

The random diffusivity approach for diffusion in heterogeneous systems

Cumulative PhD dissertation



Universidad
del País Vasco

Euskal Herriko
Unibertsitatea

Candidate: Vittoria Sposini

First supervisor: Prof. Dr. Ralf Metzler
Institute for Physics and Astronomy
University of Potsdam, Germany

Second supervisor: Dr. Gianni Pagnini
Ikerbasque & BCAM, Spain

Potsdam, 15th July 2020

*Ai miei nonni,
Franco e Marianella.*



*The research presented in this dissertation has been partially funded by
BCAM – Basque Center for Applied Mathematics – Bilbao (Spain),
where the candidate carried out a 9 months internship
in the research line of Statistical Physics.*

Declaration

I hereby declare that this dissertation contains my own work and the work that I carried out in collaboration with others, as specified in the text and Acknowledgements. Except where specific reference is made to the work of others, the contents of this dissertation are original and have not been submitted in whole or in part for consideration for any other degree or qualification in this, or any other university.

Vittoria Sposini,
Potsdam, 15th July 2020.

Acknowledgments

I would like to start by expressing my sincerest gratitude to Prof. Ralf Metzler, who provided me with the opportunity to undertake this fascinating experience that has been my PhD. I found in Prof. Metzler an inspiring model from both a scientific and personal perspective and I am thankful that I have had the chance to work with him and to be part of his group. His kindness and resourcefulness have always put me at ease, allowing me to pursue my doctoral studies with the most positive attitude possible. Secondly, I am extremely thankful to Dr. Gianni Pagnini who has been guiding me since my Master's Thesis. His frank and honest advices have always been of great help and support throughout my PhD studies, pushing me to keep moving forward and never backward. Furthermore, I would like to mention my deepest gratitude to Prof. Francesco Mainardi, who was the first to introduce me to this field and who has kept supporting me since then. Thanks to him and to my two supervisors, Prof. Metzler and Dr. Pagnini, I had the chance to discover and unveil my eagerness for science and for that I am very grateful to all of them.

I will never thank enough Prof. Aleksei V. Chechkin. His incredible commitment to science and his remarkable dedication in guiding young scientists have been of great inspiration. Prof. Chechkin has been one of the main pillars during my graduate studies, not only for his technical support in our common research but also for all the numerous shared moments full of science, literature, art, history, and joy. In particular, I would like to mention that I am extremely grateful to him for taking me along to his weekly meetings with Prof. Igor Sokolov at the Humboldt University in Berlin, to whom I also express my gratitude. Our common discussions have always been insightful and greatly edifying.

I would like to thank Prof. Gleb Oshanin with whom I started a fruitful collaboration during his visit to our group at Potsdam University. His sharpness challenged and encouraged me in learning more and more, allowing me to explore new enlightening aspects of our research.

I am deeply grateful to Prof. Flavio Seno for inviting me to visit his group at the University of Padova and for his great support in our common work. I thank Dr. Sandalo Vargas for his incredible availability, generosity and support during our attempts to work on a joint publication (we have not succeeded yet, though I am confident that we will soon). Moreover, I am grateful to both of them for their very appreciated advices for my scientific future.

I would like to thank the group in Bilbao, in particular Dr. Oleksii Sliusarenko, Dr. Silvia Vitali, Dr. Andrea Trucchia, Dr. Vera Egorova, and our close collaborator Dr. Paolo Paradisi, for the many productive discussions and for the nice time spent together inside and outside BCAM.

I am extremely grateful to all the people at Potsdam University who contributed

in creating a peaceful and yet fervent environment for our daily work, which has helped me in enjoying my PhD studies to the most from the start. Dr. Yousof Mardoukhi, Dr. Fereydoon Taheri, Dr. Hou Ru, Amin Padash, Tobias Guggenberger, Vasundhara Shaw, Pooja Arya, Joachim Jelken, Manaswita Kar, Dr. Al-Shaimaa Sad, Dr. Maria Victoria del Valle de la Cordialidad, Dr. Reinaldo Santos de Lima, and Prathitha Kar, thank you! A special thanks goes to my dear colleague and friend Samudrajit Thapa with whom I closely shared many PhD adventures. Moreover, I thank my friends Marina Pasteris, Joachim Jelken and Yousof Mardoukhi, for their help in the translation of the abstract in Spanish and German.

I cannot forget the love and support of my family, which is now spread around the world and yet so close to my heart. I deeply thank my brother, Filippo Maria Sposini, who keeps projecting me always one step ahead of where I see myself. I thank my mom and dad, Antonella Susta and Andrea Sposini, who have always believed in me and supported me unconditionally. The state of emergency due to the Covid19-crisis brought us unexpectedly close during the time of my PhD thesis writing. Their loving presence, via Skype for regular workout sessions with my mom and in a 2 months flat sharing in Potsdam with my dad, has been of great help in this last part of my doctoral studies.

Last but not least, I am immensely grateful to my partner, Vito Vurro. Despite our distance, I have always confided in him and his love to find strength, determination, and focus during my PhD time that, even if with many ups and downs, has led both of us through an extraordinary personal and scientific journey.

List of publications*

1. Sposini V, Chechkin A V, Seno F, Pagnini G & Metzler R 2018 Random diffusivity from stochastic equations: comparison of two models for Brownian yet non-Gaussian diffusion *New J. Phys.* **20**, 043044.
2. Vitali S, Sposini V, Sliusarenko O, Paradisi P, Castellani G & Pagnini G 2018 Langevin equation in complex media and anomalous diffusion *J. R. Soc. Interface* **15**, 20180282.
3. D'Ovidio M, Vitali S, Sposini V, Sliusarenko O, Paradisi P, Castellani G & Pagnini G 2018 Center-of-mass like superposition of Ornstein-Uhlenbeck processes: a pathway to non-autonomous stochastic differential equations and fractional diffusion *Fract. Calc. Appl. Anal.* **21**, 1420.
4. Sposini V, Chechkin A V & Metzler R 2019 First passage statistics for diffusing diffusivity *J. Phys. A: Math. Theor.* **52**, 04LT01.
5. Sliusarenko O, Vitali S, Sposini V, Paradisi P, Chechkin A V, Castellani G & Pagnini G 2019 Finite-energy Lévy-type motion through heterogeneous ensemble of Brownian particles *J. Phys. A: Math. Theor.* **52**, 095601.
6. Sposini V, Metzler R & Oshanin G 2019 Single-trajectory spectral analysis of scaled Brownian motion *New J. Phys.* **21**, 073043.
7. Sposini V, Grebenkov D S, Metzler R , Oshanin G & Seno F 2020 Universal spectral features of different classes of random diffusivity processes *New J. Phys.* **22**, 063056.
8. Grebenkov D S, Sposini V, Metzler R , Oshanin G & Seno F 2020 Exact first-passage time distributions for three random diffusivity models (submitted to *J. Phys. A: Math. Theor.*), pre-print: arXiv:2007.05765.

*This is the complete list of publications of the candidate, the ones contributing to the cumulative dissertation are 1, 4, 6 and 7.

Abstract

The two hallmark features of Brownian motion are the linear growth $\langle x^2(t) \rangle = 2Ddt$ of the mean squared displacement (MSD) with diffusion coefficient D in d spatial dimensions, and the Gaussian distribution of displacements. With the increasing complexity of the studied systems deviations from these two central properties have been unveiled over the years. Recently, a large variety of systems have been reported in which the MSD exhibits the linear growth in time of Brownian (Fickian) transport, however, the distribution of displacements is pronouncedly non-Gaussian (Brownian yet non-Gaussian, BNG). A similar behaviour is also observed for viscoelastic-type motion where an anomalous trend of the MSD, i.e., $\langle x^2(t) \rangle \sim t^\alpha$, is combined with *a priori* unexpected non-Gaussian distributions (anomalous yet non-Gaussian, ANG). This kind of behaviour observed in BNG and ANG diffusions has been related to the presence of heterogeneities in the systems and a common approach has been established to address it, that is, the random diffusivity approach.

This dissertation explores extensively the field of random diffusivity models. Starting from a chronological description of all the main approaches used as an attempt of describing BNG and ANG diffusion, different mathematical methodologies are defined for the resolution and study of these models. The processes that are reported in this work can be classified in three subcategories, i) randomly-scaled Gaussian processes, ii) superstatistical models and iii) diffusing diffusivity models, all belonging to the more general class of random diffusivity models. Eventually, the study focuses more on BNG diffusion, which is by now well-established and relatively well-understood. Nevertheless, many examples are discussed for the description of ANG diffusion, in order to highlight the possible scenarios which are known so far for the study of this class of processes.

The second part of the dissertation deals with the statistical analysis of random diffusivity processes. A general description based on the concept of moment-generating function is initially provided to obtain standard statistical properties of the models. Then, the discussion moves to the study of the power spectral analysis and the first passage statistics for some particular random diffusivity models. A comparison between the results coming from the random diffusivity approach and the ones for standard Brownian motion is discussed. In this way, a deeper physical understanding of the systems described by random diffusivity models is also outlined.

To conclude, a discussion based on the possible origins of the heterogeneity is sketched, with the main goal of inferring which kind of systems can actually be described by the random diffusivity approach.

Abstrakt

Die zwei grundlegenden Eigenschaften der Brownschen Molekularbewegung sind das lineare Wachstum $\langle x^2(t) \rangle = 2Ddt$ der mittleren quadratischen Verschiebung (mean squared displacement, MSD) mit dem Diffusionskoeffizienten D in Dimension d und die Gauß Verteilung der räumlichen Verschiebung. Durch die zunehmende Komplexität der untersuchten Systeme wurden in den letzten Jahren Abweichungen von diesen zwei grundlegenden Eigenschaften gefunden. Hierbei, wurde über eine große Anzahl von Systemen berichtet, in welchen die MSD das lineare Wachstum der Brownschen Bewegung (Ficksches Gesetz) zeigt, jedoch die Verteilung der Verschiebung nicht einer Gaußverteilung folgt (Brownian yet non-Gaussian, BNG). Auch in viskoelastischen Systemen Bewegung wurde ein analoges Verhalten beobachtet. Hier ist ein anomales Verhalten des MSD, $\langle x^2(t) \rangle \sim t^\alpha$, in Verbindung mit einer *a priori* unerwarteten nicht gaußchen Verteilung (anomalous yet non-Gaussian, ANG). Dieses Verhalten, welches sowohl in BNG- als auch in ANG-Diffusion beobachtet wird, ist auf eine Heterogenität in den Systemen zurückzuführen. Um diese Systeme zu beschreiben, wurde ein einheitlicher Ansatz, basierend auf den Konzept der zufälligen Diffusivität, entwickelt. Die vorliegende Dissertation widmet sich ausführlich Modellen mit zufälligen Diffusivität. Ausgehend von einem chronologischen Überblick der grundlegenden Ansätze der Beschreibung der BNG- und ANG-Diffusion werden mathematische Methoden entwickelt, um die verschiedenen Modelle zu untersuchen. Die in dieser Arbeit diskutierten Prozesse können in drei Kategorien unterteilt werden: i) *randomly-scaled Gaussian processes*, ii) *superstatistical models* und iii) *diffusing diffusivity models*, welche alle zu den allgemeinen Modellen mit zufälligen Diffusivität gehören. Der Hauptteil dieser Arbeit ist die Untersuchung auf die BNG Diffusion, welche inzwischen relativ gut verstanden ist. Dennoch werden auch viele Beispiele für die Beschreibung von ANG-Diffusion diskutiert, um die Möglichkeiten der Analyse solcher Prozesse aufzuzeigen. Der zweite Teil der Dissertation widmet sich der statistischen Analyse von Modellen mit zufälligen Diffusivität. Eine allgemeine Beschreibung basierend auf dem Konzept der momenterzeugenden Funktion wurde zuerst herangezogen, um grundsätzliche statistische Eigenschaften der Modelle zu erhalten. Anschließend konzentriert sich die Diskussion auf die Analyse der spektralen Leistungsdichte und der *first passage* Statistik für einige spezielle Modelle mit zufälligen Diffusivität. Diese Ergebnisse werden mit jenen der normalen Brownschen Molekularbewegung verglichen. Dadurch wird ein tiefergehendes physikalisches Verständnis über die Systeme erlangt, welche durch ein Modell mit zufälligen Diffusivität beschrieben werden. Abschließend, zeigt eine Diskussion mögliche Ursachen für die Heterogenität auf, mit dem Ziel darzustellen, welche Arten von Systemen durch den Zufalls-Diffusivitäts-Ansatz beschrieben werden können.

Resumen

Las dos características distintivas del movimiento Browniano son el crecimiento lineal $\langle x^2(t) \rangle = 2Ddt$ del desplazamiento cuadrático medio (*mean squared displacement*, MSD) con el coeficiente de difusión D en dimensiones espaciales d , y la distribución Gaussiana de los desplazamientos. Con los continuos avances en tecnologías experimentales y potencia de cálculo, se logra estudiar con mayor detalle sistemas cada vez más complejos y algunos sistemas revelan desviaciones de estas dos propiedades centrales. En los últimos años se ha observado una gran variedad de sistemas en los que el MSD presenta un crecimiento lineal en el tiempo (típico del transporte Browniano), no obstante, la distribución de los desplazamientos es pronunciadamente no Gaussiana (*Brownian yet non-Gaussian diffusion*, BNG). Un comportamiento similar se observa asimismo en el caso del movimiento de tipo viscoelástico, en el que se combina una tendencia anómala del MSD, es decir, $\langle x^2(t) \rangle \sim t^\alpha$, con $0 < \alpha < 2$, con distribuciones inesperadamente no Gaussianas (*Anomalous yet non-Gaussian diffusion*, ANG). Este tipo de comportamiento observado en las difusiones BNG y ANG se ha relacionado con la presencia de heterogeneidades en los sistemas y se ha establecido un enfoque común para abordarlo: el enfoque de difusividad aleatoria. En la primera parte de esta disertación se explora extensamente el área de los modelos de difusividad aleatoria. A través de una descripción cronológica de los principales enfoques utilizados para caracterizar las difusiones BNG y ANG, se definen diferentes metodologías matemáticas para la resolución y el estudio de estos modelos. Los procesos expuestos en este trabajo, pertenecientes a la clase más general de modelos de difusividad aleatoria, pueden clasificarse en tres subcategorías: i) *randomly-scaled Gaussian processes*, ii) *superstatistical models* y iii) *diffusing diffusivity models*. Fundamentalmente el enfoque de este trabajo se centra en la difusión BNG, bien establecida y ampliamente estudiada en los últimos años. No obstante, múltiples ejemplos son examinados para la descripción de la difusión ANG, a fin de remarcar los diferentes modelos de estudio disponibles hasta el momento. En la segunda parte de la disertación se desarrolla el análisis estadístico de los procesos de difusividad aleatoria. Inicialmente se expone una descripción general basada en el concepto de la *función generadora de momentos* para obtener las propiedades estadísticas estándar de los modelos. A continuación, la discusión aborda el estudio de la *densidad espectral de potencia* y la estadística del *tiempo de primer paso* para algunos modelos de difusividad aleatoria. Adicionalmente, los resultados del método de difusividad aleatoria se comparan junto a los de movimiento browniano estándar. Como resultado, se obtiene una mayor comprensión física de los sistemas descritos por los modelos de difusividad aleatoria. Para concluir, se presenta una discusión acerca de los posibles orígenes de la heterogeneidad, con el objetivo principal de inferir qué tipo de sistemas pueden describirse apropiadamente según el enfoque de la difusividad aleatoria.

Contents

List of abbreviations	1
1 Introduction	3
Synopsis	9
2 Superstatistics and randomly-scaled Gaussian models	14
2.1 Randomly-scaled Gaussian processes	14
2.1.1 Fractional dynamics	15
2.1.2 Brownian and anomalous yet non-Gaussian diffusion	16
2.2 Superstatistics	20
2.2.1 Superstatistical Brownian motion	21
2.3 Discussion	23
3 The diffusing diffusivity approach	25
3.1 In response to the experimentalists' call: the first DD model	25
3.2 Second generation models	27
3.3 Third generation models	30
3.4 Most recent developments	33
3.4.1 Viscoelastic-type motion	33
3.4.2 Many-body systems – Rouse model in crowded environment	34
3.5 Discussion	35
4 Statistical analyses of random diffusivity models	37
4.1 Power spectral analysis	39
4.2 First passage statistics	45
4.3 Discussion	51
5 Conclusions	53

Appendix	57
A Fractional Brownian motion	57
B Fractional derivatives	58
C Collection of papers	60
Bibliography	138

List of abbreviations

ANG	Anomalous yet non-Gaussian
BM	Brownian motion
BNG	Brownian yet non-Gaussian
DD	Diffusing diffusivity model
FBM	Fractional Brownian motion
FLE	Fractional Langevin equation
GGBM	Generalised grey Brownian motion
GLE	Generalised Langevin equation
HEBP	Heterogeneous ensemble of Brownian particles
<i>i.i.d.</i>	Independent and identically distributed
LE	Langevin equation
mDD	Minimal diffusing diffusivity model
MGF	Moment-generating function
MSD	Mean-squared displacement
PDF	Probability density function
PSD	Power spectral density
RSG	Randomly-scaled Gaussian process
SBM	Scaled Brownian motion
SupBM	Superstatistical Brownian motion

Chapter 1

Introduction

The systematic study of diffusion dates back to the 19th century, when Robert Brown was performing experiments to observe the jiggly motion of granules extracted from pollen grains suspended in water [1]. What is nowadays commonly known as Brownian motion (BM) represents the classical model for diffusion established by Einstein, Smoluchowski, Langevin, Fick and others [2–10]. The methodologies used to describe and investigate diffusive motion can be divided in two classes:

- The stochastic formulation in terms of random walks and stochastic processes, suitable for particle-based modelling and corresponding to a micro/mesoscopic description;
- The deterministic description through partial differential equations representing diffusion equations, suitable for the study of distribution functions at a macroscopic scale.

In the theory of standard diffusion, a clear connection exists between the two approaches. The Langevin equation (LE) represents a standard stochastic description of the diffusive motion of a mesoscopic particle in a liquid and it reads

$$\frac{dx(t)}{dt} = v(t); \quad m \frac{dv(t)}{dt} = -\gamma v(t) + \sqrt{2\sigma} \xi(t), \quad (1.1)$$

where m is the mass of the particle, γ is the damping coefficient and $\xi(t)$ is a stochastic forcing, mathematically represented by zero-mean, white Gaussian noise with δ -correlation and noise intensity σ . The second equation in (1.1) is nothing but Newton's equation of motion, where both terms in the right-hand side represent the effect of the liquid onto the particle. The stochastic forcing stands for the random kicks that the particle receives from the surrounding molecules, due to thermal motion. The deterministic term accounts for the instantaneous dissipation back into the environment of the energy transferred through each kick. If the system is in

equilibrium, the two terms are linked through the fluctuation-dissipation relation, that is $\sigma = \gamma k_B T$, where k_B is the Boltzmann constant and T is the temperature of the system. Starting from the LE, one can calculate the probability $P(x, v, t) dx dv$ of finding the diffusive entity in the interval $(x, x + dx; v, v + dv)$ at a time t . Finally, the probability density function (PDF) $P(x, v, t)$ is known to fulfil the bivariate Fokker–Planck–Smoluchowski equation

$$\frac{\partial P(x, v, t)}{\partial t} = -v \frac{\partial P(x, v, t)}{\partial x} - \frac{\gamma}{m} \frac{\partial P(x, v, t)}{\partial v} + \frac{\sigma}{m^2} \frac{\partial^2 P(x, v, t)}{\partial v^2}, \quad (1.2)$$

which in this form for (x, v, t) is also known as Klein–Kramers equation. Starting either from the LE in (1.1) or from the Fokker–Planck equation in (1.2), it is easy to prove that standard diffusion shows two hallmark features in the limit $t \gg \gamma^{-1}$:

- i) the linear growth of the mean squared displacement (MSD)

$$\langle x^2(t) \rangle = 2Dt, \quad (1.3)$$

- ii) the Gaussian distribution of displacements

$$G(x, t|D) = \frac{1}{\sqrt{4\pi Dt}} \exp\left(-\frac{x^2}{4Dt}\right), \quad (1.4)$$

where D is the diffusion coefficient. For the sake of simplicity, here and throughout the whole dissertation, one-dimensional models only are treated, nevertheless a generalisation to higher dimensions can readily be achieved component-wise.

The presence of a Gaussian distribution implies in general that the environment in which the diffusion occurs is homogeneous, such that, at any time t , larger than the single jump time Δt , the displacement performed by the particle is given by a sum of steps which can be seen as independent and identically distributed (*i.i.d.*) random variables. Then, the central limit theorem guarantees the convergence of the displacement distribution to a Gaussian. If the environment were not homogeneous, the assumption of *i.i.d.* steps would fail and, as a consequence, the displacement distribution could deviate from a Gaussian. Moreover, the presence of temporal correlations between each step, typical for instance of viscoelastic media (see figure 1.1), can cause the MSD to display a non-linear trend. Diffusion in viscoelastic environments is well understood when using the two prototypical models, fractional Brownian motion (FBM) [12] and the fractional Langevin equation (FLE) [14–16] (see Appendix A for more details). In their stochastic formulation both models consider fractional Gaussian noise, characterised by a power-law correlation function, instead of δ -correlated white Gaussian noise. A Gaussian displacement distribution is obtained for both FBM and FLE, but their variance scales as a power-law

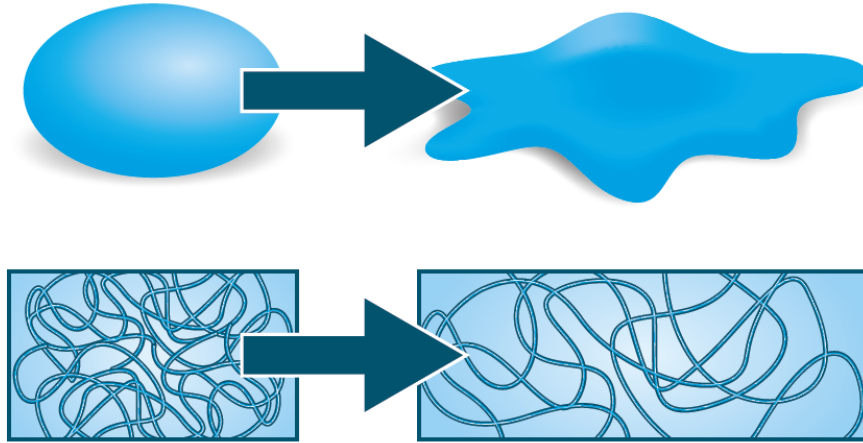


Figure 1.1: Macroscopic (top row) and microscopic (bottom row) representation of viscoelastic materials, whose behaviour depends on the magnitude and the time scale of the applied forces. The difference in the microscopic structures of the material defines the different responses. On the left, high entanglement of the fibers corresponds to elastic behaviour while, on the right, a lesser entanglement of the fibers leads to a more viscous character (image from blog.biolinscientific.com).

at long times. From a more physical perspective, FBM represents an overdamped non-equilibrium model where the particles are exposed to an external random force with long-range correlation. Conversely, the FLE depicts an underdamped equilibrium description where a generalised fluctuations-dissipation relation can be defined. This difference leads, for instance, to the fact that when fractional Gaussian noise with positive correlation is introduced (persistent noise), for FBM one has a superdiffusive behaviour, namely $\langle x^2(t) \rangle \sim t^\alpha$ with $\alpha > 1$, while from the FLE one obtains a subdiffusive behaviour, that is $\langle x^2(t) \rangle \sim t^\alpha$ with $\alpha < 1$. This is due to the fact that the fluctuation-dissipation relation in the FLE couples the persistent noise with long memory in the damping term, leading to subdiffusion. Note that FBM and FLE deviate from the models associated to the typical understanding of fractional dynamics. The latter are models that emerge if one introduces broadly distributed step lengths or waiting times (such that their variance does not exist), as in the continuous time random walk formalism [17]. These processes are characterised by displacement distributions that are inherently non-Gaussian and whose time evolution is well described by the so-called fractional diffusion equations, in which the concept of fractional derivatives is introduced (see Appendix B).

With continuous advances in experimental techniques and computational power, more and more complex systems are being studied in great detail, unveiling deviations from the *a priori* expected Gaussian behaviour of BM and viscoelastic-type motion. In particular two specific classes of diffusive processes have been identified,

Brownian (or Fickian) yet non-Gaussian diffusion (BNG) [18, 19] and, in analogy, anomalous yet non-Gaussian diffusion (ANG) [65]. The former is characterised by a linear trend of the MSD while the latter presents an anomalous trend of the MSD, i.e., $\langle x^2(t) \rangle \sim t^\alpha$, with $0 < \alpha < 2$, and both display an unexpected non-Gaussian displacement distribution. The non-Gaussianity of the displacement distribution has been associated to various sources of heterogeneity and it is often characterised by exponential (Laplace) or stretched Gaussian shape.

The study of these processes has become increasingly relevant with the growing number of complex systems discovered to exhibit such statistical features. For instance, for BNG diffusion one can mention soft matter and biological systems, in which the motion of viruses, biological macromolecules, proteins and colloidal particles along lipid tubes and through actin networks [18, 19] as well as along membranes and inside colloidal suspension [20] and colloidal nanoparticles adsorbed at fluid interfaces [21–23] are studied. Ecological processes, involving the characterisation of organism movement and dispersal [24] also exhibit similar behaviour. Moreover, there are processes, that are Brownian but non-Gaussian in certain time windows of their dynamics. These concern the dynamics of disordered solids, such as glasses and supercooled liquids [25–27] as well as interfacial dynamics [28, 29]. As far as ANG diffusion is concerned, the motion of tracer particles in the cellular cytoplasm [30–32] and the motion of lipids and proteins in protein-crowded model membranes [33] can be reported.

The most common approach employed over the last decade to describe BNG and ANG diffusion is based on the concept of random diffusivity. It is worth mentioning that two pioneering discussions of similar models are already present in the book by Van Kampen [10] under the name of composite Markov processes and in the paper by Kärger [11] on nuclear magnetic resonance self-diffusion in heterogeneous systems. In the former a model is discussed starting from a composition of Markov processes, which are obtained by randomly switching the diffusive dynamics, e.g. free motion and oscillatory motion, and its parameters at any random time τ_i . This description is useful in particular in solid-state physics. In the latter, instead, it is introduced the idea of regarding a heterogeneous systems as consisting of several subregions of different diffusivities, providing interesting results for the study of nuclear magnetic resonance self-diffusion. This view of heterogeneous systems will be largely discussed along this dissertation. Finally, it is important to mention that similar processes are ubiquitous in financial mathematics as well [34–37]. They are commonly known as stochastic volatility models and their study is motivated by various aspects of the observed financial market data concerning stock price. Recently these models have been also expanded to fractional volatility models to include the fact that historical volatility time series exhibit a much rougher behaviour than BM. This "roughness" of the volatility dynamics can indeed be better described by FBM [38].

Figure 1.2 aims at providing a general understanding of how the presence of



Figure 1.2: Artistic representation of a diffusivity map for heterogeneous systems. Differently coloured areas denote regions of different diffusivity. A diffusing particle is likely to eventually cross the boundaries and sample different diffusivities (image from www.itermar.it – Infiorata di Spello, Umbria, Italy).

heterogeneity can be mapped into the concept of random diffusivity, by associating each colour of a local region to a specific value of the diffusion coefficient. The main assumption behind this approach is that fluctuations of the system that happen at a micro- or mesoscopic scale reflect onto the value of a specific macroscopic observable, that is the diffusion coefficient (or the noise intensity for FBM where the concept of diffusion coefficient cannot be clearly defined). One could imagine that the variability in the diffusion coefficient can be due to changes in the environment and/or in some features of the diffusive entities. Indeed, the diffusion coefficient depends on both environment and particle properties. Thus, not only can one have variability along a single trajectory while the tracer explores the whole inhomogeneous space, but one could also observe fluctuations in the diffusive entities themselves, for instance, in terms of a distribution of bead sizes. Imagine the diffusion of tracers in artificial or natural gels, such as mucin or mucus, in biofilms, or in the crowded cytoplasm of cells. All these systems are heterogeneous in nature (see figure 1.1) and one cannot avoid taking this into account when modelling transport properties and diffusive motion.

This dissertation focuses on the description of the various models that have been introduced in the last decade to address the study of motion in heterogeneous systems through the random diffusivity approach. A Synopsis of the dissertation is initially reported, where specific reference is made to the original contribution of the author

to the field, which is otherwise directly integrated in the overall discussion.

The first part of this work is structured as a review and it aims at establishing a general state-of-the-art of the topic. A collection of the main models developed for the description of BNG and ANG diffusion is reported, with more emphasis on BNG diffusion, as it is so far a wider discussed topic in comparison to ANG, which still represents a quite unexplored field. This part of the dissertation is divided in two Chapters (Chapter 2 and 3), accounting for models with different origins and features. Chapter 2 reports two classes of models, randomly-scaled Gaussian processes and the theory of superstatistics. Both models, which find their origins in frameworks initially defined for other kinds of systems, have been revised only recently to be included in the topic of random diffusivity models for the study of BNG and ANG diffusion. In Chapter 3 an overview of what is called diffusing diffusivity approach is reported. This model was introduced *ad hoc* to reproduce BNG diffusion and, very recently, possible ways to extend it to the description of ANG diffusion have been studied.

The second part of the dissertation, represented by Chapter 4, moves to the study of different statistical aspects of random diffusivity models. While Chapter 2 and 3 are based on how one can mathematically reproduce BNG and ANG diffusion features known from experiments, this fourth Chapter focuses on a more advanced statistical study and characterisation of this class of models. Starting from the introduction of a general framework, able to reproduce, among others, any (overdamped) random diffusivity model for BNG diffusion, a detailed description of two specific statistical analyses is reported, namely power spectral analysis and first passage analysis. In this way, a more general view and understanding of random diffusivity models is gained.

Chapter 5 is dedicated to final discussions, conclusions and outlook. In Appendices A and B one can find some mathematical details concerning FBM, FLE and fractional derivatives. Finally, the collection of the four publications contributing to this cumulative dissertation is included in Appendix C.

Synopsis

Before proceeding with the discussion, a comprehensive view of the ideas, methods, and achievements discussed in this thesis is reported here, with the aim of highlighting the novel results obtained during this research.

As largely discussed in the introduction, a growing number of systems are being revealed which exhibit BNG and ANG dynamics. The comparison among observations coming from different systems shows that their complexity and inhomogeneity, interpreted as the cause of the non-Gaussian behaviour, influences the particles diffusive motion at different levels. In particular, for some systems the non-Gaussian dynamics may persist throughout the entire observation window, while for others one observes at long times a crossover to Gaussian diffusion.

In Chapter 2 and 3 of this work, three possible classes of models for the study of the diffusive dynamics of particles in complex systems are considered: randomly-scaled Gaussian processes (RSG) and superstatistical models (SupBM) in Chapter 2 and diffusing diffusivity models (DD) in Chapter 3. The overall review of these random diffusivity models includes and integrates the results discussed by the author and collaborators in:

Sposini V, Chechkin A V, Seno F, Pagnini G & Metzler R 2018 Random diffusivity from stochastic equations: comparison of two models for Brownian yet non-Gaussian diffusion <i>New J. Phys.</i> 20 , 043044 – see Appendix C for the full text (page 59).

Note that the very structure itself of this part of the thesis, namely the division into two Chapters, recalls the general message of the publication – a comparison of two classes of models for BNG diffusion.

Focusing on the description of BNG diffusion, for the DD models, an operative set of dynamic stochastic equations to define a time-dependent random diffusivity is needed. In this way a description based on two coupled Langevin equations, one for the dynamics of the particles and one for the fluctuations of the environment, is obtained. The different mathematical methods that can be used to solve this set of

equations are also included in the discussion. Of particular interest are those sets of equations which are able to mimic the class of the generalised Gamma distribution for the diffusivity. This class of distributions includes the Gamma and the exponential distribution, which can properly reproduce the Laplace distribution for the particle displacement observed in experiments. The same generalised Gamma distribution was also chosen in the discussion of RSG and SupBM models, where a mathematical description based on standard BM with a population of diffusivity emerges. It is discussed that the main difference among the RSG, SupBM, and the DD models is the description of the particle dynamics in the long time regime, corresponding to different physical scenarios. The RSG model does not consider an active dynamics of the environment, in contrast, the SupBM and DD models support the idea of randomly varying diffusivity along single trajectories, corresponding to a dynamics for the environment. Nevertheless, in the SupBM an explicit assumption is introduced, that is the presence of a clear time scale separation between the characteristic time of the medium fluctuations and the relaxation time of the system. As a result, two observations can be drawn: i) the SupBM provides a mathematical description at the ensemble level which is equivalent to the one given by RSG models; ii) the SupBM can be used as a short time approximation of the DD model, which presents results that are valid for any characteristic time of the medium fluctuations. The RSG and SupBM models define a specific non-Gaussian dynamics for the entire diffusion process, while DD models are able to describe a transition from a non-Gaussian to a Gaussian diffusion in the long time regime, leading to an effective value for the diffusivity. If one selects the same distribution of diffusivity for all three models, the short times non-Gaussian dynamics is equivalent in each model.

The influence of non-equilibrium initial conditions for the diffusivity dynamics is also briefly addressed. The main result emerges in the temporal evolution of the MSD, which can present different intermediate regimes. In the long time regime one obtains a description in agreement with the one for the equilibrium case, as expected.

References to models suitable for the study of ANG diffusion are also reported. While for RSG models a direct parallel with BNG diffusion results can be drawn, in the case of SupBM and DD models the mathematical and physical picture is not yet clear. Indeed, the interplay between the dynamics of the environment and the long range correlations typical of viscoelastic motion is still to be fully understood.

In Chapter 4 advanced statistical analyses of the random diffusivity models for BNG diffusion discussed above are reported, including the results obtained by the author and collaborators in:

Sposini V, Chechkin A V & Metzler R 2019 First passage statistics for diffusing diffusivity *J. Phys. A: Math. Theor.* **52**, 04LT01 – see Appendix C for the full text (page 82).

Sposini V, Grebenkov D S, Metzler R , Oshanin G & Seno F 2020 Universal spectral features of different classes of random diffusivity processes *New J. Phys.* **22**, 063056 – see Appendix C for the full text (page 111).

Initially, a general framework for the study of overdamped models for BNG diffusion is introduced. This framework is able to reproduce all three classes of models discussed in Chapter 2 and 3. In addition, a range of previously unconsidered random diffusivity processes, where the diffusivity is modelled as a functional of BM, can also be studied. A description based on the concept of the moment-generating function is provided for this general framework, such that standard statistical properties of the models, such as the PDF and its moments, can be derived. Exact forms of the PDFs span distributions in which the central part may be Gaussian or non-Gaussian, and the tails may assume Gaussian, exponential, log-normal or even power-law forms.

Two insightful approaches to study time-dependent stochastic processes are then reported, namely the single-trajectory power spectral analysis and the first passage time statistics. The former is based on the characterisation of the power spectral density (PSD) of a process. A textbook definition of the PSD provides an ensemble-averaged property defined as the Fourier transform of the autocorrelation function of the process in the asymptotic limit of long observation times. Due to experimental and computational limitations, the observation time of typical single-trajectory measurements or supercomputing studies is limited, and typically also relatively few trajectories are measured. To account for these limitations, the concept of single-trajectory PSD was introduced. The latter is a standard concept in statistical physics used to evaluate the instant in which a diffusing particle reaches a reaction centre or a stochastic process exceeds a given threshold value.

In section 4.1 results on the single-trajectory power spectral analysis for random diffusivity models are discussed. A universal scaling of the PSD as function of the frequency f is established in all cases, showing in addition that this scaling can be understood already from the single-trajectory PSD. It is shown that a first way to discriminate among models lies in the study of the ageing behaviour of the PSD. Indeed, the dependence of the PSD on the trajectory length appears only for those random diffusivity models that are characterised by an anomalous scaling of the MSD. Differences from one model to another appear in higher order moments of the single-trajectory PSD distribution as well. In particular, exact expressions for the coefficient of variation, defined as the ratio between standard deviation and mean value of the single-trajectory power spectrum distribution, are obtained, proving that the latter can be a good indicator of the specific model. Moreover, the probability density for the amplitudes of the single-trajectory PSD is studied. This observable reflects the very specific properties of the different random diffusivity models thus providing insightful results. For instance, the coefficient of variation may be directly calculated from its moments.

In section 4.2 the first passage behaviour of the random diffusivity models is studied. In particular, it is shown that at short times random diffusivity dynamics leads to a faster decay of the survival probability and thus to faster first passage. In a semi-infinite domain a universal crossover independent of the initial particle position occurs. Beyond this crossover, random diffusivity models show a dynamic which is slower than standard BM. Finally, the decay in the tails changes according to the class of model that one selects. For DD models a convergence to the conventional Lévy-Smirnov behaviour typical of BM is recovered. For RSG and SupBM models heavier tails are observed. In finite domains, one obtains similar results as for semi-infinite domains. The only difference is in the large time dynamics of DD models where the first passage behaviour is dominated by an exponential decay with a characteristic time, indicative of the mean first passage time, that is longer than that the one for BM. Thus, it is found that in general the heterogeneity of the environment does not improve the mean first passage result, in fact some of the particles are slowed down. At the same time the heterogeneity also allows other particles to have a diffusion coefficient greater than the average, and this is enough to increase the speed of the reaction activation in diffusion-limited reactions, dominated by the non-asymptotic part of the first passage time behaviour. In particular, the amount of fast particles does not depend on the initial position, representing the distance between particle and target. This suggests that the obtained results may be qualitatively generalised to any distribution of the initial particle position.

Along the discussion of Chapter 4, more emphasis is put on the study of random diffusivity models, yet one can also find comments on the results on the power spectral analysis for scaled Brownian motion (SBM) obtained by the author and collaborators in:

Sposini V, Metzler R & Oshanin G 2019 Single-trajectory spectral analysis of scaled Brownian motion *New J. Phys.* **21**, 073043 – see Appendix C for the full text (page 94).

This study was thought as a preliminary exercise to understand how to apply the framework of single-trajectory spectral analysis to diffusing diffusivity models. However, the interesting comparison that emerged between SBM and FBM by itself became worth of publication. The spectral content of SBM, which is a Markovian but non-stationary diffusion process with Gaussian distribution and scaling of the variance $\langle x^2(t) \rangle \sim t^\alpha$, $0 < \alpha < 2$, showed that the frequency dependence has the invariant scaling form $\sim 1/f^2$, where f is the frequency, fully independent of the anomalous scaling exponent α . The frequency dependence of the single-trajectory PSD is thus the same as for standard BM. Furthermore, similar to BM is also the behaviour of the coefficient of variation. However, a distinctive feature is shown to be provided by the explicit dependence of the results on the measurement time. This ageing property can be used to deduce the anomalous diffusion exponent. The res-

ults for SBM were compared to the single-trajectory PSD behaviour of FBM. Note that even if both FBM and SBM are Gaussian in nature, the former has stationary increments yet is non-Markovian due to its power-law correlated driving noise, differently from what stated above for SBM. For both sub- and superdiffusion the coefficient of variation for FBM provides different values from SBM. In addition, subdiffusive FBM is non-ageing but has an α -dependent frequency scaling of the single-trajectory PSD. In the superdiffusive regime the frequency dependence and the ageing behaviour of the single-trajectory PSD for FBM is the same as for SBM, leaving the coefficient of variation as the only way to distinguish the two processes from each other. Concurrently, the PDF of the single-trajectory PSD is the same for all cases.

Finally, in the conclusions, a discussion based on the possible origins of the heterogeneity is reported, with the main result that random diffusivity models are able to describe systems that display time-dependent heterogeneity, weak space-dependent heterogeneity and/or ensemble heterogeneity.

Chapter 2

Superstatistics and randomly-scaled Gaussian models

The intuition based on the idea that the concept of random diffusivity could be employed in the description of diffusive motion in heterogeneous environments led to a renewed interest in two models which were developed in the early 2000s, randomly-scaled Gaussian models and the so-called superstatistical models. In this Chapter, these two approaches are briefly introduced and discussed from a fresh perspective, which will turn out to be convenient for later discussions and comparisons.

2.1 Randomly-scaled Gaussian processes

A general framework for the description of diffusion in complex environments is provided by the class of stochastic processes identified as randomly-scaled Gaussian processes (RSG). The basic idea of this approach is that the complexity or heterogeneity of the medium is completely described by the random nature of a specific parameter, that is

$$X = \sqrt{\Lambda} X_g, \quad (2.1)$$

where Λ is an independent, non-negative and dimensionless random variable and X_g is a Gaussian process. The distribution function of any RSG process can be recovered following the results discussed in [39]:

Define with Z_1 and Z_2 two real independent random variables whose PDFs are $P_1(z_1)$ and $P_2(z_2)$, with $-\infty \leq z_1 \leq +\infty$ and $0 \leq z_2 \leq +\infty$, respectively, and with Z the random variable obtained by the product of Z_1 and Z_2^α , that is, $Z = Z_1 Z_2^\alpha$. Then, the PDF of Z , denoted by $P(z)$, is given by

$$P(z) = \int_0^\infty P_1\left(\frac{z}{\lambda^\alpha}\right) P_2(\lambda) \frac{d\lambda}{\lambda^\alpha}. \quad (2.2)$$

In what follows a short excursion is reported with some examples that show how this framework can be used to define models displaying fractional dynamics. Later on, it is described how the same framework can be used to model heterogeneous diffusion, namely BNG and ANG diffusion.

2.1.1 Fractional dynamics

Fractional dynamics is intended here as any process that allows for an evolution equation of its PDF that presents fractional derivatives (see Appendix B for more details on fractional derivatives).

The original generalised grey Brownian motion (GGBM) is a stochastic process defined by [40]

$$X_{\beta,H} = \sqrt{\Lambda_\beta} X_H, \quad (2.3)$$

where X_H represents FBM with $0 < H < 1$ and variance scaling as t^{2H} , while Λ_β is an independent, non-negative random variable distributed according to the M-Wright function (sometimes also called Mainardi function)

$$M_\beta(\lambda) = \sum_{k=0}^{\infty} \frac{(-\lambda)^k}{k! \Gamma(-\beta k + 1 - \beta)}, \quad 0 < \beta \leq 1, \quad \lambda \geq 0, \quad (2.4)$$

which is characterised by a Laplace transform expressed in terms of the Mittag-Leffler function

$$\int_0^{\infty} M_\beta(\lambda) e^{-\lambda s} d\lambda = E_\beta(-s) = \sum_{k=0}^{\infty} \frac{(-s)^k}{\Gamma(\beta k + 1)}, \quad 0 < \beta \leq 1, \quad \lambda \geq 0. \quad (2.5)$$

The model described in (2.3) includes grey Brownian motion [41], FBM and BM as special cases when $\beta = 2H$, $\beta = 1$ and $\beta = 2H = 1$, respectively (see [40] for more details). The evolution equation for the PDF of the GGBM can be expressed in term of the Erdély–Kober $D_\eta^{\epsilon,\mu}$ fractional derivative with respect to t in the following way [42]

$$\frac{\partial P(x,t)}{\partial t} = \frac{\nu}{\beta} t^{\nu-1} D_{\nu/\beta}^{\beta-1,1-\beta} \frac{\partial^2 P(x,t)}{\partial x^2}. \quad (2.6)$$

Equation (2.6) defines a Green's function given by

$$P(x,t) = \frac{1}{2t^H} M_{\beta/2} \left(\frac{|x|}{t^H} \right), \quad (2.7)$$

which presents the following asymptotic behaviour in the self-similar variable $y = |x|/t^H$

$$P(y) \sim y^a \exp(-by^c), \quad y \rightarrow \infty, \quad (2.8)$$

with $a = (\beta - 1)/(2 - \beta)$, $b = (2 - \beta)2^{-2/(2-\beta)}\beta^{\beta/(2-\beta)}$ and $c = 2/(2 - \beta)$.

A RSG model was used also in [39] to derive a stochastic process whose one-point one-time PDF is the solution of the symmetric space-time fractional diffusion

$${}_tD_{\star}^{\beta}P(x, t) = {}_xD^{\nu}P(x, t), \quad (2.9)$$

where ${}_tD_{\star}^{\beta}$ is the Caputo time fractional derivative and ${}_xD^{\nu}$ is the symmetric Riesz–Feller space fractional derivative. In this case we have that

$$X_{\nu, \beta}(t) = \sqrt{\Lambda_{\nu/2, \beta}}G_{2\beta/\nu}(t), \quad 0 < \beta \leq 1, \quad 0 < \nu \leq 2, \quad (2.10)$$

where $G_{2\beta/\nu}(t)$ is FBM with Hurst exponent $H = \beta/\nu$, such that its variance scales as $t^{2\beta/\nu}$, and $\Lambda_{\nu/2, \beta}$ is an independent constant non-negative random variable distributed according to the distribution function

$$K_{\nu/2, \beta}^{-\nu/2}(\lambda) = \int_0^{\infty} L_{\nu/2}^{-\nu/2}\left(\frac{\lambda}{y^{2/\nu}}\right) M_{\beta}(y) \frac{dy}{y^{2/\nu}}, \quad 0 < \beta \leq 1, \quad \lambda \geq 0, \quad (2.11)$$

where $L_{\alpha}^{-\alpha}(\lambda)$ is the extremal Lévy stable density, which can be related to the M-Wright/Mainardi function in (2.4) as follows

$$L_{\alpha}^{-\alpha}\left(\frac{1}{\lambda^{\alpha}}\right) \frac{1}{\alpha\lambda^{1/\alpha+1}} = M_{\alpha}(\lambda), \quad 0 < \alpha \leq 1, \quad \lambda \geq 0. \quad (2.12)$$

The stochastic process described in (2.10) generalises Gaussian processes and it is uniquely determined by its mean and autocovariance structure. Conversely to the GGBM, it involves also stochastic processes fractional in space but, on the other hand, it does not provide all the time fractional processes described by the GGBM.

2.1.2 Brownian and anomalous yet non-Gaussian diffusion

The class of diffusion processes which is of main interest in this dissertation is represented by BNG and ANG diffusion. As already mentioned in the introduction, these are processes characterised by a linear and anomalous trend of the MSD, respectively, combined with an unexpected non-Gaussian distribution. Many experiments have shown that these non-Gaussian PDFs often display exponential or stretched Gaussian shape. Thus, the goal of this section is to show how RSG processes can be used to reproduce this kind of behaviour.

Regardless of the Gaussian model that is chosen for (2.1), the probability density function for the particle position solely depends on the distribution of the random variable Λ , as shown in (2.2). It was proven by the author and collaborators in [43] that an appropriate general choice for $P_{\Lambda}(\lambda)$ in order to obtain exponential and stretched Gaussian shaped position PDFs is a generalised gamma distribution

$$P_{\Lambda}(\lambda) = \frac{\eta}{\Gamma(\nu/\eta)} \lambda^{\nu-1} \exp(-\lambda^{\eta}), \quad (2.13)$$

where ν and η are positive dimensionless parameter. When $\eta = 1$, the gamma distribution emerges as a special case

$$P_\Lambda(\lambda) = \frac{\lambda^{\nu-1}}{\Gamma(\nu)} \exp(-\lambda). \quad (2.14)$$

In order to get a physical understanding and interpretation of the random variable Λ in this model, one can think of it as related to the particle diffusivity. For instance, one can choose $\Lambda = \mathcal{D}/D_0$, where \mathcal{D} stands for a random diffusion coefficient and where D_0 is a dimensional parameter representing the scale. Then the result in (2.2) reads

$$\begin{aligned} P(x, t) &= \int_0^\infty \frac{P_\Lambda(D/D_0)}{\sqrt{4\pi D_0 \sigma^2(t)}} \exp\left(-\frac{\left(x/\sqrt{D/D_0}\right)^2}{4D_0 \sigma^2(t)}\right) \frac{dD}{D_0 \sqrt{D/D_0}} \\ &= \int_0^\infty \frac{1}{\sqrt{4\pi D \sigma^2(t)}} \exp\left(-\frac{x^2}{4D \sigma^2(t)}\right) P_{\mathcal{D}}(D) dD \\ &= \int_0^\infty G(x, t|D) P_{\mathcal{D}}(D) dD, \end{aligned} \quad (2.15)$$

where $\sigma^2(t)$ is the variance of the Gaussian distribution, whose explicit form will depend on the specific Gaussian process one selects, and with

$$P_{\mathcal{D}}(D) = \frac{1}{D_0} P_\Lambda(D/D_0). \quad (2.16)$$

From the result in (2.15) it is then possible to understand the system described by (2.1) as a population of particles with randomly-distributed diffusion coefficients. If one calculates $P_{\mathcal{D}}(D)$ from (2.16) by making use of (2.13), then the particle position PDF in (2.15) presents the following asymptotic behaviour in the tails [43]

$$P(x, t) \sim \frac{(x^2/(4D_0 t))^{(2\nu-\eta-1)/(2(\eta+1))}}{\Gamma(\nu/\eta) \sqrt{4\pi D_0 \sigma^2(t)}} \exp\left(-\frac{\eta+1}{\eta} \eta^{\frac{1}{\eta+1}} \left(\frac{x^2}{4D_0 \sigma^2(t)}\right)^{\frac{\eta}{\eta+1}}\right), \quad (2.17)$$

which, in the special case of gamma distributed Λ given in (2.14), simplifies as

$$P(x, t) \sim \frac{|x|^{\nu-1}}{\sqrt{\pi} (4D_0 \sigma^2(t))^\nu} \exp\left(-\frac{|x|}{\sqrt{D_0 \sigma^2(t)}}\right). \quad (2.18)$$

This result confirms the initial assumption that a RSG model defined as in (2.1) with $P_\Lambda(\lambda)$ given by (2.13), which can be seen as a diffusive model with random diffusion coefficient distributed according to (2.16), allows for a description of BNG

and ANG diffusion. Note that from the results in (2.17) and (2.18) it is possible to observe explicitly that within the framework of RSG models, the features of the selected Gaussian model are the only ones responsible for the temporal spreading of the position PDF, and thus of the MSD scaling. Indeed, the random parameter Λ rescales the amplitude of each realisation, hence the reshaping of the ensemble PDF, but does not affect at all the temporal trend.

Heterogeneous ensemble of Brownian particles

The most general stochastic model to define a Gaussian process is provided by the LE reported in (1.1), where the particle position and velocity are here renamed as $x_g(t)$ and $v_g(t)$, respectively, to make clear that they identify the Gaussian model in (2.1). As already discussed in the introduction, it is well known that, with this description, one observes an initial ballistic behaviour of the MSD for $t \ll \gamma^{-1}$, during which the system is equilibrating, followed by a linear trend when $t \gg \gamma^{-1}$. By making use of this Gaussian model, the RSG process in (2.1) can be written as

$$X = \sqrt{\Lambda} X_g, \quad (2.19)$$

$$V = \sqrt{\Lambda} V_g, \quad (2.20)$$

where it is clear that the velocity gets rescaled as well, with same coefficient as the position. Then, by recalling that the random variable Λ is time independent, the RSG model will fulfil the following stochastic differential equations

$$\frac{dx(t)}{dt} = \sqrt{\lambda} \frac{dx_g(t)}{dt} = \sqrt{\lambda} v_g(t), \quad (2.21)$$

$$\frac{dv(t)}{dt} = \sqrt{\lambda} \frac{dv_g(t)}{dt} = \frac{\sqrt{\lambda}}{m} \left(-\gamma v_g(t) + \sqrt{2\sigma} \xi(t) \right), \quad (2.22)$$

which finally lead to the following LE for the RSG process

$$\frac{dx(t)}{dt} = v(t), \quad (2.23)$$

$$m \frac{dv(t)}{dt} = -\gamma v(t) + \sqrt{2\sigma\lambda} \xi(t). \quad (2.24)$$

This model was first introduced within a more general framework to study fractional dynamics (see [44–46]) and it is referred to as heterogeneous ensemble of Brownian particles (HEBP). For the purposes of this dissertation only a simple version of it is needed, where (2.23)-(2.24) are combined with the distribution of Λ provided in (2.13).

Once the stationary equilibrium is reached, represented by the linear trend of the MSD, it is possible to define the diffusivity coefficient given by $\mathcal{D} = (\sigma/\gamma^2) \Lambda = D_0 \Lambda$,

with $D_0 = \sigma/\gamma^2$. This confirms the physical interpretation of the model explained above: the introduction of a random scaling in a Gaussian model represents a way to deal with systems where a population of diffusivities is observed.

For some systems, under the assumption that the equilibration process is so fast that one is not able to observe it, i.e., $\gamma^{-1} \ll \Delta t$, where Δt represents the experimental time resolution, it is possible to consider the overdamped limit of the LE. This means that the Gaussian process can be described by the differential equation

$$\frac{dx_g(t)}{dt} = \sqrt{2D_0} \xi(t), \quad (2.25)$$

which represents the Wiener process. In this model the MSD presents a linear trend only. The RSG process associated to this Gaussian model becomes simply

$$\frac{dx(t)}{dt} = \sqrt{2D_0 \lambda} \xi(t) = \sqrt{2\mathcal{D}} \xi(t), \quad (2.26)$$

where the relation $\mathcal{D} = D_0 \Lambda$ was introduced again. This description in the overdamped limit, always combined with the distribution of Λ provided in (2.13), has been largely employed for the study of BNG diffusion [43].

RSG models for ANG diffusion

By following the procedure described above for the HEBP, it is possible to define a RSG model for ANG diffusion starting from FBM as Gaussian process. In particular, one can start from the stochastic differential equation

$$\frac{dx_g(t)}{dt} = \sqrt{2\sigma_H} \xi_H(t), \quad (2.27)$$

where $0 < H < 1$ is the Hurst exponent and $\xi_H(t)$ is fractional Gaussian noise. Then, with the introduction of a random scaling $\sqrt{\Lambda}$ as defined in (2.1), it is possible to obtain

$$\frac{dx(t)}{dt} = \sqrt{2\sigma_H \lambda} \xi(t) = \sqrt{2\mathcal{D}_H} \xi(t), \quad (2.28)$$

where $\mathcal{D}_H = \sigma_H \Lambda$. This model can indeed be used to model ANG diffusion. In particular, by choosing Λ to be distributed according to the Weibull distribution, which is a special case of the one in (2.13) with $\nu = \eta$, it was shown [47] that it is possible to properly reproduce the Golding-Cox data [48], a paradigmatic dataset in the field of anomalous diffusion describing the random motion of individual molecules inside bacteria cells.

Finally, it is worth mentioning that an interesting study was performed in [49] following a similar approach but starting from a different dynamical equation, namely

the generalised Langevin equation (GLE)

$$\frac{dx(t)}{dt} = v(t), \quad (2.29)$$

$$\frac{dv(t)}{dt} = - \int_{-\infty}^t \gamma(t - \tau)v(\tau)d\tau + \sqrt{2\sigma}\xi(t), \quad (2.30)$$

where a memory kernel $\gamma(t)$ is introduced. In this description, the assumption of equilibrium leads to a relation between the memory kernel and the stochastic forcing $\xi(t)$ given by the Kubo fluctuation-dissipation relation, that is $\langle \xi(t')\xi(t+t') \rangle = \sqrt{k_B T} \gamma(t)$. The standard LE can be obtained from the GLE considering an exponential memory kernel, while the GLE with power-law kernel identifies the FLE that is usually related to the study of viscoelastic systems, as an alternative description to the one provided by FBM, as discussed in the introduction.

2.2 Superstatistics

The term superstatistics stands for "superposition of statistics" and it was coined by Beck and Cohen in the early 2000s [50–52]. In fact, as already mentioned in the introduction, pioneering discussions of this theory can be found in the book by Van Kampen [10] and in the paper by Kärger [11].

The theory of superstatistics introduced by Beck and Cohen aims at describing the dynamics of complex systems in a non-equilibrium state, hence displaying fluctuations in space and/or time. If one assumes that the spatio-temporal inhomogeneities of the systems happen on a large scale, effectively they can be represented via many spatial cells or time slices, each presenting a different value of some relevant system parameter β . Additionally, the theory of superstatistics is based on the assumption that the relaxation time of the system is small compared to the typical time scale of changes of β . Then, each cell, whose size can be associated with the correlation length/time of the varying quantity β , can be approximately considered to be at a local equilibrium. In this way, a stationary non-equilibrium complex system is mapped into a superposition of inhomogeneous smaller systems at equilibrium.

If E represents an effective energy for each cell, the stationary distribution of a superstatistical system can be written as a superposition of a local Boltzmann factor $e^{-\beta E}$ weighted over the global probability $P_\beta(\beta)$ to observe some value β ,

$$P(E) = \int_0^\infty P_\beta(\beta) \frac{1}{Z(\beta)} \rho(E) e^{-\beta E} d\beta, \quad (2.31)$$

where $\rho(E)$ is the density of states and $Z(\beta)$ is the normalisation constant of $\rho(E)e^{-\beta E}$ for a given β . It is important to stress that the meaning of the variables at hand

depend on the specific complex system under consideration. Thus, local equilibrium is meant in a generalised sense and the result in (2.31) is valid for any corresponding counterpart of the Boltzmann factor of the specific system dynamics.

In general, the distribution $P_\beta(\beta)$ is determined by the spatio-temporal dynamics of the non-equilibrium system. Important examples usually considered in the superstatistical framework are:

- i) the χ^2 -distribution with integer degree k

$$P_\beta(\beta) = \frac{1}{\Gamma(k/2)} \left(\frac{k}{2\beta_0} \right)^{k/2} \beta^{k/2-1} \exp\left(-\frac{k\beta}{2\beta_0}\right), \quad (2.32)$$

when one considers many independent microscopic random variables contributing to β in an additive way;

- ii) the inverse χ^2 -distribution with integer degree k

$$P_\beta(\beta) = \frac{\beta_0}{\Gamma(k/2)} \left(\frac{k\beta_0}{2} \right)^{k/2} \beta^{-k/2-2} \exp\left(-\frac{k\beta_0}{2\beta}\right), \quad (2.33)$$

when the same observation holds for random variables that contribute in an additive way to β^{-1} ;

- iii) a lognormal distribution

$$P_\beta(\beta) = \frac{a}{\beta} \left(-c(\ln \beta - b)^2 \right), \quad (2.34)$$

when the random variable β may be generated by multiplicative random processes.

2.2.1 Superstatistical Brownian motion

Coming back to the main topic of this dissertation, one can apply the theory of superstatistics to model the motion of a Brownian particle of mass m moving through a changing environment, hence introducing the superstatistical Brownian motion (SupBM). The dynamics of the system can be described starting from the LE in (1.1) that, for the sake of clarity, is recalled here

$$m \frac{dv(t)}{dt} = -\gamma v(t) + \sqrt{2\sigma} \xi(t). \quad (2.35)$$

Then, in order to account for the environment fluctuations, one can follow the superstatistics theory discussed above and define the parameter

$$\beta = \frac{\gamma}{m\sigma}, \quad (2.36)$$

which will be fluctuating according to a certain probability $P_\beta(\beta)$. The superstatistical description of the system is completely provided by (2.35), (2.36) and $P_\beta(\beta)$.

The effective energy of the system can be identified with $E = \frac{1}{2}mv^2$ and the local equilibrium assumption for each cell allows us to write the local stationary distribution as a Gaussian

$$P(v|\beta) = \sqrt{\frac{m\beta}{2\pi}} \exp\left(-\frac{1}{2}\beta mv^2\right), \quad (2.37)$$

where the local equilibrium correlation is given by

$$C(t-t'|\beta) = \langle v(t)v(t') \rangle = \frac{1}{m\beta} \exp(-\gamma|t-t'|). \quad (2.38)$$

Finally, according to (2.31), the marginal distribution describing the superstatistical system can be written as

$$P(v, t) = \int_0^\infty P_\beta(\beta) P(v, t|\beta) d\beta, \quad (2.39)$$

which will lead to an analogous result for $P(x, t)$, while, the superstatistical correlation function is given by

$$C(t-t') = \int_0^\infty P_\beta(\beta) C(t-t'|\beta) d\beta = \frac{1}{m} \int_0^\infty \frac{P_\beta(\beta)}{\beta} \exp(-\gamma|t-t'|) d\beta. \quad (2.40)$$

Note that in (2.39) no distinction between which of the parameters is fluctuating, if γ , σ , and/or m , can be made, as there is no explicit dependence on the single parameters. Conversely, the correlation function in (2.40) bares a clear and distinct dependence on both β and γ , such that a larger amount of information can be extrapolated from it. Note that, as the velocity correlation function provides the MSD trend by

$$\langle (x(t) - x(0))^2 \rangle = \int_0^t \int_0^t \langle [v(t') - v(0)][v(t'') - v(0)] \rangle dt' dt'', \quad (2.41)$$

insightful information can be extracted from the MSD behaviour as well. Here, an observation is due concerning the local equilibrium of each cell in connection to the fluctuations of the parameter β . First of all, as already mentioned in the introduction, at equilibrium the fluctuation-dissipation relation, i.e., $\sigma = k_B T \gamma$, must be valid, hence there is no variability of γ without variability of σ , and vice versa. By employing this relation in (2.36) one obtains that $\beta = (mk_B T)^{-1}$. Two important conclusions can be drawn from this observation with respect to the superstatistical Brownian motion formalism discussed in this section:

- i) fluctuations of β are related to fluctuations in the temperature of the system and/or to fluctuations in the mass of the particle;
- ii) if one wants to relate the fluctuations of β to a random diffusion coefficient $D = \sigma/\gamma^2$, such that $\beta = (m\gamma D)^{-1}$, one must not forget to include in the description the corresponding fluctuations of γ due to the fluctuation-dissipation relation, i.e., $\gamma D = k_B T$, leading to possible variability in the MSD trend, according to (2.41).

From the results reported in (2.39), (2.40) and (2.41) it is straightforward to notice, after the discussion in section 2.1.2 for RSG models, that the superstatistical Brownian motion can be used, under certain prescriptions for $P_\beta(\beta)$, to describe BNG diffusion and that it can be interpreted, under the constraints described in point ii), as a random diffusivity model.

2.3 Discussion

In this Chapter two models were introduced, namely RSG and SupBM models, with the main goal of showing that the description that they provide for BNG and ANG diffusion is based on common results with many similarities. This is why in the recent literature on random diffusivity models, one often sees that the two approaches are used interchangeably. In fact, even if they mathematically present some formulae in common, the physical description provided by the two models is very different. On the one hand, the theory of superstatistics represents an effective description of diffusion in a non-equilibrium system and it is based on the strong assumption that there is a clear time scale separation between the characteristic time of the medium fluctuations and the relaxation time of the system. On the other hand, the RSG models describe systems at equilibrium where a population of parameters can be introduced, due to inherent variabilities of the system, for instance in the size of the diffusive tracers (for more details see also the discussion in [46] on HEPB and SupBM). Nevertheless, one could imagine taking a snap-shot of a system described by the SupBM and compare it with one taken from a second system defined by a RSG model: they would be indistinguishable. If one is interested in understanding in more detail the physical properties of the system under consideration, and thus in differentiating between the two models, one must consider the time evolution of single realisations and extract, for instance, the single trajectory velocity autocorrelation function and the single trajectory time-averaged mean squared displacement. This observation opens the door to a standard discussion in statistical physics, concerning ensemble average analysis *versus* time average analysis, leading to the concept of ergodicity, which will be briefly addressed in Chapter 4. To conclude this discussion, it is worth mentioning that, if one considers the system described in the SupBM,

when the realisations are long enough, the allegedly large separation between the relaxation time of the system and the characteristic time of the environment fluctuations actually becomes small, if compared to the timescale at which the system is observed, and then the superstatistical description may not be valid any longer. If this is the case, the models discussed in the next Chapter could be of help in the description of such systems.

Finally, before moving to the next Chapter, note that, in order to avoid misunderstandings, throughout this dissertation the term superstatistics (or superstatistical) refers to the theory introduced by Beck and Cohen and discussed above in section 2.2. Any other description with time-independent random parameters comes under the framework defined as randomly-scaled Gaussian processes, introduced in section 2.1.

Chapter 3

The diffusing diffusivity approach

In this Chapter, a short review on the diffusing diffusivity (DD) approach is reported. The discussion evolves chronologically; starting from the model in which the term *diffusing diffusivity* was coined, it then moves to different developments and expansions, showing how the DD approach was able to drive the focus of the anomalous diffusion community towards the study of random diffusivity processes.

3.1 In response to the experimentalists' call: the first DD model

The work from Granick's group [18,19] brought to light the fact that in experiments often no check is performed on the displacement distribution, given for granted that whenever a linear trend of the MSD is observed, one is dealing with BM. In fact, the authors showed that this is not always the case. Two independent systems were reported to display a linear trend of the MSD combined with exponential tailed distributions. As discussed already in the introduction, the same behaviour was later on observed by many other experimentalists in different systems, confirming the universality of BNG diffusion. Moreover, in the discussions reported in [18,19], the idea of SupBM, described in Chapter 2, was invoked as a possible basis for the understanding of this class of processes. The authors immediately came to the conclusion that, while this model could be used for certain systems, it does not provide a complete answer to the scenario at hand. Indeed, the invariance of the displacement PDF at any time, typical of superstatistical models, is not able to reproduce the final crossover to Gaussian diffusion and the recovered ergodicity observed in many systems displaying BNG diffusion. Following these observations, a call for new diffusive models able to describe BNG diffusion features was explicitly placed.

In response to the experimentalists' call, Chubinsky and Slater introduced the

first DD model in 2014 [53]. The main idea behind their work is based on the assumption that, when deviations from BM are observed, a clear discrimination between the origin of non-linearity in time of the MSD and the non-Gaussianity can be made. Starting from a simple one-dimensional unbiased random walk,

$$x_N = \sum_{i=1}^N \Delta x_i, \quad (3.1)$$

Chubinsky and Slater proved that, in order to obtain a linear trend of the MSD, what is needed are uncorrelated step directions only. Thus, the step lengths may display correlations and still the MSD would be linear. Actually, correlations of such kind are to be expected in heterogeneous environment and they can give rise to non-Gaussian displacement distribution. Then, one can imagine to have a random walk as in (3.1), where the steps Δx_i are distributed according to

$$P(\Delta x_i) = \frac{1}{\sqrt{4\pi D_i \Delta t}} \exp\left(-\frac{\Delta x_i^2}{4D_i \Delta t}\right), \quad (3.2)$$

and where it is assumed that the diffusivity D_i varies slowly in time, such that the correlation time $\tau_D \gg \Delta t$. Considering that small changes in D allow for a continuous-time description, one can additionally consider the diffusivity to fulfil the advection-diffusion equation (from here the name *diffusing diffusivity*) which, at stationarity, reads

$$\frac{\partial p_D(D)}{\partial D} = \frac{1}{D_0} p_D(D), \quad (3.3)$$

also known as the barometric formula. Reflecting boundary conditions in $D = 0$ and $D = D_{max}$ are needed to avoid the negativity of D . The solution of (3.3) for $D_{max} \rightarrow \infty$ is given by the exponential distribution

$$p_D(D) = \frac{1}{D_0} \exp\left(-\frac{D}{D_0}\right). \quad (3.4)$$

At short times ($t \ll \tau_D$) the diffusivity of a particle can be assumed constant and the displacement distribution can be obtained, as in the SupBM and RSG models, by

$$P(x, t) = \int_0^{D_{max}} p_D(D) G(x, t|D) dD \sim \frac{1}{2\sqrt{D_0 t}} \exp\left(-\frac{|x|}{\sqrt{D_0 t}}\right). \quad (3.5)$$

At times large enough ($t \gg \tau_D$) the particles have explored the whole diffusivity space and the central limit theorem guarantees the convergence to a Gaussian distribution

$$P(x, t) = \frac{1}{\sqrt{4\langle D \rangle t}} \exp\left(-\frac{x^2}{4\langle D \rangle t}\right). \quad (3.6)$$

The numerical results reported in [53] established the first model able to fully reproduce the BNG behaviour observed in many systems.

To summarise, the key physical interpretation of any DD model reads:

When observing an ensemble of particles performing diffusion in a fluctuating, heterogeneous environment, at short times, each of them will present a different diffusivity, depending on their local environment. Going on in time, the diffusivity will change, either because the environment itself is changing or because the particle is moving. When (and if) the particles will have experienced the whole diffusivity space, the displacement distribution will eventually turn into a Gaussian.

3.2 Second generation models

Starting from the results obtained by Chubinsky and Slater [53], a wide interest in the topic emerged. In particular, one can identify as second generation models the work from two groups reported in [54] and [55, 56]. Published just a couple of years after the paper by Chubinsky and Slater, the main idea behind these two novel works was to provide a DD model which would be analytically treatable. Both started from a common approach based on the idea of having two coupled stochastic equations, one for the evolution of the particle position and one for the evolution of the diffusivity. Eventually, the two works followed different mathematical methods to solve the model, succeeding in reporting an explicit analytical derivation and solution for the DD models considered. In what follows, a short description of the two formalisms is reported.

Subordination approach

Checkkin and coauthors introduced [54] a model that they called *minimal diffusing diffusivity model* (mDD), which can be solved analytically through the Feller subordination approach [58]. The system dynamics is defined starting from the coupled Langevin equations

$$\frac{d}{dt}x(t) = \sqrt{2D(t)} \xi_1(t), \quad (3.7)$$

$$D(t) = y^2(t), \quad (3.8)$$

$$\frac{d}{dt}y(t) = -\frac{1}{\tau}y(t) + \sigma\xi_2(t), \quad (3.9)$$

where $\xi_1(t)$ and $\xi_2(t)$ are independent, white Gaussian noises with δ -correlation. The auxiliary variable $y(t)$ undergoes an Ornstein-Uhlenbeck process (OU) and the time-dependent random diffusion coefficient $D(t)$ is given by the squared of this auxiliary variable. In this way, one avoids the need to introduce boundary conditions

for the dynamic equation of $D(t)$, hence simplifying the resolution of the set of equations in (3.7)-(3.9). Note that in the original work in [54] an n -dimensional overdamped LE in (3.7) and a d -dimensional OU in (3.9) were considered, with independent dimensionalities n and d . Here only the 1-dimensional case for both cases is discussed. A generalisation to the multi-dimensional description can readily be obtained component-wise. For simplicity, dimensionless variables $t \rightarrow t/\tau$ and $x \rightarrow x/(\sigma\tau)$ are considered, such that $y(t)$ is also renormalized according to $y(t) \rightarrow y(t)/(\sigma\tau^{1/2})$. Then, following the subordination approach, one can introduce a path variable (subordinator), which in this case can be defined as the integrated diffusivity

$$\tau(t) = \int_0^t D(s)ds = \int_0^t y^2(s)ds. \quad (3.10)$$

Thanks to this new variable, it is possible to redefine the set of equations in (3.7)-(3.9), in dimensionless units, as

$$\frac{d}{d\tau}x(\tau) = \sqrt{2}\xi_1(\tau), \quad (3.11)$$

$$\frac{d}{dt}\tau(t) = D(t). \quad (3.12)$$

One can immediately observe that equation (3.11) represents the equation for standard BM with $D = 1$, such that the Green's function in the path variable $\tau(t)$ can be written as a Gaussian, namely $G(x, \tau|D = 1)$. Then, in order to calculate the probability density in the real time, one has to integrate over all possible path lengths

$$P(x, t) = \int_0^\infty G(x, \tau|D = 1)T(\tau, t)d\tau, \quad (3.13)$$

where $T(\tau, t)$ is the PDF of the process $\tau(t)$, defined via its Laplace transform

$$\tilde{T}(s, t) = \frac{\exp(t/2)}{\left[\frac{1}{2}(\sqrt{1+2s^2} + \frac{1}{\sqrt{1+2s^2}})\sinh(t\sqrt{1+2s^2}) + \cosh(t\sqrt{1+2s^2})\right]^{1/2}}. \quad (3.14)$$

Starting from the subordination formula in (3.13), the probability density function of the mDD is finally given, in the Fourier space, by

$$\begin{aligned} \hat{P}(k, t) &= \int_{-\infty}^{+\infty} e^{ikx}P(x, t)dx = \int_{-\infty}^{+\infty} e^{ikx} \left[\int_0^\infty G(x, \tau|D = 1)T(\tau, t)d\tau \right] dx \\ &= \int_0^\infty T(\tau, t)\hat{G}(x, \tau|D = 1)d\tau = \int_0^\infty T(\tau, t)e^{-k^2\tau}d\tau \\ &= \tilde{T}(k^2, t). \end{aligned} \quad (3.15)$$

This result can be explicitly evaluated in the limit of short and long times starting from (3.14). By recalling that the description is reported in dimensionless variables, the short and long time limits can be expressed as $t \ll 1$ and $t \gg 1$, respectively. In the former case one has

$$\hat{P}(k, t) \sim t^{-1/2} \left(k^2 + \frac{1}{t} \right)^{-1/2} \rightarrow P(x, t) \sim \frac{1}{\pi t} K_0 \left(\frac{x}{t^{1/2}} \right), \quad (3.16)$$

where $K_0(z)$ is the modified Bessel function of second kind that for small arguments presents an asymptotic behaviour $K_0(z) \sim \sqrt{\pi/2z} e^{-z}$. In the long time regime instead one finds, considering the tails of the distribution, namely for $k \ll 1$, that the PDF displays a Gaussian behaviour

$$\hat{P}(k, t) \sim \exp \left(-\frac{k^2 t}{2} \right) = \exp \left(-\langle D \rangle_{\text{st}} k^2 t \right) \rightarrow P(x, t) \sim G(x, t | D = \langle D \rangle_{\text{st}}). \quad (3.17)$$

Phase space path integral approach

Jain and Sebastian [55,56] introduced a model that can be solved analytically through the phase space path integral approach. Considering the description of simple BM

$$\frac{d}{dt} x(t) = \eta(t), \quad (3.18)$$

where $\langle \eta(t_1) \eta(t_2) \rangle = 2D \delta(t_1 - t_2)$, they showed that the introduction of a stochastic diffusivity in this framework is quite straightforward. Starting from the idea that it is possible to characterise the noise through its characteristic functional defined as [55]

$$\left\langle \exp \left(i \int_0^t \eta(t') p(t') dt' \right) \right\rangle = \exp \left(-D \int_0^t p^2(t') dt' \right), \quad (3.19)$$

it is possible to obtain the probability distribution functional for the noise as the Fourier transform

$$\hat{\mathcal{P}}[\eta(t)] = \int \exp \left(-i \int_0^t \eta(t') p(t') dt' - D \int_0^t p^2(t') dt' \right) dp(t). \quad (3.20)$$

Using equation (3.18), it is then possible to write the probability distribution functional for the Brownian path $x(t)$ as

$$\mathcal{P}[x(t)] = \int \exp \left(-i \int_0^t \dot{x}(t') p(t') dt' - D \int_0^t p^2(t') dt' \right) dp(t). \quad (3.21)$$

Finally, the probability of finding a particle at x at time t , given that it started at $x_0 = 0$ at time $t = 0$, is given by

$$P(x, t) = \int \int \exp \left(-i \int_0^t \dot{x}(t') p(t') dt' - D \int_0^t p^2(t') dt' \right) dp(t) dx(t). \quad (3.22)$$

If one wants to consider a diffusing diffusivity picture describing an environment that fluctuates in time, an effective time dependent and random diffusion coefficient $D(t)$, constrained to be positive, needs to be introduced in the formalism. For this case, it is possible to generalise expression (3.22) as follows

$$P(x, t) = \int \int \left\langle \exp \left(- \int_0^t D(t') p^2(t') dt' + i \int_0^t \dot{x}(t') p(t') dt' \right) \right\rangle_D dp(t) dx(t), \quad (3.23)$$

where the angular brackets indicate the average over all realisations of $D(t)$. The easier way to introduce a random fluctuating, positive diffusion coefficient is to consider the following assumption

$$D(t) = y^2(t), \quad (3.24)$$

where $y(t)$ is a random vector (note that one can select a d -dimensional random vector as well). In particular, Jain and Sebastian selected for $y(t)$ the position vector of a harmonic oscillator that undergoes overdamped Brownian motion. This choice represents exactly the same set of equations described by the mDD above and, as a consequence, by working out equation (3.23) with these assumptions for $D(t)$ and $y(t)$, the authors found the exact same result reported in (3.15).

3.3 Third generation models

After having defined the building blocks of the DD approach, its physical interpretation and how to analytically treat it, the evolution of the DD models moves to the introduction and study of alternative descriptions. These further generalisations are summarised in the class of third generation models that, based on similar methodologies to the ones already discussed, provide new insights on random diffusivity processes.

Lanoiselée and Grebenkov [59] proposed to model the time-dependent diffusivity $D(t)$ as a Cox-Ingersoll-Ross process (CIR) [34], also known as Feller's process or square root process. This model is equivalent to the mDD, as shown by Checkin *et al.* in [54], but presents a description where the introduction of the auxiliary variable is avoided. In particular, the dynamics is defined by the coupled stochastic equations

$$\frac{d}{dt} x(t) = \sqrt{2D(t)} \xi_1(t) \quad (3.25)$$

$$\frac{d}{dt} D(t) = \frac{1}{\tau} (D - \bar{D}) + \sigma \sqrt{2D(t)} \xi_2(t), \quad (3.26)$$

where $\xi_1(t)$ and $\xi_2(t)$ are independent, white Gaussian noises with zero average and δ -correlation. Thanks to this formalism, the connection with the stochastic volatility models mentioned in the introduction and used in financial mathematics for the modelling of stock price emerges naturally.

Tyagi and Cherayil introduced [60] a simple alternative approach that not only verifies the earlier findings on DD models, but also identifies another process for the random diffusivity, i.e., the two-state white noise, that exhibits the same BNG behaviour. The mathematical methodology used in their work is a hybrid between the subordination approach and the phase space path integral approach, both explained in section 3.2. The set of coupled LEs is first expressed in its equivalent Fokker–Planck form. Then, the solution of this FPE, which contains the time dependent diffusion coefficient $D(t)$, is represented as a Fourier integral. This expression is finally averaged over the stochastic trajectories of $D(t)$, using path integration methods. The results reported by Tyagi and Cherayil allow for a broader understanding of DD models. Indeed, they proved that the modulation of white noise by any stochastic process whose time correlation function decays exponentially presents similar features, thus providing a motivation of why BNG behaviour appears to be so widespread. In particular, they argued that the MSD of any particle whose dynamics is driven by randomly modulated white noise will vary linearly with time (in some interval) if the time-correlation function of the modulating variable decays exponentially. In order to see that explicitly, it is useful to recall some of their results. Consider the set of equations defined by the mDD, that is (3.7)-(3.9). It is straightforward to check that the correlation function of $y(t)$ is given by

$$\langle y(t_1)y(t_2) \rangle = y^2(0)e^{-(t_1+t_2)/\tau} + \frac{\sigma\tau}{2} [e^{-|t_1-t_2|/\tau} - e^{-(t_1+t_2)/\tau}], \quad (3.27)$$

where $y(0)$ represents the initial condition. Then, the MSD of the particle position will be given by

$$\begin{aligned} \langle x^2(t) \rangle &= 2 \int_0^t \int_0^t \langle y(t_1)y(t_2) \rangle \langle \xi(t_1)\xi(t_2) \rangle dt_1 dt_2 \\ &= (\sigma\tau)t + \tau \left(y^2(0) - \frac{\sigma\tau}{2} \right) (1 - e^{-2t/\tau}) \\ &\sim \begin{cases} 2y^2(0)t, & t \ll \tau, \\ (\sigma\tau)t, & t \gg \tau. \end{cases} \end{aligned} \quad (3.28)$$

From this result one observes that the position MSD always shows a linear trend, but with a slope that can vary, depending on the initial condition for $y(t)$. It is worth noticing that by selecting an equilibrium initial condition for $y(t)$ one has that $y^2(0) = \sigma\tau/2$, such that the two limits in (3.28) coincide and a single overall behaviour is observed for the particle MSD. Conversely, if one selects a non-equilibrium initial condition for $y(t)$ the two different trends become visible. See for instance the discussion by the author and collaborators in [43] where a study on non-equilibrium initial conditions for the diffusivity in the mDD model was explicitly addressed.

The result in (3.28) holds in general whenever $y(t)$ presents a correlation with an exponential decay, similar to the one in (3.27). Following this idea, Tyagi and

Cherayil showed that there is at least one other stochastic process that could replace $D(t)$ in (3.8)-(3.9) and still produce BNG diffusion: the dichotomic or two-state noise. Quite some literature is present on this kind of processes, which are often referred to as switching models [10, 61–63]. Indeed, a two-state noise $\zeta(t)$ can be defined as a process that fluctuates between two values c_1 and c_2 and is characterised by:

1. $\langle \zeta(t) \rangle = \bar{\zeta} = (\nu_{12}c_2 + \nu_{21}c_1)/(2\bar{\nu})$, where $\bar{\nu} = (\nu_{12} + \nu_{21})/2$ and ν_{ij} is the transition rate from i to j ;
2. $\langle \zeta(t_1)\zeta(t_2) \rangle = \bar{\zeta}^2 + (\nu_{21}\nu_{12}/(4\bar{\nu}^2))(c_1 - c_2)^2 \exp(-2\bar{\nu}|t_1 - t_2|)$;
3. $\zeta^2(t) = (c_1 + c_2)\zeta(t) - c_1c_2$.

Then, by taking $D(t) = \zeta^2(t)$ and by following the mathematical procedure described above, Tyagi and Cherayil proved that BNG diffusion with features very similar to the one of the mDD is obtained. A similar two-state model was also analysed in the paper by Miyaguchi and coauthors in [64].

Finally, expanding the idea that any stochastic modulation of Brownian motion with exponential relaxation can lead to BNG, in the work by the author and collaborators [43], a generalisation of the mDD was defined, where instead of a OU process for the auxiliary variable, a more general non-linear stochastic equation was selected

$$\frac{d}{dt}x(t) = \sqrt{2D(t)}\xi_1(t), \quad (3.29)$$

$$D(t) = y^2(t), \quad (3.30)$$

$$\frac{d}{dt}y(t) = \frac{\sigma^2}{2y} \left[2\nu - 1 - 2\eta \left(\frac{y}{y_0} \right)^{2\eta} \right] + \sigma \xi_2(t), \quad (3.31)$$

where ν and η are positive constants and y_0 is a dimensional constant defined by $D_0 = y_0^2$. The correlation function of $y(t)$ in (3.31) still behaves exponentially, hence the linear trend of MSD is observed, yet this model is able to extend the formalism of the DD approach to a more general class of distributions. In particular, all the models discussed up until now provide a distribution of the diffusion coefficient which is well described by a Gamma distribution. The latter leads to the characteristic exponential tails for the particle displacement distribution in the non-Gaussian regime. In the description reported in the set of equations (3.29)-(3.31), a broader class of distributions for the diffusion coefficient is introduced, namely the generalised Gamma distribution

$$p_{\mathcal{D}}(D) = \frac{\eta}{D_0^\nu \Gamma(\nu/\eta)} D^{\nu-1} e^{-(D/D_0)^\eta}, \quad (3.32)$$

whose moments are given by $\langle D^n \rangle = D_0^n \Gamma(\frac{\nu+n}{\eta})/\Gamma(\frac{\nu}{\eta})$ and which was already mentioned in Chapter 2. Within this model, stretched Gaussian tails for the particle

displacement distribution can be recovered, in addition to the more common Laplacian shape obtained by setting $\nu = 0.5$ and $\eta = 1$. Note that distributions of this kind are indeed observed in experiments, see for instance the results for lateral diffusion in lipid membranes reported in [33].

3.4 Most recent developments

In this section some insights on the most recent developments in the field of the DD approach are reported. First of all, it is worth mentioning that, thanks to the study reported in very recent works [69–71], a clear connection can be drawn between DD models and the continuous time random walk approach (CTRW). This interpretation can be seen as a more direct generalisation of the first DD model, where a random walk approach was discussed. Indeed, while most of the studies preferred to move towards a continuum description, as widely discussed above, in [69–71] a different path was undertaken. In particular, the concept of fluctuating diffusivity is replaced by fluctuations in the number of steps of the random walker and jump length distributions. A large deviation description is employed to show that, under the condition that the jump length distribution decays exponentially or faster (power-law distributed jump lengths are excluded), and that the distribution of the waiting times is analytic for short waiting times, the particle displacement distribution presents exponential tails, with a logarithmic correction.

Before moving to the final discussion, it is worth reporting some details concerning developments of the DD approach where the focus is shifted towards different types of systems and/or diffusion behaviours. In particular two different but equally interesting directions are chosen, i) models for ANG diffusion and ii) many-body system descriptions.

3.4.1 Viscoelastic-type motion

As discussed in the introduction, a behaviour similar to BNG diffusion has been observed for viscoelastic-type motion as well, where an anomalous scaling of the MSD is combined with an unexpected non-Gaussian displacement distribution [65].

Very recently, a work was published by Sabri and coauthors [66] in which a model was developed for describing the heterogeneous anomalous diffusion in the cytoplasm of mammalian cells. Through a comparison with simulations they showed that the motion can be fully reproduced as an intermittent FBM, alternating between two states of different motility K_α^{on} and K_α^{off} . The dichotomous switching between these states was modeled as a Markov process with transition rates k_{on} and k_{off} . This resembles the two-state noise model described above in section 3.3, combined with FBM-like motion instead of standard BM. Sabri and coauthors claimed a very good

overlap with experimental data and thus, they showed that the resulting diffusion heterogeneity does not require a full and elaborate model but rather a switching between two modes of motion, which is sufficient to reproduce the experimental results. Conversely, in the paper by Wang and coauthors [67], various possible extensions of the DD approach to viscoelastic-type motion and ANG diffusion were reported. All these models show a crossover from non-Gaussian to Gaussian distributions, yet their MSDs exhibit very different behaviours. These observations highlight the strong non-universality of random-diffusivity viscoelastic anomalous diffusion and show the need for more studies in this direction, in order to arrive at a full understanding of ANG diffusion.

3.4.2 Many-body systems – Rouse model in crowded environment

A recent development of the DD approach emerged in the direction of modelling many-body systems. Indeed, all the models mentioned above are based on the study of single particle systems. The work by Ahamad and Debnath [68] represents the first attempt in this new direction. The authors studied and derived exact results for the dynamics of Rouse model in crowded environment modeled by the concept of DD. The Rouse model is a standard model describing the random motion of interacting connected beads through a chain of harmonic oscillators and it represents the basis of dynamics of dilute polymer solutions. The novelty of the work comes from the idea that each Rouse mode is allowed to diffuse with stochastically varying time dependent diffusivities. In this way, it is possible to model diffusion in the crowded rearranging environment.

In the Rouse model, each bead follows a Langevin dynamics given by

$$\frac{\partial}{\partial t} r_i(\tau, t) = \frac{g}{\zeta} \frac{\partial^2}{\partial \tau^2} r_i(\tau, t) + \sqrt{2D} \xi_i(\tau, t), \quad (3.33)$$

where $\mathbf{r}(\tau, t)$ is the position vector of the bead at point τ along the chain contour at time t and i represents the index for the Cartesian coordinates. The chain contour length τ varies from 0 to N and free boundary conditions are considered, namely $\left. \frac{\partial}{\partial \tau} r_i(\tau, t) \right|_{\tau=0, N} = 0$. The compression modulus for the spring is identified with g and ζ is the friction coefficient per unit length of the chain. Finally $\xi_i(\tau, t)$ are white Gaussian noises with 0 average and δ -correlation, that is $\langle \xi_i(\tau_1, t_1) \xi_j(\tau_2, t_2) \rangle = \delta_{ij} \delta(\tau_1 - \tau_2) \delta(t_1 - t_2)$. In order to proceed further with the study of the model, a decoupling of the variable τ and t is obtained through the normal mode analysis. In this way, the Rouse modes are defined as

$$\mathbf{X}_p(t) = \frac{1}{N} \int_0^N \cos\left(\frac{p\pi\tau}{N}\right) \mathbf{r}(\tau, t) d\tau, \quad p \leq 0, \quad (3.34)$$

such that $\mathbf{r}(\tau, t) = \mathbf{X}_0(t) + 2 \sum_{p=1}^N \mathbf{X}_p(t) \cos\left(\frac{p\pi\tau}{N}\right)$. Note that the zeroth mode represents the center of mass of the chain $\mathbf{X}_0(t) = \frac{1}{N} \int_0^N \mathbf{r}(\tau, t) d\tau = \mathbf{R}(t)$. Then, equations of motion for normal modes are given by

$$\frac{d}{dt} \mathbf{X}_p(t) = -\frac{g_p}{\zeta_p} \mathbf{X}_p(t) + \sqrt{2D_p} \eta_p(t). \quad (3.35)$$

In the standard Rouse model, all mode diffusion coefficients D_p are equal and related to zeroth mode diffusivity by $D_p = D_0/2$. This relation holds for an isotropic environment, as each bead is experiencing the same field. To account for a crowded environment, following the idea introduced in the DD approach, it is possible to model the square root of the diffusion coefficient D_p for each mode as an independent stochastic process

$$D_0(t) = \mathbf{Y}_0^2(t) = \sum_{i=0}^{n_0} Y_{0i}^2, \quad (3.36)$$

$$2D_p(t) = \mathbf{Y}_p^2(t) = \sum_{i=0}^{n_p} Y_{pi}^2, \quad p \geq 1, \quad (3.37)$$

where each $\mathbf{Y}_p(t)$ is an independent n_p -dimensional OU process. Thus, following the results of the DD approach, a non-Gaussian behavior of derived modes displacement distributions is obtained. Finally, the authors explained how one can compare predictions from this theory with experiments on polymeric liquids. Indeed, even if normal modes are not resolved so readily in experiments, it is possible to relate them to measurable quantities such as relaxation modulus, viscosity and others.

3.5 Discussion

This Chapter, even if far from being a complete review on the DD concept, presents a quite general overview of this modelling approach. In a constructive way, it was shown how, from a general idea and physical understanding of the class of systems initially under study, a structured and detailed theoretical framework has emerged. DD models are based on a very general statistical approach, whose flexibility has been employed for the study of many physical systems.

Focusing on all of those DD models describing BNG diffusion, an interesting observation is due. In the final discussion reported in Chapter 2 it was briefly mentioned that the DD approach would come at hand in the characterisation of those systems where SupBM fails. After the detailed description reported in this Chapter, it is now possible to elaborate on this idea. It was amply discussed that an exponential relaxation of the diffusion dynamics is needed to be able to reproduce the

linear trend of the particle MSD. In the presence of exponential relaxation, it is immediate to identify the characteristic time τ_D of the environment fluctuations. In order to use a superstatistical description, one must be able to identify a clear distinction between τ_D and the relaxation time of the system. If one starts from an overdamped Brownian motion description, the system relaxes instantaneously, such that a realistic choice for its relaxation time can only be given by the experimental (or numerical) time resolution Δt . Moreover, one can imagine that any system will be studied for an observation time $T \gg \Delta t$. Then, it is possible to compare τ_D with the observation time T and come to the conclusion that, whenever $\tau_D \ll T$, a DD approach is needed, as at the timescale T at which the systems is observed one actually has $\tau_D \sim \Delta t$. Conversely, when $\tau_D \gtrsim T$, a SupBM description can be employed. See for instance the analysis reported in [72] where a characterisation of mDD single trajectories is reported for different values of τ_D and fixed T . Following this argument one can better understand why SupBM can be used as a short time approximation of the DD models, as widely discussed in literature. Finally, if one starts from an underdamped Brownian motion description, the argumentation becomes more involved, but one can still arrive at similar conclusions. This, however, is still work in progress.

To conclude, with this Chapter a full understanding of the emergence of BNG diffusion in heterogeneous environments was reached. The discussion will now move to more detailed statistical analyses based on this class of diffusion processes.

Chapter 4

Statistical analyses of random diffusivity models

A general framework to describe random diffusivity models, based on results and discussions reported in the previous Chapters, is defined here. This framework is given by the class of one-dimensional stochastic processes $x(t)$ that obey the Langevin equation

$$\frac{dx(t)}{dt} = \sqrt{2D_0\Psi(t)} \xi(t), \quad (4.1)$$

where D_0 is a constant, dimensional coefficient of units $\text{length}^2/\text{time}$, $\xi(t)$ denotes a standard Gaussian white noise with zero mean and δ -correlation, and $\Psi(t)$ is a positive-definite random function, which multiplies D_0 and thus introduces a (time-dependent) randomness into the effective noise amplitude.

The representation in (4.1) was introduced in the work by the author and collaborators in [74] and is able to reproduce, among others (for instance, models in which $\Psi(t)$ is defined as a functional of BM—see [74] for more details), any of the (overdamped) random diffusivity models that were defined along this dissertation to describe BNG diffusion. On the one hand, the connection with DD models is clear just by noticing that $\Psi(t)$ represents the dimensionless counterpart of the random, time-dependent diffusion coefficient $D(t)$ extensively discussed in Chapter 3. On the other hand, SupBM models can be introduced if one defines $\Psi(t)$ as a jump process, that is a process that attains a new random value after a fixed time interval. Then, RSG models can be obtained as a limiting case in this representation, by considering that the time interval for each draw is always equal to the length of the trajectory. In this way the variability in time of $\Psi(t)$ within each realisation is lost. Generally, the models introduced in Chapter 2 can be described by dividing the interval $(0, T)$ into N equal subintervals of duration $\delta = T/N$ and supposing that $\Psi(t) = \psi_k$, where k represents the different subintervals and where ψ_k are *i.i.d.* and positive-definite random variables distributed according to a distribution $\rho(\psi)$. In the case of RSG

models one has that $\delta = T$.

In addition, the framework defined in (4.1) allows also for the study of those models in which $\Psi(t)$ is a deterministic function of time. For instance, a choice of the form $\Psi(t) = t^{\alpha-1}$ produces the so-called scaled Brownian motion [73, 76, 77]. Finally, by setting $\Psi(t) \equiv 1$, one simply obtains standard BM.

Regardless of the choice of $\Psi(t)$, the Langevin equation in (4.1) can be solved for any fixed realisation of the noise and of $\Psi(t)$, to obtain

$$x(t) = (2D_0)^{1/2} \int_0^t \Psi^{1/2}(t') \xi(t') dt'. \quad (4.2)$$

Then, if one can calculate its characteristic function $\Phi(t, w)$, the PDF $P(x, t)$ of the model can be defined as

$$P(x, t) = \frac{1}{2\pi} \int_{-\infty}^{\infty} e^{-iwx} \Phi(t, w) dw. \quad (4.3)$$

In general, starting from (4.2), the characteristic function of $x(t)$ can be written as

$$\Phi(t, w) = \left\langle \overline{\exp \left(iw(2D_0)^{1/2} \int_0^t \Psi^{1/2}(t') \xi(t') dt' \right)} \right\rangle_{\Psi}, \quad (4.4)$$

where the bar stands for averaging over thermal histories while the angular brackets denote averaging over the realisations of the random function $\Psi(t)$. After performing the thermal average, one readily obtains

$$\Phi(t, w) = \left\langle \exp \left(-D_0 w^2 \int_0^t \Psi(t') dt' \right) \right\rangle_{\Psi}. \quad (4.5)$$

From this result, it is possible to observe that the main character in defining the features of any random diffusivity model is played by the integrated random diffusivity

$$\tau(t) = \int_0^t \Psi(t') dt'. \quad (4.6)$$

Indeed, if one defines the moment generating function of $\tau(t)$ as

$$\Upsilon(t, \lambda) = \langle \exp(-\lambda\tau(t)) \rangle_{\Psi}, \quad \lambda \geq 0, \quad (4.7)$$

it is straightforward to see that $\Phi(t, w) = \Upsilon(t, D_0 w^2)$, such that the PDF in (4.3) is solely defined by the integrated random diffusivity selected for the model. Note that, within the subordination approach (and the phase space path integral approach) for DD models discussed in Chapter 3, the same result was obtained just with a slightly

different notation where $\Upsilon(t, \lambda)$ was identified as the PDF of the subordinator in Laplace space—see equation (3.15).

In the following sections two kinds of advanced statistical analyses are reported, namely power spectral analysis and first passage statistics, which discuss and integrate the studies performed by the author and collaborators in [73, 74] and [75], respectively. The study is focused mainly on the class of processes defined in Chapter 2 and 3 for the description of BNG diffusion. Nevertheless, the general formalism introduced above in this section allows for an easy generalisation of the presented results to a broader class of random diffusivity models.

4.1 Power spectral analysis

The power spectral analysis of a stochastic trajectory $x(t)$ is developed in the frequency domain and provides important insights into short and long time behaviour and temporal correlations [78]. Starting from standard textbook settings, this analysis is based on the study of the so-called power spectral density (PSD) of the process, defined as

$$\mu(f) = \lim_{T \rightarrow \infty} \frac{1}{T} \left\langle \left| \int_0^T e^{ift} x(t) dt \right|^2 \right\rangle, \quad (4.8)$$

where f denotes the frequency. From a more practical point of view, the PSD is calculated by first performing a Fourier transform of an individual trajectory $x(t)$ over the finite observation time T ,

$$S(f, T) = \frac{1}{T} \left| \int_0^T e^{ift} x(t) dt \right|^2, \quad (4.9)$$

then, by averaging $S(f, T)$ over a statistical ensemble of possible trajectories and finally, by taking the asymptotic limit $T \rightarrow \infty$. This definition involves averages over a very large number of trajectories and it requires the trajectories to be very long in order to be able to consider the limit in T . Often these two assumptions are not possible to be implemented when dealing with experimental data. Indeed, single particle tracking experiments are typically limited in the measurement time, for instance, due to the lifetime of the employed fluorescent tags or to the time that a particle stays in the microscope focus. Additionally, such experiments are often limited to a relatively small number of individual trajectories. If these limitations are to be taken into account when defining the statistical analysis, one must avoid taking long time limits and ensemble averages. This is why the concept of single-trajectory power spectral density was introduced [79–81].

The quantity $S(f, T)$ defined in (4.9) for a single trajectory $x(t)$ and for finite observation times T is, of course, a random variable. Thus, the most general inform-

ation about its properties is contained in the moment-generating function (MGF)

$$\phi(T, \lambda) = \langle \exp(-\lambda S(f, T)) \rangle, \quad \lambda \geq 0. \quad (4.10)$$

By considering expression (4.1), the MGF of single-trajectory PSD for random diffusivity models presents the following exact analytic high-frequency form

$$\phi(T, \lambda) \sim \left\langle \left[1 + \frac{8\lambda D_0}{f^2 T} \int_0^T \Psi(t) dt + \frac{12\lambda^2 D_0^2}{f^4 T^2} \left(\int_0^T \Psi(t) dt \right)^2 \right]^{-1/2} \right\rangle_{\Psi}, \quad (4.11)$$

in which the vanishing terms were dropped and solely the leading terms in $1/f$ are kept. This equation is valid for any fixed realisation of $\Psi(t)$ and holds for arbitrary T and arbitrary f . It also represents the form of the MGF in the case when $\Psi(t)$ is non-fluctuating: in particular, for $\Psi(t) = 1$ it describes the MGF in case of standard Brownian motion [79], while the choice $\Psi(t) = t^{\alpha-1}$ corresponds to the case of scaled Brownian motion studied in [73].

One can see that the Laplace parameter λ appears in (4.11) in the combination $D_0\lambda/f^2$ only, so that the high- f spectrum of a single-trajectory PSD has the universal form

$$S(f, T) \sim \frac{4D_0}{f^2} \mathcal{A}, \quad (4.12)$$

regardless of the specific choice of $\Psi(t)$. Here \mathcal{A} , with realisation A , is a dimensionless, random amplitude, which differs from realisation to realisation. The result in (4.12) shows that the characteristic high-frequency dependence of the PSD can be learnt already at the single trajectory level, in agreement with the conclusions in [73, 79, 80].

The MGF $\Phi(T, \lambda)$ of the random amplitude \mathcal{A} follows from (4.11) and (4.12) and can be written as

$$\begin{aligned} \Phi(T, \lambda) &= \int_0^{\infty} e^{-\lambda A} P_{\mathcal{A}}(A) dA \\ &= \frac{2}{\sqrt{3}} \int_0^{\infty} \exp\left(-\frac{4p}{3}\right) I_0\left(\frac{2p}{3}\right) \Upsilon(T, \lambda p/T) dp, \end{aligned} \quad (4.13)$$

where $I_0(z)$ is the modified Bessel function of the first kind and $\Upsilon(T, \lambda)$ is the MGF of the integrated diffusivity defined in (4.7). Relation (4.13) links the MGF of \mathcal{A} to the one of $\tau(T)$, showing how $\Upsilon(T, \lambda)$ controls the high-frequency behavior of the PSD. By taking the inverse Laplace transform of (4.13) with respect to the parameter λ one can evaluate the PDF of \mathcal{A} , which then provides, thanks to the relation in (4.12), the high- f expression of the PDF $P(S(f, T) = S)$ according to

$$P(S(f, T) = S) \sim \frac{f^2}{4D_0} P_{\mathcal{A}}\left(A = \frac{Sf^2}{4D_0}\right), \quad f \rightarrow \infty. \quad (4.14)$$

One can readily obtain the moments of $S(f, T)$, relate them to the moments of \mathcal{A} and thus to the behaviour of $\tau(T)$. For instance, its average value is given by

$$\langle S(f, T) \rangle = \frac{4D_0 C_1}{f^2 T} \langle \tau(T) \rangle_\Psi = \frac{2C_1}{f^2 T} \langle \overline{x^2(T)} \rangle_\Psi, \quad (4.15)$$

where $C_1 = (3/4)^{3/2} {}_2F_1(1, 3/2; 1; 1/4)$, with ${}_2F_1(a, b; c; z)$ being the Gauss hypergeometric function. This result shows that those random diffusivity models that display anomalous scaling of the MSD, i.e., $\langle \overline{x^2(T)} \rangle_\Psi \not\propto T$, will show ageing behaviour as well, namely a dependence of the PSD properties on the trajectory length T (see, for instance, the discussion in [73]). Moreover, starting from the results for the moments of $S(f, T)$, one can also calculate the coefficient of variation γ of the PDF $P(S(f, T) = S)$ in the high- f limit, which is given by

$$\gamma = \left(\frac{\langle \overline{S^2(f, T)} \rangle_\Psi - \langle \overline{S(f, T)} \rangle_\Psi^2}{\langle \overline{S(f, T)} \rangle_\Psi^2} \right)^{1/2} \approx \left(\frac{9}{4} \frac{\partial_\lambda^2 \Upsilon(T; \lambda)|_{\lambda=0}}{(\partial_\lambda \Upsilon(T; \lambda)|_{\lambda=0})^2} - 1 \right)^{1/2}.$$

This implies that the effective broadness of $P(S(f, T) = S)$ is entirely defined by the first two moments of the random variable $\tau(T)$ in (4.6) and, more specifically, that the value of γ is independent of D_0 and f , when f is large enough.

The results reported until now are valid regardless of the choice of $\Psi(t)$. One can now focus on the analysis of the BNG models introduced in Chapter 2 and 3, recalling the connection established at the beginning of this Chapter between them and the general formalism used here.

Results for the SupBM and RSG models are reported in figure 4.1, where $\Psi(t)$ is selected to be a jump process with values drawn anew any δ time from a gamma distribution

$$\rho(\psi) = \frac{\psi^{\nu-1}}{\Gamma(\nu)\psi_0^\nu} \exp(-\psi/\psi_0), \quad (4.16)$$

with shape parameter $\nu = 0.5$ and scale parameter $\psi_0 = 1$. Recalling that δ represents the duration of each subinterval during which $\Psi(t)$ remains fixed before extracting a new value from (4.16), the RSG models is obtained in the limiting case $\delta = T$, while for the SupBM one can in principle choose any value of δ . The MGF of $\tau(t)$ for a jump process with gamma distributed values is given by

$$\Upsilon(T, \lambda) = (1 + \lambda\delta\psi_0)^{-\nu T/\delta}, \quad (4.17)$$

and its average value is given by $\langle \tau(T) \rangle = T \langle \psi \rangle = T\nu\psi_0$. Then, by making use of (4.15) one easily gets that $\langle S(f, T) \rangle = 2D_0 C_1 / f^2$, where the values $\nu = 0.5$ and $\psi_0 = 1$ have been considered. Indeed, in figure 4.1 (top and central panels) one can observe that the average value of the power spectrum is not affected by the value

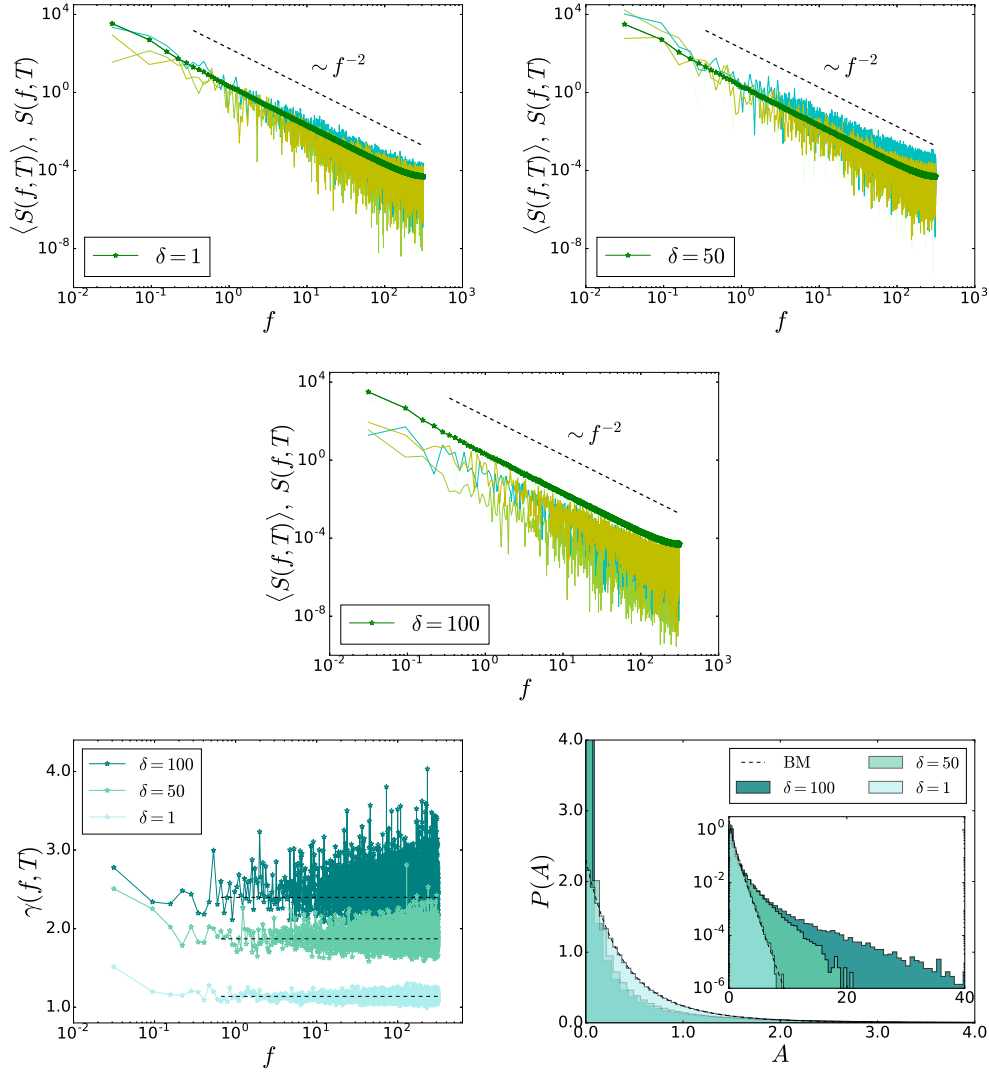


Figure 4.1: $\Psi(t)$ modelled as a jump process with Gamma distribution ($\psi_0 = 1$ and $\nu = 0.5$), for varying subinterval size δ and with trajectory length $T = 100$. When $\delta = T = 100$, the results can be associated to a RSG model. Top & central panels: few realisations of the power spectra from individual trajectories and its mean value for $\delta = 1, 50$, and 100 . Bottom-left panel: coefficient of variation for the three values of δ were the black dashed lines represent the analytical trend in (4.20). Bottom-right panel: distribution of the random amplitude \mathcal{A} in linear and semi-log scale (inset). Black dashed lines correspond to theoretical results for BM [79], showing that for $\delta = 1$ the limiting behaviour found in (4.19) for $\delta \rightarrow 0$ already dominates.

of δ . Nevertheless, the scattering among single-trajectory realisations is greater for larger values of δ . This may be detected in the distribution of the random variable \mathcal{A} as well, which is broader for larger values of δ —see the bottom-right panel of figure 4.1. The expression for the distribution of the random variable \mathcal{A} can be obtained by Laplace inverting the result in (4.13), considering the specific MGF of $\tau(t)$ defined in (4.17). This leads to

$$P_{\mathcal{A}}(A) = \frac{2}{\sqrt{3}} \int_0^\infty \frac{J_0\left(\left(1 + 1/\sqrt{3}\right)\sqrt{2zA}\right)}{(1 + z\psi_0\delta/T)^{\nu T/\delta}} J_0\left(\left(1 - 1/\sqrt{3}\right)\sqrt{2zA}\right) dz, \quad (4.18)$$

which, in the limit $\delta \rightarrow 0$ and $N \rightarrow \infty$, with $\delta N = T$, becomes

$$P_{\mathcal{A}}(A) = \frac{2}{\sqrt{3\nu\psi_0}} \exp\left(-\frac{4A}{3\nu\psi_0}\right) I_0\left(\frac{2A}{3\nu\psi_0}\right), \quad (4.19)$$

representing the same behavior as for standard BM [79], however, with renormalised coefficients. As a consequence of the different broadness of $P_{\mathcal{A}}(A)$ for changing δ , the coefficient of variation shows different limiting values—see the bottom-left panel of figure 4.1. Indeed, by recalling the result in (4.16), for this specific case one obtains

$$\gamma = \left[\frac{9}{4} \left(1 + \frac{\delta}{\nu T}\right) - 1\right]^{1/2}. \quad (4.20)$$

To conclude, it was shown that, for these models, the fluctuations of the power spectral behaviour are sensitive to different parameter values of the distribution (4.16), while the average trend is not. Moreover, the smaller the value of δ , the more the results approach a trend similar to the BM one, with properly rescaled coefficients as defined in (4.19). A similar result will be obtained for the DD model below and this is due to the final homogenisation of the process which does not happen, for instance, if one selects a heavy-tailed distribution for ψ_k , as shown in [74].

Moving to the DD models, an example is treated here where $\Psi(t)$ is defined, according to the mDD description, as the squared Ornstein-Uhlenbeck process $y(t)$ given by

$$\frac{dy(t)}{dt} = -\frac{1}{\tau_\star} y(t) + \sigma_\star \xi(t), \quad (4.21)$$

with time scale τ_\star and noise amplitude σ_\star . In this case the MGF of $\tau(T)$ is expressed in (3.14) with a slightly different notation (the exact form in the current notation is reported in [74]). Focusing on the numerical results reported in figure 4.2, top-left panel, one can see that the $1/f^2$ scaling is recovered, as expected, but in this case the value of τ_\star does affect the average power spectrum. Indeed, one can start by showing that in this case $\langle \tau(T) \rangle = \sigma_\star^2 \tau_\star T/2$, which then, thanks to the expression in (4.15), leads to $\langle S(f, T) \rangle = 2D_0 C_1 \sigma_\star^2 \tau_\star / f^2$, where an explicit dependence on both σ_\star

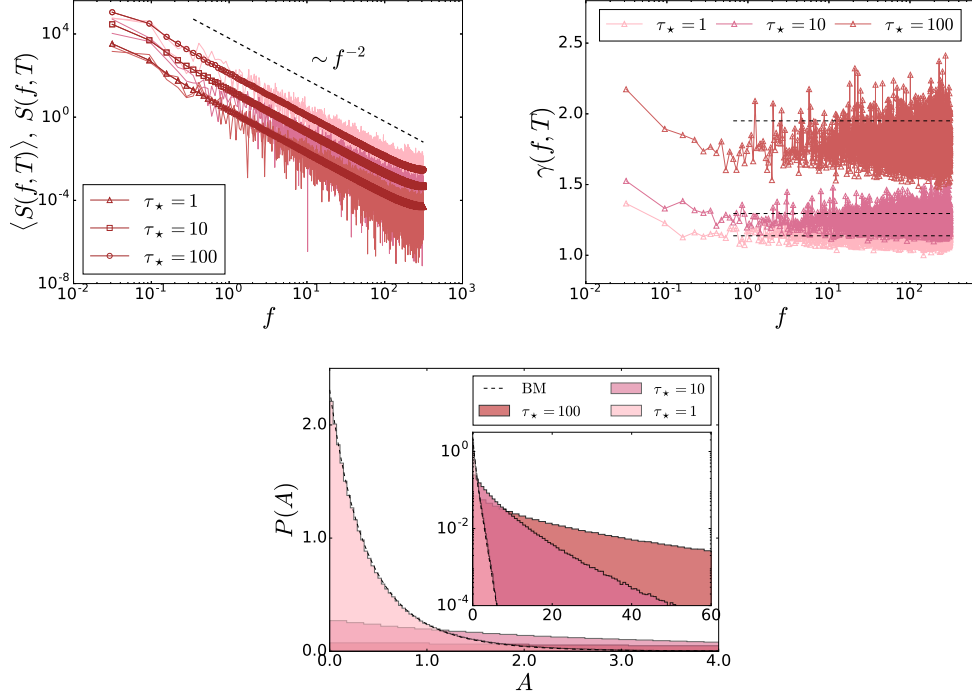


Figure 4.2: $\Psi(t)$ modelled as the squared Ornstein-Uhlenbeck process reported in (4.21), for three different values of τ_* . Other parameters are $T = 100$ and $\sigma_* = 1$. Top-left panel: few realisations of the power spectra from individual trajectories and its average value for $\tau_* = 1, 10, 100$. Top-right panel: coefficient of variation; blacked dashed lines represent the analytical result in (4.22). Bottom panel: distribution of the random amplitude \mathcal{A} in linear and semi-log scale (inset). Black dashed lines correspond to theoretical results for BM [79], showing that for small values of τ_* one approaches a trend comparable with that for BM.

and τ_* is present. Because of this dependence, the coefficient of variation γ converges to different values when τ_* is changed, namely

$$\gamma = \left[\frac{3}{4} \left(3 + \frac{3\tau_*}{\nu T} \left(1 - \frac{\tau_*}{2T} (1 - e^{-2T/\tau_*}) \right) \right) - 1 \right]^{1/2}, \quad (4.22)$$

as shown in the top-right panel of figure 4.2. Consequently, different degrees of broadness of the PDF of the random amplitude \mathcal{A} are also observed—see the bottom panel of figure 4.2. Note that for $\tau_* \ll T$ one obtains results that are very similar to the ones of BM (see [79]), while for increasing τ_* , the PDF of the random amplitude \mathcal{A} becomes increasingly broader, similarly to what discussed above for the jump process model with the Gamma distribution for ψ_k .

To conclude, it is possible, first of all, to define a general result from this analysis: regardless of the different properties of the random diffusivity model, a universal high- f behaviour of the PSD is obtained. This behaviour is characterised by a $1/f^2$ scaling, in analogy with BM [79] and SBM [73]. A first way to discriminate among different diffusion models lies in the study of the ageing behaviour of the PSD. Indeed, it was shown that the dependence of the PSD on the trajectory length T appears only for those random diffusivity models characterised by anomalous scaling of the MSD. This is still not of help when dealing with BNG diffusion models, which are all defined by a linear trend of the MSD. Then, differences from one model to another will appear in higher order moments of $P(S = S(f, T))$, for instance when studying the coefficient of variation γ . Finally, it was established that the PDF of the random amplitude \mathcal{A} carries most of the meaningful information. Indeed, the coefficient of variation may be directly calculated from its moments. Moreover, the MGF of \mathcal{A} is tightly related to the one of the integrated diffusivity $\tau(t)$ as shown in (4.13), underlining the observation that in the study of random diffusivity models the integrated diffusivity appears to act as the main player.

4.2 First passage statistics

The concept of first passage is ubiquitously used in statistical physics and its applications lie, for instance, in the quantification of the moment in time when a diffusing particle reaches a reaction centre or a stochastic process exceeds a given threshold value [82, 83]. Mathematically this is treated starting from the diffusion equation of the specific random walk and assuming absorbing boundary conditions in the position where the target or threshold is located. In addition to this simple setting, many factors enter in the analysis, starting from the domain geometry, the kind of target and its interaction with the diffusive entities. The easiest configuration is to consider a point target and to assume that the diffusive entity interacts with probability 1 with the target as soon as it finds it. Finally, one can start from a one-dimensional

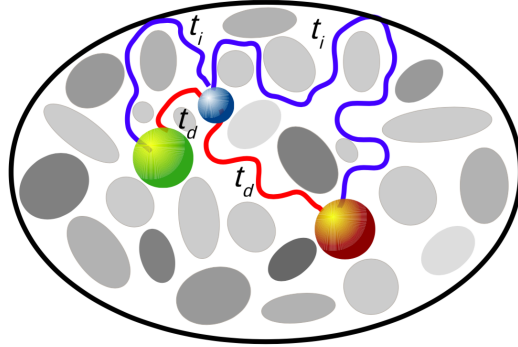


Figure 4.3: Schematic representation of two diffusive entities (large spheres) performing direct and indirect trajectories, red and blue respectively, towards the target (small sphere). While direct trajectories are typical and quite alike, indirect ones display a large dissimilarity (image adapted from reference [86]).

description, where only 2 choices can be considered: a semi-line and an interval. Already in this very simple problem set up, the first passage problem is not an easy one. The main difficulty is due to the fact that the first passage time is a stochastic variable itself and thus not easy to quantify deterministically. As a first attempt, one can consider the mean first passage time (MFPT) to quantify the first passage behaviour of the system. Nevertheless, depending on the specific diffusive process, the MFPT could be either a good or a bad estimator. Often fluctuations around this average value are significant and thus the best way to proceed is to consider the full distribution instead of its first moment only. The first passage time density function, $\varphi(t)$, is directly linked to the survival probability

$$S(t) = \int_0^t P(x, t') dt', \quad (4.23)$$

through its negative derivative, that is $\varphi(t) = -dS(t)/dt$. In (4.23), $P(x, t)$ represents the solution of the diffusion equation with absorbing boundary conditions at the targets, as discussed above. Another important element of the first passage analysis is the dependence on the initial position x_0 (see figure 4.3). The diffusive entities starting very close to the target will most likely perform a direct motion towards it, while those starting far away from the target will have to explore a large part of the domain before locating the target, or they may even not find it at all as they keep diffusing away from it. The MFPT is representative for the latter set of trajectories, namely the indirect ones, for which the dependence on the initial position is eventually lost. The former set of trajectories, the direct ones, instead strongly depend on the initial position and they are responsible for the so-called most likely first passage time, defined by the maximum of the first passage time PDF, i.e.,

$d\wp(t)/dt = 0$ [84–86].

Focusing on the analysis of random diffusivity models, it is reported here a study on the first passage behaviour of the RSG/SupBM models and the DD models, with comparison to standard BM results as well. Note that in this analysis the study of RSG and SupBM models will provide the same results as it starts from the definition of the probability $P(x, t)$ that can be expressed in the same way for both models, as discussed in Chapter 2. Thus, for simplicity, hereafter the results for both RSG and SupBM models are associated to the subscript $-_S$, while the ones for the DD models are identified by the subscript $-_{DD}$.

Starting from a semi-infinite domain with a target located at the origin and with initial position $x_0 > 0$, the corresponding diffusion equation with absorbing boundary conditions at the target can be solved by making use of the method of images [75,82]. In particular, by recalling the results from Chapter 2 and 3, one readily obtains

$$P_{DD}(x, t|x_0) = \int_0^\infty [G(x, \tau|x_0, D = 1) - G(x, \tau | -x_0, D = 1)] T(\tau, t) d\tau, \quad (4.24)$$

$$P_S(x, t|x_0) = \int_0^\infty [G(x, t|x_0, D) - G(x, t | -x_0, D)] p_{\mathcal{D}}(D) dD, \quad (4.25)$$

where $T(\tau, t)$ represents the PDF of the subordinator corresponding to the specific DD model and $p_{\mathcal{D}}(D)$ is the diffusivity distribution. Note that an explicit dependence on the initial position x_0 is introduced in the notation for clarity. The survival probability defined in (4.23) is then given by

$$S_{DD}(t|x_0) = \int_0^\infty S_{BM}(\tau|x_0, D = 1) T(\tau, t) d\tau, \quad (4.26)$$

$$S_S(t|x_0) = \int_0^\infty S_{BM}(t|x_0, D) p_{\mathcal{D}}(D) dD, \quad (4.27)$$

where $S_{BM}(t|x_0, D)$, defined as

$$S_{BM}(t|x_0, D) = G(x, t|x_0, D) - G(x, t | -x_0, D) = \operatorname{erf} \left(\frac{x_0}{\sqrt{4Dt}} \right), \quad (4.28)$$

stands for the result of BM in the same problem set up. This corresponds to a FPT density function for BM that is given by the well-known Lévy-Smirnov distribution

$$\wp_{BM}(t) = \frac{x_0}{\sqrt{4\pi Dt^3}} \exp \left(-\frac{x_0^2}{4Dt} \right), \quad (4.29)$$

which shows an interesting dichotomy: despite the certain return to the origin ($\int_0^\infty \wp_{BM}(t|x_0) dt = 1$), the MFPT $\langle t_{BM} \rangle = \int_0^\infty t \wp_{BM}(t|x_0) dt$ is infinite.

Following a similar procedure one can obtain results for the finite interval $[0, L]$ with absorbing boundaries at both $x = 0$ and $x = L$

$$S_{\text{BM}}(t|x_0) = \frac{4}{\pi} \sum_{n=0}^{\infty} \sin\left(\frac{\pi(2n+1)}{L}x_0\right) \frac{\exp(-D\lambda_{2n+1}^2 t)}{(2n+1)}, \quad (4.30)$$

$$S_{\text{DD}}(t|x_0) = \frac{4}{\pi} \sum_{n=0}^{\infty} \sin\left(\frac{\pi(2n+1)}{L}x_0\right) \frac{\tilde{T}(\lambda_{2n+1}^2, t)}{(2n+1)}, \quad (4.31)$$

$$S_{\text{S}}(t|x_0) = \frac{4}{\pi} \sum_{n=0}^{\infty} \sin\left(\frac{\pi(2n+1)}{L}x_0\right) \frac{1}{(2n+1)\sqrt{\lambda_{2n+1}^2 t + 1}}, \quad (4.32)$$

where $\lambda_n = n\pi/L$ are the eigenvalues coming from the solution of the diffusion equation for the displacement PDF in a finite domain [75, 82]. From the results in (4.30) it is immediate to see that the FPT density function for BM can be approximated, at long time, by its eigenstate with smallest eigenvalue,

$$\varphi_{\text{BM}}(t) \sim \exp(-t/\tau_1), \quad \tau_1 = L^2/\pi^2 D, \quad (4.33)$$

such that a finite MFPT is guaranteed in the finite domain.

Note that similar results for the random diffusivity models can be obtained by using the formalism of MGFs discussed in the sections above, see for instance the results in [91]. While the formalism based on the MGF is more useful for generalising the results to different random diffusivity models, as shown above for the power spectral analysis, the framework used here, based on the results obtained in Chapter 2 and 3, is more suitable for a clear comparison with BM first passage behaviour, as one can see, for instance, from the results in (4.26) and (4.27).

Results for the survival probability behaviour from this analysis are depicted in figure 4.4. Focusing first on the top panels, while for BM one observes a universal rescaling variable, i.e., x_0/\sqrt{t} , when introducing heterogeneity in the system through a random diffusivity, the universal rescaling is partially lost—see especially the top-left panel of figure 4.4. In particular, the effect of direct trajectories, which acts on the short time trend of the survival probability, appears to be stronger for random diffusivity models than for BM and it varies when changing initial position and kind of heterogeneity (identified by the diffusivity distribution). By using a random walk description it is possible to understand this effect more easily. In a random walk picture, each particle will perform jumps with random directions, each with a jump length $\Delta x = (D \Delta t)^{1/2}$. By assuming the time interval between each jump to be constant, e.g. $\Delta t = 1$, the jump length Δx will be defined solely by the diffusion coefficient. Then, considering a target located at a distance $N\Delta x$ from the initial position x_0 , the direct trajectories will be those that perform N consecutive jumps in the direction of the target. If D does not change in time and it is the same

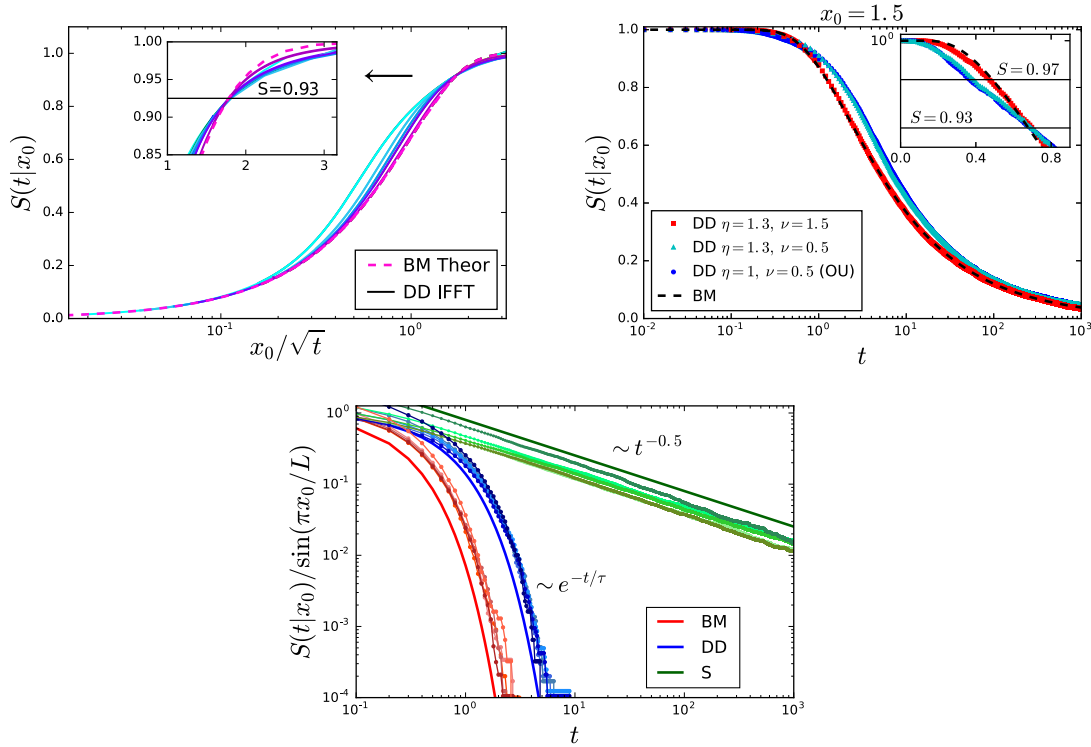


Figure 4.4: Top-left panel: numerical estimation of the analytical result for the survival probability in the semi-infinite domain as defined in (4.26) as function of x_0/\sqrt{t} . Different colours represent different initial positions x_0 , the pink dashed line represents the BM result in (4.28). In the inset the short time behaviour of $S(t|x_0)$ is reported, the universal crossover at $S \approx 0.93$ is distinct. Top-right panel: numerical results for the survival probability for fixed initial value $x_0 = 1.5$ obtained from simulations of the DD model discussed in section 3.3 in the expressions (3.29)-(3.31) and defined in [43], where different kinds of heterogeneity can be introduced. The black dashed line represents the BM result in (4.28). In the inset the short time behaviour of $S(t|x_0)$ is reported; the crossover level is different when varying the kind of heterogeneity. Bottom panel: survival probability for the finite interval $[0, 1]$, showing a comparison of the results coming from simulations of BM, mDD, and RSG/SupBM. Different colour shades represent different initial positions x_0 . The solid lines represent the analytical results in (4.30) - (4.32). Note that since all the three results in (4.30), (4.31) and (4.32) present the same dependence on the initial condition x_0 , the curves are normalised over this dependence, evaluated at the leading eigenvalue. Indeed, different colour shades eventually merge into a common curve for large times.

for each trajectory (BM case), one will observe a specific average number of direct trajectories that corresponds to the BM case. If one introduces a distribution of diffusivity values, each particle will have its own jump length and the particles with greater D will need less jumps to reach the target. In this way, one can understand that, on the ensemble level, the number of direct particles increases with respect to the BM case if one introduces a distribution of diffusivities. Moreover, this effect will depend on the kind of heterogeneity considered, which is responsible for the specific diffusivity distributions, as depicted in figure 4.4, top-right panel.

Note that the random walk description for the interpretation of direct trajectories is valid for both RSG/SupBM models and DD models, since the latter can be approximated, at short times, by SupBM with a description based mainly on realisation-to-realisation variability. Nevertheless, for RSG/SupBM models the argument concerning larger or smaller jump lengths holds for the entire time window, playing a crucial role in the behaviour of indirect trajectories as well. If one instead considers DD models, the fluctuations of the diffusion coefficient along the single trajectory will lead the particles to explore the whole diffusivity space and eventually to homogenise. Then, the argument above will not be valid any longer, and one sees that the indirect trajectories present results similar to the BM ones (see the long time behaviour in figure 4.4, top panels). Indeed, in the long time behaviour the two classes of random diffusivity models, that is RSG/SupBM models and DD models, show large discrepancies. To describe more details about the last observation one can focus on the bottom panel of figure 4.4, where results from simulations of both classes of random diffusivity models in a finite interval $[0, L]$ with boundary conditions at both $x = 0$ and $x = L$ are reported. Similarly to the discussion reported for the semi-infinite domain, the homogenisation process in the DD model allows the survival probability to reach a long time trend which is exponential, as for BM, yet a slower rate is observed. This corresponds to the behaviour in figure 4.4, top-left panel, where the initial faster drop of $S(t|x_0)$ is followed by an increase due to the fact that all the particles with initial greater diffusivities have already reached the target. If in the DD models this is just a transient behaviour that for a domain large enough (or for τ_D small enough, see [91]) disappears, for RSG/SupBM models this influences the long time trend as well. Indeed, as no variations (or very few in the case of SupBM) of D along each trajectory are expected in these models, the longer the time the more the system is left with particles with very low diffusivity values. These particles are responsible for the heavy-tailed behaviour of the survival probability in RSG/SupBM models.

Many of the results discussed above about the survival probability can also be argued in terms of the first passage time density function. In order to do so, one can focus on figure 4.5, where the first passage time PDF is displayed for both semi-infinite and finite domain (left and right panel, respectively). For the sake of simplicity, results for one initial position only are reported. One can immediately see

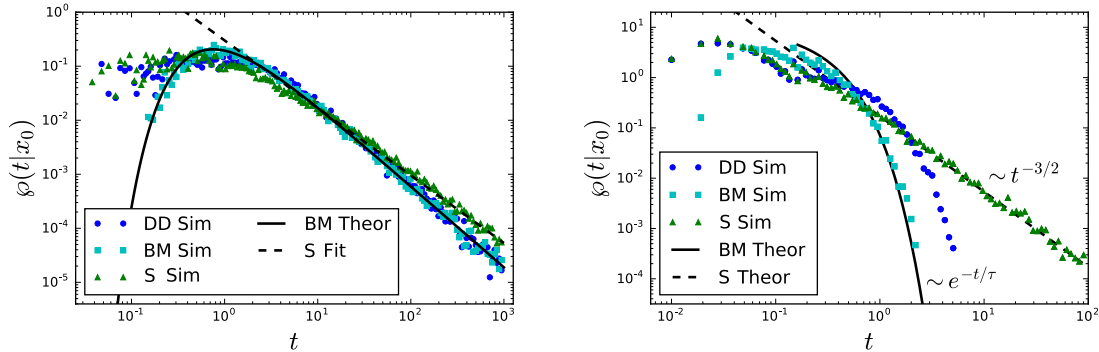


Figure 4.5: Comparison between BM, mDD, and RSG/SupBM first passage time distributions obtained from simulations. The black solid lines represent the analytical results for BM in (4.29) and (4.33), while the black dashed lines depict a power-law fit identifying the long time trend for SupBM. Left panel: semi-infinite domain with initial condition $x_0 = 1.5$; right panel: finite interval $[0, 1]$ with initial condition $x_0 = 0.5$.

that both classes of random diffusivity models (RSG/SupBM models and DD models) show the same behaviour at short times. In particular, the peak of the distribution is shifted to the left, towards shorter first passage times, if compared with the BM result. In the case of a semi-infinite domain, it is interesting to observe that a plateau emerges instead of a peak. Moving towards the tails of the distributions, one again observes a discrepancy between the two classes of models, as amply discussed above. As a general result, one can conclude that the effect of the heterogeneity is to stretch the first passage time distribution.

4.3 Discussion

In this Chapter, the effect of the system heterogeneity in diffusion models through the introduction of a random diffusivity was addressed and extensively discussed from a statistical point of view. Quite typically stochastic processes are evaluated in terms of their displacement distribution, i.e., $P(x, t)$, and by defining their ensemble averaged MSD and/or time-averaged MSD,

$$\langle x^2(t) \rangle = \int_{-\infty}^{\infty} x^2 P(x, t) dx, \quad (4.34)$$

$$\overline{\delta^2(\Delta)} = \frac{1}{T - \Delta} \int_0^{T - \Delta} (x(t - \Delta) - x(t))^2 dt, \quad (4.35)$$

where T is the measurement time and Δ is referred to as lagtime, with $\Delta \ll T$. Note that for ergodic processes, in the limit $T \rightarrow \infty$, the two quantities in (4.34) and (4.35) coincide. The models described in Chapter 2, namely RSG and SupBM models, are clearly non-ergodic, yet the DD approach allows for a recovery of the ergodicity, as already mentioned along this dissertation (note that studies about statistical properties typical of DD models, among which the ergodicity, are reported in [59]). Finally, the general framework defined in (4.1) describes models which can be both ergodic or non ergodic, depending on the choice of $\Psi(t)$.

The study performed here slightly deviates from this standard methodologies and focuses more on other statistical analyses, with relation to power spectral densities and first passage statistics. This is of help not only for the classifications of the models in data analyses, but also for gaining a deeper physical understanding of those systems which can be potentially described by random diffusivity models, as widely discussed in sections 4.1 and 4.2. At the same time, a general procedure to obtain the MGF for all the random diffusivity models that can be defined through the definition in (4.1) is provided. Starting from the expression of the MGF in (4.5), the position PDF $P(x, t)$ and all its moments can be derived.

Finally, before concluding, it is worth noticing that other approaches and studies focused on the role of heterogeneity in the target location are present in literature, both for SupBM [87] and DD models [88–93], showing results in agreement with the discussion reported here.

Chapter 5

Conclusions

Random diffusivity processes have gradually established themselves as a new paradigm in the modelling of diffusion beyond Brownian motion. Extensively studied by the community of stochastic processes in the last ten years, this class of models aims at the description of complex systems where new experimental techniques have displayed the presence of heterogeneities that appear or manifest themselves on a mesoscopic scale, comparable with the one at which the diffusion occurs. The randomness responsible for the diffusive dynamics is thought to obey standard stochastic processes, namely BM or FBM-like for diffusion in viscoelastic media, yet fluctuations are observed for the main parameters of the driving diffusive model. The origin of these fluctuations and their timescale result to be the key aspects in defining an appropriate modelling approach for this kind of systems.

In this dissertation a pathway from individual models to a general framework to address diffusion in heterogenous systems through the concept of random diffusivity was presented. Proceeding in chronological order, a review of the main models leading to the state-of-the-art on the random diffusivity approach was provided. Thanks to this step-by-step description the reader had the chance to both get a closer look at those particular models that have been successful in the description of experimental data and, at the same time, to understand the potential of this approach in a broader sense. Indeed, it is worthwhile to emphasise the great number of different mathematical methodologies that have been used to develop, study and analyse this class of diffusion processes. Furthermore, an attempt to introduce a general methodology for the study and description of random diffusivity models was made, in order to finally report results obtained from the statistical analysis of this class of stochastic processes. In particular, it was shown how fluctuations along single trajectories and realisation-to-realisation fluctuations of a stochastic process turn out to be relevant in establishing its power spectral behaviour and in many scenarios of first-passage time statistics as well. The interplay between the relaxation time of the systems and the timescale of the fluctuations represents an essential feature in

the study of these models. Recent works by Hartich and Godec [94, 95] reported a link between relaxation and first-passage phenomena in Markovian dynamics and it would be compelling to see what similar studies can tell about random diffusivity models.

From the overall discussion reported in this dissertation, it is clear that random diffusivity models are able to fully describe BNG diffusion, yet the study of ANG diffusion remains to be fully understood. To address the latter, a few directions have been tested in literature by making use of the random diffusivity approach. Results on this topic were discussed in this dissertation, with the main goal of emphasising both strong points and shortcomings of the theory to foster future developments. One interesting direction for future work in this topic could be to extend the general framework introduced in Chapter 4 to the case of fractional Gaussian noise, in order to understand whether the statistical features of the model after introducing long-range correlation would still show some kind of universality, as was shown for BNG diffusion. Eventually one could relate this study to the results obtained in [66, 67], briefly discussed in section 3.4.

Before concluding, a discussion on the possible origin of those heterogeneities responsible for the emergence of random diffusivity models is due. As a first step, one must identify the kind of heterogeneity that one is dealing with. Two main distinctions can be considered, ensemble heterogeneity *vs* medium heterogeneity and time-dependent heterogeneity *vs* space-dependent heterogeneity. Not always it is possible to differentiate between these two sets, and even more, a clear distinction between medium and ensemble heterogeneity is not always well defined. Nevertheless, one can still try to create a sort of classification of heterogeneities.

On the one hand, whenever one considers ensemble heterogeneity the presence of space-dependent heterogeneity can be excluded. In other words, from the point of view considered in this dissertation, it is assumed that ensemble heterogeneity is not caused by space-dependent heterogeneity, but rather it emerges from inherent realisation-to-realisation variability of the system configuration, for instance, from changes in specific *a priori* features of the diffusive entities. Still, ensemble heterogeneity can be both time-dependent and time-independent. In the latter case, one has realisation-to-realisation fluctuations only, leading to non-ergodic behaviour, while in the former case the ergodicity can be recovered if one thinks of a system in which, for instance, the diffusive entities are characterised by features that fluctuates in time (see the case of polymerisation [96]).

On the other hand, the medium heterogeneity can be mapped into both time-dependent and space-dependent heterogeneity. Despite the quite involved picture, there are some general observations that can be made. The random diffusivity approach mathematically describes fluctuations that vary in time and not in space. However, this does not mean that the physical origin of those fluctuations must be found in time-dependent heterogeneity only, but rather it implies that if, and when,

those fluctuations come from space-dependent heterogeneity, a process of homogenisation, which one could think of as a coarse-graining procedure, can be defined, such that a direct link can be drawn between variability in space and variability in time [97]. This connection is of course not always possible, as it depends on which kind of space-dependent heterogeneity the system presents. For simplicity, one could identify with *weak space-dependent heterogeneity* the one in which this process of homogenisation can be defined and with *strong space-dependent heterogeneity* the one in which it cannot. Consider for instance the model described by Spakowitz in [98] where Brownian simulations are performed with a diffusion coefficient that presents an explicit dependence on the space-variable. In particular, focusing on the 1D case, $D(x)$ is modelled as a superposition of M Gaussian pockets located randomly in the domain, that is

$$D(x) = 1 + \sum_{i=1}^M \delta_i \exp\left(-\frac{(x - c_i)^2}{2\sigma_i^2}\right). \quad (5.1)$$

where c_i identifies the random locations of the Gaussian pockets, σ_i their size and δ_i their magnitude. In this description the diffusivity map is indeed similar to the picture reported in figure 1.2, where one can imagine the different colours to correspond to the different δ_i values and the different region sizes to the different values of σ_i . In the study reported in [98] a fixed size σ was selected and the same value was chosen for every $\delta_i = \delta$, emphasising also that small values of δ lead to a weak heterogeneity while large values lead to a strong heterogeneity. Then, the weak heterogeneity case was studied and the results show a very interesting behaviour, close to the one of BNG diffusion treated in this dissertation. In particular, the authors claim that the MSD is slightly affected by the heterogeneity, while the displacement distribution displays a clear non-Gaussian behaviour at short times that eventually crosses over to a Gaussian. This shows that systems with *weak space-dependent heterogeneity* can be described quite well by time-dependent random diffusivity models.

With such concepts, it is possible to conclude that random diffusivity models describe systems that display time-dependent heterogeneity, *weak space-dependent heterogeneity* and/or ensemble heterogeneity.

It would be interesting to study the model represented by the expression in (5.1) and defined in [98], in the case of strong heterogeneity to see whether it is still possible to draw a mapping between space-dependence and time-dependence and, if not, to understand where in the parameter space the critical behaviour appears. Moreover, it would be interesting to study the case in which, instead of random location of the pockets one introduces a random magnitude or a random size for them, meaning selecting a randomly distributed δ_i and/or σ_i . Finally, also a study to understand the role of randomness in the location of the pockets by changing the distribution in space of c_i could be interesting. This study could then be linked to the experiments performed by Chakraborty & Roichman in [99]. Indeed, in order

to characterise quantitatively the effect of spatial heterogeneities they studied the diffusion of fluorescent colloidal particles in a matrix of micropillars having a range of structural configurations: from completely ordered to completely random.

To conclude, understanding the role of heterogeneity is of great relevance for the study of transport properties in many systems, such as, biological systems, polymers, gels, and porous materials and surely there is still much to be explored. This dissertation is thought to represent a step forward in this direction.

Appendix

A Fractional Brownian motion

Fractional Brownian motion was originally introduced by Mandelbrot and Van Ness in [12]. If one defines $X_H(t)$, where $t \geq 0$, with values in \mathbb{R} as a *Hurst Self-Similar with stationary Increments* (H-SSSI) process if:

- (i) it is a self-similar process, $X(at) = a^H X(t)$;
- (ii) it has stationary increments, namely $X(t+t') - X(t)$ is invariant under time shift transformation,

then FBM represents the only H-SSSI Gaussian process. The Hurst exponent for FBM varies between $0 < H \leq 1$ and its correlation function is given by

$$\langle X_H(t)X_H(t') \rangle = \frac{1}{2} (|t|^{2H} + |t'|^{2H} - |t - t'|^{2H}), \quad (5.2)$$

such that FBM describes processes with an antipersistent behavior if $0 < H < 1/2$ and with persistent behaviour if $1/2 < H \leq 1$. Note that for $H = 1/2$ one obtains standard BM.

A common description of FBM is given by the stochastic differential equation

$$\frac{dx_H(t)}{dt} = \sqrt{2K_H} \xi_H(t), \quad (5.3)$$

where $\xi_H(t)$ is the so-called fractional Gaussian noise [13]. This is a Gaussian noise with zero mean and power-law correlation function $\langle \xi_H(t)\xi_H(t') \rangle = H(2H - 1)|t - t'|^{2(H-1)}$, such that the antipersistent behaviour ($0 < H < 1/2$) correspond to negative correlated noise while the persistent behaviour ($1/2 < H \leq 1$) is related to positive correlation of the noise. The probability density function of FBM follows the evolution equation

$$\frac{\partial P(x, t)}{\partial t} = 2HKt^{(2H-1)} \frac{\partial^2 P(x, t)}{\partial x^2}. \quad (5.4)$$

and it is given by the Gaussian

$$P(x, t) = \frac{1}{\sqrt{4\pi K_H t^{2H}}} \exp\left(-\frac{x^2}{4K_H t^{2H}}\right), \quad (5.5)$$

where $K_H = 2HK$, with variance $\langle x^2(t) \rangle = 2K_H t^{2H}$.

Note that fractional Gaussian noise is also employed in the definition of the fractional Langevin equation (FLE). More specifically, the FLE is a special case of the GLE defined in (2.29)-(2.30) where the fractional Gaussian noise is used as stochastic forcing. The PDF of both its velocity and its position are Gaussian and the MSD crosses over from ballistic behavior at short times to anomalous diffusion at long times.

B Fractional derivatives

The Riesz–Feller space-fractional derivative ${}_x D_\theta^\nu$ is defined by its Fourier transform according to

$$\int_{-\infty}^{+\infty} e^{+i\kappa x} \{ {}_x D_\theta^\nu u(x, t) \} dx = -|\kappa|^\nu e^{i(\text{sign}\kappa)\theta\pi/2} \widehat{u}(\kappa, t), \quad (5.6)$$

with $0 < \nu \leq 2$, $|\theta| \leq \min\{\nu, 2 - \nu\}$ and where $\theta = 0$ represents the symmetric case.

The Caputo time-fractional derivative ${}_t D_\star^\beta$ is defined by its Laplace transform as

$$\int_0^{+\infty} e^{-st} \{ {}_t D_\star^\beta u(x, t) \} dt = s^\beta \widetilde{u}(x, s) - \sum_{n=0}^{m-1} s^{\beta-1-n} u^{(n)}(x, 0^+), \quad (5.7)$$

with $m - 1 < \beta \leq m$ and $m \in \mathbb{N}$. In literature the time-fractional derivative is sometimes considered in the Riemann–Liouville sense, which is identified as ${}_t D^\beta$. The relation between the time-fractional Riemann–Liouville derivative and the time-fractional derivative in the Caputo sense is given by

$${}_t D_\star^\beta u(x, t) = {}_t D^\beta u(x, t) - \frac{t^{-\beta}}{\Gamma(1 - \beta)} u(x, 0). \quad (5.8)$$

The difference between the two definitions stands in the initial condition. For instance, the Caputo and Riemann–Liouville fractional derivatives of an exponential function $u(t) = e^{\lambda t}$, are given by

$${}_t D_\star^\beta e^{\lambda t} = \lambda^m t^{m-\beta} E_{1, m-\beta+1}(\lambda t), \quad (5.9)$$

$${}_t D^\beta e^{\lambda t} = t^{-\beta} E_{1, 1-\beta}(\lambda t), \quad (5.10)$$

with $m - 1 < \beta \leq m$ and $m \in \mathbb{N}$ and where $E_{\alpha,\beta}(z)$ is the two parameter Mittag-Leffler function defined as

$$E_{\alpha,\beta}(z) = \sum_{k=0}^{\infty} \frac{z^k}{\Gamma(\alpha k + \beta)}, \quad z \in \mathbb{C}. \quad (5.11)$$

The Erdélyi-Kober time-fractional derivative is defined as

$$D_{\eta}^{\gamma,\mu} \phi(t) = \prod_{j=1}^n \left(\gamma + j + \frac{1}{\eta} t \frac{d}{dt} \right) (I_{\eta}^{\gamma+\mu, n-\mu} \phi(t)), \quad (5.12)$$

where $n - 1 < \mu \leq n$ and $I_{\eta}^{\gamma,\mu}$ is the Erdélyi-Kober fractional integral operator given by

$$I_{\eta}^{\gamma,\mu} \phi(t) = \frac{t^{-\eta(\mu+\gamma)}}{\Gamma(\mu)} \int_0^t s^{\eta\gamma} (t-s)^{\mu-1} \phi(s) d(s^{\eta}), \quad (5.13)$$

with $\mu > 0$, $\eta > 0$ and $\gamma \in \mathbb{R}$. In the particular case if $\mu = \eta$, the Erdélyi-Kober time-fractional derivative can be related to the Riemann-Liouville derivative through

$$D_1^{-\mu,\mu} u(x, t) = t^{\mu} {}_t D^{\mu} u(x, t). \quad (5.14)$$

C Collection of papers

Sposini V, Checkin A V, Seno F, Pagnini G & Metzler R 2018 Random diffusivity from stochastic equations: comparison of two models for Brownian yet non-Gaussian diffusion *New J. Phys.* **20**, 043044.



PAPER

Random diffusivity from stochastic equations: comparison of two models for Brownian yet non-Gaussian diffusion

OPEN ACCESS

RECEIVED

15 January 2018

REVISED

24 February 2018

ACCEPTED FOR PUBLICATION

14 March 2018


PUBLISHED

25 April 2018

Original content from this work may be used under the terms of the [Creative Commons Attribution 3.0 licence](https://creativecommons.org/licenses/by/4.0/).

Any further distribution of this work must maintain attribution to the author(s) and the title of the work, journal citation and DOI.



Vittoria Sposini^{1,2}, Aleksei V Chechkin^{1,3}, Flavio Seno⁴, Gianni Pagnini^{2,5} and Ralf Metzler¹ 

¹ Institute for Physics & Astronomy, University of Potsdam, D-14476, Potsdam-Golm, Germany

² Basque Center for Applied Mathematics, E-48009, Bilbao, Spain

³ Akhiezer Institute for Theoretical Physics, 61108 Kharkov, Ukraine

⁴ INFN, Padova section and Department of Physics and Astronomy 'Galileo Galilei', University of Padova, I-35131, Padova, Italy

⁵ Ikerbasque—Basque Foundation for Science, Bilbao, Spain

E-mail: rmetzler@uni-potsdam.de

Keywords: diffusion, non-Gaussian statistics, superstatistics

Abstract

A considerable number of systems have recently been reported in which Brownian yet non-Gaussian dynamics was observed. These are processes characterised by a linear growth in time of the mean squared displacement, yet the probability density function of the particle displacement is distinctly non-Gaussian, and often of exponential (Laplace) shape. This apparently ubiquitous behaviour observed in very different physical systems has been interpreted as resulting from diffusion in inhomogeneous environments and mathematically represented through a variable, stochastic diffusion coefficient. Indeed different models describing a fluctuating diffusivity have been studied. Here we present a new view of the stochastic basis describing time-dependent random diffusivities within a broad spectrum of distributions. Concretely, our study is based on the very generic class of the generalised Gamma distribution. Two models for the particle spreading in such random diffusivity settings are studied. The first belongs to the class of generalised grey Brownian motion while the second follows from the idea of diffusing diffusivities. The two processes exhibit significant characteristics which reproduce experimental results from different biological and physical systems. We promote these two physical models for the description of stochastic particle motion in complex environments.

1. Introduction

The systematic study of the diffusive motion of tracer particles in fluids dates back to the 19th century, particularly referring to Robert Brown's experiments observing the erratic motion of granules extracted from pollen grains which were suspended in water [1]. Since then numerous scientists contributed by improving the experiments [2–4] as well as in defining the basis of the theory of diffusion [5–9]. In brief, Brownian or standard diffusion processes are mainly characterised by two central features: (i) the linear growth in time of the mean-squared displacement (MSD),

$$\langle x^2(t) \rangle = 2Dt, \quad (1)$$

where D is the diffusion coefficient, and (ii) the Gaussian probability density function (PDF) for the particle displacement,

$$G(x, t|D) = \frac{1}{\sqrt{4\pi Dt}} \exp\left(-\frac{x^2}{4Dt}\right). \quad (2)$$

Here and in the following we focus on a one-dimensional formulation of the model, a generalisation to higher dimensions can be achieved component-wise.

Discoveries of deviations from the linear time dependence (1) have a long history. Thus, Richardson already in 1926 reported his famed t -cubed law for the relative particle diffusion in turbulence [10]. Scher and Montroll

uncovered anomalous diffusion of the power-law form

$$\langle x^2(t) \rangle \simeq D_\alpha t^\alpha, \quad (3)$$

with the anomalous diffusion exponent $0 < \alpha < 1$ and the generalised diffusion coefficient D_α [11], for the motion of charge carriers in amorphous semiconductors [12]. With the advance of modern microscopy techniques, in particular, superresolution microscopy, as well as massive progress in supercomputing, anomalous diffusion of the type (3) has been reported in numerous complex and biological systems [13, 14]. Thus, subdiffusion with $0 < \alpha < 1$ was observed for submicron tracers in the crowded cytoplasm of biological cells [15–19] as well as in artificially crowded environments [20–23]. Further reports of subdiffusion come from the motion of proteins embedded in the membranes of living cells [24–26]. Subdiffusion is also seen in extensive simulations studies, for instance, of lipid bilayer membranes [27–30] and relative diffusion in proteins [31]. Superdiffusion, due to active motion of molecular motors, was observed in various biological cell types for both introduced and endogenous tracers [16, 17, 32, 33].

Most of the anomalous diffusion phenomena mentioned here belong to two main classes of anomalous diffusion: (i) the class of continuous time random walk processes, in which scale-free power-law waiting times in between motion events give rise to the law (3) [12, 34], along with a stretched Gaussian displacement probability density $G(x, t)$ [11, 12, 34] as well as weak ergodicity breaking and ageing [35, 36]. We note that similar effects of non-Gaussianity, weak non-ergodicity, and ageing also occur in spatially heterogeneous diffusion processes [37–40]. (ii) The second one is the class of viscoelastic diffusion described by the generalised Langevin equation with power-law friction kernel [41, 42] and of fractional Brownian motion (FBM) [43]. These processes are both fuelled by long-range, power-law correlated noise. Its distribution is Gaussian, so that the displacement probability density $G(x, t)$ is Gaussian, as well. Moreover, these are ergodic processes [23, 42, 44–46].

Over the last few years a new class of diffusive processes has been reported, namely, so-called Brownian yet non-Gaussian diffusion [47, 48]. This class identifies a dynamics characterised by a linear growth (1) of the MSD combined with a non-Gaussian PDF for the particle displacement. The emergence of a non-Gaussian distribution, despite the Brownian MSD scaling, suggests the presence of an inhomogeneity that can be located both on the single tracer particle and on the ensemble levels. The study of these processes is becoming increasingly relevant with the growing number of complex systems discovered to exhibit such statistical features. For instance, we mention soft matter and biological systems, in which the motion of biological macromolecules, proteins and viruses along lipid tubes and through actin networks [47, 48], as well as along membranes and inside colloidal suspension [49] and colloidal nanoparticles adsorbed at fluid interfaces [50–52] are studied. We also mention ecological processes, involving the characterisation of organism movement and dispersal [53, 54], as well as processes, that are Brownian but non-Gaussian in certain time windows of their dynamics. These concern the dynamics of disordered solids, such as glasses and supercooled liquids [55–57] as well as interfacial dynamics [58, 59]. Also anomalous diffusion processes of the viscoelastic class that typically are expected to exhibit Gaussian statistic of displacements, were reported to have non-Gaussian displacements along with distinct distributions of diffusivity values. These concern the motion of tracer particles in the cellular cytoplasm [60–62] and the motion of lipids and proteins in protein-crowded model membranes [29].

Here we study two alternative stochastic approaches to non-Gaussian diffusion due to random diffusivity parameters, namely, generalised grey Brownian motion (ggBM) and diffusing diffusivities (DD). We analyse their exact behaviour and relate these approaches to the idea of superstatistics. To prepare the discussion, section 2 presents a primer on the approach of superstatistics and what has been done in the context of ggBM and DD models. In section 3 we then study the ggBM model with a random diffusivity distributed according to the generalised Gamma distribution. In particular, ggBM will be shown to represent a stochastic description of the superstatistics approach and is equivalent to the short time (ST) limit of the DD model. In section 4 we formulate a set of stochastic equations for the dynamics within the DD framework, in which the diffusivity statistic is governed by the generalised Gamma distribution. This is then incorporated in the framework of the minimal model of DD in section 5. In section 5.4 we describe the behaviour of the kurtosis of the two models, an important quantity for data analysis. Section 6 introduces an analysis for an initial non-equilibrium setting for the random diffusivity, relevant, for instance, for the description of single particle trajectories. To transfer this concept to the ggBM approach we propose a non-equilibrium version of ggBM. Finally our conclusions are reported in section 7. In the appendices some mathematical details are collected.

2. Pathways to Brownian yet non-Gaussian diffusion: superstatistics and DD, and ggBM

When we talk about an ensemble of particles, we could imagine that non-Gaussian statistic in this ensemble sense emerges due to the fact that different particles are located in different environments with different transport characteristics, such as the diffusion coefficient. If during the observation time each particle remains in its own environment characterised by a given value D of the diffusivity, the ensemble of particles shows a

mixture of individual Gaussians, weighted by some distribution $p(D)$ of local diffusivities. This is the idea behind superstatistics, an approach promoted by Beck and Cohen [63], see also [64]. As a result, the ensemble dynamics is still Brownian yet the PDF of particle displacements will correspond to a sum or integral of single Gaussians with specific value of D , weighted by the distribution $p(D)$. For instance, an exponential form for $p(D)$ will produce an exponential shape of the ensemble displacement PDF, sometimes called a Laplace distribution. We note that there also exist superstatistical formulations on the basis of the stochastic Langevin equation, leading to Brownian yet non-Gaussian behaviour [65]. A quite general superstatistical formulation in terms of the gamma distribution was put forward by Hapca *et al* [53].

More recently, similar concepts have been sought to describe non-Gaussian viscoelastic subdiffusion. Thus, Lampo *et al* [61] observed exponential distributions of the generalised diffusivity D_α for the motion of submicron tracers in living bacteria and eukaryotic cells. As a theoretical description they used a superstatistical formulation of the stochastic equation for FBM [61]. Following the observation of stretched Gaussian shapes of the displacement PDF in protein-crowded lipid bilayer membranes [29], more general forms for the distribution of the generalised diffusion coefficient were introduced, see, for instance, [66, 67]. Viscoelastic, non-Gaussian diffusion was also described in terms of the generalised Langevin equation with superstatistical distribution of the friction amplitude [68, 69].

Some other models instead introduce a fluctuating diffusivity, for instance to describe segregation in solids [70] or to analyse data from diffusion processes assessed by modern measurement techniques [71]. Brownian motion in fluctuating environments, or governed by temperature or friction fluctuations has been studied in [72–74] and models with intermittency between two values of the diffusivity are considered in [75, 76]. Anomalous diffusion in a disordered system was also described in terms of a superstatistical model based on a Langevin equation formulation, combining a Rayleigh-shaped diffusivity distribution with deterministic power-law growth or decay of the mean diffusivity [77].

A general framework for the description of diffusion in a complex environment is provided also by the class of stochastic processes identified as ggBM [78–82]. The basic idea of this approach is that the complexity or heterogeneity of the medium is completely described by the random nature of a specific parameter. Choosing this parameter to be the diffusivity leads to a stochastic interpretation of the system that may be viewed as complementary to the superstatistics concept and thus suitable for the description of the class of Brownian yet non-Gaussian processes. We will define ggBM with a random diffusivity in more detail in the next section 3, and in the following demonstrate that ggBM is equivalent to the ST limit of the DD model.

Recently the idea of DD has received considerable attention. According to this approach, in addition to the introduction of a population of diffusivities, each particle during its motion is affected by a continuously changing diffusivity. Chubynsky and Slater first introduced this model describing the dynamics of the diffusion coefficient by a biased, stationary random walk with reflecting boundary conditions [83]. With this assumption the diffusivity changes slowly step by step, in the ST limit giving rise to normal diffusion with exponential displacement PDF⁶. In the long time (LT) regime simulations showed a crossover to Gaussian diffusion with a single, effective diffusion coefficient [83]. In a more recent work a direct test of the DD mechanism for diffusion in inhomogeneous media is reported [86].

The DD concept was further studied by Jain and Sebastian [87, 88] and Chechkin *et al* [67]. While Jain and Sebastian use a path integral approach, Chechkin *et al* invoke the concept of subordination and an explicit exact solution for the PDF in Fourier space. Despite the different mathematical approach, both models recover the linear trend of the MSD and a distribution of displacements that at ST is exponential, while, at LT, it crosses over to a Gaussian with effective diffusivity, in agreement with the results in [83]. Tyagi and Cherayil [89] present a hybrid procedure between the two approaches, finding that the modulation of white noise by any stochastic process, whose time correlation function decays exponentially, is likely to have features similar to the ones obtained in [67, 83, 87, 88]. As a recent result we also report the work by Lanoiselée and Grebenkov in which the concept of DD is further investigated, for instance, with respect to time averages and ergodicity breaking properties [90].

In this paper we present a detailed comparison between the concept of ggBM with random diffusivity and the DD model. The main difference between the DD and ggBM model is represented by the interaction between environment and particles. On the one hand, in the DD model two different statistical levels are taken into account, one for the motion of the environment and one for the motion of the particles. The relation between these two gives rise to specific characteristics. Thus, at ST the slow variability of the environment guarantees the superstatistical limit. In the LT regime the diffusivity reaches a stationary average value leading the particles to develop a Gaussian statistic. On the other hand, the ggBM model does not directly involve an environment dynamics but only implies a dynamics in which the statistical features of the environment continuously drives the particles in their motion, see below for more details.

⁶This approach has some commonalities in spirit with the correlated continuous time random walk model [84, 85].

Concretely, for both ggBM and DD models a set of stochastic equations is introduced to generate a random diffusivity with a well defined stationary distribution. Until now mainly exponential or Gamma distributions have been considered for the random diffusivity. We here base the discussion on the generalised Gamma distribution, which represents an even broader class of distributions including the ones mentioned above, as particular cases. We define the generalised Gamma distribution by

$$\gamma_{\nu,\eta}^{\text{gen}}(D) = \frac{\eta}{D_*^\nu \Gamma(\nu/\eta)} D^{\nu-1} \exp\left(-\left[\frac{D}{D_*}\right]^\eta\right), \quad (4)$$

where D_* is a positive and dimensional constant and ν and η are positive constants. This distribution encodes the n th order stationary moments

$$\langle D^n \rangle_{\text{stat}} = D_*^n \frac{\Gamma([\nu + n]/\eta)}{\Gamma(\nu/\eta)}. \quad (5)$$

The choice of the generalised Gamma distribution is based on experimental evidence demonstrating its role as a versatile description for generalised distributions in various complex systems. Indeed, in the context of superstatistics the generalised Gamma distribution was studied by Beck in [91]. Importantly, the generalised Gamma distribution includes those cases labelled as Gamma or exponential distribution that have already shown good agreement with several systems [53, 55–57]. Moreover it comprises the cases of stretched and compressed exponential distributions which may be useful for the interpretation of various systems [26, 53, 92, 93].

In the following we generalise the ggBM model from [78–82] to incorporate the generalised Gamma function (4). We then demonstrate how to reformulate the Ornstein–Uhlenbeck picture of the DD minimal model [67] and the closely related DD models [83, 87, 88] to include the distribution (4). With this extension both models are considerably more flexible for the description of measured data. Moreover, we will show that the ggBM model is a powerful stochastic representation of the superstatistics approach, and that the ggBM model equals the ST limit of the DD model. Finally, we consider non-equilibrium conditions in the DD model and propose a non-equilibrium extension of the ggBM model to consider similar effects in the stochastic setting of superstatistics. Such non-equilibrium initial conditions represent an important extension of the random diffusivity models, especially for experimentally relevant cases of single particle trajectory measurements.

3. Generalised grey Brownian motion with random diffusivity

GgBM is defined through the stochastic equation [78–82]

$$X_{\text{ggBM}}(t) = \sqrt{2D} \times W(t), \quad (6)$$

for the particle trajectory $X_{\text{ggBM}}(t)$, in which $W(t) = \int_0^t \xi(t') dt'$ is standard Brownian motion, the Wiener process defined as the integral over the white Gaussian noise $\xi(t)$ with zero mean. Moreover, D is a random diffusivity, here taken to be distributed according to the generalised Gamma distribution (4). The idea is that different, but physically identical particles move in disjointed environments, in which they experience different diffusivities, the essential view of the superstatistics approach. Alternatively, we could also think of physically different particles, with different diffusion coefficients, moving in an identical environment. The latter could, for instance, correspond to an ensemble of tracer beads with varying radius or different surface properties.

More mathematically speaking, ggBM is defined through the explicit construction of the underlying probability space based on self-similar increments, and it can be represented by the stochastic equation $X_{\text{ggBM}} = \sqrt{\Lambda} X_g$, where Λ is an independent, non-negative random variable, and X_g is a Gaussian process [78–82]. The characterisation of this class has also been studied for the case when X_g is a standard FBM and Λ is distributed according to the quite general class of M –Wright functions [81, 94]. We note that the definition (6) is similar to the superstatistical Langevin equation models in [65, 77].

Figure 1 shows trajectories obtained from direct simulations of the scheme (6), for which the diffusivity values D are chosen from the generalised Gamma distribution (4). As a result we obtain a Brownian motion characterised by a random amplitude, as demonstrated explicitly by the MSD plots for the same trajectories shown in the bottom panel of figure 1. For the value $\nu = 1.5$ (right panels) larger D values are observed, in accordance with the shape of the distribution (4). The ggBM description is indeed close to the superstatistical concept and fundamentally different from the time evolution of the sample paths for the DD model, compare figure 7. However, at very ST both processes look much alike, as the DD model at ST will be shown to reduce to the ggBM model.

The particle displacement distribution can be recovered following Pagnini and Paradisi [94]. If we define with Z_1 and Z_2 two real independent random variables whose PDFs are $p_1(z_1)$ and $p_2(z_2)$ with $-\infty \leq z_1 \leq +\infty$ and $0 \leq z_2 \leq +\infty$, respectively, and with the random variable Z obtained by the product of Z_1 and Z_2 , that is,

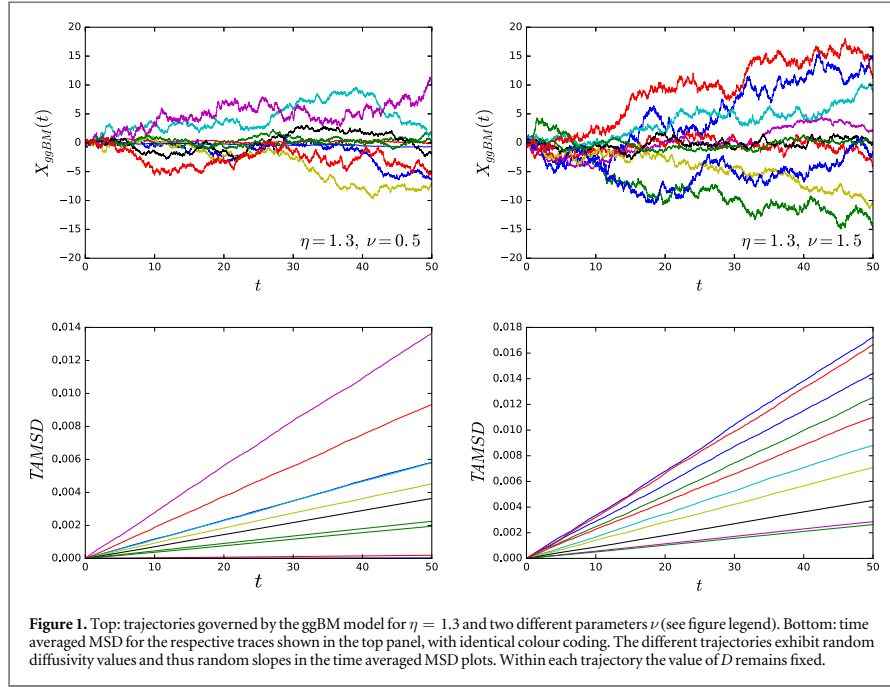


Figure 1. Top: trajectories governed by the ggBM model for $\eta = 1.3$ and two different parameters ν (see figure legend). Bottom: time averaged MSD for the respective traces shown in the top panel, with identical colour coding. The different trajectories exhibit random diffusivity values and thus random slopes in the time averaged MSD plots. Within each trajectory the value of D remains fixed.

$Z = Z_1 Z_2^{-1}$, then, if we denote the PDF of Z with $p(z)$, we find that

$$p(z) = \int_0^\infty p_1\left(\frac{z}{\lambda'}\right) p_2(\lambda) \frac{d\lambda}{\lambda'}. \tag{7}$$

In the present case we identify $X_{\text{ggBM}}(t)$, $W(t)$, and the random diffusivity D with Z, Z_1 , and Z_2 , respectively. The PDF for the particle displacement encoded by equations (6) and (7) is given by

$$\begin{aligned} f_{\text{ggBM}}(x, t) &= \int_0^\infty \frac{1}{\sqrt{2\pi t}} \exp\left(-\frac{(x/\sqrt{2D})^2}{2t}\right) p_D(D) \frac{dD}{\sqrt{2D}} \\ &= \int_0^\infty \frac{1}{\sqrt{4\pi D t}} \exp\left(-\frac{x^2}{4D t}\right) p_D(D) dD \\ &= \int_0^\infty G(x, t|D) p_D(D) dD, \end{aligned} \tag{8}$$

where $G(x, t|D)$ is the Gaussian distribution (2) for given D . Such a representation of the PDF corresponds to the one of the superstatistical approach, proving the similarity of the two methods. The distribution $p_D(D)$ is defined in (4) and the integral in (8), which can be solved exactly through different methods (appendix), provides the result (A.6) in terms of a Fox H -function (see appendix, where also the series expansion is given). The asymptotic behaviour of this result acquires the generalised exponential shape

$$f_{\text{ggBM}}(x, t) \sim \frac{(x^2/[4D_* t])^{(2\nu-\eta-1)/(2(\eta+1))}}{\Gamma(\nu/\eta) \sqrt{4\pi D_* t}} \exp\left(-\frac{\eta+1}{\eta} \eta^{\frac{1}{\eta+1}} \left[\frac{x^2}{4D_* t}\right]^{\eta/(\eta+1)}\right). \tag{9}$$

In particular, the choice $\eta = 1$ leads us back to exponential distributions, with power-law prefactor. Figure 2 demonstrates the agreement between the analytical result (9) for the PDF and the result of stochastic simulations of the underlying ggBM process, for different times and a fixed set of the parameters ν and η . In particular, we see that the shape of the distribution remains invariant—as for the superstatistical approach—and in contrast to the DD model analysed below.

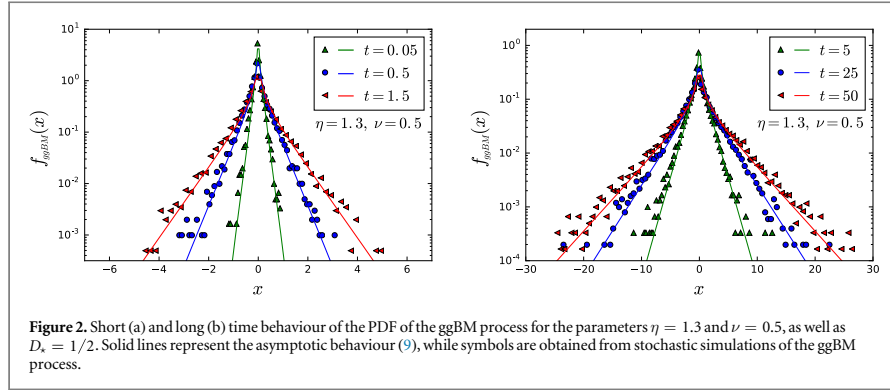


Figure 2. Short (a) and long (b) time behaviour of the PDF of the ggBM process for the parameters $\eta = 1.3$ and $\nu = 0.5$, as well as $D_* = 1/2$. Solid lines represent the asymptotic behaviour (9), while symbols are obtained from stochastic simulations of the ggBM process.

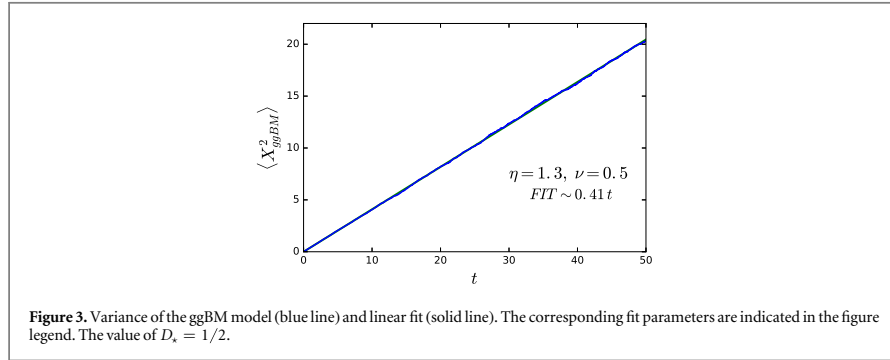


Figure 3. Variance of the ggBM model (blue line) and linear fit (solid line). The corresponding fit parameters are indicated in the figure legend. The value of $D_* = 1/2$.

The MSD follows immediately from the following transformations,

$$\begin{aligned}
 \langle X_{ggBM}^2(t) \rangle &= \int_{-\infty}^{\infty} x^2 f_{ggBM}(x, t) dx \\
 &= \int_0^{\infty} p_D(D) \int_{-\infty}^{\infty} x^2 G(x, t|D) dx dD \\
 &= \int_0^{\infty} p_D(D) 2Dt dD = 2t \int_0^{\infty} D p_D(D) dD \\
 &= 2 \langle D \rangle_{stat} t,
 \end{aligned}
 \tag{10}$$

where, according to (5), the effective diffusivity becomes

$$\langle D \rangle_{stat} = D_* \Gamma([\nu + 1]/\eta) / \Gamma(\nu/\eta).
 \tag{11}$$

Figure 3 demonstrates the linearity of the variance. The fitted parameters are consistent with the model prediction, $\langle D \rangle_{stat} = 0.20$ comparing to the values chosen in the simulations.

By means of the ggBM approach and with the introduction of a generalised Gamma distribution for the diffusivity we are able to reproduce a diffusive motion with a linear scaling of the MSD and a PDF characterised by a stretched or compressed Gaussian with a power-law prefactor. This is our first main result.

4. Diffusing diffusivity: stochastic equations for random diffusivity

We now consider the diffusion coefficient $D(t)$ to be a random function of time, defined by means of the auxiliary variable $Y(t)$ through $D(t) = Y^2(t)$, similarly to the DD minimal model introduced earlier [67]. Our goal is to construct a stochastic equation for the additional variable $Y(t)$ such that the stationary PDF for its square is the generalised Gamma distribution in (4). Thus, our present model is represented by the following set of stochastic equations

$$dY = a(Y)dt + \sigma \times dW(t)
 \tag{12a}$$

$$D(t) = Y^2(t), \tag{12b}$$

where $a(Y)$ is a nonlinear function whose explicit shape is obtained below, σ is a constant and $W(t)$ is a Wiener process with variance $\langle W^2(t) \rangle = t$. The physical dimension of the auxiliary variable is $[Y] = \text{cm s}^{-1/2}$ and for the constant σ we have $[\sigma] = \text{cm s}^{-1}$.

Our approach is based on the central idea that it is possible to establish a direct relation between the PDFs of the two variables $Y(t)$ and $D(t)$. This allows us to introduce a completely new dynamics for the auxiliary variable. Such a dynamics, even though more complex, allows to reproduce a more general class of PDFs for the random diffusivity and thus provides a significant extension of the DD model, which will be our second main result.

To proceed we set $p(Y, t)$ to represent the PDF of the process $Y(t)$ described in (12a). It fulfils the Fokker–Plank equation [9]

$$\frac{\partial p(Y, t)}{\partial t} + \frac{\partial a(Y)p(Y, t)}{\partial Y} = \frac{\sigma^2}{2} \frac{\partial^2 p(Y, t)}{\partial Y^2}. \tag{13}$$

Considering the stationary situation the corresponding time independent PDF $p_Y(Y)$ fulfils the equation

$$\frac{\partial a(Y)p_Y(Y)}{\partial Y} = \frac{\sigma^2}{2} \frac{\partial^2 p_Y(Y)}{\partial Y^2}, \tag{14}$$

from which we infer the relation

$$a(Y) = \frac{\sigma^2}{2p_Y(Y)} \frac{\partial p_Y(Y)}{\partial Y}, \tag{15}$$

directly relating the drift coefficient $a(Y)$ with the stationary distribution of $Y(t)$ [95].

We then recall that, given two random variables Z_1 and Z_2 related by $Z_2 = g(Z_1)$, for appropriate functions $g(z)$ we have [96]

$$p_{Z_2}(z_2) = p_{Z_1}(g^{-1}(z_2)) \left| \frac{d}{dz_2} g^{-1}(z_2) \right|. \tag{16}$$

This implies that the distributions of the variables $Y(t)$ and $D(t)$ are related via

$$p_Y(Y, t) = |Y| p_D(Y^2, t). \tag{17}$$

Based on this we construct a set of stochastic equations for the desired quantity $D(t)$. Starting from the chosen stationary distribution $p_D(D)$ of the random diffusivity we define the stationary distribution $p_Y(Y)$ for the auxiliary variable $Y(t)$ by means of equation (17). Finally relation (15) allows us to recover the suitable coefficient $a(Y)$ in equation (12a). Following the described scheme for the generalised Gamma distribution (4) we obtain

$$p_Y(Y) = |Y| \frac{\eta}{D_*^\nu \Gamma(\nu/\eta)} Y^{2(\nu-1)} \exp\left(-\left[\frac{Y}{\sqrt{D_*}}\right]^{2\eta}\right), \tag{18}$$

and thus

$$\frac{\partial p_Y(Y)}{\partial Y}(Y) = \frac{\eta \operatorname{sgn}(Y)}{D_*^\nu \Gamma(\nu/\eta)} Y^{2(\nu-1)} \exp\left(-\left[\frac{Y}{\sqrt{D_*}}\right]^{2\eta}\right) \left(2\nu - 1 - 2\eta \left[\frac{Y}{\sqrt{D_*}}\right]^{2\eta}\right). \tag{19}$$

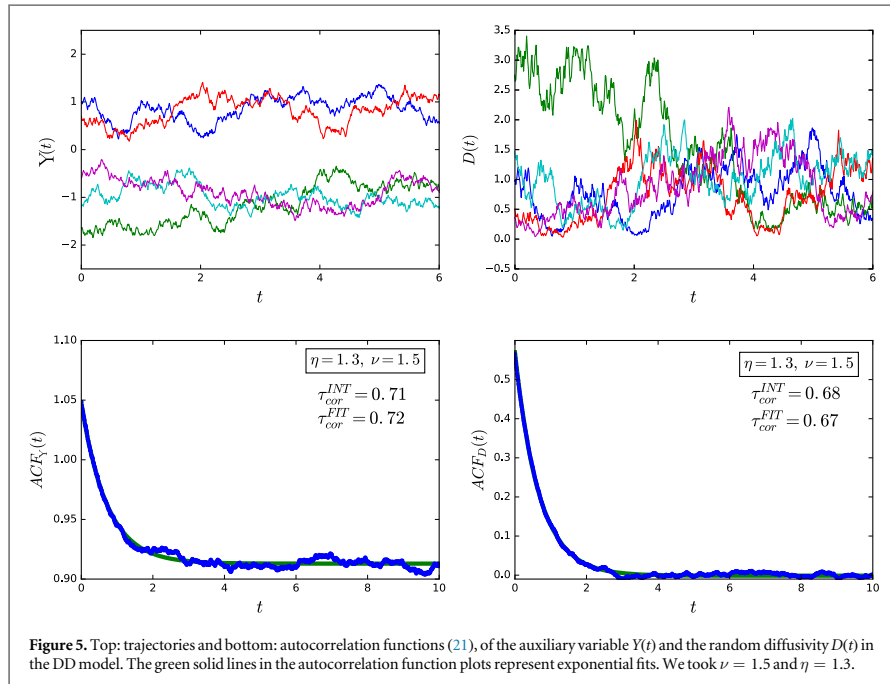
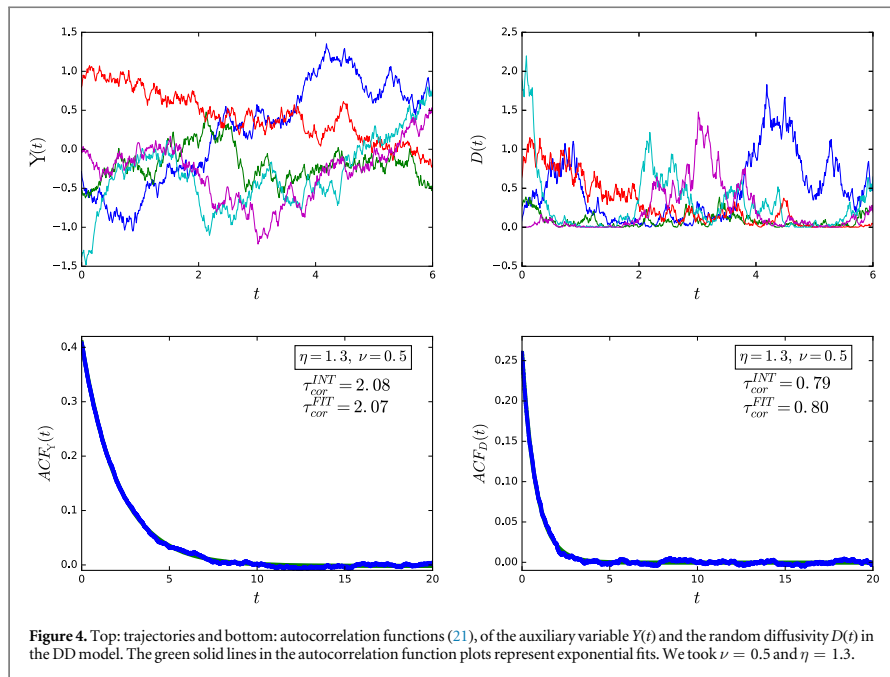
This finally leads us to the desired drift coefficient

$$a(Y) = \frac{\sigma^2}{2Y} \left(2\nu - 1 - 2\eta \left[\frac{Y}{\sqrt{D_*}}\right]^{2\eta}\right). \tag{20}$$

The stochastic equations (12a) together with the explicit form (20) of the drift coefficient for the diffusivity fluctuations provide a complete and generalised analogue of the DD model, which is extremely flexible for the modelling of experimental data.

We notice that in the particular case of $\nu = 0.5$ and $\eta = 1$ we recover the Ornstein–Uhlenbeck model (diffusion in an harmonic potential) considered in the original minimal DD model [67]. As already remarked in [67] in this setting the resulting stochastic equation for $D(t)$ is nothing else than the Heston model, that is widely used in financial mathematics and specifies the time evolution of the stochastic volatility of a given asset [90, 97, 98].

Equation (12a) can be readily solved numerically with initial conditions taken randomly from the equilibrium distribution (18). Figures 4 and 5 show sample time evolutions of the auxiliary variable Y and the diffusivity $D = Y^2$ for the DD process based on the steady state generalised Gamma distribution, as obtained below. We note that for the case $\nu = 0.5$ in figure 4 the sample paths of the variable $Y(t)$ frequently cross the zero line, while for the case $\nu = 1.5$ in figure 5 the zero line is avoided, corresponding to the uni- and bimodal shapes of the PDFs of the variable $Y(t)$ evaluated in figure 6. The existence of a pole in the generalised Gamma



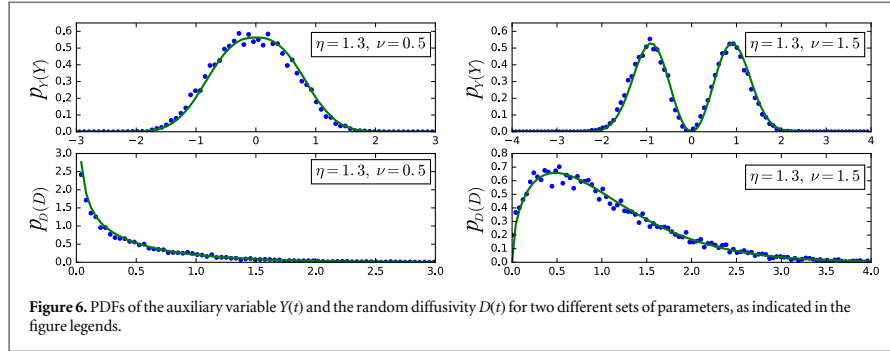


Figure 6. PDFs of the auxiliary variable $Y(t)$ and the random diffusivity $D(t)$ for two different sets of parameters, as indicated in the figure legends.

distribution (4) at $D = 0$ for the case $\nu = 0.5$ thus creates a very different behaviour than for the case $\nu = 1.5$ without singularity. For the diffusivity variable $D(t)$ in figures 4 and 5 the regions of $Y(t)$ close to the zero line lead to smaller $D(t)$ values in the same regions. Finally, figures 4 and 5 demonstrate the exponential shape of the autocorrelation functions for both $Y(t)$ and $D(t)$,

$$\text{ACF}_Y(t, t') = \langle (Y(t) - \langle Y \rangle)(Y(t + t') - \langle Y \rangle) \rangle \tag{21}$$

and an analogous expression for $D(t)$.

We know from previous studies of DD models that the correlation time of the random diffusivity represents a key factor in the study of the particle dynamics. The correlation time τ_c is evaluated both by means of a two-parametric numerical fit to the exponential function and through the integral

$$\tau_c \sim \frac{1}{\text{ACF}(0)} \int_0^\infty \text{ACF}(\tau) d\tau, \tag{22}$$

which is exact for pure exponential autocorrelation functions. The results obtained by the two methods are reported in figure 4 and 5 and they are in excellent agreement, from which we conclude that the diffusivity autocorrelation is exponential to leading order and thus the correlation time τ_c well defined.

It is interesting to notice that the auxiliary function $Y(t)$ in the case of a bimodal distribution possesses a non-zero correlation function in the stationary state. This is due to the fact that despite a vanishing global mean of the PDF, depending on the initial setting each trajectory is representative of only one side of the bimodal PDF.

5. A generalised minimal model for DD

With the set of equations defined in section 4 we can consider the generalisation of the DD minimal model described in [67], and obtain the process in position space, $X_{\text{DD}}(t)$. Recalling the idea of introducing an analytic description for the dynamics of the random diffusivity, we take that the motion of the particle is defined by the integral version of the overdamped Langevin equation,

$$X_{\text{DD}}(t) = \int_0^t \sqrt{2D(t')} \times \xi(t') dt', \tag{23}$$

where $\xi(t)$ is white Gaussian noise and $D(t)$ is the random time-dependent diffusivity obtained in section 4. This dynamics based on the above results for the diffusivity dynamics generalises the idea introduced in [67], where an Ornstein–Uhlenbeck process was selected for the auxiliary variable. Figure 7 shows trajectories obtained from the stochastic equation (23) where the diffusivity was generated from (12a) with initial conditions taken randomly from the stationary distribution. In ggBM each trajectory has the same D value, while in the DD model the value of D changes as function of time. In turn, individual trajectories of the DD model are quite similar.

Since the DD model is a direct generalisation of the minimal DD model we expect a crossover to a Gaussian displacement PDF for times longer than the correlation time τ_c . We thus carry on our analysis for the ST and LT regimes separately, before analysing the MSD and kurtosis of this DD process.

5.1. Short time regime

Since the dynamics of the environment is determined by the correlation time τ_c we expect that on ST scales with $t \ll \tau_c$ the diffusion coefficient is approximately fixed for each particle and we thus suppose the validity of a superstatistical description at ST,

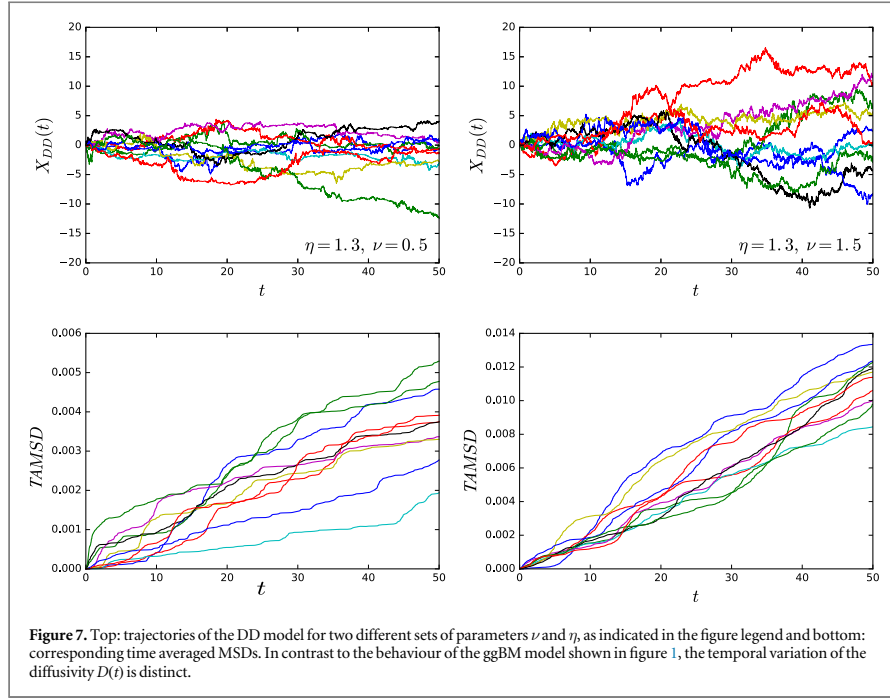


Figure 7. Top: trajectories of the DD model for two different sets of parameters ν and η , as indicated in the figure legend and bottom: corresponding time averaged MSDs. In contrast to the behaviour of the ggBM model shown in figure 1, the temporal variation of the diffusivity $D(t)$ is distinct.

$$X_{DD}^{ST} \sim \sqrt{2D} \int_0^t \xi(t') dt' = \sqrt{2D} \times W(t). \tag{24}$$

The existence of the superstatistical regime at $t \ll \tau_c$ is consistent with the model considered in [67] and with the results reported in [89] concerning the modulation of white noise by any stochastic process whose time correlation function decays exponentially. The superstatistical approach allows us to estimate the ST distribution of the particle displacement by means of

$$f_{DD}^{ST}(x, t) \sim \int_0^\infty p_D(D) G(x, t|D) dD. \tag{25}$$

This representation corresponds to the ggBM scenario established above, which means that we can borrow its results in equations (A.6) and (9), considering that $f_{DD}^{ST}(x, t) \sim f_{ggBM}(x, t)$.

The expected behaviour (9) is confirmed by extensive numerical simulations. Figures 8(a) and 9(a) show the ST PDFs for two different sets of the parameters ν and η , and in both cases we observe excellent agreement with the asymptotic behaviour (9).

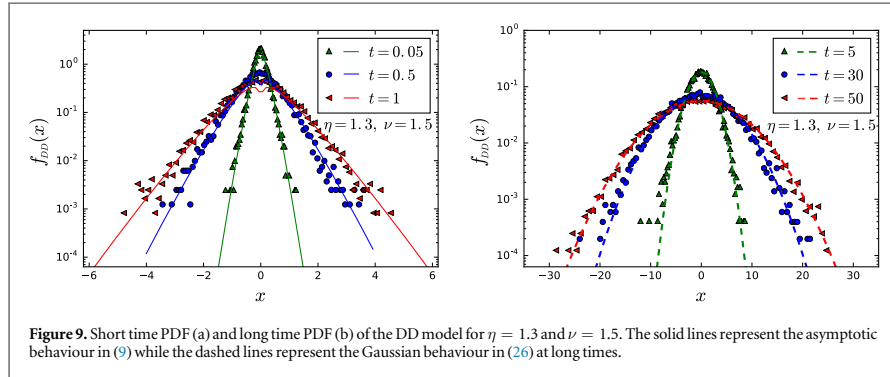
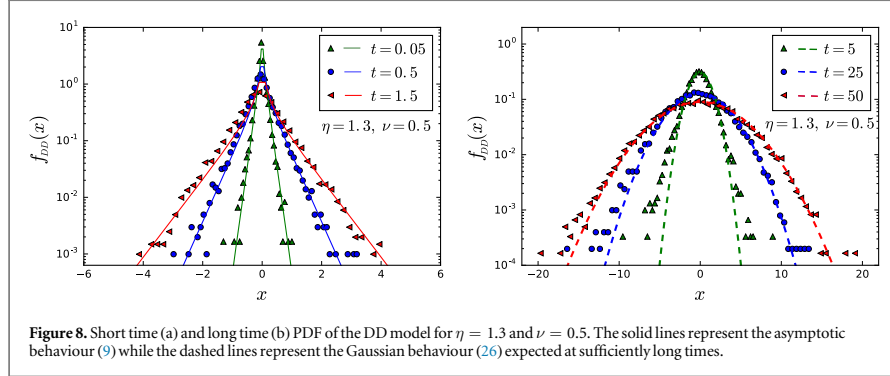
Comparing figure 2 with figure 8(a) we notice that the ggBM model allows one to describe a process that preserves the exact non-Gaussian PDF, which is exactly the same PDF we obtain in the DD model in the ST regime. Both approaches describe the same superstatistical frame but the DD model then crosses over to a Gaussian beyond the correlation time τ_c , see below the discussion of the kurtosis. The establishment of the relation between the DD model and the previously devised ggBM at ST is our third main result.

5.2. Long time regime

At LT, again taking our clue from [67] and from the general results in [89], we expect that eventually a crossover to a Gaussian distribution is observed (as already anticipated in figures 8 and 9). Above the correlation time, that is, for times $t \gg \tau_c$ we thus look for a PDF given by

$$f_{DD}^{LT}(x, t) \sim \frac{1}{\sqrt{4\pi \langle D \rangle_{stat} t}} \exp\left(-\frac{x^2}{4 \langle D \rangle_{stat} t}\right), \tag{26}$$

with the effective diffusivity (11). The numerical results reported in figures 8(b) and 9(b) prove the validity of this behaviour. At sufficient LT the particles have explored all the diffusivity space and a Gaussian behaviour with an effective diffusivity emerges. This leads to a standard Brownian diffusive behaviour. We stress again that the



transition from a non-Gaussian to a Gaussian profile depends on the value of the correlation time τ_c of the diffusivity process.

5.3. Mean squared displacement

For the DD model we found a crossover of the PDF of the spreading particles. An initial non-Gaussian behaviour is slowly replaced by a Gaussian one. The superstatistical behaviour of the DD approach at ST is equivalent to the ggBM model and is characterised by the non-Gaussianity. Nevertheless, as expected from previous studies [67], the MSD does not change in the course of time and is the same at ST and LT regimes. Direct calculation indeed produces the invariant form

$$\langle X_{DD}^2(t) \rangle = 2 \langle D \rangle_{\text{stat}} t. \quad (27)$$

This continuity of the MSD is demonstrated in figure 10, together with a linear fit proving the validity of the linear trend.

5.4. Kurtosis

In what follows the second and fourth moments of the non-Gaussian PDF identified in equations (8) and (25) are studied in terms of the kurtosis that represents one of the first checks for non-Gaussianity. We recall the second order moment calculated in (10) and in a similar way we obtain the fourth order moment

$$\langle X_{\text{ggBM}}^4(t) \rangle = \langle X_{DD}^4(t) \rangle_{\text{ST}} = 12 \langle D^2 \rangle_{\text{stat}} t^2, \quad (28)$$

where $\langle D^2 \rangle_{\text{stat}}$ is the second moment of the diffusivity in the stationary state. By means of results (10) and (28) and recalling the definition of the diffusivity moments in equation (5), the kurtosis $K = \langle x^4(t) \rangle / \langle x^2(t) \rangle^2$ is given by

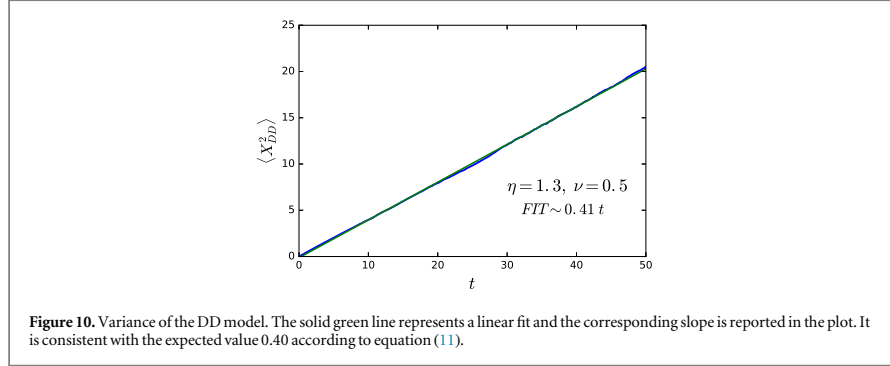


Figure 10. Variance of the DD model. The solid green line represents a linear fit and the corresponding slope is reported in the plot. It is consistent with the expected value 0.40 according to equation (11).

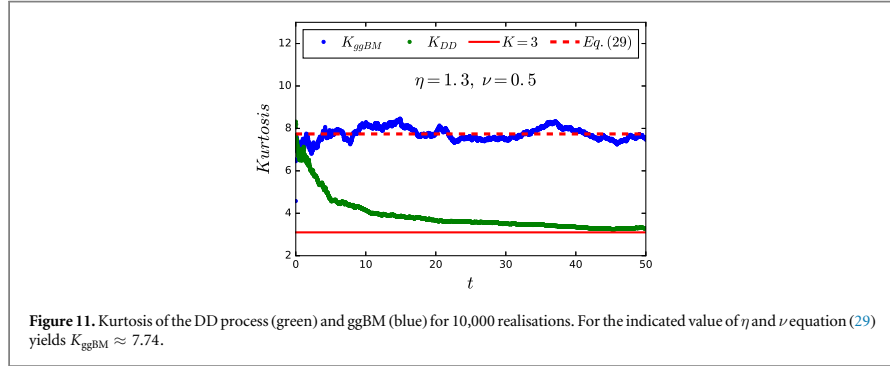


Figure 11. Kurtosis of the DD process (green) and ggBM (blue) for 10,000 realisations. For the indicated value of η and ν equation (29) yields $K_{\text{ggBM}} \approx 7.74$.

$$\begin{aligned}
 K_{\text{ggBM}} &= K_{\text{DD}}^{\text{ST}} = 4t^2 D_*^2 \frac{3\Gamma([\nu + 2]/\eta)}{\Gamma(\nu/\eta)} \times \frac{1}{4t^2 D_*^2} \left(\frac{\Gamma(\nu/\eta)}{\Gamma([\nu + 1]/\eta)} \right)^2 \\
 &= 3 \frac{\Gamma([\nu + 2]/\eta)\Gamma(\nu/\eta)}{\Gamma([\nu + 1]/\eta)^2} > 3,
 \end{aligned} \tag{29}$$

for ggBM and the short-time DD process. The non-Gaussian PDF represents a leptokurtic behaviour as can be observed in figure 11, showing the kurtosis of the DD and ggBM models. The value for the kurtosis at ST is in agreement with the value reported in (29). At LT the DD kurtosis approaches the value 3 characteristic of the Gaussian distribution, while the ggBM one keeps fluctuating around the same initial value.

6. Non-equilibrium initial conditions

The results discussed above consider equilibrium initial conditions for the diffusivity fluctuations. In particular, results (10) and (27) for the particle MSD exhibit the invariant form $\langle X^2(t) \rangle = 2\langle D \rangle_{\text{stat}} t$ in both cases. Such equilibrium initial conditions will in general not be fulfilled for particles that are initially seeded in a non-equilibrium environment. For instance, in single particle tracking a tracer bead can be introduced into the system at $t = 0$, or similar in computer simulations. After this disturbance the environment equilibrates again. To accommodate for such a case we here study a minimal model for the case of non-equilibrium initial conditions, which leads to another main result of this work. As we are going to see, this non-equilibrium scenario gives rise to differences in the characteristics of the two studied models. In particular, we observe an initial ballistic behaviour. The LT behaviour, of course, does not show differences since in this range the diffusivity reaches its stationary state and we can again consider the results obtained in the previous sections for the LT limit.

We illustrate the role of non-equilibrium conditions by taking a specific, and in fact the simplest, set of parameters, $\nu = 0.5$ and $\eta = 1$. This defines the stochastic dynamical equation in (12a) as

$$D(t) = Y^2(t) \tag{30a}$$

$$dY = -\frac{\sigma^2}{D_*} Y dt + \sigma dW(t), \quad (30b)$$

that corresponds to the well known dynamics of the Ornstein–Uhlenbeck process for the study in [67] with the correlation time $\tau_c = D_*/\sigma^2$. We start considering the related Fokker–Planck equation

$$\frac{\partial}{\partial t} p(Y, t) = \frac{\sigma^2}{D_*} \frac{\partial}{\partial Y} Y p(Y, t) + \frac{\sigma^2}{2} \frac{\partial^2}{\partial Y^2} p(Y, t). \quad (31)$$

We can solve this equation with a non-equilibrium condition, for instance, $p(Y, 0) = \delta(Y - Y_0)$, using the method of characteristics in Fourier space. We readily derive the general solution

$$p(Y, t|Y_0) = (\pi D_* [1 - \exp(-2t\sigma^2/D_*)])^{-1/2} \exp\left(-\frac{(Y - Y_0 \exp(-t\sigma^2/D_*))^2}{D_* (1 - \exp(-2t\sigma^2/D_*))}\right). \quad (32)$$

Recalling relation (16) for the diffusivity PDF we then obtain

$$\begin{aligned} p_D(D, t|D_0 = Y_0^2) &= \frac{1}{2\sqrt{D}} [p(\sqrt{D}, t) + p(-\sqrt{D}, t)] \\ &= (4\pi D_* D [1 - \exp(-2t\sigma^2/D_*)])^{-1/2} \\ &\quad \times \left\{ \exp\left(-\frac{(\sqrt{D} - \sqrt{D_0} \exp(-t\sigma^2/D_*))^2}{D_* (1 - \exp(-2t\sigma^2/D_*))}\right) \right. \\ &\quad \left. + \exp\left(-\frac{(-\sqrt{D} - \sqrt{D_0} \exp(-t\sigma^2/D_*))^2}{D_* (1 - \exp(-2t\sigma^2/D_*))}\right) \right\}. \end{aligned} \quad (33)$$

We point out that in the limit of LT this result provides exactly the stationary distribution described in (4) with the specific set of parameters defined above. This is also verified by the trend of the average value

$$\langle D(t) \rangle = \frac{1}{2} (D_* (1 - e^{-2t\sigma^2/D_*}) + 2D_0 e^{-2t\sigma^2/D_*}), \quad (34)$$

in agreement with result (4).

In contrast to the previous analysis, we observe an explicit dependence on time of $p_D(D, t)$, which makes the calculations more involved. Thus, we select an initial condition for the diffusivity, $D_0 = 0$, which is convenient for the study of the particles displacement distribution. This leads to a reduction in (33), namely,

$$p(D, t|D_0 = 0) = (\pi D_* D (1 - \exp(-2t\sigma^2/D_*)))^{-1/2} \exp\left(\frac{D}{D_* (1 - \exp(-2t\sigma^2/D_*))}\right). \quad (35)$$

We now study the two models in this particular case of a non-equilibrium initial condition for the diffusivity.

6.1. Diffusing diffusivities with non-equilibrium initial diffusivity condition

The dynamics for the diffusivity encoded in equations (30a) and (30b) when choosing the specific set of parameters $\nu = 0.5$ and $\eta = 1$ is the same as described in [67] when $d = n = 1$. Thus, in this paragraph, we extend the description of the minimal DD model studied in [67] to the case of non-equilibrium initial conditions for the diffusivity. In order to proceed with the same notation we introduce dimensionless units for relations (30a) and (30b) as well as for the overdamped Langevin equation describing the particle motion [67], such that the full set of stochastic equations reads

$$\begin{aligned} X_{DD} &= \int_0^t \sqrt{2D(t')} \xi(t') dt' \\ D(t) &= Y^2(t) \\ dY &= -Y dt + dW(t). \end{aligned} \quad (36)$$

A subordination approach can then be used to obtain the distribution of the particle displacement [67], namely,

$$f_{DD}(x, t) = \int_0^\infty T(\tau, t) G(x, \tau) d\tau, \quad (37)$$

where $G(x, \tau)$ is the Gaussian (2) and $T(\tau, t)$ represents the PDF of the process $\tau(t) = \int_0^t Y^2(t') dt'$. Starting from the subordination formula (37) we obtain the relation

$$\hat{f}_{DD}(k, t) = \tilde{T}(s = k^2, t) \quad (38)$$

where with the symbols $\hat{\cdot}$ and $\tilde{\cdot}$ we indicate the Fourier and Laplace transforms, respectively. For the particular initial condition $D_0 = 0$, which is equivalent to $y_0 = 0$, the solution is known [99, 100],

$$\tilde{T}(s, t) = \exp\left(\frac{t}{2}\right) / \left(\frac{1}{\sqrt{1+2s}} \sinh(t\sqrt{1+2s}) + \cosh(t\sqrt{1+2s})\right)^{1/2}. \tag{39}$$

This latter quantity is directly related to the MSD of the particles through [67]

$$\langle X_{DD}^2(t) \rangle = -2 \frac{\partial \tilde{T}(s, t)}{\partial s} \Big|_{s=0}. \tag{40}$$

We readily obtain the closed form result

$$\langle X_{DD}^2(t) \rangle = t - \frac{1}{2}(1 - e^{-2t}) \sim \begin{cases} t^2, & t \ll 1 \\ 2t, & t \gg 1 \end{cases}. \tag{41}$$

The resulting dynamics is thus no longer Brownian at all times. In contrast, at times shorter than the correlation time (in the dimensionless units used here $\tau_c = 1$) we obtain a ballistic scaling of the MSD. This behaviour reflects the fact that the diffusivity equilibration in this case with $D_0 = 0$ leads to an initial acceleration.

Starting from equations (38) and (39) we consider approximations of the PDF for ST and LT which, since we are in dimensionless units, correspond to $t \ll 1$ and $t \gg 1$ respectively. In the ST limit, the Fourier transform of the PDF becomes

$$\hat{f}_{DD}^{ST}(k, t) \sim \frac{(1 + t + t^2/2)^{1/2}}{(1 + t + t^2/2 + k^2 t^2)^{1/2}} \sim \frac{1}{t} \left(k^2 + \frac{1}{t^2}\right)^{-1/2}. \tag{42}$$

Note that this expression is normalised, $\hat{f}_{DD}(k = 0, t) = 1$. After taking the inverse Fourier transform we find

$$\begin{aligned} f_{DD}^{ST}(x, t) &\sim \frac{1}{\pi t} \int_0^\infty \frac{\cos(kx)}{(k^2 + 1/t^2)^{1/2}} dk \\ &= \frac{1}{\pi t} K_0\left(\frac{|x|}{t}\right). \end{aligned} \tag{43}$$

Re-establishing dimensional units, this result becomes

$$f_{DD}^{ST}(x, t) \sim \frac{1}{\pi \sigma t} K_0\left(\frac{|x|}{\sigma t}\right). \tag{44}$$

Here $K_\nu(z)$ is the modified Bessel function of second type. The asymptotic behaviour of this distribution for $|x| \rightarrow \infty$ is the Laplace distribution

$$f_{DD}^{ST}(x, t) \sim \frac{1}{\sqrt{2\pi\sigma t|x|}} \exp\left(-\frac{|x|}{\sigma t}\right). \tag{45}$$

In the LT limit equations (38) and (39) yield

$$\hat{f}_{DD}^{LT}(k, t) \sim \frac{2^{1/2} \exp(t[1 - \sqrt{1 + 2k^2}]/2)}{(1 + 1/\sqrt{1 + 2k^2})^{1/2}}, \tag{46}$$

that again is normalised. If we focus on the tails of the distribution in the limit $k \ll 1$ we obtain the Gaussian

$$\hat{f}_{DD}^{LT}(k, t) \sim \exp(-k^2 t/2) \tag{47}$$

in Fourier space, corresponding to the Gaussian

$$f_{DD}^{LT}(x, t) \sim \frac{1}{\sqrt{2\pi t}} \exp\left(-\frac{x^2}{2t}\right) \tag{48}$$

in direct space. Restoring dimensional units and recalling that $\langle D \rangle_{\text{stat}} = D_*/2$, eventually provides

$$\begin{aligned} f_{DD}^{LT}(x, t) &\sim \frac{1}{\sqrt{2\pi D_* t}} \exp\left(-\frac{x^2}{2D_* t}\right) \\ &= \frac{1}{\sqrt{4\pi \langle D \rangle_{\text{stat}} t}} \exp\left(-\frac{x^2}{4 \langle D \rangle_{\text{stat}} t}\right), \end{aligned} \tag{49}$$

where in the last step we identified the equilibrium value $\langle D \rangle_{\text{stat}}$ of the diffusivity. From the approximations (45) and (49) we readily recover the two limiting scaling laws for the variance in equation (41).

Figure 12 nicely corroborates these findings, comparing the non-equilibrium DD model results for the PDF obtained above with results from stochastic simulations. The crossover behaviour of the associated MSD is displayed in figure 13, again showing very good agreement with the theory.

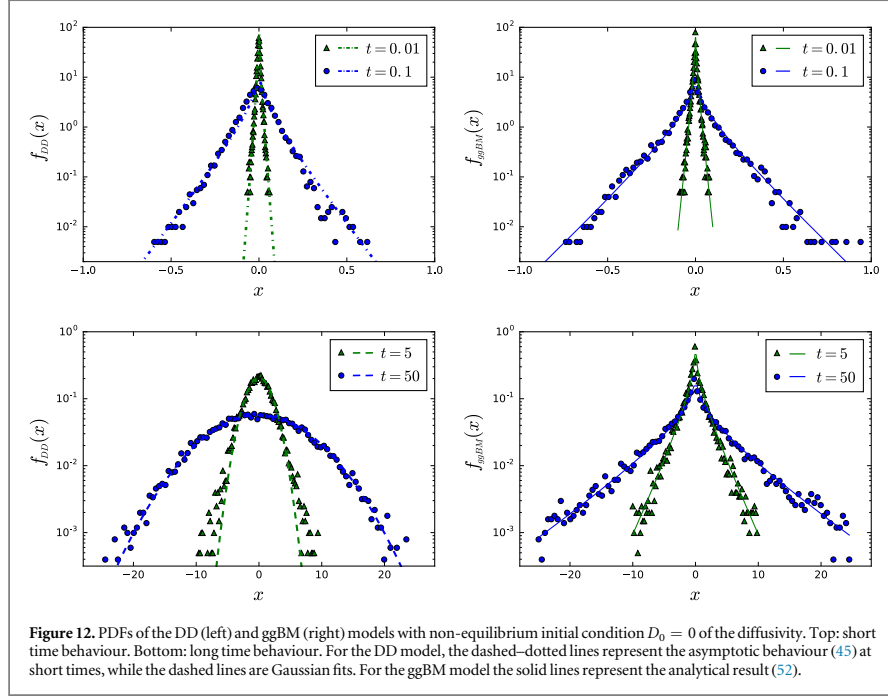


Figure 12. PDFs of the DD (left) and ggBM (right) models with non-equilibrium initial condition $D_0 = 0$ of the diffusivity. Top: short time behaviour. Bottom: long time behaviour. For the DD model, the dashed–dotted lines represent the asymptotic behaviour (45) at short times, while the dashed lines are Gaussian fits. For the ggBM model the solid lines represent the analytical result (52).

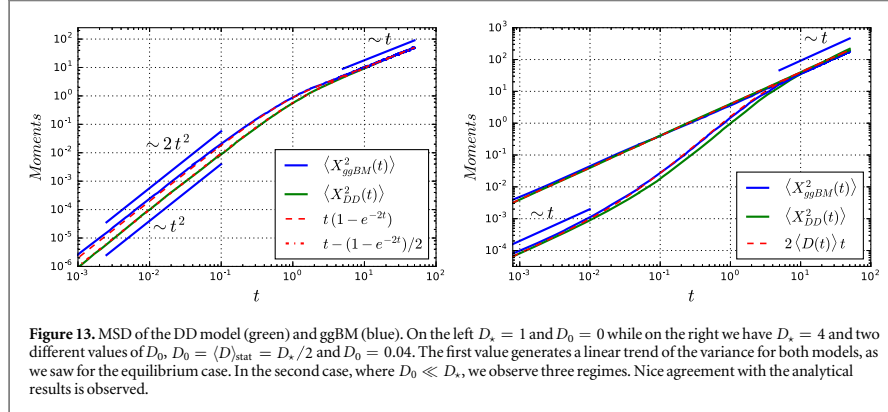


Figure 13. MSD of the DD model (green) and ggBM (blue). On the left $D_s = 1$ and $D_0 = 0$ while on the right we have $D_s = 4$ and two different values of D_0 , $D_0 = (D)_{\text{stat}} = D_s/2$ and $D_0 = 0.04$. The first value generates a linear trend of the variance for both models, as we saw for the equilibrium case. In the second case, where $D_0 \ll D_s$, we observe three regimes. Nice agreement with the analytical results is observed.

6.2. Non-equilibrium ggBM

The ggBM model discussed in section 3 is based on the static distribution $p_D(D)$ of the diffusivity. In order to explore non-equilibrium effects as discussed above for the DD model also within the superstatistical approach, we here propose a non-equilibrium generalisation of the ggBM model. Thus, we generalise the standard ggBM definition (6) and introduce a variability of D in time, according to the stochastic equation

$$X_{\text{ggBM}}(t) = \sqrt{2D(t)} \times W(t). \quad (50)$$

Physically, this new concept may be interpreted as fluctuations of the disjointed environments experienced by the different particles or to temporal changes of the particle size, for instance, due to agglomeration–separation dynamics.

Based on the definition (50) it is then straightforward to take the dynamics of $D(t)$ to be the same as the one considered for the DD model. This guarantees that the ensemble properties of this generalised process (50) are

exactly the same as the ones of the standard ggBM model studied in section 3. In particular, the dependence on time of the diffusivity does not affect the validity of equation (7), so in order to estimate the PDF of the particle displacement of the ggBM model, we consider the distribution (35) in the calculation of the integral

$$f_{\text{ggBM}}(x, t|D_0) = \int_0^\infty p_D(D, t|D_0)G(x, t|D)dD, \tag{51}$$

which may be defined in general as a dynamic superstatistics because of the dependence of $p_D(D, t)$ on t . We obtain an explicit solution by means of the Mellin transform following the same procedure as described in appendix A.2,

$$f_{\text{ggBM}}(x, t|D_0 = 0) = (\pi^2 D_* t (1 - \exp(-2t\sigma^2/D_*))^{-1/2} \times K_0\left(\frac{|x|}{\sqrt{D_* t (1 - \exp(-2t\sigma^2/D_*))}}\right), \tag{52}$$

where $K_\nu(z)$ is the modified Bessel function of second type. The asymptotic behaviour for $|x| \rightarrow \infty$ is given by the exponential

$$f_{\text{ggBM}}(x, t|D_0 = 0) \sim \frac{1}{\sqrt{2\pi|x|\sqrt{D_* t (1 - \exp(-2t\sigma^2/D_*))}}} \exp\left(-\frac{|x|}{\sqrt{D_* t (1 - \exp(-2t\sigma^2/D_*))}}\right). \tag{53}$$

However, in comparison with the result (9) in the equilibrium situation we now observe a different time scaling in the exponent. For ST we see that

$$f_{\text{ggBM}}^{\text{ST}}(x, t|D_0 = 0) \sim \frac{1}{\sqrt{\sqrt{2}\pi\sigma t|x|}} \exp\left(-\frac{|x|}{\sqrt{2}\sigma t}\right), \tag{54}$$

while at LT

$$f_{\text{ggBM}}^{\text{LT}}(x, t|D_0 = 0) \sim \frac{1}{\sqrt{2\pi|x|\sqrt{D_* t}}} \exp\left(-\frac{|x|}{\sqrt{D_* t}}\right). \tag{55}$$

Comparing the ST PDF in (54) with the DD model obtained in (45) we notice that they show a difference in the time scaling of a factor $\sqrt{2}$ which is exactly what we observe in figure 12.

Starting from equation (51) the MSD can be written as

$$\begin{aligned} \langle X_{\text{ggBM}}^2(t) \rangle &= \langle (\sqrt{2D(t)} W(t))^2 \rangle = 2\langle D(t) \rangle t \\ &= [D_*(1 - e^{-2t\sigma^2/D_*}) + 2D_0 e^{-2t\sigma^2/D_*}]t. \end{aligned} \tag{56}$$

Note that this result is valid for any initial conditions D_0 , not only for the case $D_0 = 0$. As already suggested above, the scaling of the variance is no longer linear at all times. According to the relation between the parameters it is possible to observe the different scaling behaviours

$$\langle X_{\text{ggBM}}^2(t) \rangle = \begin{cases} 2D_0 t, & \sigma^2 t \ll D_0 \\ 2D_0 t + 2\sigma^2 t^2, & D_0 \ll \sigma^2 t \ll D_*, \quad 0 \leq D_0 \ll D_*, \\ D_* t, & \sigma^2 t \gg D_* \end{cases} \tag{57}$$

$$\langle X_{\text{ggBM}}^2(t) \rangle = \begin{cases} 2D_0 t - 4\sigma^2(D_0/D_*)t^2 & \sigma^2 t \ll D_* \\ D_* t & \sigma^2 t \gg D_* \end{cases} \text{ elsewhere.} \tag{58}$$

Thus, when $D_0 \ll D_*$ we observe three regimes for the MSD. When $D_0 = 0$ or when the relation $D_0 \ll D_*$ does not hold we directly observe an initial ballistic behaviour followed by the stationary linear trend. This behaviour is nicely corroborated in figure 13.

7. Conclusions

A growing range of systems are being revealed which exhibit Brownian yet non-Gaussian diffusion dynamics. Often, an exponential (Laplace) shape of the displacement PDF is observed, however, also stretched Gaussian shapes have been reported. The comparison of diffusion processes recorded by new experimental techniques suggests that the complexity and inhomogeneity of the medium, interpreted as the cause of non-Gaussian behaviour, may influence the spreading of particles in specific fashion and at different levels. In particular, experiments have demonstrated that a non-Gaussian dynamic may persist throughout the observation window and that there are systems that, instead, at LT, exhibit a crossover to Gaussian diffusion. In this article we introduced an analytic approach to generate a random and time-dependent diffusivity with specific features and

we proposed two possible models for the spreading dynamics of particles in complex systems: one belonging to the class of ggBM and the other supporting the idea of DD.

We saw that the two models have in common the idea that the non-Gaussianity of the PDF is a direct consequence of an inhomogeneity of the environment, represented by a population of diffusivities. The same PDF for the random diffusivity was introduced for both models. We defined an operative set of dynamic stochastic equations to study random diffusivity effects within the broad class of generalised Gamma distributions. This includes the Gamma distribution, or the exponential PDF which produces the Laplace distribution for the particle displacements.

We observed that the main difference between the ggBM and the DD model is the description of the particle dynamics in the LT regime, corresponding to different physical scenarios for the environment. GgBM does not consider an active dynamics of the environment, and the characteristic that mainly influences the particle motion is the randomness of the medium. This means that the statistical features of the medium completely drive the particles in their entire motion. In contrast the DD model supports the idea of randomly evolving diffusivity corresponding to a dynamics also for the environment. In this way the particles evolve experiencing both a continuous variability in time and a stochasticity in the ensemble. The first model delineates a specific non-Gaussian dynamics for the entire diffusion process, while the second allows to describe a transition from a non-Gaussian to a Gaussian diffusion. In fact, it was shown that the ST non-Gaussian dynamics is the same in the two models, whereas at longer times the ggBM model retains the diffusivity distribution and the DD model leads to an effective value for the diffusivity.

We here also studied the influence of non-equilibrium initial conditions for the diffusivity dynamics and found two main effects. First, the non-equilibrium case breaks the equivalence of the DD and the dynamic generalisation of the ggBM models at ST and, second, it causes changes in the temporal evolution of the MSD. In this case the ggBM model, which in the static case we showed to represent a stochastic interpretation of superstatistical Brownian motion, describes what we may call a dynamical superstatistics that leads to the presence of different time scaling regimes in the process. The DD model, which we investigated in this case via a subordination approach, at ST can no longer be described through a superstatistic approximation, since the subordination results in that regime diverge from the behaviour of ggBM. Furthermore we observed different time scaling regimes for the DD model, as well. Nevertheless, we note that for both models we never obtained an anomalous time scaling for the MSD, only a crossover between ballistic and linear (Brownian or Fickian) behaviour. In the LT regime we obtained a description of the two models which is in agreement with the one for the equilibrium case, as it should be.

It will be interesting to generalise the present findings to anomalous dynamics with stochastic diffusivity by implementing different types of noise. Maintaining the same population of diffusivities the results obtained for the PDF of the particle displacement will not be affected, yet the MSD scaling will become anomalous.

Acknowledgements

AVC and RM acknowledge funding from the DFG within project ME 1535/6-1. This research is supported by the Basque Government through the BERC 2014–2017 programme and by the Spanish Ministry of Economy and Competitiveness MINECO through BCAM Severo Ochoa excellence accreditation SEV-2013-0323 and through project MTM2016-76016-R MIP.

Appendix. Computation of the superstatistical integral

In this appendix we provide different methods to solve the integral representing the non-Gaussian PDF of the two models discussed in this work,

$$\bar{P}(x, t) = \int_0^\infty p_D(D) G(x, t|D) dD, \quad (\text{A.1})$$

where $G(x, t|D)$ represents a Gaussian distribution and $p_D(D)$ is the generalised Gamma distribution (4).

A.1. Computation via Fox H -function

Recalling equation (A.1) we have

$$\begin{aligned} \bar{P}(x, t) &= \int_0^\infty \frac{\eta}{D_*^\nu \Gamma(\nu/\eta)} D^{\nu-1} e^{-(D/D_*)^\eta} \frac{1}{\sqrt{4\pi Dt}} e^{-\frac{x^2}{4Dt}} dD \\ &= \frac{\eta}{D_*^\nu \Gamma(\nu/\eta) \sqrt{4\pi t}} \int_0^\infty D^{\nu-3/2} e^{-D^\eta} e^{-\lambda D_*/D} dD, \end{aligned} \quad (\text{A.2})$$

where we set $\lambda = x^2/4D_*t$. Changing the variable of integration to $y = (D/D_*)^\eta$ we get

$$\begin{aligned} \bar{P}(x, t) &= \frac{\eta}{\Gamma(\nu/\eta)\sqrt{4\pi D_*t}} \int_0^\infty y^{\frac{\nu-3/2}{\eta}} e^{-y} e^{-\lambda y^{-1/\eta}} \frac{1}{\eta} y^{\frac{1}{\eta}-1} dy \\ &= \frac{1}{\Gamma(\nu/\eta)\sqrt{4\pi D_*t}} \int_0^\infty y^{-1-(1/2-\nu)/\eta} e^{-y-\lambda y^{-1/\eta}} dy. \end{aligned} \tag{A.3}$$

With the identification

$$e^{-z} = H_{0,1}^{1,0} \left[z \mid \overline{(0, 1)} \right] \tag{A.4}$$

with the Fox H -function and exploiting some (very convenient) properties of the H -function [101] we then obtain

$$\bar{P}(x, t) = \frac{1}{\Gamma(\nu/\eta)\sqrt{4\pi D_*t}} H_{0,2}^{2,0} \left[\lambda \mid \overline{((\nu - 1/2)/\eta, 1/\eta)} (0, 1) \right]. \tag{A.5}$$

The Fox function is defined as a generalised Mellin-Barnes integral and has very convenient properties under integral transformations. The Fox function comprises a large range of special functions, including Mejer's G -function, hypergeometric functions, or Bessel functions [102]. In the notation used here the vertical line separates the argument from the function's parameters, and the horizontal line denotes the lack of upper parameters [102].

Recalling that $\lambda = x^2/4D_*t$, we finally obtain

$$\begin{aligned} \bar{P}(x, t) &= \frac{1}{\Gamma(\nu/\eta)\sqrt{4\pi D_*t}} H_{0,2}^{2,0} \left[\frac{x^2}{4D_*t} \mid \overline{((\nu - 1/2)/\eta, 1/\eta)} (0, 1) \right] \\ &= \frac{1}{\Gamma(\nu/\eta)\sqrt{4\pi D_*t}} \left(\frac{x^2}{4D_*t} \right)^{\nu-1/2} \\ &\quad \times H_{0,2}^{2,0} \left[\frac{x^2}{4D_*t} \mid \overline{(0, 1/\eta)} (-\nu + 1/2, 1) \right]. \end{aligned} \tag{A.6}$$

The series expansion of this function reads [102]

$$\begin{aligned} H_{0,2}^{2,0} \left[z \mid \overline{(0, 1/\eta)} (-\nu + 1/2, 1) \right] &= \sum_{n=0}^\infty \frac{(-1)^n}{n!} \Gamma(1/2 - \nu - \eta n) \eta z^{\eta n} \\ &\quad + \sum_{n=0}^\infty \frac{(-1)^n}{n!} \Gamma\left(\frac{\nu - 1/2 - n}{\eta}\right) z^{1/2-\nu+n}. \end{aligned} \tag{A.7}$$

The asymptotic behaviour is then obtained in the form [102]

$$f_{DD}^{ST}(x, t) \sim \frac{1}{\Gamma(\nu/\eta)\sqrt{4\pi D_*t}} \left(\frac{x^2}{4D_*t} \right)^{\frac{2\nu-\eta-1}{2(\eta+1)}} \exp\left(-\frac{\eta+1}{\eta} \frac{1}{\eta^{\eta+1}} \left(\frac{x^2}{4D_*t} \right)^{\eta/(\eta+1)}\right), \tag{A.8}$$

for $|x| \rightarrow \infty$.

A.2. Computation via Mellin transform

It is possible to rearrange the integral in equation (A.1) as a convolution integral,

$$\begin{aligned} \bar{P}(x, t) &= \int_0^\infty p_D(D) \frac{\exp\left(-\frac{(x/\sqrt{t})^2}{4D}\right)}{\sqrt{4\pi t} \sqrt{D}} dD \\ &= \frac{2}{\sqrt{4t}} \int_0^\infty \sqrt{D} p_D((\sqrt{D})^2) \frac{\exp\left(-\frac{(x/\sqrt{D})^2}{4}\right)}{\sqrt{\pi}} \frac{d\sqrt{D}}{\sqrt{D}} \\ &= \frac{1}{\sqrt{4t}} \int_0^\infty 2\xi p_D(\xi^2) M_{1/2}\left(\frac{\bar{x}}{\xi}\right) \frac{d\xi}{\xi}, \end{aligned} \tag{A.9}$$

where we defined $\bar{x} = x/t^{1/2}$ and $\xi = D^{1/2}$, and $M_{1/2}$ denotes the M -Wright function with parameter $\beta = 1/2$ [78]. Considering the convolution formula for the Mellin transform

$$\int_0^\infty f(\xi) g\left(\frac{x}{\xi}\right) \frac{d\xi}{\xi} \stackrel{M}{\longleftrightarrow} f^M(s) g^M(s), \tag{A.10}$$

and remembering the property

$$x^\beta f(ax^h) \xleftrightarrow{\mathcal{M}} h^{-1} a^{-(s+\beta)/h} f\left(\frac{s+\beta}{h}\right), \tag{A.11}$$

we compute the Mellin transform of the obtained integral in equation (A.9), recovering

$$\sqrt{4t} \bar{P}(\bar{x}) = \int_0^\infty 2\xi p_D(\xi^2) M_{1/2}\left(\frac{\bar{x}}{\xi}\right) \frac{d\xi}{\xi} \xleftrightarrow{\mathcal{M}} p_D^M\left(\frac{s+1}{2}\right) M_{1/2}^M(s). \tag{A.12}$$

The Mellin transforms for the M -Wright function [78] and the generalised Gamma distribution [102] are known and given by

$$\begin{aligned} M_\beta(x) &\xleftrightarrow{\mathcal{M}} \frac{\Gamma(s)}{\Gamma(1+(s-1)/\beta)}, \\ \gamma_{(\nu,\eta)}^{\text{gen}}(x) &\xleftrightarrow{\mathcal{M}} D_*^{s-1} \frac{\Gamma((\nu+s-1)/\eta)}{\Gamma(\nu/\eta)}. \end{aligned} \tag{A.13}$$

We can thus rewrite equation (A.12) in the form

$$\begin{aligned} p_D^M\left(\frac{s+1}{2}\right) M_{1/2}^M(s) &= D_*^{\frac{s-1}{2}} \frac{\Gamma\left(\frac{\nu+(s+1)/2-1}{\eta}\right)}{\Gamma\left(\frac{\nu}{\eta}\right)} \frac{\Gamma(s)}{\Gamma\left(1+\frac{1}{2}(s-1)\right)} \\ &= \frac{2D_*^{\frac{s-1}{2}} \Gamma\left(\frac{\nu-1/2+s/2}{\eta}\right) \Gamma(s-1)}{\Gamma\left(\frac{\nu}{\eta}\right) \Gamma\left(\frac{s-1}{2}\right)} \\ &= \frac{2D_*^{\frac{s-1}{2}} \Gamma\left(\frac{\nu-1/2+s/2}{\eta}\right) \Gamma((s-1)/2+1/2)}{\Gamma\left(\frac{\nu}{\eta}\right) 2^{1-(s-1)} \sqrt{\pi}} \\ &= \frac{1}{2\sqrt{D_*\pi} \Gamma\left(\frac{\nu}{\eta}\right)} \left(\frac{1}{4D_*}\right)^{-s/2} \Gamma\left(\frac{\nu-1/2}{\eta} + \frac{s/2}{\eta}\right) \Gamma\left(\frac{s}{2}\right). \end{aligned} \tag{A.14}$$

Now we notice that the Mellin transform of the H -function is [102]

$$H_{p,q}^{m,n} \left[ax \left| \begin{matrix} (a_p, A_p) \\ (b_q, B_q) \end{matrix} \right. \right] \xleftrightarrow{\mathcal{M}} a^{-s} \frac{\left(\prod_{j=1}^m \Gamma(b_j + B_j s) \right) \left(\prod_{j=1}^n \Gamma(1 - a_j - A_j s) \right)}{\left(\prod_{j=m+1}^q \Gamma(1 - b_j - B_j s) \right) \left(\prod_{j=n+1}^p \Gamma(a_j + A_j s) \right)}. \tag{A.16}$$

Thus, recalling also the property of the Mellin transform in equation (A.11) we obtain that

$$\sqrt{4t} \bar{P}(\bar{x}) = \frac{1}{\Gamma(\nu/\eta) \sqrt{\pi D_*}} H_{0,2}^{2,0} \left[\frac{\bar{x}^2}{4D_*} \left| \left(\frac{\nu-1/2}{\eta}, \frac{1}{\eta} \right) (0, 1) \right. \right], \tag{A.17}$$

and finally

$$\bar{P}(x, t) = \frac{1}{\Gamma(\nu/\eta) \sqrt{4\pi D_* t}} H_{0,2}^{2,0} \left[\frac{x^2}{4D_* t} \left| \left(\frac{\nu-1/2}{\eta}, \frac{1}{\eta} \right) (0, 1) \right. \right]. \tag{A.18}$$

The result here recovered is consistent with equation (A.6).

A.3. Asymptotic trend via Laplace method

Starting again from equation (A.1) it is also possible to calculate directly the asymptotic behaviour through the Laplace method. We introduce the new variable $y = D_* / D$ in equation (A.1),

$$\begin{aligned} \bar{P}(x, t) &= \frac{\eta}{D_*^\nu \Gamma(\nu/\eta) \sqrt{4\pi t}} \int_0^\infty D^{\nu-3/2} e^{-(D/D_*)y} e^{-\lambda D_*/D} dD \\ &= \frac{\eta}{\Gamma(\nu/\eta) \sqrt{4\pi D_* t}} \int_0^\infty y^{-\nu-1/2} e^{-y^\eta - \lambda y} dy \end{aligned} \tag{A.19}$$

Now the integral looks like a Laplace integral of the form

$$I(\lambda) = \int_0^\infty f(y)e^{-\lambda y} dy. \tag{A.20}$$

In order to apply the Laplace method we need $f(0) \neq 0$ which is not our case since $f(0) = 0$ together with all its derivatives. Thus, to evaluate the asymptotics, we define the maximum of the function,

$$\phi(y) = -\lambda y - y^{-\eta}, \tag{A.21}$$

which is located at $y_m = (\eta/\lambda)^{1/(\eta+1)}$. Introducing of the new variable $\bar{z} = z\eta^{1/(\eta+1)}$ the integral becomes

$$\begin{aligned} I(\lambda) &= \lambda^{\frac{2\nu-1}{2(\eta+1)}} \int_0^\infty \bar{z}^{\frac{2\nu-1}{2(\eta+1)}} \exp[-\lambda^{\frac{\eta}{\eta+1}}(\bar{z}^{-\eta} + \bar{z})] d\bar{z} \\ &= \lambda^{\frac{2\nu-1}{2(\eta+1)}} \int_0^\infty \bar{z}^{\frac{2\nu-1}{2(\eta+1)}} e^{\bar{\lambda} f(\bar{z})} d\bar{z}, \end{aligned} \tag{A.22}$$

where we defined $f(\bar{z}) = -\bar{z} - \bar{z}^{-\eta}$ and $\bar{\lambda} = \lambda^{\eta/(\eta+1)}$. Now the standard Laplace method can be applied considering that the function $f(\bar{z})$ reaches its maximum at $\bar{z}_m = \eta^{1/(\eta+1)}$, such that

$$\begin{aligned} I(\lambda) &= \lambda^{\frac{2\nu-1}{2(\eta+1)}} \bar{z}_m^{\frac{2\nu-1}{2(\eta+1)}} e^{\bar{\lambda} f(\bar{z}_m)} \sqrt{\frac{2\pi}{|\lambda| f''(\bar{z}_m)}} \\ &= \sqrt{\frac{2\pi}{\eta+1}} \frac{\eta^{2\nu+\eta+1}}{\eta^{2(\eta+1)^2}} \lambda^{\frac{2\nu-\eta-1}{2(\eta+1)}} \exp\left[-\frac{\eta+1}{\eta} \eta^{\frac{1}{\eta+1}} \lambda^{\frac{\eta}{\eta+1}}\right]. \end{aligned} \tag{A.23}$$

This finally leads to

$$\bar{P}(x, t) \simeq \frac{\eta^{2\nu+\eta+1} + 1}{\Gamma(\nu/\eta) \sqrt{4\pi D_* t}} \sqrt{\frac{2\pi}{\eta+1}} \left(\frac{x^2}{4D_* t}\right)^{\frac{2\nu-\eta-1}{2(\eta+1)}} \exp\left[-\frac{\eta+1}{\eta} \eta^{\frac{1}{\eta+1}} \left(\frac{x^2}{4D_* t}\right)^{\frac{\eta}{\eta+1}}\right], \tag{A.24}$$

for $|x| \rightarrow \infty$. This result is, up to a numerical prefactor, identical to the asymptotic behaviour obtained in (A.1).

ORCID iDs

Ralf Metzler  <https://orcid.org/0000-0002-6013-7020>

References

- [1] Brown R 1828 A brief account of microscopical observations made on the particles contained in the pollen of plants *Phil. Mag.* **4** 161
- [2] Perrin J 1908 L'agitation moléculaire et le mouvement Brownien *Compt. Rend.* **146** 967
- [3] Perrin J 1909 Mouvement Brownien et réalité moléculaire *Ann. Chim. Phys.* **18** 5
- [4] Nordlund I 1914 A new determination of avogadro's number from Brownian motion of small mercury spherules *Z. Phys. Chem.* **87** 40
- [5] Kappler E 1931 Versuche zur messung der avogadro-loschmidtschen zahl aus der Brownschen bewegung einer drehwaage *Ann. Phys.* **11** 233
- [6] Einstein A 1905 Über die von der molekularkinetischen theorie der Wärme geforderte bewegung von in ruhenden flüssigkeiten suspendierten teilchen *Ann. Phys.* **322** 549
- [7] Sutherland W 1905 A dynamical theory of diffusion for non-electrolytes and the molecular mass of albumin *Phil. Mag.* **9** 781
- [8] von Smoluchowski M 1906 Zur kinetischen theorie der Brownschen molekularbewegung und der suspensionen *Ann. Phys.* **21** 756
- [9] Langevin P 1908 Sur la théorie de mouvement Brownien *C.R. Hebd. Seances Acad. Sci.* **146** 530
- [10] van Kampen N G 1981 *Stochastic Processes in Physics and Chemistry* (Amsterdam: North Holland)
- [11] Richardson L F 1926 Atmospheric diffusion shown on a distance-neighbour graph *Proc. R. Soc. A* **110** 709
- [12] Metzler R and Klafter J 2004 The restaurant at the end of the random walk: recent developments in the description of anomalous transport by fractional dynamics *J. Phys. A: Math. Gen.* **37** R161
- [13] Scher H and Montroll E W 1975 Anomalous transit-time dispersion in amorphous solids *Phys. Rev. B* **12** 2455
- [14] Höfling F and Franosch T 2013 Anomalous transport in the crowded world of biological cells *Rep. Prog. Phys.* **76** 046602
- [15] Nørregaard K, Metzler R, Ritter C M, Berg-Sørensen K and Oddershede L B 2017 Manipulation and motion of organelles and single molecules in living cells *Chem. Rev.* **117** 4342–75
- [16] Weiss M, Elsner M, Kartberg F and Nilsson T 2004 Anomalous subdiffusion is a measure for cytoplasmic crowding in living cells *Biophys. J.* **87** 3518–24
- [17] Caspi A, Granek R and Elbaum M 2000 Enhanced diffusion in active intracellular transport *Phys. Rev. Lett.* **85** 5655–8
- [18] Seisenberger G, Ried M U, Endreß T, Büning H, Hallek M and Bräuchle C 2001 Real-time single-molecule imaging of the infection pathway of an adeno-associated virus *Science* **294** 1929–32
- [19] Golding I and Cox E C 2006 Physical nature of bacterial cytoplasm *Phys. Rev. Lett.* **96** 098102
- [20] Jeon J H, Tejedor V, Burov S, Barkai E, Selhuber-Unkel C, Berg-Sørensen K, Oddershede L and Metzler R 2011 *In vivo* anomalous diffusion and weak ergodicity breaking of lipid granules *Phys. Rev. Lett.* **106** 048103
- [21] Banks D S and Fradin C 2005 Anomalous diffusion of proteins due to molecular crowding *Biophys. J.* **89** 2960–71
- [22] Wong I Y, Gardel M L, Reichman D R, Weeks E R, Valentine M T, Bausch A R and Weitz D A 2004 Anomalous diffusion probes microstructure dynamics of entangled F-actin networks *Phys. Rev. Lett.* **92** 178101
- [23] Szymanski J and Weiss M 2009 Elucidating the origin of anomalous diffusion in crowded fluids *Phys. Rev. Lett.* **103** 038102

- [23] Jeon J-H, Leijnse N, Oddershede L B and Metzler R 2013 Anomalous diffusion and power-law relaxation of the time averaged mean square displacement in worm-like micellar solution *New J. Phys.* **15** 045011
- [24] Weiss M, Hashimoto H and Nilsson T 2003 Anomalous protein diffusion in living cells as seen by fluorescence correlation spectroscopy *Biophys. J.* **84** 4043–52
- [25] Weigel A V, Simon B, Tamkun M M and Krapf D 2011 Ergodic and nonergodic processes coexist in the plasma membrane as observed by single-molecule tracking *Proc. Natl Acad. Sci. USA* **108** 6438–43
- [26] Manzo C, Torreno-Pina J A, Massignan P, Lapeyre G J Jr, Lewenstein M and Garcia Parajo M F 2015 Weak ergodicity breaking of receptor motion in living cells stemming from random diffusivity *Phys. Rev. X* **5** 011021
- [27] Kneller G 2014 Communication: a scaling approach to anomalous diffusion *J. Chem. Phys.* **141** 041105
- [28] Jeon J-H, Martinez-Seara Monne H, Javanainen M and Metzler R 2012 Anomalous diffusion of phospholipids and cholesterol in a lipid bilayer and its origins *Phys. Rev. Lett.* **109** 188103
- [29] Jeon J-H, Javanainen M, Martinez-Seara H, Metzler R and Vattulainen I 2016 Protein crowding in lipid bilayers gives rise to non-Gaussian anomalous lateral diffusion of phospholipids and proteins *Phys. Rev. X* **6** 021006
- [30] Metzler R, Jeon J-H and Cherstvy A G 2016 Non-Brownian diffusion in lipid membranes: experiments and simulations *Biochim. Biophys. Acta—Biomembranes* **1858** 2451–67
- [31] Hu X, Hong L, Smith M D, Neusius T, Cheng X and Smith J C 2016 The dynamics of single protein molecules is non-equilibrium and self-similar over thirteen decades in time *Nat. Phys.* **12** 171–4
- [32] Robert D, Nguyen T H, Gallet F and Wilhelm C 2010 *In vivo* determination of fluctuating forces during endosome trafficking using a combination of active and passive microrheology *PLoS One* **4** e10046
- [33] Reverey J F, Jeon J-H, Leippe M, Metzler R and Selhuber-Unkel C 2015 Superdiffusion dominates intracellular particle motion in the supercrowded cytoplasm of pathogenic *Acanthamoeba castellanii* *Sci. Rep.* **5** 11690
- [34] Hughes B D 1995 *Random Walks and Random Environments* vol 1 (Oxford: Oxford University Press)
- [35] Metzler R, Jeon J H, Cherstvy A G and Barkai E 2014 Anomalous diffusion models and their properties: non-stationarity, non-ergodicity and ageing at the centenary of single particle tracking *Phys. Chem. Chem. Phys.* **16** 24128–64
- [36] Schulz J H P, Barkai E and Metzler R 2013 Aging effects and population splitting in single-particle trajectory averages *Phys. Rev. Lett.* **110** 020602
- [37] Schulz J H P, Barkai E and Metzler R 2014 Aging renewal theory and application to random walks *Phys. Rev. X* **4** 011028
- [38] Cherstvy A G, Chechkin A V and Metzler R 2013 Anomalous diffusion and ergodicity breaking in heterogeneous diffusion processes *New J. Phys.* **15** 083039
- [39] Cherstvy A G and Metzler R 2014 Nonergodicity, fluctuations, and criticality in heterogeneous diffusion processes *Phys. Rev. E* **90** 012134
- [40] Cherstvy A G, Chechkin A V and Metzler R 2014 Ageing and confinement in non-ergodic heterogeneous diffusion processes *J. Phys. A: Math. Theor.* **47** 485002
- [41] Massignan P, Manzo C, Torreno-Pina J A, García-Parajo M F, Lewenstein M and Lapeyre G L Jr. 2014 Nonergodic subdiffusion from Brownian motion in an inhomogeneous medium *Phys. Rev. Lett.* **112** 150603
- [42] Lutz E 2001 Fractional Langevin equation *Phys. Rev. E* **64** 051106
- [43] Goychuk I 2009 Viscoelastic subdiffusion: from anomalous to normal *Phys. Rev. E* **80** 046125
- [44] Goychuk I 2012 Viscoelastic subdiffusion: generalized Langevin equation approach *Adv. Chem. Phys.* **150** 187–253
- [45] Mandelbrot B B and van Ness J W 1968 Fractional Brownian motions, fractional noises and applications *SIAM Rev.* **10** 422–37
- [46] Deng W and Barkai E 2009 Ergodic properties of fractional Brownian–Langevin motion *Phys. Rev. E* **79** 011112
- [47] Schwarzl M, Godec A and Metzler R 2017 Quantifying non-ergodicity of anomalous diffusion with higher order moments *Sci Rep.* **7** 3878
- [48] Jeon J-H and Metzler R 2012 Inequivalence of time and ensemble averages in ergodic systems: exponential versus power-law relaxation in confinement *Phys. Rev. E* **85** 021147
- [49] Wang B, Kuo J, Bae S C and Granick S 2012 When Brownian diffusion is not Gaussian *Nat. Mater.* **11** 481–5
- [50] Wang B, Antony S M, Bae S C and Granick S 2009 Anomalous yet Brownian *Proc. Natl Acad. Sci. USA* **106** 15160–4
- [51] Leptos K C, Guasto J S, Gollub J P, Pesci A I and Goldstein R E 2009 Dynamics of enhanced tracer diffusion in suspensions of swimming Eukaryotic microorganisms *Phys. Rev. Lett.* **103** 198103
- [52] Xue C, Zheng X, Chen K, Tian Y and Hu G 2016 Probing non-Gaussianity in confined diffusion of nanoparticles *J. Phys. Chem. Lett.* **7** 514–9
- [53] Wang D, Hu R, Skaug M J and Schwartz D K 2015 Temporally anticorrelated motion of nanoparticles at a liquid interface *J. Phys. Chem. Lett.* **6** 54–9
- [54] Dutta S and Chakrabarti J 2016 Anomalous dynamical responses in a driven system *Europhys. Lett.* **116** 38001
- [55] Hapca S, Crawford J W and Young I M 2009 Anomalous diffusion of heterogeneous populations characterized by normal diffusion at the individual level *J. R. Soc. Interface* **6** 111–22
- [56] Cherstvy A G, Günther O, Beta C and Metzler R unpublished
- [57] Kob W and Andersen H C 1995 Testing mode-coupling theory for a supercooled binary Leonard–Jones mixture: the van Hove correlation function *Phys. Rev. E* **51** 4626–41
- [58] Chaudhuri P, Berthier L and Kob W 2007 Universal nature of particle displacements close to glass and jamming transitions *Phys. Rev. Lett.* **99** 060604
- [59] R-Vargas S, Rovigatti L and Sciortino F 2017 Connectivity, dynamics, and structure in a tetrahedral network liquid *Soft Matter* **13** 514–30
- [60] Samanta N and Chakrabarti R 2016 Tracer diffusion in a sea of polymers with binding zones: mobile versus frozen traps *Soft Matter* **12** 8554–63
- [61] Skaug M J, Wang L, Ding Y and Schwartz D K 2015 Hindered nanoparticle diffusion and void accessibility in a three-dimensional porous medium *ACS Nano* **9** 2148–56
- [62] Stuhrmann B, Soares Silva M, Depken M, Mackintosh F C and Koenderink G H 2012 Nonequilibrium fluctuations of a remodeling *in vitro* cytoskeleton *Phys. Rev. E* **86** 020901
- [63] Lampo T, Stylianidis S, Backlund M P, Wiggins P A and Spakowitz A J 2017 Cytoplasmic RNA-protein particles exhibit non-Gaussian subdiffusive behaviour *Biophys. J.* **112** 532–42
- [64] Soares Silva M, Stuhrmann B, Betz T and Koenderink G H 2014 Time-resolved microrheology of actively remodeling actomyosin networks *New J. Phys.* **16** 075010
- [65] Beck C and Cohen E D B 2003 Superstatistics *Physica A* **322** 267

- [64] Beck C 2006 Superstatistical Brownian motion *Prog. Theor. Phys. Suppl.* **162** 29–36
- [65] van der Straeten E and Beck C 2009 Superstatistical fluctuations in time series: applications to share-price dynamics and turbulence *Phys. Rev. E* **80** 036108
- [66] Metzler R 2017 Gaussianity fair: the riddle of anomalous yet non-Gaussian diffusion *Biophys. J.* **112** 413–5
- [67] Chechkin A V, Seno F, Metzler R and Sokolov I 2017 Brownian yet non-Gaussian diffusion: from superstatistics to subordination of diffusing diffusivities *Phys. Rev. X* **7** 021002
- [68] van der Straeten E and Beck C 2011 Dynamical modelling of superstatistical complex systems *Physica A* **390** 951–6
- [69] Slezak J, Metzler R and Magdziarz M 2018 Superstatistical generalised Langevin equation: non-Gaussian viscoelastic anomalous diffusion *New J. Phys.* **20** 023026
- [70] Dubinko V I, Tur A V, Turkin A A and Yanovsky V V 1990 Diffusion in fluctuating medium *Radiat. Effects Defects Solid* **112** 233–43
- [71] Albers T and Radons G 2013 Subdiffusive continuous time random walks and weak ergodicity breaking analyzed with the distribution of generalized diffusivities *Eur. Phys. Lett.* **102** 40006
- [72] Rozenfeld R, Luczka J and Talkner P 1998 Brownian motion in a fluctuating medium *Phys. Lett. A* **249** 409–14
- [73] Luczka J, Talkner P and Hänggi P 2000 Diffusion of Brownian particles governed by fluctuating friction *Physica A* **278** 18–31
- [74] Luczka J and Zaborek B 2004 Brownian motion: a case of temperature fluctuation *Acta Phys. Pol. B* **35** 2151–64
- [75] Uneyama T, Miyaguchi T and Akimoto T 2015 Fluctuation analysis of time-averaged mean-square displacement for the Langevin equation with time-dependent and fluctuating diffusivity *Phys. Rev. E* **92** 032140
- [76] Akimoto T and Yamamoto E 2016 Distributional behaviours of time-averaged observables in the Langevin equation with fluctuating diffusivity: normal diffusion but anomalous fluctuations *Phys. Rev. E* **93** 062109
- [77] Cherstvy A G and Metzler R 2016 Anomalous diffusion in time-fluctuating non-stationary diffusivity landscapes *Phys. Chem. Chem. Phys.* **18** 23840–52
- [78] Mura A, Taqqu M S and Mainardi F 2008 Non-Markovian diffusion equations and processes: analysis and simulations *Physica A* **387** 5033–64
- [79] Mura A and Mainardi F 2009 A class of self-similar stochastic processes with stationary increments to model anomalous diffusion in physics *Int. Transf. Spe. Funct.* **20** 185–98
- [80] Pagnini G 2012 Erdélyi Kober fractional diffusion *Fractional Calculus Appl. Anal.* **5** 117–27
- [81] Mura A and Pagnini G 2008 Characterizations and simulations of a class of stochastic processes to model anomalous diffusion *J. Phys. A: Math. Theor.* **41** 285003
- [82] Molina-García D, Pham T M, Paradisi P and Pagnini P 2016 Fractional kinetics emerging from ergodicity breaking in random media *Phys. Rev. E* **94** 052147
- [83] Chubynsky M V and Slater G W 2014 Diffusing diffusivities: a model for anomalous, yet Brownian diffusion *Phys. Rev. Lett.* **113** 098302
- [84] Tejedor V and Metzler R 2010 Anomalous diffusion in correlated continuous time random walks *J. Phys. A: Math. Theor.* **43** 082002
- [85] Magdziarz M, Metzler R, Szczotka W and Zebrowski P 2012 Correlated continuous time random walks in external force fields *Phys. Rev. E* **85** 051103
- [86] Matse M, Chubynsky M V and Bechhoefer J 2017 Test of the diffusing-diffusivity mechanism using nearwall colloidal dynamics *Phys. Rev. E* **96** 042604
- [87] Jain R and Sebastian K L 2016 Diffusion in a crowded, rearranging environment *J. Phys. Chem. B* **120** 3988–92
- [88] Jain R and Sebastian K L 2017 Diffusing diffusivity: a new derivation and comparison with simulations *J. Chem. Sci.* **129** 929–37
- [89] Tyagi N and Cherayil B J 2017 Non-Gaussian Brownian diffusion in dynamically disordered thermal environments *J. Phys. Chem. B* **121** 7204–9
- [90] Lanoiselée Y and Grebenkov D 2018 A model of non-Gaussian diffusion in heterogeneous media *J. Phys. A: Math. Theor.* **51** 145602
- [91] Beck C 2006 Stretched exponentials from superstatistics *Physica A* **365** 96
- [92] Javanainen M, Hammaren H, Monticelli L, Jeon J-H, Miettinen M S, Martinez-Seara H, Metzler R and Vattulainen I 2013 Anomalous and normal diffusion of proteins and lipids in crowded lipid membranes *Faraday Discuss.* **161** 397–417
- [93] Jeon J-H, Javanainen M, Martinez-Seara H, Metzler R and Vattulainen I 2016 Protein crowding in lipid bilayers gives rise to non-Gaussian anomalous lateral diffusion of phospholipids and proteins *Phys. Rev. X* **6** 021006
- [94] Pagnini G and Paradisi P 2016 A stochastic solution with Gaussian stationary increments of the symmetric space-time fractional diffusion equation *Fractional Calculus Appl. Anal.* **19** 408–40
- [95] Thomson D J 1987 Criteria for the selection of stochastic models of particle trajectories in turbulent flows *J. Fluid Mech.* **180** 529–56
- [96] Ross S 2010 *A First Course in Probability* 8th edn (Upper Saddle River, NJ: Prentice Hall)
- [97] Heston S L 1993 A closed-form solution for options with stochastic volatility with applications to bond and currency options *Rev. Financ. Studies* **6** 327
- [98] Dragulescu A and Yakovenko V 2002 Probability distribution of returns in the Heston model with stochastic volatility *Quant. Finance* **2** 443
- [99] Liptser R S and Shiryaev A N 2001 *Statistics of Random Processes II* (Berlin: Springer)
- [100] Dankel T Jr 1991 On the distribution of the integrated square of the Ornstein–Uhlenbeck process *SIAM J. Appl. Math.* **51** 568–74
- [101] Prudnikov A P 1990 *Integrals and Series. 3: More Special Functions* (Boca Raton, FL: CRC Press)
- [102] Mathai A M and Saxena R K 1978 *The H-function with applications in statistics and other disciplines* (New Delhi: Wiley Eastern)

Sposini V, Checkin A V & Metzler R 2019 First passage statistics for diffusing diffusivity *J. Phys. A: Math. Theor.* **52**, 04LT01.

Letter

First passage statistics for diffusing diffusivity

Vittoria Sposini^{1,2}, Aleksei Chechkin^{1,3} and Ralf Metzler^{1,4}

¹ Institute for Physics & Astronomy, University of Potsdam, 14476 Potsdam-Golm, Germany

² Basque Centre for Applied Mathematics, 48009 Bilbao, Spain

³ Akhiezer Institute for Theoretical Physics, 61108 Kharkov, Ukraine

 E-mail: rmetzler@uni-potsdam.de (Ralf Metzler)

Received 24 September 2018, revised 23 November 2018

Accepted for publication 7 December 2018

Published 28 December 2018



CrossMark

Abstract

A rapidly increasing number of systems is identified in which the stochastic motion of tracer particles follows the Brownian law $\langle \mathbf{r}^2(t) \rangle \simeq Dt$ yet the distribution of particle displacements is strongly non-Gaussian. A central approach to describe this effect is the diffusing diffusivity (DD) model in which the diffusion coefficient itself is a stochastic quantity, mimicking heterogeneities of the environment encountered by the tracer particle on its path. We here quantify in terms of analytical and numerical approaches the first passage behaviour of the DD model. We observe significant modifications compared to Brownian–Gaussian diffusion, in particular that the DD model may have a faster first passage dynamics. Moreover we find a universal crossover point of the survival probability independent of the initial condition.

Keywords: diffusion, superstatistics, first passage

(Some figures may appear in colour only in the online journal)

1. Introduction

Since its original systematic study 190 years ago by Brown [1], diffusion of molecular and (sub-)micron-sized entities has been identified as the dominant form of thermally driven, passive transport in numerous biological and inanimate systems. The two hallmark features of diffusion is the linear growth $\langle \mathbf{r}^2(t) \rangle = 2Ddt$ of the mean squared displacement (MSD) with diffusion coefficient D in d spatial dimensions, and the Gaussian distribution of displacements [2]. With increasing complexity of the studied systems deviations from these two central properties have been unveiled over the years. Thus, anomalous diffusion with an MSD of the form

⁴ Author to whom any correspondence should be addressed.

$\langle \mathbf{r}^2(t) \rangle \simeq t^\alpha$ was observed in a large range of systems [3, 4]. Along with such observations a rich variety of generalised stochastic processes has been developed [5, 6]. The displacement distribution of anomalous diffusion processes may be inherently Gaussian (such as for fractional Brownian motion [7]) or non-Gaussian (for instance, for processes characterised by scale-free trapping time distributions [8] or space-dependent diffusivity models [9]).

Recently a large variety of systems have been reported in which the MSD exhibits the linear growth in time $\langle \mathbf{r}^2(t) \rangle \simeq Dt$ of Brownian (Fickian) transport, however, the distribution of displacements $P(\mathbf{r}, t)$ is pronouncedly non-Gaussian due to randomly distributed values of the diffusion coefficient that can be extracted from experiments [10–12]. Pertinent examples include the motion of tracer beads along tubular or membrane structures or in gels and colloidal suspensions [10, 13, 14], and the motion of nematodes [11] and single cells on substrates [15]. As long as the displacement distribution $P(\mathbf{r}, t)$ has a fixed shape for any time t , one possible way to model the non-Gaussianity is the concept of superstatistics [16, 17] which introduces a distribution $p_D(D)$ of the diffusion coefficient and then averages individual Gaussian distributions with one given D value over this $p_D(D)$ ⁵. However, this approach does not work when eventually a crossover to an effective Gaussian is observed [10, 13]. For the latter case Chubynsky and Slater introduced the diffusing diffusivity (DD) model [18], see also [19–25]. In this popular approach the diffusion coefficient is assumed to be a stochastic variable itself, described by a stationary process. Consequently the system is initially described by a non-Gaussian displacement distribution. Beyond a characteristic time scale a crossover occurs to a Gaussian behaviour characterised by an effective value of the diffusivity.

Here, we study the first passage behaviour of the DD model. The concept of first passage is ubiquitously used in statistical physics and its applications, for instance, to quantify when a diffusing particle reaches a reaction centre or a stochastic process exceeds a given threshold value [26, 27]. Based on the minimal model for DD [23] we derive the first passage behaviour in both semi-infinite and finite systems. We find that the DD dynamics may be faster than Brownian–Gaussian diffusion (ordinary Brownian motion in mathematics literature) at intermittent times in a semi-infinite domain while the long time behaviour matches exactly the Brownian–Gaussian result with an effective diffusivity. We also observe an interesting universal crossover point of the survival probability which is independent of the initial particle position. In finite domains the mean first passage time of the DD model is longer than in the Brownian–Gaussian case. Concurrently, in the DD model the divergence of the mean first passage time observed in the superstatistical approach is rectified.

In section 2 we briefly recall the basic properties of the minimal diffusing diffusivity model [23]. The survival probabilities for the semi-infinite and finite domains are then derived in section 3 along with their short and long time asymptotes. Section 4 provides a detailed discussion of the results including a relation to the standard Brownian–Gaussian first passage behaviour. A short conclusion is presented in section 5.

2. Minimal model for Brownian yet non-Gaussian diffusion

The model we study is the so-called minimal diffusing diffusivity (DD) model which was introduced to describe diffusion in heterogeneous environments [23]. In this model the diffusivity is defined as a stochastic process itself, in terms of the squared Ornstein–Uhlenbeck

⁵ Such a distribution $p(D)$ could be effected by distributed properties of the observed particles such as a distribution of tracer bead sizes or diffusing bacteria mobilities. In the original picture for superstatistics [16, 17] particles are assumed to move on disjunct spatial patches with different transport properties.

process, guaranteeing the stationarity of $D(t)$. In dimensionless units the minimal DD model is defined by the set of Langevin equations [23]

$$\begin{aligned} \frac{d}{dt}\mathbf{r}(t) &= \sqrt{2D(t)}\boldsymbol{\xi}(t) \\ D(t) &= \mathbf{Y}^2(t), \quad \frac{d}{dt}\mathbf{Y}(t) = -\mathbf{Y} + \boldsymbol{\eta}(t), \end{aligned} \tag{1}$$

where the components of $\boldsymbol{\xi}(t)$ and $\boldsymbol{\eta}(t)$ are independent white Gaussian noises and \mathbf{Y} represents a d -dimensional Ornstein–Uhlenbeck process. The dimensionless Ornstein–Uhlenbeck process here has a characteristic crossover time of unity. We assume the diffusivity to start from equilibrium initial conditions (the non-equilibrium case is discussed in [24]). This leads to the superstatistical short time diffusivity distribution

$$p_D(D) = \begin{cases} (\sqrt{\pi D})^{-1}e^{-D}, & d = 1 \\ e^{-D}, & d = 2, \\ (2\sqrt{D/\pi})e^{-D}, & d = 3 \end{cases} \tag{2}$$

for 1, 2 and 3 dimensions. While the dominating exponential tail is common to all d , there is a pole at $D \rightarrow 0$ in $d = 1$ [23]. As we showed previously, the minimal DD model can be written using the concepts of subordination [28] through the relation [23]

$$P(\mathbf{r}, t|\mathbf{r}_0) = \int_0^\infty G(\mathbf{r}, \tau|\mathbf{r}_0, D = 1)T_d(\tau, t)d\tau, \tag{3}$$

of the probability density function (PDF) $P(\mathbf{r}, t|\mathbf{r}_0)$ of displacement and the Gaussian

$$G(\mathbf{r}, t|\mathbf{r}_0, D) = (4\pi Dt)^{-d/2} \exp(-(\mathbf{r} - \mathbf{r}_0)^2/[4Dt]) \tag{4}$$

with fixed diffusion coefficient D . The subordinator $T_d(\tau, t)$ represents the PDF of the process $\tau(t) = \int_0^t \mathbf{Y}^2(t')dt'$ and is defined through its Laplace transform [23]

$$\tilde{T}_d(s, t) = \exp(dt/2) \left[\frac{1}{2}(\sqrt{1+2s} + \frac{1}{\sqrt{1+2s}}) \sinh(t\sqrt{1+2s}) + \cosh(t\sqrt{1+2s}) \right]^{-d/2} \tag{5}$$

with short and long time limits

$$\tilde{T}_d(s, t) \sim t^{-d/2} (s + 1/t)^{-d/2}, \quad t \ll 1, \tag{6}$$

$$\tilde{T}_d(s, t) \sim 2^{d/2} \exp\left(\frac{dt}{2}(1 - \sqrt{1+2s})\right) \left(1 + \frac{1}{2}\left(\sqrt{1+2s} + \frac{1}{\sqrt{1+2s}}\right)\right)^{-d/2}, \quad t \gg 1. \tag{7}$$

At short times the diffusivity varies slowly and we can assume it to be almost constant. In this limit the DD model thus reduces to the superstatistical approximation of the DD model in which each particle has a constant random diffusion coefficient with distribution $p_D(D)$ [16, 17]: on the ensemble level this implies that the PDF can be written as $P_{\text{sup}}(\mathbf{r}, t|\mathbf{r}_0) = \int_0^\infty G(\mathbf{r}, t|\mathbf{r}_0, D)p_D(D)dD$, such that the short time PDF explicitly reads

$$P_{\text{ST}}(\mathbf{r}, t|\mathbf{r}_0) = P_{\text{sup}}(\mathbf{r}, t|\mathbf{r}_0) = \begin{cases} (\pi t^{1/2})^{-1}K_0(|x - x_0|/t^{1/2}), & d = 1 \\ (2\pi t)^{-1}K_0(|r - r_0|/t^{1/2}), & d = 2 \\ (2\pi^2 t^{3/2})^{-1}K_0(|r - r_0|/t^{1/2}), & d = 3 \end{cases} \tag{8}$$

where $K_0(x)$ is a modified Bessel function of the second kind with exponential asymptote $K_0(z) \sim \sqrt{\pi/(2z)}e^{-z}$ [29]. At long times the DD process crosses over to a purely Gaussian process with PDF $P_{LT}(\mathbf{r}, t|\mathbf{r}_0) = G(\mathbf{r}, t|\mathbf{r}_0, D = \langle D \rangle_{st})$ with the stationary diffusivity $\langle D \rangle_{st} = d/2$ [23]. For all t the MSD is given by $\langle (\mathbf{r}(t) - \mathbf{r}_0)^2 \rangle = 2d\langle D \rangle_{st}t$.

We showed in [24] that there is a stochastic counterpart to this superstatistical approximation, defined through the generalised grey Brownian motion (ggBM) formalism [30], $\mathbf{r}(t) = \sqrt{2D} \times \mathbf{W}(t)$, where D is the random and constant diffusion coefficient and $\mathbf{W}(t)$ is the d -dimensional Wiener process or standard Brownian motion. Note that while the DD model represents the heterogeneity of the medium in some mean field sense [23] the ggBM model describes a heterogeneous ensemble of particles [31].

The following reasons motivated our concrete choice of the minimal DD model [23]: the Ornstein–Uhlenbeck process is stationary and thus provides a well defined crossover time as observed experimentally: at short times this model produces the desired exponential tails of the displacement distribution while at times longer than the Ornstein–Uhlenbeck relaxation time the behaviour crosses over to a Gaussian shape. Of course, other models provide similar behaviour, such as the ‘barometric formula’ model used in [18]. However, the Ornstein–Uhlenbeck based approach is exactly solvable analytically, which has clear advantages. Below we show that the behaviour revealed for our specific model is shared by more general models.

3. Results for the survival probabilities

The first passage time PDF of a stochastic process is the negative time derivative of the survival probability, $\wp(t) = -dS(t)/dt$. We here obtain the survival probability for semi-infinite and finite domains using the above subordination relation.

3.1. Survival of diffusing diffusivity model in semi-infinite domain

We begin our study with the semi-infinite interval $d = 1$ with absorbing boundary condition at $x = 0$. Following the approach for standard diffusion [26] we use the method of images for the initial particle position x_0 . Combined with the subordination principle (3) we get the image propagator

$$P(x, t|x_0) = \int_0^\infty (G(x, \tau|x_0, D = 1) - G(x, \tau|-x_0, D = 1)) T_1(\tau, t) d\tau. \quad (9)$$

After Fourier transform we obtain

$$\hat{P}(k, t|x_0) = \int_0^\infty T_1(\tau, t) e^{-k^2\tau} (e^{ikx_0} - e^{-ikx_0}) d\tau = (e^{ikx_0} - e^{-ikx_0}) \tilde{T}_1(s = k^2, t). \quad (10)$$

Here $\hat{\cdot}$ and $\tilde{\cdot}$ indicate the Fourier and Laplace transforms of the functions, respectively. We then calculate the survival probability in the semi-infinite domain,

$$S(t|x_0) = \int_0^\infty P(x, t|x_0) dx = \int_0^\infty dx \int_{-\infty}^{+\infty} \frac{dk}{2\pi} e^{-ikx} \hat{P}(k, t|x_0). \quad (11)$$

To check normalisation, we first see from expression (5) that $\tilde{T}_1(s, 0) = 1$. Then,

$$S(0|x_0) = \int_0^\infty dx \int_{-\infty}^{+\infty} \frac{dk}{2\pi} (e^{-ik(x-x_0)} - e^{-ik(x+x_0)}) = 1, \tag{12}$$

where we used that $\int_{-\infty}^\infty dk/(2\pi) \exp(-ikx) = \delta(x)$. Moreover, plugging the long time limit for $\tilde{T}_1(s = k^2, t)$ in (7) into the expression for $S(t|x_0)$ one can readily show that $S(t \rightarrow \infty|x_0) = 0$, as it should.

The direct calculation of the integral (11) is not easy to perform, we here focus on the short and long time regimes. At short times, $\tilde{T}_1(s = k^2, t)$ is given by (6) and thus

$$\begin{aligned} S_{ST}(t|x_0) &= \int_0^\infty dx \int_{-\infty}^\infty \frac{dk}{2\pi} e^{-ikx} (e^{ikx_0} - e^{-ikx_0}) \frac{t^{-1/2}}{\sqrt{k^2 + 1/t}} \\ &= \frac{1}{2\pi\sqrt{t}} \left(\int_0^\infty dx \int_{-\infty}^\infty dk \frac{e^{-ik(x-x_0)}}{\sqrt{k^2 + 1/t}} - \int_0^\infty dx \int_{-\infty}^\infty dk \frac{e^{-ik(x+x_0)}}{\sqrt{k^2 + 1/t}} \right) \\ &= \frac{1}{\pi\sqrt{t}} \int_0^\infty \left[K_0\left(\frac{|x-x_0|}{\sqrt{t}}\right) - K_0\left(\frac{|x+x_0|}{\sqrt{t}}\right) \right] dx. \end{aligned} \tag{13}$$

Splitting the integral and changing variables we obtain

$$\begin{aligned} S_{ST}(t|x_0) &= \frac{1}{\pi\sqrt{t}} \left[\int_0^{x_0} K_0\left(\frac{x_0-x}{\sqrt{t}}\right) dx + \int_{x_0}^\infty K_0\left(\frac{x-x_0}{\sqrt{t}}\right) dx - \int_0^\infty K_0\left(\frac{x+x_0}{\sqrt{t}}\right) dx \right] \\ &= \frac{2}{\pi} \int_0^{x_0/\sqrt{t}} K_0(z) dz. \end{aligned} \tag{14}$$

Using $\int_0^a K_0(z) dz = a\pi/2 (K_0(a)L_{-1}(a) + K_1(a)L_0(a))$, with the modified Struve function $L_\nu(z)$ [29],

$$S_{ST}(t|x_0) = \frac{x_0}{\sqrt{t}} \left[K_0\left(\frac{x_0}{\sqrt{t}}\right) L_{-1}\left(\frac{x_0}{\sqrt{t}}\right) + K_1\left(\frac{x_0}{\sqrt{t}}\right) L_0\left(\frac{x_0}{\sqrt{t}}\right) \right]. \tag{15}$$

The same result can be obtained both inserting directly the short time approximation (8) of the propagator in the result of the method of images and calculating directly the superstatistical integral valid for the survival probability.

At long times, when in equation (7) we only consider the tails of the distribution, $\tilde{T}_1(s = k^2, t) \sim \exp(-k^2 t/2)$. This approximation leads to

$$\begin{aligned} S_{LT}(t|x_0) &= \int_0^\infty dx \left[\int_{-\infty}^\infty \frac{dk}{2\pi} \exp\left(-ik(x-x_0) - \frac{k^2 t}{2}\right) - \exp\left(-ik(x+x_0) - \frac{k^2 t}{2}\right) \right] \\ &= \frac{1}{\sqrt{2\pi t}} \int_0^\infty dx \left[\exp\left(-\frac{(x-x_0)^2}{2t}\right) - \exp\left(-\frac{(x+x_0)^2}{2t}\right) \right] \\ &= \text{erf}\left(\frac{x_0}{\sqrt{2t}}\right) = \text{erf}\left(\frac{x_0}{\sqrt{4\langle D \rangle_{st} t}}\right). \end{aligned} \tag{16}$$

This result equals the one for Brownian diffusion in a semi-infinite domain, in agreement with the fact that at long times the DD model shows a crossover to Gaussian diffusion with effective diffusivity $\langle D \rangle_{st}$. In analogy with Brownian diffusion, this particularly leads to the divergence of the mean first passage time, $\langle t \rangle = \infty$.

3.2. Survival of diffusing diffusivity model in a finite domain

We now turn to a finite domain $[0, L]$ with absorbing boundaries at $x = 0$ and $x = L$. Drawing on the subordination approach again, we map the images result for the finite domain to obtain the DD propagator,

$$P(x, t|x_0) = \frac{2}{L} \sum_{n=1}^{\infty} \sin\left(\frac{\pi n}{L}x_0\right) \sin\left(\frac{\pi n}{L}x\right) \tilde{T}_1(\lambda_{2n}^2, t). \tag{17}$$

By integration we obtain the survival probability

$$S(t|x_0) = \frac{4}{\pi} \sum_{n=0}^{\infty} \sin\left(\frac{\pi(2n+1)}{L}x_0\right) \frac{\tilde{T}_1(\lambda_{2n+1}^2, t)}{(2n+1)}, \tag{18}$$

from which we obtain the limiting behaviours for short times,

$$S_{ST}(t|x_0) \sim \frac{4}{\pi} \sum_{n=0}^{\infty} \sin\left(\frac{\pi(2n+1)}{L}x_0\right) \frac{1}{(2n+1)\sqrt{\lambda_{2n+1}^2 t + 1}}, \tag{19}$$

and for long times,

$$S_{LT}(t|x_0) \sim \frac{4\sqrt{2}}{\pi} \sum_{n=0}^{\infty} \sin\left(\frac{\pi(2n+1)}{L}x_0\right) \exp\left(-\frac{t}{2} \left[\sqrt{1 + 2\lambda_{2n+1}^2} - 1\right]\right) \times (2n+1) \left(1 + \frac{1}{2} \left(\sqrt{1 + 2\lambda_{2n+1}^2} + \frac{1}{\sqrt{1 + 2\lambda_{2n+1}^2}}\right)\right)^{1/2}. \tag{20}$$

Note that, as in the previous case, the asymptotic behaviour at short times can also be found through direct calculation of the superstatistical integral.

4. Discussion of results

Figures 1 and 2 show a comparison of the results obtained for the DD model with the classical ones for Brownian–Gaussian motion in the semi-infinite and finite domains, respectively. In figures 1 (left) and 2 we include results from simulations, demonstrating excellent agreement with our analytical results. As expected, we observe significant dissimilarities between the two models mostly in the short time limit. At intermediate time scales the DD model shows a crossover from short time superstatistical behaviour to the limiting Brownian–Gaussian behaviour with effective diffusivity $\langle D \rangle_{st}$.

For the semi-infinite domain figure 1 demonstrates that in the short time regime the DD process exhibits a faster decay of the survival probability and thus a faster first passage dynamics. This effect is particularly visible in the right panel, in which short times correspond to large values on the abscissa x_0/\sqrt{t} . To clarify this effect we express result (15) and the one for Brownian motion in terms of elementary functions,

$$S_{BM}(t|x_0) \sim 1 - \frac{\sqrt{2}e^{-(x_0^2/2t)}}{\sqrt{\pi}x_0} t^{1/2}, \quad x_0/\sqrt{t} \rightarrow \infty, \tag{21}$$

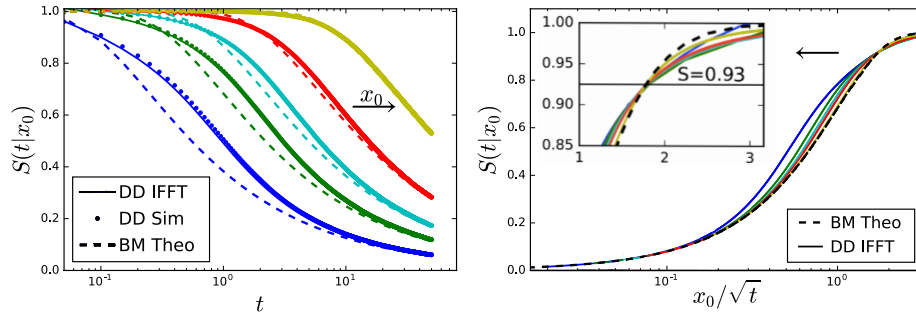


Figure 1. Left: comparison of numerical and analytical results for the survival probability $S(t|x_0)$ in the semi-infinite interval. Different colours represent the initial positions $x_0 = 0.5, 1, 1.5, 2,$ and 5 . Dashed lines in both panels represent the theoretical results of the corresponding Brownian–Gaussian motion (BM Theo). The numerical results (dots) obtained through Monte Carlo simulations are in full agreement with the analytical trend (solid line) obtained from numerical integration of the inverse Fourier transform (11) using the inverse fast Fourier transform (IFFT) algorithm. Right: analytical results for the survival probability in rescaled units in the semi-infinite domain as function of x_0/\sqrt{t} . In the inset the short time behaviour of $S(t|x_0)$ is reported, the universal crossover at $S \approx 0.93$ (corresponding to the crossover point $x_0/\sqrt{t} \approx 1.78$) is distinct. The same colour coding for different initial positions x_0 is used as in the left panel. The Brownian–Gaussian result is fully independent of the value of x_0 , as the survival probability exclusively depends on the scaling variable x_0/\sqrt{t} , see equations (15) and (16).

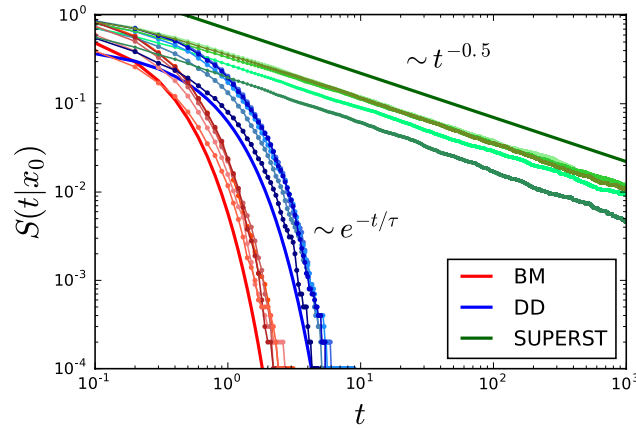


Figure 2. Survival probability for the finite interval $[0, L]$, showing a comparison between Brownian–Gaussian diffusion, DD, and superstatistical dynamics. Different colour shades represent different initial positions x_0 , and the solid lines represent the analytical trends. We observe that at long times the asymptotic behaviour is the expected power law for the superstatistical model and exponential tails for the DD and Brownian–Gaussian models, the latter with two different characteristic decay times τ .

$$S_{\text{ST}}(t|x_0) \sim 1 - \frac{\sqrt{2}e^{-(x_0/\sqrt{t})}}{\sqrt{\pi x_0}} t^{1/4} + \frac{5e^{-(x_0/\sqrt{t})}}{4\sqrt{2\pi x_0^3}} t^{3/4}, \quad x_0/\sqrt{t} \rightarrow \infty. \quad (22)$$

Comparing the asymptotes (21) with (22) along with the inset in figure 1 (right), we observe that for a fixed initial position x_0 the DD survival probability initially indeed drops faster than the one for Brownian–Gaussian motion. This behaviour is more pronounced when x_0 is closer to the absorbing boundary and less relevant for larger x_0 . From a physical point of view, this can be understood due to the fact that the closer to the boundary we place the particle initially the more likely it is that the particle is absorbed immediately, independently from the underlying diffusive model.

Figure 1 (right) demonstrates two universalities. First, we observe that at intermediate times the survival probabilities for any initial position show a universal convergence to a common crossover point at around $S(t|x_0) \approx 0.93$, including the Brownian–Gaussian survival probability. For sufficiently large values of x_0/\sqrt{t} , the DD model results in a smaller survival probability, whereas the behaviour is the opposite below the crossover value of x_0/\sqrt{t} . Second, the initial advantage of faster first passage of the DD process over Brownian–Gaussian motion which reverts after the universal crossover point, appears to balance out: at long times the survival probability in all cases converges to the exact result of Brownian–Gaussian motion with effective diffusivity $\langle D \rangle_{\text{st}}$. This can be seen directly from result (16), the associated first passage density of which is exactly the well-known Lévy–Smirnov form $\wp(t) = (x_0/\sqrt{4\pi\langle D \rangle_{\text{st}}t^3}) \exp(-x_0^2/[4\langle D \rangle_{\text{st}}t])$.

Qualitatively a similar behaviour is observed for finite domains at short times. As shown in figure 2, in contrast, the long time behaviour is dominated by the exponential shoulder (20) corresponding to the lowest non-zero eigenvalue in the DD model. The corresponding characteristic time scale τ in figure 2 is longer than for Brownian–Gaussian motion. This is due to the fact that in the finite interval the particles will reach the boundary before experiencing the entire diffusivity space, and so the effective Brownian limit is not recovered. The larger the interval L is the smaller the difference between the characteristic times of DD and Brownian–Gaussian models will be. In the limit of $L \rightarrow \infty$ the same long time behaviour is observed. Figure 2 also demonstrates an interesting behaviour of the superstatistical model. When the diffusivity distribution (2) governs the particle motion at all times t , even in the finite domain a power law scaling of the survival probability emerges, and thus a diverging mean first passage time is produced. This behaviour is caused by an appreciable fraction of immobile particles manifested in the divergence or nonzero value of $p_D(D = 0)$ in $d = 1$ and $d = 2$, respectively. This behaviour is rectified in the DD model.

How universal is the observed behaviour of the DD model based on the Ornstein–Uhlenbeck process? To assess this question we analyse the generalised DD model based on the superstatistical short time distribution $p(D) = \eta/[D_*\Gamma(\nu/\eta)]D^{\nu-1} \exp(-[D/D_*]^\eta)$ in the form of a generalised Gamma distribution. In [24] this model was studied as a generalisation of the Ornstein–Uhlenbeck process for the diffusivity. For the different models we rescaled space-time such that the MSD has the same value, $\langle x^2(t) \rangle = t$ in our dimensionless units. The comparison for different values of the parameters ν and η shows that the distribution $p(D)$ may have significantly distinct forms, which reflects upon the behaviour of the survival probability, as shown in figure 3. In particular, for certain parameters the faster first passage behaviour at shorter times persists, while for other parameter values the performance is close

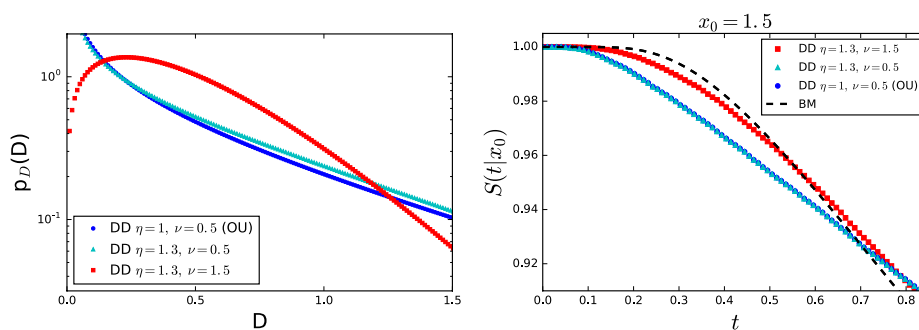


Figure 3. Comparison of the DD model based on the Ornstein–Uhlenbeck (OU) process with the generalised DD model from [24] based on the generalised Gamma distribution. Left: depending on the parameters ν and η the distribution $p(D)$ may be significantly different. Right: survival probability for the different models, demonstrating that for certain parameter values the first passage behaviour remains faster while for others the performance is getting close to that of Brownian–Gaussian motion. Note that the results for the two cases with $\nu = 0.5$ almost coincide.

to the Brownian case. We also note that the positions of the crossover points may vary with the different DD models.

5. Conclusions

We studied the first passage behaviour of the popular DD model used as a mean field proxy for diffusion of test particles in heterogeneous environments, in which the particle experiences varying diffusivities. Our analysis demonstrated that at short times the DD dynamics leads to a faster decay of the survival probability and thus to faster first passage. In a semi-infinite domain, fully independent of the initial particle position a universal crossover occurs, beyond which the DD dynamics becomes slower than pure Brownian–Gaussian motion, and the ultimate decay is determined by the conventional Lévy–Smirnov behaviour for initial particle position x_0 and effective diffusivity $\langle D \rangle_{st}$. The initially faster DD dynamics may be particularly relevant in cases of molecular regulation processes at very low concentrations (few-encounter limit) [32]. A similar crossover in the first passage behaviour occurs in the case of a finite domain (not shown here). At long times in finite domains the DD first passage behaviour is dominated by an exponential shoulder with a characteristic time (approximately the mean first passage time) that is longer than that for Brownian–Gaussian motion.

These results are in agreement with the expectation that rare events, represented by the exponential tails of the particles displacement distribution at short times, may dominate triggered actions. Thus, even if in general heterogeneity in the environment does not improve the mean first passage result (in fact some of the particles are slowed down) it allows some other particles to have a diffusion coefficient greater than the average, and this is enough to increase the speed of the reaction activation in diffusion-limited reactions. Moreover, we proved that the amount of fast particles does not depend on the initial position, representing the distance between particle and target. This suggests that the obtained results may be qualitatively generalised to any distribution of the initial particle position.

The study developed here is not limited to the one-dimensional case. First of all, we know that in the semi-infinite domain the results of the survival probability of Brownian–Gaussian

motion in $d = 2$ and $d = 3$ are the same as the one in $d = 1$. Then, the same analysis of the first passage problem can be performed by solely changing to the corresponding d -dimensional subordinator. For finite domains the analysis is also similar since, for all d we have an exponential behaviour in time of the propagator which allows us to relate the DD survival probability to the Laplace transform of the corresponding subordinator, as we did for the one-dimensional case.

We finally note that similar non-Gaussian effects have been reported for systems, in which the (subdiffusive) motion is dominated by viscoelastic effects. With a fixed diffusivity this would be a Gaussian process, and the non-Gaussianity was shown to stem from varying diffusivity values [12, 33, 34]. It will be interesting to study the associated first passage behaviour in this case, as well.

Acknowledgments

VS thanks the organisers of the 671st WE-Heraeus-Seminar on Search and Problem Solving by Random Walks: Drunkards vs Quantum Computers at Bad Honnef, Germany, in May 2018 where the main results of this work were presented. RM and AVC acknowledge funding from Deutsche Forschungsgemeinschaft, grants ME 1535/6-1 and ME 1535/7-1. RM acknowledges the Foundation for Polish Science (Fundacja na rzecz Nauki Polski) for funding within an Alexander von Humboldt Polish Honorary Research Scholarship.

ORCID iDs

Ralf Metzler  <https://orcid.org/0000-0002-6013-7020>

References

- [1] Brown R 1828 A brief account of microscopical observations made on the particles contained in the pollen of plants *Phil. Mag.* **4** 161
- [2] van Kampen NG 1981 *Stochastic Processes in Physics and Chemistry* (Amsterdam: North-Holland)
- [3] Höfling F and Franosch T 2013 Anomalous transport in the crowded world of biological cells *Rep. Prog. Phys.* **76** 046602
- [4] Nørregaard K, Metzler R, Ritter C, Berg-Sørensen K and Oddershede L 2017 Manipulation and motion of organelles and single molecules in living cells *Chem. Rev.* **117** 4342
- [5] Bouchaud J P and Georges A 1990 Anomalous diffusion in disordered media: statistical mechanisms, models and physical applications *Phys. Rep.* **195** 127–293
- [6] Metzler R, Jeon J H, Cherstvy A G and Barkai E 2014 Anomalous diffusion models and their properties: non-stationarity, non-ergodicity and ageing at the centenary of single particle tracking *Phys. Chem. Chem. Phys.* **16** 24128–64
- [7] Mandelbrot B B and van Ness J W 1968 Fractional Brownian motions, fractional noises and applications *SIAM Rev.* **10** 422–37
- [8] Scher H and Montroll E W 1975 Anomalous transit-time dispersion in amorphous solids *Phys. Rev. B* **12** 2455
- [9] Cherstvy A G, Chechkin A V and Metzler R 2013 Anomalous diffusion and ergodicity breaking in heterogeneous diffusion processes *New J. Phys.* **15** 083039
- [10] Wang B, Kuo J, Bae S C and Granick S 2012 When Brownian diffusion is not Gaussian *Nat. Mater.* **11** 481–5
- [11] Hapca S, Crawford J W and Young I M 2009 Anomalous diffusion of heterogeneous populations characterized by normal diffusion at the individual level *J. R. Soc. Interface* **6** 111–22

- [12] Lampo T, Stylianido S, Backlund M P, Wiggins P A and Spakowitz A J 2017 Cytoplasmic RNA-protein particles exhibit non-Gaussian subdiffusive behaviour *Biophys. J.* **112** 532–42
Metzler R 2017 Gaussianity fair: the riddle of anomalous yet non-Gaussian diffusion *Biophys. J.* **112** 413–5
- [13] Wang B, Antony S M, Bae S C and Granick S 2009 Anomalous yet Brownian *Proc. Natl Acad. Sci. USA* **106** 15160–4
- [14] Leptos K C, Guasto J S, Gollub J P, Pesci A I and Goldstein R E 2009 Dynamics of enhanced tracer diffusion in suspensions of swimming eukaryotic microorganisms *Phys. Rev. Lett.* **103** 198103
- [15] Cherstvy A G, Nagel O, Beta C and Metzler R 2018 Non-Gaussianity, population heterogeneity, and transient superdiffusion in the spreading dynamics of amoeboid cells *Phys. Chem. Chem. Phys.* **20** 23034
- [16] Beck C and Cohen E D B 2003 Superstatistics *Physica A* **322** 267
- [17] Beck C 2006 Superstatistical Brownian motion *Prog. Theor. Phys. Suppl.* **162** 29–36
- [18] Chubynsky M V and Slater G W 2014 Diffusing diffusivities: a model for anomalous, yet Brownian diffusion *Phys. Rev. Lett.* **113** 098302
- [19] Matse M, Chubynsky M V and Bechhoefer J 2017 Test of the diffusing-diffusivity mechanism using nearwall colloidal dynamics *Phys. Rev. E* **96** 042604
- [20] Jain R and Sebastian K L 2016 Diffusion in a crowded, rearranging environment *J. Phys. Chem. B* **120** 3988–92
- [21] Jain R and Sebastian K L 2017 Diffusing diffusivity: a new derivation and comparison with simulations *J. Chem. Sci.* **129** 929–37
- [22] Tyagi N and Cherayil B J 2017 Non-Gaussian Brownian diffusion in dynamically disordered thermal environments *J. Phys. Chem. B* **121** 7204–9
- [23] Chechkin A V, Seno F, Metzler R and Sokolov I 2017 Brownian yet non-Gaussian diffusion: from superstatistics to subordination of diffusing diffusivities *Phys. Rev. X* **7** 021002
- [24] Sposini V, Chechkin A V, Seno F, Pagnini G and Metzler R 2018 Random diffusivity from stochastic equations: comparison of two models for Brownian yet non-Gaussian diffusion *New J. Phys.* **20** 043044
- [25] Lanoiselée Y and Grebenkov D 2018 A model of non-Gaussian diffusion in heterogeneous media *J. Phys. A: Math. Theor.* **51** 145602
- [26] Redner S 2001 *A Guide to First Passage Processes* (Cambridge: Cambridge University Press)
- [27] Metzler R, Oshanin G and Redner S 2014 *First-Passage Phenomena and their Applications* (Singapore: World Scientific)
- [28] Bochner S 1960 *Harmonic Analysis and the Theory of Probability* (Berkeley, CA: Berkeley University Press)
- [29] Prudnikov A P 1986 *Integrals and Series. Volume 2: Special Functions* (Boca Raton, FL: CRC Press)
- [30] Mura A and Pagnini G 2008 Characterizations and simulations of a class of stochastic processes to model anomalous diffusion *J. Phys. A: Math. Theor.* **41** 285003
- [31] Sliusarenko O, Vitali S, Sposini V, Paradisi P, Chechkin A V, Castellani G and Pagnini G 2018 Finite-energy Lévy-type motion through heterogeneous ensemble of Brownian particles (arXiv:1807.07883 [cond-mat.stat-mech])
- [32] Godec A and Metzler R 2016 Universal proximity effect in target search kinetics in the few encounter limit *Phys. Rev. X* **6** 041037
Godec A and Metzler R 2017 First passage time statistics for two-channel diffusion *J. Phys. A: Math. Theor.* **50** 084001
- [33] Jeon J-H, Javanainen M, Martinez-Seara H, Metzler R and Vattulainen I 2016 Protein crowding in lipid bilayers gives rise to non-Gaussian anomalous lateral diffusion of phospholipids and proteins *Phys. Rev. X* **6** 021006
- [34] He W, Song H, Su Y, Geng L, Ackerson B J, Peng H B and Tong P 2016 Dynamic heterogeneity and non-Gaussian statistics for acetylcholine receptors on live cell membranes *Nat. Commun.* **7** 11701



Sposini V, Metzler R & Oshanin G 2019 Single-trajectory spectral analysis of scaled Brownian motion *New J. Phys.* **21**, 073043.



PAPER

Single-trajectory spectral analysis of scaled Brownian motion

OPEN ACCESS

RECEIVED
15 March 2019REVISED
18 June 2019ACCEPTED FOR PUBLICATION
4 July 2019PUBLISHED
23 July 2019Original content from this
work may be used under
the terms of the [Creative
Commons Attribution 3.0
licence](https://creativecommons.org/licenses/by/4.0/).Any further distribution of
this work must maintain
attribution to the
author(s) and the title of
the work, journal citation
and DOI.Vittoria Sposini^{1,2}, Ralf Metzler¹  and Gleb Oshanin^{3,4} ¹ Institute for Physics & Astronomy, University of Potsdam, D-14476 Potsdam-Golm, Germany² Basque Centre for Applied Mathematics, E-48009 Bilbao, Spain³ Sorbonne Université, CNRS, Laboratoire de Physique Théorique de la Matière Condensée (UMR 7600), 4 Place Jussieu, F-75252 Paris Cedex 05, France⁴ Interdisciplinary Scientific Center Poncelet (ISCP), 119002, Moscow, RussiaE-mail: rmetzler@uni-potsdam.de**Keywords:** diffusion, anomalous diffusion, power spectral analysis, single trajectory analysis**Abstract**

A standard approach to study time-dependent stochastic processes is the power spectral density (PSD), an ensemble-averaged property defined as the Fourier transform of the autocorrelation function of the process in the asymptotic limit of long observation times, $T \rightarrow \infty$. In many experimental situations one is able to garner only relatively few stochastic time series of finite T , such that practically neither an ensemble average nor the asymptotic limit $T \rightarrow \infty$ can be achieved. To accommodate for a meaningful analysis of such finite-length data we here develop the framework of single-trajectory spectral analysis for one of the standard models of anomalous diffusion, scaled Brownian motion. We demonstrate that the frequency dependence of the single-trajectory PSD is exactly the same as for standard Brownian motion, which may lead one to the erroneous conclusion that the observed motion is normal-diffusive. However, a distinctive feature is shown to be provided by the explicit dependence on the measurement time T , and this ageing phenomenon can be used to deduce the anomalous diffusion exponent. We also compare our results to the single-trajectory PSD behaviour of another standard anomalous diffusion process, fractional Brownian motion, and work out the commonalities and differences. Our results represent an important step in establishing single-trajectory PSDs as an alternative (or complement) to analyses based on the time-averaged mean squared displacement.

1. Introduction

The spectral analysis of measured position time series ('trajectories') $X(t)$ of a stochastic process provides important insight into its short and long time behaviour, and also unveils its temporal correlations [1]. In standard textbook settings, spectral analyses are carried out by determining the so-called power spectral density (PSD) $\mu(f)$ of the process. The PSD is classically calculated by first performing a Fourier transform of an individual trajectory $X(t)$ over the finite observation time T

$$S(f, T) = \frac{1}{T} \left| \int_0^T e^{if t} X(t) dt \right|^2, \quad (1)$$

where f denotes the frequency. The quantity $S(f, T)$ for finite observation times T is, of course, a random variable. The standard PSD yields from $S(f, T)$ by averaging it over a statistical *ensemble* of all possible trajectories. After taking the asymptotic limit $T \rightarrow \infty$, one obtains the standard PSD

$$\begin{aligned} \mu(f) &= \lim_{T \rightarrow \infty} \frac{1}{T} \left\langle \left| \int_0^T e^{if t} X(t) dt \right|^2 \right\rangle \\ &= \lim_{T \rightarrow \infty} \frac{1}{T} \int_0^T \int_0^T \cos(f[t_1 - t_2]) \langle X(t_1) X(t_2) \rangle dt_1 dt_2, \end{aligned} \quad (2)$$

where the angular brackets denote the statistical averaging. In the second line of (2), taking into account that $X(t)$ is real-valued, we took the absolute square and used the summation relation for trigonometric functions [2] to obtain the cosine function with the difference of the two times and the autocorrelation function $\langle X(t_1)X(t_2) \rangle$ of the process $X(t)$; see [1, 3, 4] for more details.

The PSD (2) is widely used to evaluate measured time traces $X(t)$, especially in experimental setups measuring in frequency domain, such as spectroscopic methods. The PSD provides information complementary to the autocorrelation $\langle X(t_1)X(t_2) \rangle$, and the relation between the PSD $\mu(f)$ and $\langle X(t_1)X(t_2) \rangle$ is in fact the famed Wiener–Khinchine theorem. Moreover, in physical terms the PSD corresponds to the spectral net power (energy per unit time). Following definition (2), the standard, ensemble-averaged PSD was determined for various processes across many disciplines. This includes, for instance, the variation of the loudness of musical performances [5], the temporal evolution of climate data [6] and of the waiting-times between earthquakes [7], the retention times of chemical tracers in groundwater [8] and noises in graphene devices [9], fluorescence intermittency in nano-devices [10], current fluctuations in nanoscale electrodes [11], or ionic currents across nanopores [12]. The PSD was also calculated analytically for individual time series in a stochastic model describing blinking quantum dots [13], for non-stationary processes taking advantage of a generalised Wiener–Khinchine theorem [14, 15], for the process of fractional Brownian motion (FBM) with random reset [16], the running maximum of a Brownian motion [17], as well as for diffusion in strongly disordered Sinai-type systems [18], to name but a few stray examples.

An alternative approach geared towards realistic experimental situations was recently proposed—based directly on the finite-time, single-trajectory PSD (1) [3, 4] (see also [19]). The need for such an alternative to the standard PSD (2) is two-fold. First, while the asymptotic limit $T \rightarrow \infty$ can well be taken in mathematical expressions, it cannot be realistically achieved experimentally. This especially holds for typical, modern single particle tracking experiments, in which the observation time is limited by the microscope’s focus or the fluorescence lifetime of the dye label tagging the moving particle of interest [20]. In general, apart from the dependence on the frequency f the single-trajectory PSD (1) therefore explicitly is a function of the observation time T . Moreover, fluctuations between individual results $S(f, T)$ of the single-trajectory PSD will be observed, even for normal Brownian motion [3]. Second, and maybe even more importantly, while such fluctuations between trajectories may, of course, be mitigated by taking an average over a statistical ensemble, in many cases the number of measured trajectories is too small for a meaningful statistical averaging. Indeed, for the data garnered in, for instance, *in vivo* experiments [20], climate evolution [21], or the evolution of financial markets [22] one necessarily deals with a single or just a few realisations of the process. As we will show, despite the fluctuations between individual trajectories relevant information can be extracted from the frequency and observation time-dependence of single-trajectory PSDs. Even more, the very trajectory-to-trajectory amplitude fluctuations encode relevant information, that can be used to dissect the physical character of the observed process.

How would we understand an observation time-dependence? This is not an issue, of course, for stationary random processes, but apart from Brownian motion, only very few naturally occurring random processes are stationary. A T -dependent evolution of the PSD can in fact be rather peculiar and system dependent. For instance, the PSD may be ageing and its amplitude may decay with T , as it happens for non-stationary random signals [15], or conversely, it can exhibit an unbounded growth with T , a behaviour predicted analytically and observed experimentally for superdiffusive processes of FBM type [4]. As a consequence, the standard textbook definition (2) of the PSD which emphasises the limit $T \rightarrow \infty$, can become rather meaningless.

Motivated by the two arguments in favour of using a single-trajectory approach to the PSD—the lack of sufficient trajectories in a typical experiment in order to form an ensemble average and insufficiently long observation times T —[3, 4] concentrated on the analysis of the random variable $S(f, T)$ defined in (1) for arbitrary finite T and f . Both for Brownian motion and FBM with arbitrary Hurst index (anomalous diffusion exponent, see below) a range of interesting, and sometimes quite unexpected features were unveiled, as detailed in the comparative discussion at the end of section 3.

While FBM, whose single-trajectory PSD is studied in [4] is a quite widespread anomalous diffusion process, it is far from the only relevant example of naturally occurring random processes with anomalous diffusive behaviour. As, in principle, $S(f, T)$ may behave distinctly for different stochastic processes, in order to get a general and comprehensive picture of the evolution in the frequency domain, one needs to study systematically the single-trajectory PSDs of other experimentally-relevant processes, such as, scaled Brownian motion (SBM), the continuous time random walk, or diffusing diffusivity models, to name just a few. In all these examples the microscopic physical processes underlying the global departure from standard Brownian motion are different, and we would expect that this difference in the microscopic behaviour translates into the behaviour in the frequency domain.

Here we concentrate on trajectories $X_\alpha(t)$ generated by SBM, a class of non-stationary anomalous diffusion processes encoding the mean squared displacement (MSD) $\langle X_\alpha^2(t) \rangle \simeq t^\alpha$ with anomalous diffusion exponent α .

SBM was formally studied within different contexts in the last two decades [23–25]. Historically, it was introduced already by Batchelor in 1952 in the context of the turbulent motion of clouds of marked fluids [26], originally studied by Richardson in 1926 [27]. An important application of SBM is for particle motion in the homogeneous cooling state of force-free cooling granular gases, in which the continuously decaying temperature (defined via the continuously dissipating kinetic energy) effectively leads to a time-dependence of the self-diffusion coefficient of the gas [28]. SBM also describes the dynamics of a tagged monomer involved in processes of irreversible polymerisation [29]. Similar dynamics emerge in the analysis of fluorescence recovery after photobleaching (FRAP) data [30], as well as of fluorescence correlation spectroscopy data [31], which are both widely used techniques to measure diffusion of macromolecules in living cells and their membranes. Lastly, essentially the same type of anomalous diffusion modelling was used for the analysis of potential water availability in a region due to precipitation (snow and rain) [32].

As an application of SBM in a broader sense, one may envisage a material undergoing an annealing process—a slow, externally imposed decrease of the temperature used in metallurgy or in preparations of glasses to get rid of internal defects. Effectively, the dynamics of the latter can be considered as an SBM—a Brownian motion with a diffusion coefficient being a slowly decreasing function of the temperature. In a similar way, one uses such a slow annealing in computer search for a global minimum of a complex energy landscape, which prevents trapping by local minima. Here, as well, if the search process proceeds by jumps of a fixed length, one encounters effectively an SBM-type process. Moreover, SBM may be used to describe the effective diffusion in an expanding medium [33]. Finally, SBM may be considered as a mean field description of continuous time random walks with scale-free waiting time densities [24].

A different perspective for applications of our PSD analysis are areas, in which the time variable represents other, complementary quantities. Thus, the height profile of an effectively one-dimensional surface may be thought of as a time series. While such modelling typically involves FBM-type statistics [34], it may be of interest to compare the predictions to those of the Markovian yet non-stationary SBM. We also mention the connection of time series to the visibility graph in complex networks [35].

The outline of the paper is as follows. In section 2 we present the basics of SBM, introduce our notation, and define the properties under study. Section 3 is devoted to the spectral analysis of single-trajectory PSDs governed by SBM. Here, we first derive an exact expression for the moment-generating function of the random variable $S(f, T)$ and evaluate the exact form of the associated probability density function (PDF). The form of the latter turns out to be entirely defined by its first two moments, in analogy to the parental process $X_\alpha(t)$. We then present explicit forms of these two moments, valid for arbitrary anomalous diffusion exponent α , frequency f , and observation time T . Section 3 ends with a comparative discussion of our results with the behaviour of the single-trajectory PSD for FBM, the only anomalous diffusion process for which the behaviour of a single-trajectory PSD is known exhaustively well at present [4]. Finally, we conclude with a brief summary of our results and a perspective in section 4.

2. Model and basic notations

SBM $X_\alpha(t)$ is an α -parametrised family of Gaussian stochastic processes defined by the (stochastic) Langevin equation [23–25]

$$\frac{dX_\alpha(t)}{dt} = \sqrt{2D_\alpha(t)} \times \xi(t), \quad (3)$$

where $\xi(t)$ denotes Gaussian white-noise with zero mean and variance 1/2, such that

$$\langle \xi(t_1) \xi(t_2) \rangle = \delta(t_1 - t_2). \quad (4)$$

Moreover, $D_\alpha(t)$ is the diffusion coefficient, that follows the deterministic power-law in time⁵

$$D_\alpha(t) = \alpha K_\alpha t^{\alpha-1}, \quad 0 < \alpha < 2, \quad (5)$$

where the coefficient K_α has physical dimension $\text{cm}^2/\text{s}^\alpha$. In general, SBM describes anomalous diffusion, such that the ensemble-averaged MSD scales as a power law in time

$$\langle X_\alpha^2(t) \rangle = 2K_\alpha t^\alpha. \quad (6)$$

When $0 < \alpha < 1$ one observes subdiffusive behaviour, while for $1 < \alpha < 2$ SBM describes superdiffusion. Standard Brownian motion is recovered in the limit $\alpha = 1$. In figure 1 we depict four representative trajectories of $X_\alpha(t)$ for the subdiffusive, normal-diffusive, and superdiffusive cases. We note that, especially for the subdiffusive case $\alpha = 1/2$ the non-stationary character is not immediately obvious from the graph of $X_\alpha(t)$ ⁶,

⁵ The limit $\alpha = 0$ corresponds to the case of ultraslow diffusion with a logarithmic MSD, as studied in [36].

⁶ One may infer the slower spreading rather from comparison of the span of $X_\alpha(t)$ on the vertical axis.

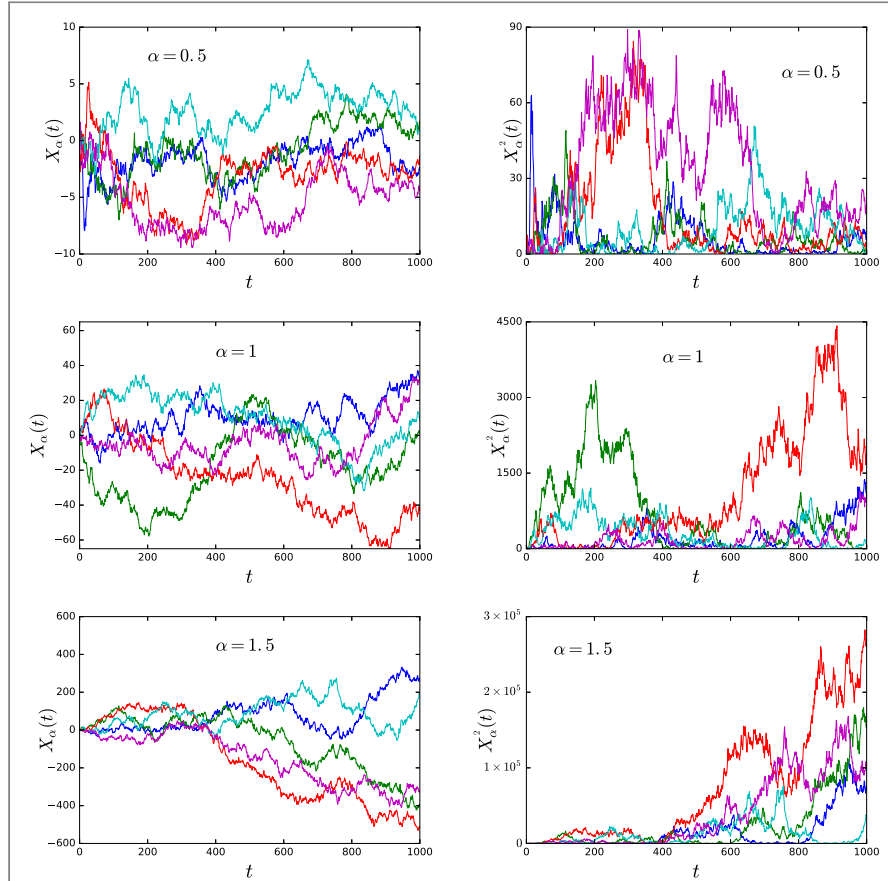


Figure 1. Four individual realisations $X_\alpha(t)$ for SBM with different anomalous diffusion exponent for subdiffusion ($\alpha = 0.5$, top), normal diffusion ($\alpha = 1$, middle), and superdiffusion ($\alpha = 1.5$, bottom). In the left column we show the process $X_\alpha(t)$ itself, while in the right column we display its square, $X_\alpha^2(t)$.

while the character of the process becomes somewhat more obvious when we plot the square process, $X_\alpha^2(t)$. Concurrently, in the superdiffusive case the growing fluctuations and large excursions away from the origin appear relatively more pronounced.

Before we proceed, it is expedient to recall other salient properties of SBM. In particular, its autocorrelation function can be readily calculated to give

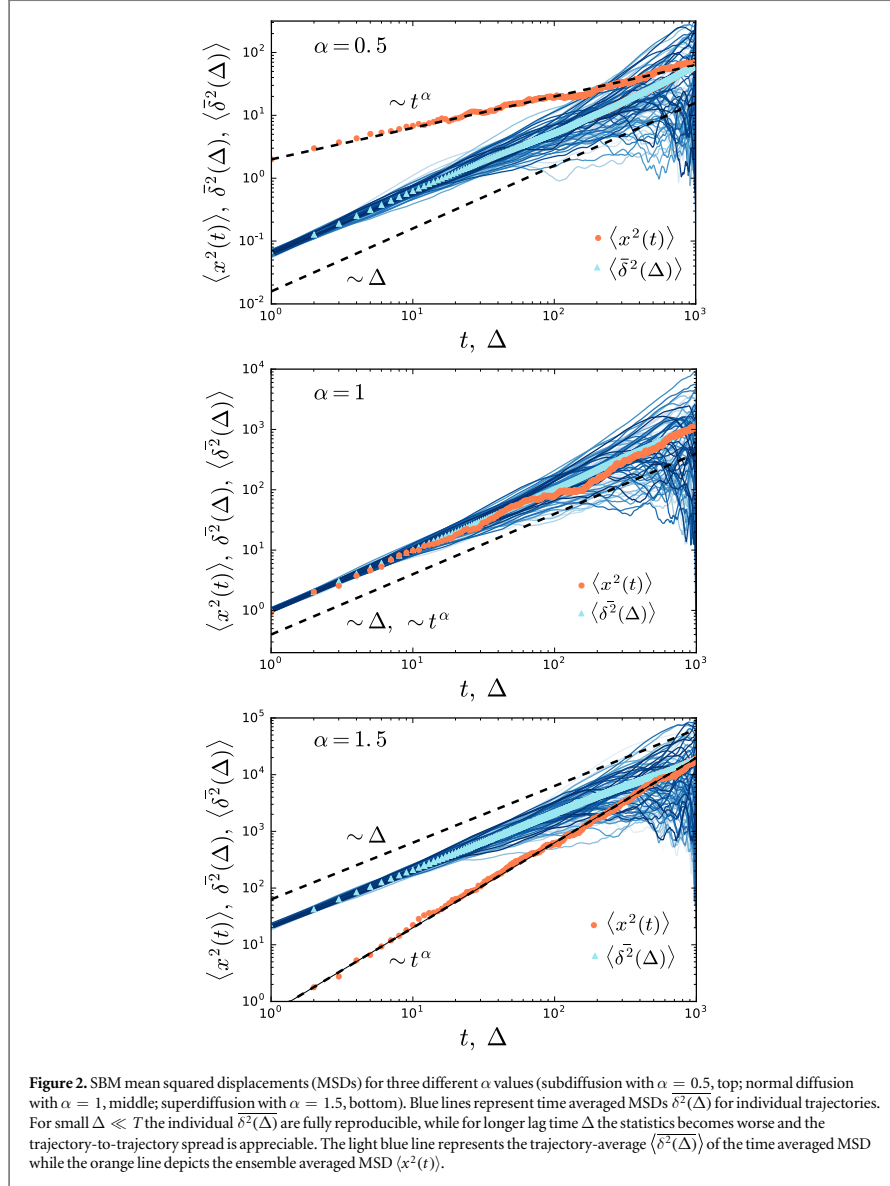
$$\langle X_\alpha(t_1)X_\alpha(t_2) \rangle = 2K_\alpha[\min\{t_1, t_2\}]^\alpha. \quad (7)$$

Hence, the covariance of $X_\alpha(t)$ has essentially the same form as the one for standard Brownian motion, except that the time variable is ‘scaled’⁷. A basic quantity to analyse the behaviour of individual trajectories is the time-averaged MSD of the time series $X_\alpha(t)$ in the time interval $[0, T]$ [38]

$$\overline{\delta^2(\Delta)} = \frac{1}{T - \Delta} \int_0^{T-\Delta} (X_\alpha(t + \Delta) - X_\alpha(t))^2 dt, \quad (8)$$

and its ensemble-averaged counterpart, which, taking into account expression (7), can be explicitly calculated as [25]

⁷ The definition of SBM would allow us to transform (subordinate [37]) time t such that the main calculations could be done for normal Brownian motion. However, as this would change the meaning of the frequency, we prefer to proceed in terms of the non-transformed time (and frequency).



$$\langle \overline{\delta^2}(\Delta) \rangle = \frac{2K_\alpha}{\alpha + 1} \left(\frac{T^{\alpha+1} - \Delta^{\alpha+1}}{T - \Delta} - (T - \Delta)^\alpha \right). \quad (9)$$

In the limit $\Delta \ll T$ we thus find $\langle \overline{\delta^2}(\Delta) \rangle \sim 2K_\alpha \Delta / T^{1-\alpha}$, a behaviour fundamentally different from the ensemble-averaged MSD (6), a feature of so-called weak ergodicity breaking: $\langle \overline{\delta^2}(\Delta) \rangle \neq \langle X_\alpha^2(\Delta) \rangle$ [38]. We display the behaviour of individual time-averaged MSDs $\overline{\delta^2}(\Delta)$ in figure 2, along with their ensemble average $\langle \overline{\delta^2}(\Delta) \rangle$ and the standard MSD $\langle X_\alpha^2(t) \rangle$. The non-ergodic behaviour of SBM is clearly highlighted by the different slopes of $\langle \overline{\delta^2}(\Delta) \rangle$ and $\langle X_\alpha^2(t) \rangle$.

Equipped with all necessary knowledge on the properties of SBM $X_\alpha(t)$, we now turn to the question of interest here, the analysis of its single-trajectory PSD. As $S(f, T)$ is a random variable, the most general information about its properties is contained in the moment-generating function

$$\Phi_\lambda = \langle \exp(-\lambda S(f, T)) \rangle, \quad \lambda \geq 0. \quad (10)$$

Once Φ_λ is determined, the PDF $P(S(f, T) = S)$ of the random variable $S(f, T)$ can be simply derived from equation (10) by an inverse Laplace transform with respect to the parameter λ . As we proceed to show below, both Φ_λ and $P(S(f, T) = S)$ are entirely defined by the first two moments, due to the Gaussian nature of the process $X_\alpha(t)$. The mean value, which represents the standard time-dependent PSD, is given by

$$\mu(f, T) = \langle S(f, T) \rangle, \quad (11)$$

while the variance of the random variable $S(f, T)$ obeys

$$\sigma^2(f, T) = \langle S^2(f, T) \rangle - \mu^2(f, T). \quad (12)$$

The quantities $\mu(f, T)$ and $\sigma^2(f, T)$ define the coefficient of variation

$$\gamma = \frac{\sigma(f, T)}{\mu(f, T)} \quad (13)$$

of the PDF of the single-trajectory PSD. As such, γ is a measure for the ‘broadness’ of a given distribution: when $\gamma > 1$ the spread $\sigma(f, T)$ of the distribution exceeds its mean value $\mu(f, T)$, and then the mean value can no longer be considered representative for the actual distribution. The calculation of the exact explicit forms of the properties defined in equations (10)–(13) represents the chief goal of our work.

3. Spectral analysis of individual trajectories of SBM

The single-trajectory PSDs $S(f, T)$ for four different sample trajectories for the three anomalous diffusion exponents $\alpha = 1/2$, $\alpha = 1$, and $\alpha = 3/2$ are shown in figure 3 (top). While, naturally, we observe distinct fluctuations within $S(f, T)$ and between different realisations, all data clearly show a $S(f, T) \simeq 1/f^2$ -scaling. The middle and bottom panels of figure 3 demonstrate the apparent scaling of the trajectory-averaged single-trajectory PSD as function of the observation time T (ageing behaviour) for two different frequency values—the respective T -scaling laws are derived below. We are now going to quantify these behaviours in detail.

3.1. Moment-generating function of the single-trajectory PSD

We start from definition (1) of the single-trajectory PSD and rewrite it in the form

$$S(f, T) = \frac{1}{T} \int_0^T \int_0^T \cos(f(t_1 - t_2)) X_\alpha(t_1) X_\alpha(t_2) dt_1 dt_2, \quad (14)$$

which is just a formal procedure since $X_\alpha(t)$ is a real-valued process. Relegating the intermediate steps of the derivation to appendix A, we eventually find the exact result

$$\begin{aligned} \Phi_\lambda &= \left\langle \exp\left(-\frac{\lambda}{T} \int_0^T \int_0^T \cos(f(t_1 - t_2)) X_\alpha(t_1) X_\alpha(t_2) dt_1 dt_2\right) \right\rangle \\ &= \frac{1}{\sqrt{1 + 2\mu\lambda + (2\mu^2 - \sigma^2)\lambda^2}}, \end{aligned} \quad (15)$$

where μ and σ^2 are defined in equations (11) and (12), respectively. Result (15) shows that the PDF of the single-trajectory PSD for SBM is fully defined through its first and second moment, and that it has exactly the same functional form as the results for Brownian motion and FBM derived in [3, 4]. As we have already remarked, this is a direct consequence of the Gaussian nature of the parental process $X_\alpha(t)$ of SBM.

Inverting the Laplace transform with respect to λ we obtain the PDF of the random variable $S(f, T)$,

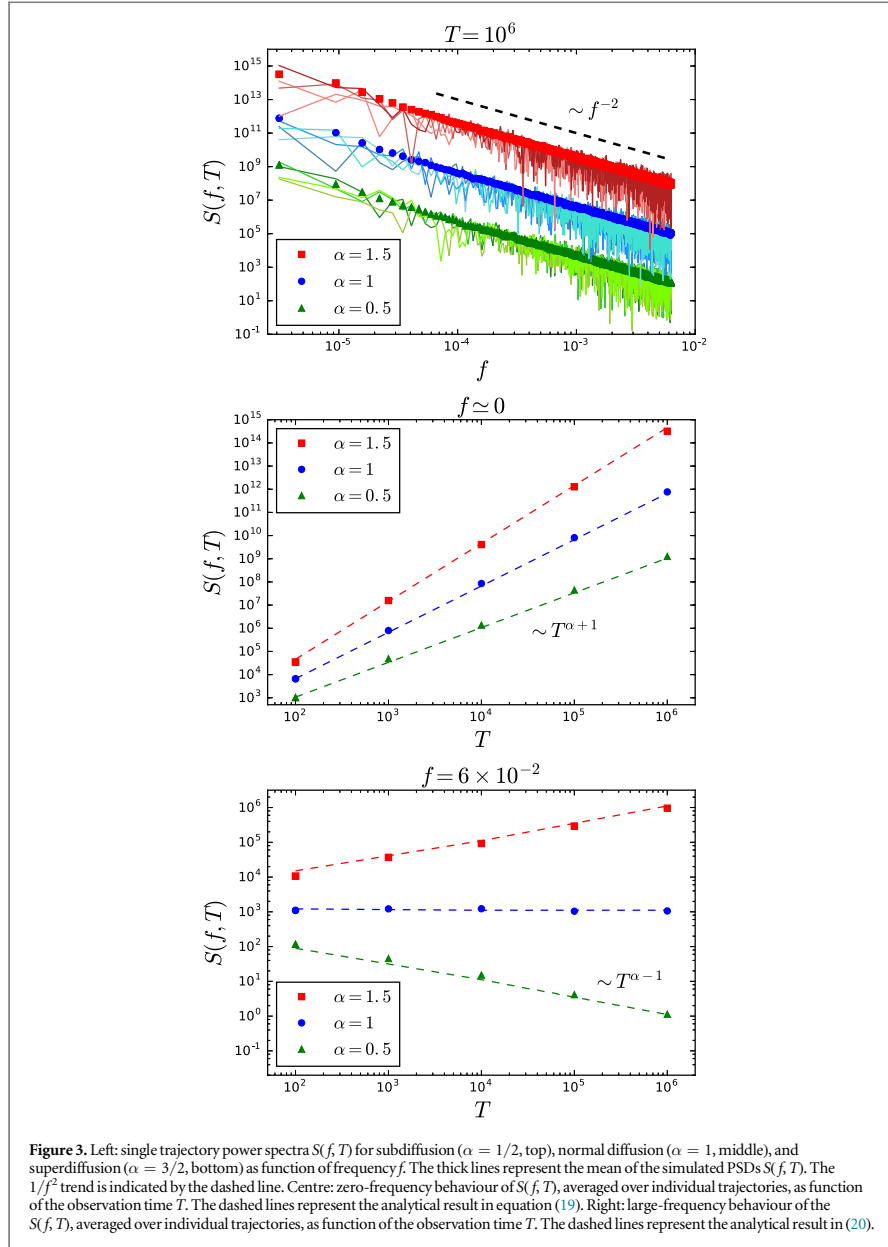
$$P(S(f, T) = S) = \frac{1}{\mu\sqrt{2 - \gamma^2}} \exp\left(-\frac{S}{\mu(2 - \gamma^2)}\right) I_0\left(\frac{\sqrt{\gamma^2 - 1}}{\mu(2 - \gamma^2)} S\right), \quad (16)$$

where I_ν is the modified Bessel function of the first kind. This function is known to be a distribution with heavier-than-Gaussian tails.

In figure 4 we present a comparison of the analytical result (16) for $P(S(f, T) = S)$ with simulations. The agreement is excellent. The width of the PDF $P(S(f, T) = S)$ becomes narrower for increasing α (note the different scales on the axes). In particular, the insets show the exponential shape of the PDF $P(S(f, T) = S)$ in the semi-logarithmic plots.

3.2. Ensemble-averaged PSD

We now proceed further and calculate the first moment of the PSD, defined in equation (11). Recalling the expression for the autocorrelation function (7) of SBM, we perform the integrations explicitly in appendix A, to find the final expression



$$\mu(f, T) = \frac{4K_\alpha T^{\alpha+1}}{fT} \left[\sin(fT) g_1\left(\frac{\alpha}{2}, fT\right) - \cos(fT) g_2\left(\frac{\alpha}{2}, fT\right) \right], \quad (17)$$

where we introduced the functions g_1 and g_2 defined in appendix A. It is straightforward to check that for $\alpha = 1$ equation (17) yields the standard expression of the PSD for Brownian motion

$$\mu(f, T)|_{\alpha=1} = \frac{4K_1}{f^2} \left(1 - \frac{\sin(fT)}{fT} \right), \quad (18)$$

where K_1 is the normal diffusion coefficient of dimensionality cm^2/s .

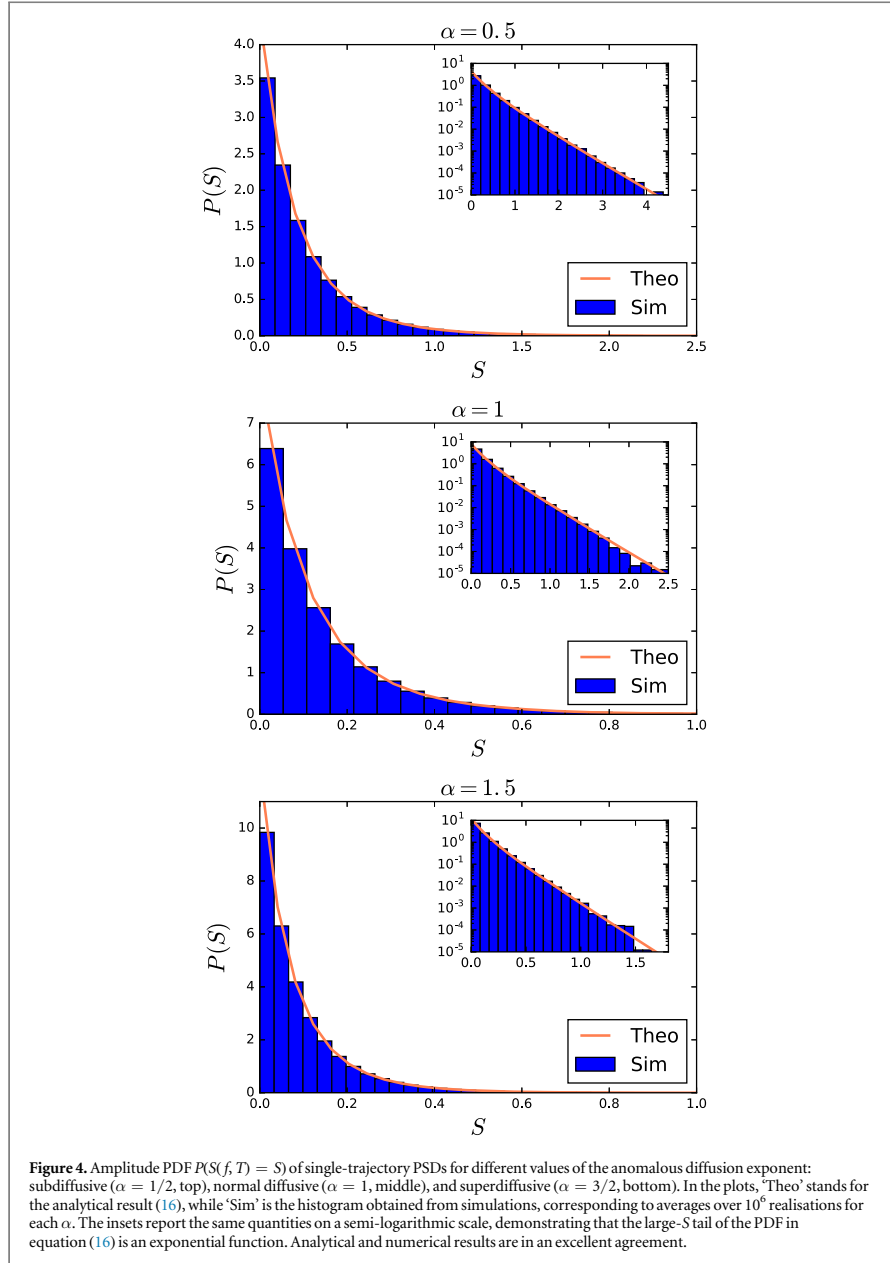


Figure 4. Amplitude PDF $P(S(f, T) = S)$ of single-trajectory PSDs for different values of the anomalous diffusion exponent: subdiffusive ($\alpha = 1/2$, top), normal diffusive ($\alpha = 1$, middle), and superdiffusive ($\alpha = 3/2$, bottom). In the plots, ‘Theo’ stands for the analytical result (16), while ‘Sim’ is the histogram obtained from simulations, corresponding to averages over 10^6 realisations for each α . The insets report the same quantities on a semi-logarithmic scale, demonstrating that the large- S tail of the PDF in equation (16) is an exponential function. Analytical and numerical results are in an excellent agreement.

Next, we focus on the asymptotic behaviour of the general expression (17) in the limit $fT \rightarrow \infty$, which is equivalent to either the limit $f \rightarrow \infty$ with T fixed, or vice versa. We get

$$\mu(f, T) \sim \frac{4K_\alpha T^{\alpha-1}}{f^2} \left\{ 1 - \frac{\Gamma(\alpha + 1) \cos(fT - \frac{\pi\alpha}{2})}{(fT)^\alpha} \right\}. \tag{19}$$

Interestingly, the f -dependence of the leading term is the same for *any* α , in particular, it is equal to the one for Brownian motion. The fact that we are not able to distinguish SBM from Brownian motion by just looking at the

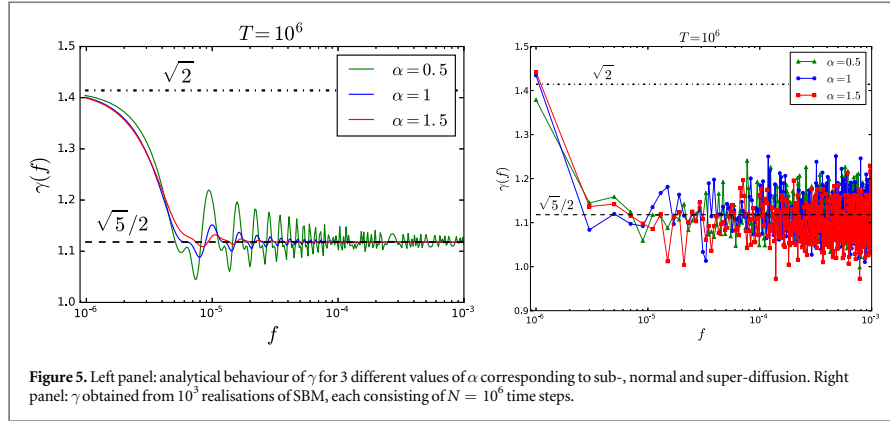


Figure 5. Left panel: analytical behaviour of γ for 3 different values of α corresponding to sub-, normal and super-diffusion. Right panel: γ obtained from 10^3 realisations of SBM, each consisting of $N = 10^6$ time steps.

frequency domain can lead, when analysing data, to the wrong conclusion that one deals with standard Brownian motion. Only when we have sufficiently precise data over a large frequency window, we could use the α -dependent subleading term to identify the anomalous diffusion exponent α . The only explicit α -dependence in the leading order of expression (19) is in the ageing behaviour encoded by the dependence on $T^{\alpha-1}$ in the prefactor, which therefore becomes a relevant behaviour to check. The dependence on α of the ageing factor leads to the convergence of the limit $T \rightarrow \infty$ in the subdiffusive case and to a divergence in the superdiffusive case. A second interesting limit is given by the low-frequency limit $f = 0$. In this case we obtain

$$\mu(f = 0, T) = \frac{4K_\alpha T^{\alpha+1}}{(\alpha + 1)(\alpha + 2)}. \quad (20)$$

This result represents the averaged squared area under the random curve $X_\alpha(t)$.

3.3. Variance and the coefficient of variation

The variance of the single-trajectory PSD is defined in equation (12). It can be calculated exactly for arbitrary α , f and T , and the details of the intermediate steps are presented in appendix A. Here we report the asymptotic behaviour for $fT \rightarrow \infty$, reading

$$\begin{aligned} \sigma^2(f, T) \sim \frac{16K_\alpha^2 T^{2\alpha-2}}{f^4} & \left\{ \frac{5}{4} + \frac{\Gamma^2(\alpha + 1)}{(fT)^{2\alpha}} + \frac{2\Gamma(\alpha + 1)\cos^2(fT - \frac{\pi\alpha}{2})}{2^{\alpha+2}(fT)^\alpha} \right. \\ & - \frac{3\Gamma(\alpha + 1)\cos(fT - \frac{\pi\alpha}{2})}{(fT)^\alpha} + \frac{\Gamma^2(\alpha + 1)\cos^2(fT - \frac{\pi\alpha}{2})}{(fT)^{2\alpha}} \\ & \left. - \frac{\Gamma^2(\alpha + 1)}{2^{\alpha+2}(fT)^{2\alpha}} [4\cos(fT) - 1] \right\}. \end{aligned} \quad (21)$$

As for the mean value, the f -dependence of the leading term does not involve α , and it has the same scaling as Brownian motion. Similarly, the explicit dependence on α of the frequency appears only in subleading order. Once again, studying the leading frequency scaling only we are not able to distinguish SBM from Brownian motion. Instead, we should pay attention to the ageing behaviour of the amplitude.

We summarise the results for the mean and variance of the single-trajectory PSD in the behaviour of the coefficient of variation, γ . It was shown that for FBM this dimensionless factor plays the role of a delicate key criterion to identifying anomalous diffusion. Namely γ assumes three different values in the limit of large frequency depending on whether we have sub-, normal or superdiffusion, but independent of the precise value of α . In the SBM case, recalling the asymptotic results for the mean and variance in equations (19) and (21) respectively, we obtain at fixed observation time T (see figure 5 for the behaviour for arbitrary f)

$$\gamma \sim \sqrt{5}/2, \quad f \rightarrow \infty \quad (22)$$

for any α . Moreover in the limit of $fT \rightarrow 0$ we obtain

$$\sigma^2(f = 0, T) = \frac{32K_\alpha^2 T^{2\alpha+2}}{(\alpha + 1)^2(\alpha + 2)^2} \text{ and hence } \gamma \sim \sqrt{2}. \quad (23)$$

In this limit the moment-generating function simplifies and the PDF is the gamma distribution with scale 2μ ($f = 0, T$) and shape parameter $1/2$.

In figure 5 analytical and numerical results for the coefficient of variation γ are shown. Analytically, in the case of subdiffusion we observe heavier oscillation of γ as function of the frequency, while in the superdiffusive case the convergence to the limiting value (22) is faster. Such a distinction is not so clear in the numerics, where the behaviour of γ is essentially the same for the three different values of α , showing again the difficulties in differentiating SBM from Brownian motion.

3.4. Comparison with FBM

As we have already remarked, the behaviour of the single-trajectory PSD is well-understood only for the anomalous diffusive processes of the FBM-type. The results obtained for SBM show both similarities and dissimilarities with the ones for FBM reported in [4]. In fact, both processes share the same form for the PDF $P(x, t)$ in an infinite space and are therefore often confused with one another in literature, see the caveats raised in [25, 38]. However, while both processes are obviously Gaussian, FBM has stationary increments with long-ranged, power-law noise correlations. In contrast, SBM is non-stationary but driven by uncorrelated noise. After our results above a natural question is whether in terms of the single-trajectory PSD the two processes can be told apart.

For the frequency dependence of the single-trajectory PSD $S(f, T)$, and thus also the mean $\mu(f, T)$, SBM shares the $1/f^2$ scaling with that of Brownian motion for any value of the anomalous diffusion exponent α in the range $0 < \alpha < 2$. Subdiffusive FBM, in contrast, exhibits a completely different behaviour with the explicitly α -dependent frequency scaling $1/f^{\alpha+1}$. Moreover, while in the subdiffusive regime SBM shows the ageing dependence $\mu \simeq T^{\alpha-1}$, FBM is independent of T . Thus, SBM and FBM can be told apart quite easily from both f and T dependencies. In contrast, in the superdiffusive regime the results for SBM and FBM are the same for the functional behaviours with respect to both f and T , and the processes therefore cannot be told apart from each other by use of the single-trajectory PSD or its mean. However, indeed there exists a difference when we consider the coefficient of variation γ . Namely, for SBM γ always converges to the value $\gamma \sim \sqrt{5}/2$ at high frequencies, the value shared with Brownian motion. FBM, in contrast, assumes three distinct values in the high frequency limit: $\gamma \sim 1$ for subdiffusion ($0 < \alpha < 1$), $\gamma \sim \sqrt{5}/2$ for normal diffusion ($\alpha = 1$), and $\gamma \sim \sqrt{2}$ for superdiffusion ($1 < \alpha < 2$). These predictions are confirmed by numerical and experimental data [3, 4]. The coefficient of variation therefore provides a suitable tool to distinguish SBM from FBM. We note that it is not necessary that the value of γ has fully converged within the frequency window probed by experiment or simulation. It is sufficient to see from the data whether a clear trend for a departure from the value $\sqrt{5}/2$ assumed by Brownian motion and SBM.

4. Conclusions

The textbook definition of the PSD takes the Fourier transform of a time series $X(t)$ over an (ideally) infinite observation time, averaged over an ensemble of trajectories $X(t)$ [1]. Due to experimental and computational limitation, the observation time of typical single-trajectory measurements or supercomputing studies is limited, and typically also relatively few trajectories are measured. To account for these limitation, we introduced the concept of the single-trajectory PSD in [3] and studied it for both normal Brownian motion and FBM in [3, 4]. Apart from the more suitable definition in view of modern single particle experiments, another feature of the single-trajectory PSD $S(f, T)$ are the amplitude fluctuations of $S(f, T)$: instead of being considered as a nuisance, these fluctuations indeed provide important information about the specific stochastic process generating the data [3, 4]—similar to the amplitude fluctuations of the time averaged MSD of $X(t)$ [38–40].

We here studied the spectral content of SBM, a standard model for anomalous diffusion which is Markovian but non-stationary, in terms of the single-trajectory PSD and its full distribution. From analytical and numerical analyses we showed that the frequency dependence has the invariant scaling form $\sim 1/f^2$, fully independent of the anomalous scaling exponent α . We also showed that the coefficient of variation for any α practically has the same frequency dependence as for Brownian motion. The main difference between SBM and Brownian motion is the ageing behaviour of single-trajectory PSD and its mean, that is, their dependence on the observation time T . Similar to Brownian motion, the single-trajectory PSD of SBM was shown to be broad in the sense that its coefficient of variation is larger than unity, such that the information of the textbook definition (2) of the PSD has a limited information content, and relevant additional information can be obtained from the single-trajectory analysis.

FBM, in contrast, has stationary increments yet is non-Markovian due to its power-law correlated driving noise. Both FBM and SBM are Gaussian in nature, and we found both emerging similarities and dissimilarities. For both sub- and superdiffusion the coefficient of variation for FBM provides different values from SBM. In

addition, subdiffusive FBM is non-ageing but has an α -dependent frequency scaling of the single-trajectory PSD. The situation is different in the superdiffusive regime: here the frequency dependence and the ageing behaviour of the single-trajectory PSD for FBM is the same as for SBM, leaving the coefficient of variation as the only way to distinguish the two processes from each other. Concurrently, the PDF of the single-trajectory PSD is the same for all three cases. Taking together all observables, we conclude that the single-trajectory PSD is able to distinguish SBM, FBM, and normal Brownian motion. In addition to its ability to identify SBM as a Gaussian diffusion process, we note that the single-trajectory PSD provides a finite-time analogue of the Wiener–Khinchine relation, that can be tested based on experimental data.

The results reported here for SBM adds an important additional piece to the development of a complete picture for single-trajectory PSD analysis of modern single particle tracking data. We demonstrated that it is a suitable tool to identify the anomalous scaling exponent α from an individual particle trajectory $X_\alpha(t)$. Moreover, within the Gaussian processes studied so far, the single-trajectory PSD framework allows one to tell the different processes apart from each other, and is thus an outstanding physical observable, providing complementary information to the (more) standard analyses in terms of ensemble and time averaged MSDs.

Acknowledgments

RM acknowledges funding through grants ME 1535/6-1 and ME 1535/7-1 of Deutsche Forschungsgemeinschaft (DFG), as well as through an Alexander von Humboldt Polish Honorary Research Scholarship from the Polish Science Foundation. We acknowledge the support of Deutsche Forschungsgemeinschaft (German Research Foundation) and Open Access Publication Fund of Potsdam University.

Appendix A. Moment-generating function of the single-trajectory PSD

The moment-generating function is calculated as

$$\begin{aligned}
 \Phi_\lambda &= \langle \exp\{-\lambda S(f, T)\} \rangle = \left\langle \exp\left\{-\frac{\lambda}{T} \int_0^T \int_0^T dt_1 dt_2 \cos(f(t_1 - t_2)) X_\alpha(t_1) X_\alpha(t_2)\right\} \right\rangle \\
 &= \left\langle \exp\left\{-\frac{\lambda}{T} \left[\int_0^T dt \cos(ft) X_\alpha(t) \right]^2 - \frac{\lambda}{T} \left[\int_0^T dt \sin(ft) X_\alpha(t) \right]^2 \right\} \right\rangle \\
 &= \frac{T}{4\pi\lambda} \int_{-\infty}^{+\infty} dz_1 \int_{-\infty}^{+\infty} dz_2 \exp\left(-T \frac{z_1^2 + z_2^2}{4\lambda}\right) \\
 &\quad \times \left\langle \exp\left\{iz_1 \int_0^T dt \cos(ft) X_\alpha(t) + iz_2 \int_0^T dt \sin(ft) X_\alpha(t)\right\} \right\rangle \\
 &= \frac{T}{4\pi\lambda} \int_{-\infty}^{+\infty} dz_1 \int_{-\infty}^{+\infty} dz_2 \exp\left(-T \frac{z_1^2 + z_2^2}{4\lambda}\right) \\
 &\quad \times \left\langle \exp\left\{i \int_0^T dt \xi(t) (z_1 Q_1 + z_2 Q_2)\right\} \right\rangle, \tag{A.1}
 \end{aligned}$$

where we used the identity $\exp(-b^2/4a) = \sqrt{a/\pi} \int_{-\infty}^{+\infty} dx \exp(-ax^2 + ibx)$ and we defined

$$\begin{aligned}
 Q_1 &= \sqrt{2D_\alpha(t)} \left(\frac{\sin(fT)}{f} - \frac{\sin(ft)}{f} \right), \\
 Q_2 &= \sqrt{2D_\alpha(t)} \left(\frac{\cos(ft)}{f} - \frac{\cos(fT)}{f} \right). \tag{A.2}
 \end{aligned}$$

We can now average over the exponential of Gaussian variable and obtain

$$\begin{aligned}
 \Phi_\lambda &= \frac{T}{4\pi\lambda} \int_{-\infty}^{+\infty} dz_1 \int_{-\infty}^{+\infty} dz_2 \exp\left(-T \frac{z_1^2 + z_2^2}{4\lambda}\right) \\
 &\quad \times \exp\left(-\frac{1}{2} \int_0^T dt z_1^2 Q_1^2 - \frac{1}{2} \int_0^T dt z_2^2 Q_2^2 - \int_0^T dt z_1 z_2 Q_1 Q_2\right) \\
 &= \left[1 + \frac{4\lambda}{T} \left(\frac{A+B}{2} \right) + \left(\frac{4\lambda}{T} \right)^2 \frac{AB-C^2}{4} \right]^{-1/2}, \tag{A.3}
 \end{aligned}$$

where for the last equality we used the identity $\int_{-\infty}^{+\infty} dz_1 \int_{-\infty}^{+\infty} dz_2 \exp(-\alpha z_1^2 + \beta z_2^2 - 2\gamma z_1 z_2) = \pi(\alpha\beta - \gamma^2)^{-1/2}$ and we defined

$$\begin{aligned} A &= \int_0^T dt Q_1^2 = \frac{2K_\alpha T^{\alpha+2}}{\omega} \left[2 \sin \omega g_1\left(\frac{\alpha}{2}, \omega\right) - g_2\left(\frac{\alpha}{2}, 2\omega\right) \right], \\ B &= \int_0^T dt Q_2^2 = \frac{2K_\alpha T^{\alpha+2}}{\omega} \left[g_2\left(\frac{\alpha}{2}, 2\omega\right) - 2 \cos \omega g_2\left(\frac{\alpha}{2}, \omega\right) \right], \\ C &= \int_0^T dt Q_1 Q_2 = \frac{2K_\alpha T^{\alpha+2}}{\omega} \left[\sin \omega g_2\left(\frac{\alpha}{2}, \omega\right) - \cos \omega g_1\left(\frac{\alpha}{2}, \omega\right) + g_1\left(\frac{\alpha}{2}, 2\omega\right) \right]. \end{aligned} \tag{A.4}$$

It is possible to show that

$$\frac{(A + B)}{T} = \mu(f, T), \tag{A.5}$$

$$\frac{4(AB - C^2)}{T^2} = 2\mu^2(f, T) - \sigma^2(f, T). \tag{A.6}$$

Relations (A.5) and (A.6) allows us to rewrite the moment-generating function as

$$\Phi_\lambda = [1 + 2\mu\lambda + (2\mu^2 - \sigma^2)\lambda^2]^{-1/2}. \tag{A.7}$$

Appendix B. Ensemble-averaged single-trajectory PSD

Recalling definition (19) we have

$$\begin{aligned} \mu(f, T) &= \frac{1}{T} \int_0^T dt_1 \int_0^T dt_2 \cos(f(t_1 - t_2)) 2K_\alpha \min(t_1, t_2)^\alpha \\ &= \frac{2K_\alpha}{T} \int_0^T dt_1 \left\{ \int_0^{t_1} dt_2 \cos(f(t_1 - t_2)) t_2^\alpha + \int_{t_1}^T dt_2 \cos(f(t_1 - t_2)) t_1^\alpha \right\} \\ &= \frac{2K_\alpha}{T} \left\{ \int_0^T dt_1 \int_0^{t_1} dt_2 [\cos(ft_1)\cos(ft_2) + \sin(ft_1)\sin(ft_2)] t_2^\alpha \right. \\ &\quad \left. + \int_0^T dt_1 \int_{t_1}^T dt_2 [\cos(ft_1)\cos(ft_2) + \sin(ft_1)\sin(ft_2)] t_1^\alpha \right\} \\ &= \frac{2K_\alpha}{T} \{I_1 + I_2 + I_3 + I_4\}. \end{aligned} \tag{B.1}$$

We focus on the explicit calculation of each integral individually, starting with

$$\begin{aligned} I_1 &= \int_0^T dt_1 \int_0^{t_1} dt_2 \cos(ft_1)\cos(ft_2) t_2^\alpha = \int_0^T dt_1 \cos(ft_1) \int_0^{t_1} dt_2 \cos(ft_2) t_2^\alpha \\ &= T^{\alpha+2} \int_0^1 dy \cos(\omega y) y^{\alpha+1} \int_0^1 dz \cos(\omega y z) z^\alpha \\ &= T^{\alpha+2} \int_0^1 dy \cos(\omega y) y^{\alpha+1} g_1\left(\frac{\alpha}{2}, \omega y\right), \end{aligned} \tag{B.2}$$

where $\omega = fT$ and

$$\begin{aligned} g_1(\alpha, \omega) &= \int_0^1 \tau^{2\alpha} \cos(\omega\tau) d\tau \\ &= -\frac{\Gamma(2\alpha + 1)\sin(\pi\alpha)}{\omega^{2\alpha+1}} \\ &\quad - \frac{i}{2\omega^{2\alpha+1}} (e^{i\pi\alpha}\Gamma(2\alpha + 1, -i\omega) - e^{-i\pi\alpha}\Gamma(2\alpha + 1, i\omega)). \end{aligned} \tag{B.3}$$

Similarly for the second integral we obtain

$$\begin{aligned} I_2 &= \int_0^T dt_1 \sin(ft_1) \int_0^{t_1} dt_2 \sin(ft_2) t_2^\alpha \\ &= T^{\alpha+2} \int_0^1 dy \sin(\omega y) y^{\alpha+1} g_2\left(\frac{\alpha}{2}, \omega y\right), \end{aligned} \tag{B.4}$$

where

$$\begin{aligned}
 g_2(\alpha, \omega) &= \int_0^1 \tau^{2\alpha} \sin(\omega\tau) d\tau \\
 &= \frac{\Gamma(2\alpha + 1) \cos(\pi\alpha)}{\omega^{2\alpha+1}} \\
 &\quad - \frac{1}{2\omega^{2\alpha+1}} (e^{i\pi\alpha} \Gamma(2\alpha + 1, -i\omega) + e^{-i\pi\alpha} \Gamma(2\alpha + 1, i\omega)).
 \end{aligned} \tag{B.5}$$

Plugging in the explicit expressions of $g_1(\alpha, \omega)$ and $g_2(\alpha, \omega)$ and working out the integrals we arrive at

$$\begin{aligned}
 I_1 &= T^{\alpha+2} \left\{ -\frac{\Gamma(\alpha + 1) \sin(\pi\alpha/2) \sin(\omega)}{\omega^{\alpha+2}} - \frac{\Gamma(\alpha + 1) \cos(\pi\alpha/2)}{(2\omega)^{\alpha+2}} \right. \\
 &\quad - i \frac{\sin(\omega)}{2\omega^{\alpha+2}} [e^{i\pi\alpha/2} \Gamma(\alpha + 1, -i\omega) - e^{-i\pi\alpha/2} \Gamma(\alpha + 1, i\omega)] \\
 &\quad \left. + \frac{1}{2(2\omega)^{\alpha+2}} [e^{i\pi\alpha/2} \Gamma(\alpha + 1, -2i\omega) + e^{-i\pi\alpha/2} \Gamma(\alpha + 1, 2i\omega)] \right\},
 \end{aligned} \tag{B.6}$$

$$\begin{aligned}
 I_2 &= T^{\alpha+2} \left\{ -\frac{\Gamma(\alpha + 1) \cos(\pi\alpha/2) \cos(\omega)}{\omega^{\alpha+2}} + \frac{\Gamma(\alpha + 1) \cos(\pi\alpha/2)}{(2\omega)^{\alpha+2}} \right. \\
 &\quad + \frac{\cos(\omega)}{2\omega^{\alpha+2}} [e^{i\pi\alpha/2} \Gamma(\alpha + 1, -i\omega) + e^{-i\pi\alpha/2} \Gamma(\alpha + 1, i\omega)] \\
 &\quad \left. - \frac{1}{2(2\omega)^{\alpha+2}} [e^{i\pi\alpha/2} \Gamma(\alpha + 1, -2i\omega) + e^{-i\pi\alpha/2} \Gamma(\alpha + 1, 2i\omega)] \right\}.
 \end{aligned} \tag{B.7}$$

The last two integrals are given by

$$\begin{aligned}
 I_3 &= \int_0^T dt_1 \cos(ft_1) t_1^\alpha \int_{t_1}^T dt_2 \cos(ft_2) \\
 &= \frac{T^{\alpha+2}}{\omega} \left\{ \sin(\omega) g_1\left(\frac{\alpha}{2}, \omega\right) - \frac{1}{2} \int_0^1 dy y^\alpha \sin(2\omega y) \right\},
 \end{aligned} \tag{B.8}$$

$$\begin{aligned}
 I_4 &= \int_0^T dt_1 \sin(ft_1) t_1^\alpha \int_{t_1}^T dt_2 \sin(ft_2) \\
 &= \frac{T^{\alpha+2}}{\omega} \left\{ -\cos(\omega) g_2\left(\frac{\alpha}{2}, \omega\right) + \frac{1}{2} \int_0^1 dy y^\alpha \sin(2\omega y) \right\},
 \end{aligned} \tag{B.9}$$

so that we finally obtain

$$\begin{aligned}
 \mu(f, T) &= 2K_\alpha T^{\alpha+1} \left\{ -\frac{\Gamma(\alpha + 1)}{\omega^{\alpha+2}} \cos\left(\omega - \frac{\pi\alpha}{2}\right) \right. \\
 &\quad + \frac{\cos(\omega - \frac{\pi\alpha}{2})}{2\omega^{\alpha+2}} [\Gamma(\alpha + 1, i\omega) + \Gamma(\alpha + 1, -i\omega)] \\
 &\quad + \frac{i \sin(\omega - \frac{\pi\alpha}{2})}{2\omega^{\alpha+2}} [\Gamma(\alpha + 1, i\omega) - \Gamma(\alpha + 1, -i\omega)] \\
 &\quad \left. + \frac{1}{\omega} \left[\sin(\omega) g_1\left(\frac{\alpha}{2}, \omega\right) - \cos(\omega) g_2\left(\frac{\alpha}{2}, \omega\right) \right] \right\},
 \end{aligned} \tag{B.10}$$

which can be simplified to the form (17).

Appendix C. Variance of the single-trajectory PSD

In order to obtain the PSD variance, given in (12) we first focus on the calculation of the second moment

$$\begin{aligned} \langle S^2(f, T) \rangle &= \frac{1}{T^2} \left\langle \int_0^T \int_0^T dt_1 dt_2 \cos(f(t_1 - t_2)) X_\alpha(t_1) X_\alpha(t_2) \right. \\ &\quad \times \left. \int_0^T \int_0^T dt_3 dt_4 \cos(f(t_3 - t_4)) X_\alpha(t_3) X_\alpha(t_4) \right\rangle \\ &= \frac{1}{T^2} \int_0^T \int_0^T \int_0^T \int_0^T dt_1 dt_2 dt_3 dt_4 \cos(f(t_1 - t_2)) \cos(f(t_3 - t_4)) \\ &\quad \times \langle X_\alpha(t_1) X_\alpha(t_2) X_\alpha(t_3) X_\alpha(t_4) \rangle. \end{aligned} \quad (\text{C.1})$$

Following the Wick/Isserlis theorem we have

$$\begin{aligned} \langle X_\alpha(t_1) X_\alpha(t_2) X_\alpha(t_3) X_\alpha(t_4) \rangle &= \langle X_\alpha(t_1) X_\alpha(t_2) \rangle \langle X_\alpha(t_3) X_\alpha(t_4) \rangle \\ &\quad + \langle X_\alpha(t_1) X_\alpha(t_3) \rangle \langle X_\alpha(t_2) X_\alpha(t_4) \rangle \\ &\quad + \langle X_\alpha(t_1) X_\alpha(t_4) \rangle \langle X_\alpha(t_3) X_\alpha(t_2) \rangle. \end{aligned} \quad (\text{C.2})$$

This allows us to rewrite (C.1) as

$$\begin{aligned} \langle S^2(f, T) \rangle &= \frac{1}{T^2} \left[\int_0^T \int_0^T dt_1 dt_2 \cos(f(t_1 - t_2)) \langle X_\alpha(t_1) X_\alpha(t_2) \rangle \right]^2 \\ &\quad + \int_0^T \int_0^T \int_0^T \int_0^T dt_1 dt_2 dt_3 dt_4 \cos(f(t_1 - t_2)) \cos(f(t_3 - t_4)) \\ &\quad \times \langle X_\alpha(t_1) X_\alpha(t_3) \rangle \langle X_\alpha(t_2) X_\alpha(t_4) \rangle \\ &\quad + \int_0^T \int_0^T \int_0^T \int_0^T dt_1 dt_2 dt_3 dt_4 \cos(f(t_1 - t_2)) \cos(f(t_3 - t_4)) \\ &\quad \times \langle X_\alpha(t_1) X_\alpha(t_4) \rangle \langle X_\alpha(t_3) X_\alpha(t_2) \rangle \\ &= \mu^2(f, T) + \frac{4K_\alpha^2}{T^2} \left\{ \int_0^T \int_0^T \int_0^T \int_0^T dt_1 dt_2 dt_3 dt_4 \cos(f(t_1 - t_2)) \cos(f(t_3 - t_4)) \right. \\ &\quad \times \min(t_1, t_3)^\alpha \min(t_2, t_4)^\alpha \\ &\quad \left. + \int_0^T \int_0^T \int_0^T \int_0^T dt_1 dt_2 dt_3 dt_4 \cos(f(t_1 - t_2)) \cos(f(t_3 - t_4)) \right. \\ &\quad \times \left. \min(t_1, t_4)^\alpha \min(t_2, t_3)^\alpha \right\}. \end{aligned} \quad (\text{C.3})$$

The variance is thus given by

$$\begin{aligned} \sigma^2(f, T) &= \frac{8K_\alpha^2}{T^2} \int_0^T \int_0^T \int_0^T \int_0^T dt_1 dt_2 dt_3 dt_4 \cos(f(t_1 - t_2)) \cos(f(t_3 - t_4)) \\ &\quad \times \min(t_1, t_3)^\alpha \min(t_2, t_4)^\alpha \\ &= \frac{8K_\alpha^2}{T^2} \left\{ \int_0^T \int_0^T dt_1 dt_2 \cos(f(t_1 - t_2)) \int_0^{t_1} dt_3 \int_0^{t_2} dt_4 \cos(f(t_3 - t_4)) t_3^\alpha t_4^\alpha \right. \\ &\quad + 2 \int_0^T \int_0^T dt_1 dt_2 \cos(f(t_1 - t_2)) \int_{t_1}^T dt_3 \int_0^{t_2} dt_4 \cos(f(t_3 - t_4)) t_1^\alpha t_4^\alpha \\ &\quad \left. + \int_0^T \int_0^T dt_1 dt_2 \cos(f(t_1 - t_2)) \int_{t_1}^T dt_3 \int_{t_2}^T dt_4 \cos(f(t_3 - t_4)) t_1^\alpha t_2^\alpha \right\} \\ &= \frac{8K_\alpha^2}{T^2} \{I_5 + 2I_6 + I_7\}. \end{aligned} \quad (\text{C.4})$$

Following the same procedure used above for calculating the mean we can show that the integrals are given by

$$I_5 = I_1^2 + I_2^2 + I_8^2 + I_9^2, \quad (\text{C.5})$$

$$\begin{aligned}
I_6 = \frac{T^{\alpha+2}}{\omega} & \left\{ I_1 \left[\sin(\omega) g_1\left(\frac{\alpha}{2}, \omega\right) - \frac{g_2\left(\frac{\alpha}{2}, 2\omega\right)}{2} \right] \right. \\
& + I_8 \left[\frac{1}{2(\alpha+1)} + \frac{g_1\left(\frac{\alpha}{2}, 2\omega\right)}{2} - \cos(\omega) g_1\left(\frac{\alpha}{2}, \omega\right) \right] \\
& + I_9 \left[-\frac{1}{2(\alpha+1)} + \frac{g_1\left(\frac{\alpha}{2}, 2\omega\right)}{2} + \sin(\omega) g_2\left(\frac{\alpha}{2}, \omega\right) \right] \\
& \left. + I_2 \left[-\cos(\omega) g_2\left(\frac{\alpha}{2}, \omega\right) + \frac{g_2\left(\frac{\alpha}{2}, 2\omega\right)}{2} \right] \right\}, \tag{C.6}
\end{aligned}$$

$$\begin{aligned}
I_7 = \frac{T^{\alpha+2}}{\omega^2} & \left\{ \frac{1}{2(\alpha+1)^2} + g_1\left(\frac{\alpha}{2}, \omega\right)^2 + g_2\left(\frac{\alpha}{2}, \omega\right)^2 + \frac{g_1\left(\frac{\alpha}{2}, 2\omega\right)^2}{2} + \frac{g_2\left(\frac{\alpha}{2}, 2\omega\right)^2}{2} \right. \\
& - \sin(\omega) \left[\frac{g_2\left(\frac{\alpha}{2}, \omega\right)}{\alpha+1} + g_1\left(\frac{\alpha}{2}, \omega\right) g_2\left(\frac{\alpha}{2}, 2\omega\right) - g_2\left(\frac{\alpha}{2}, \omega\right) g_1\left(\frac{\alpha}{2}, 2\omega\right) \right] \\
& \left. - \cos(\omega) \left[\frac{g_1\left(\frac{\alpha}{2}, \omega\right)}{\alpha+1} + g_1\left(\frac{\alpha}{2}, \omega\right) g_1\left(\frac{\alpha}{2}, 2\omega\right) + g_2\left(\frac{\alpha}{2}, \omega\right) g_2\left(\frac{\alpha}{2}, 2\omega\right) \right] \right\}, \tag{C.7}
\end{aligned}$$

where I_1 and I_2 are defined in (B.7) and

$$\begin{aligned}
I_8 = T^{\alpha+2} & \left\{ \frac{\Gamma(\alpha+1) \cos(\pi\alpha/2) \sin(\omega)}{\omega^{\alpha+2}} - \frac{\Gamma(\alpha+1) \sin(\pi\alpha/2)}{(2\omega)^{\alpha+2}} \right. \\
& - \frac{\sin(\omega)}{2\omega^{\alpha+2}} [e^{i\pi\alpha/2} \Gamma(\alpha+1, -i\omega) + e^{-i\pi\alpha/2} \Gamma(\alpha+1, i\omega)] \\
& \left. - \frac{1}{2\omega(\alpha+1)} - \frac{i}{2(2\omega)^{\alpha+2}} [e^{i\pi\alpha/2} \Gamma(\alpha+1, -2i\omega) - e^{-i\pi\alpha/2} \Gamma(\alpha+1, 2i\omega)] \right\}, \tag{C.8}
\end{aligned}$$

$$\begin{aligned}
I_9 = T^{\alpha+2} & \left\{ -\frac{\Gamma(\alpha+1) \sin(\pi\alpha/2) \cos(\omega)}{\omega^{\alpha+2}} - \frac{\Gamma(\alpha+1) \sin(\pi\alpha/2)}{(2\omega)^{\alpha+2}} \right. \\
& + i \frac{\cos(\omega)}{2\omega^{\alpha+2}} [e^{i\pi\alpha/2} \Gamma(\alpha+1, -i\omega) - e^{-i\pi\alpha/2} \Gamma(\alpha+1, i\omega)] \\
& \left. + \frac{1}{2\omega(\alpha+1)} - \frac{i}{2(2\omega)^{\alpha+2}} [e^{i\pi\alpha/2} \Gamma(\alpha+1, -2i\omega) - e^{-i\pi\alpha/2} \Gamma(\alpha+1, 2i\omega)] \right\}. \tag{C.10}
\end{aligned}$$

ORCID iDs

Ralf Metzler  <https://orcid.org/0000-0002-6013-7020>

Gleb Oshanin  <https://orcid.org/0000-0001-8467-3226>

References

- [1] Norton M P and Karczub D G 2003 *Fundamentals of Noise and Vibration Analysis for Engineers* (Cambridge: Cambridge University Press)
- [2] Abramowitz M and Stegun I A 1965 *Handbook of Mathematical Functions* (New York: Dover)
- [3] Krapf D, Marinari E, Metzler R, Oshanin G, Xu X and Squarcini A 2018 *New J. Phys.* **20** 023029
- [4] Krapf D, Lukat N, Marinari E, Metzler R, Oshanin G, Selhuber-Unkel C, Squarcini A, Stadler L, Weiss M and Xu X 2019 *Phys. Rev. X* **9** 011019
- [5] Voss R and Clarke J 1975 *Nature* **258** 317
Hennig H, Fleischmann R, Fredebohm A, Haggmayer Y, Nagler J, Witt A, Theis F J and Geisel T 2011 *PLoS One* **6** e26457
- [6] Weber R O and Talkner P 2001 *J. Geophys. Res.* **106** 20131
- [7] Sornette A and Sornette D 1989 *Europhys. Lett.* **9** 197
- [8] Kirchner J W, Feng X and Neal C 2000 *Nature* **403** 524
See also Scher H, Margolin G, Metzler R, Klafter J and Berkowitz B 2002 *Geophys. Res. Lett.* **29** 1061

- [9] Balandin A A 2013 *Nat. Nanotechnol.* **8** 549
- [10] Frantsuzov P A, Volkán-Kacsó Sand Jank B 2013 *Nano Lett.* **13** 402
- [11] Krapf D 2013 *Phys. Chem. Chem. Phys.* **15** 459
- [12] Zorkot M, Golestanian R and Bonthuis D J 2016 *Nano Lett.* **16** 2205
- [13] Niemann M, Kantz H and Barkai E 2013 *Phys. Rev. Lett.* **110** 140603
- Sadegh S, Barkai E and Krapf D 2014 *New J. Phys.* **16** 113054
- [14] Leibovich N, Dechant A, Lutz E and Barkai E 2016 *Phys. Rev. E* **94** 052130
- [15] Leibovich N and Barkai E 2017 *Eur. Phys. J. B* **90** 229
- [16] Majumdar S N and Oshanin G 2018 *J. Phys. A: Math. Theor.* **51** 435001
- [17] Bénichou O, Krapivsky P L, Mejía-Monasterio C and Oshanin G 2016 *Phys. Rev. Lett.* **117** 080601
- [18] Marinari E, Parisi G, Ruelle D and Windey P 1983 *Phys. Rev. Lett.* **50** 1223
- Dean D S, Iorio A, Marinari E and Oshanin G 2016 *Phys. Rev. E* **94** 032131
- [19] Schnellbacher N D and Schwarz U S 2018 *New J. Phys.* **20** 031001
- [20] Nørregaard K, Metzler R, Ritter C M, Berg-Sørensen K and Oddershede L B 2017 *Chem. Rev.* **117** 4342
- Höfling F and Franosch T 2013 *Rep. Prog. Phys.* **76** 046602
- [21] Kemp D B, Eichenseer K and Kiessling W 2015 *Nat. Commun.* **6** 8890
- [22] Tóth B, Lempérière Y, Deremble C, de Lataillade J, Kockelkoren J and Bouchaud J-P 2011 *Phys. Rev. X* **1** 021006
- Cherstvy A G, Vinod D, Aghion E, Chechkin A V and Metzler R 2017 *New J. Phys.* **19** 063045
- [23] Lim S C and Muniandy S V 2002 *Phys. Rev. E* **66** 021114
- Fulinski A 2011 *Phys. Rev. E* **83** 061140
- Fulinski A 2013 *J. Chem. Phys.* **138** 021101
- Fulinski A 2013 *Acta Phys. Pol.* **44** 1137
- [24] Thiel F and Sokolov I 2014 *Phys. Rev. E* **89** 012115
- [25] Jeon J-H, Chechkin A V and Metzler R 2014 *Phys. Chem. Chem. Phys.* **16** 15811
- Safdari H, Cherstvy A G, Chechkin A V, Thiel F, Sokolov I M and Metzler R 2015 *J. Phys. A: Math. Theor.* **48** 375002
- [26] Batchelor G K 1952 *Math. Proc. Camb. Phil. Soc.* **48** 345
- [27] Richardson L F 1926 *Proc. R. Soc. A* **110** 709
- [28] Bodrova A, Chechkin A V, Cherstvy A G and Metzler R 2015 *Phys. Chem. Chem. Phys.* **17** 21791
- [29] Oshanin G and Moreau M 1995 *J. Chem. Phys.* **102** 2977
- [30] Saxton M J 2001 *Biophys. J.* **75** 2226
- Periasamy N and Verkman A S 1998 *Biophys. J.* **75** 557
- [31] Wu J and Berland M 2008 *Biophys. J.* **95** 2049
- [32] Molini A, Talkner P, Katul G G and Porporato A 2011 *Physica A* **390** 1841
- [33] Le Vot F and Yuste S B 2018 *Phys. Rev. E* **98** 042117
- Yuste S B, Abad E and Escudero C 2016 *Phys. Rev. E* **94** 032118
- [34] Taloni A, Chechkin A and Klafter J 2010 *Phys. Rev. Lett.* **104** 160602
- Ghasemi Nezhadhighi M, Chechkin A V and Metzler R 2014 *J. Chem. Phys.* **140** 024106
- Schumer R, Taloni A and Furbish D J 2017 *Geophys. Res. Lett.* **44** 2016GL072134
- [35] Lacasa L, Luque B, Ballesteros F, Luque J and Nuño J C 2008 *Proc. Natl Acad. Sci. USA* **105** 4972
- Mira-Iglesias A, Navarro-Pardo E and Alberto Conejero J 2019 *Symmetry* **11** 563
- [36] Bodrova A S, Chechkin A V, Cherstvy A G and Metzler R 2015 *New J. Phys.* **17** 063038
- [37] Feller W 1971 *An Introduction to Probability Theory and Its Applications* (New York: Wiley)
- [38] Metzler R, Jeon J-H, Cherstvy A G and Barkai E 2014 *Phys. Chem. Chem. Phys.* **16** 24128
- Barkai E, Garini Y and Metzler R 2012 *Phys. Today* **65** 29
- [39] Bouchaud J-P 1992 *J. Phys.* **12** 1705
- Bel G and Barkai E 2005 *Phys. Rev. Lett.* **94** 240602
- Rebenshtok A and Barkai E 2007 *Phys. Rev. Lett.* **99** 210601
- Lomholt M A, Zaid I M and Metzler R 2007 *Phys. Rev. Lett.* **98** 200603
- Aquino G, Grigolini P and West B J 2007 *Europhys. Lett.* **80** 10002
- [40] Schulz J H P, Barkai E and Metzler R 2014 *Phys. Rev. X* **4** 011028
- Jeon J-H, Tejedor V, Burov S, Barkai E, Selhuber-Unkel C, Berg-Sørensen K, Oddershede L and Metzler R 2011 *Phys. Rev. Lett.* **106** 048103

Sposini V, Grebenkov D S, Metzler R , Oshanin G & Seno F 2020 Universal spectral features of different classes of random diffusivity processes *New J. Phys.* **22**, 063056.



OPEN ACCESS

RECEIVED
23 February 2020REVISED
6 May 2020ACCEPTED FOR PUBLICATION
11 May 2020PUBLISHED
26 June 2020

Original content from
this work may be used
under the terms of the
[Creative Commons
Attribution 4.0 licence](#).

Any further distribution
of this work must
maintain attribution to
the author(s) and the
title of the work, journal
citation and DOI.



PAPER

Universal spectral features of different classes of random-diffusivity processes

Vittoria Sposini^{1,2} , Denis S Grebenkov³ , Ralf Metzler^{1,7} , Gleb Oshanin^{4,5}  and Flavio Seno⁶¹ Institute for Physics & Astronomy, University of Potsdam, 14476 Potsdam-Golm, Germany² Basque Centre for Applied Mathematics, 48009 Bilbao, Spain³ Laboratoire de Physique de la Matière Condensée (UMR 7643), CNRS—Ecole Polytechnique, IP Paris, 91128 Palaiseau, France⁴ Sorbonne Université, CNRS, Laboratoire de Physique Théorique de la Matière Condensée (UMR 7600), 4 Place Jussieu, 75252 Paris Cedex 05, France⁵ Interdisciplinary Scientific Center J-V Poncelet (ISCP), CNRS UMI 2615, 11 Bol. Vlassievsky per., 119002 Moscow, Russia⁶ INFN, Padova Section and Department of Physics and Astronomy “Galileo Galilei”, University of Padova, 35131 Padova, Italy⁷ Author to whom any correspondence should be addressed.E-mail: rmetzler@uni-potsdam.de**Keywords:** diffusion, power spectrum, random diffusivity, single trajectories

Abstract

Stochastic models based on random diffusivities, such as the diffusing-diffusivity approach, are popular concepts for the description of non-Gaussian diffusion in heterogeneous media. Studies of these models typically focus on the moments and the displacement probability density function. Here we develop the complementary power spectral description for a broad class of random-diffusivity processes. In our approach we cater for typical single particle tracking data in which a small number of trajectories with finite duration are garnered. Apart from the diffusing-diffusivity model we study a range of previously unconsidered random-diffusivity processes, for which we obtain exact forms of the probability density function. These new processes are different versions of jump processes as well as functionals of Brownian motion. The resulting behaviour subtly depends on the specific model details. Thus, the central part of the probability density function may be Gaussian or non-Gaussian, and the tails may assume Gaussian, exponential, log-normal, or even power-law forms. For all these models we derive analytically the moment-generating function for the single-trajectory power spectral density. We establish the generic $1/f^2$ -scaling of the power spectral density as function of frequency in all cases. Moreover, we establish the probability density for the amplitudes of the random power spectral density of individual trajectories. The latter functions reflect the very specific properties of the different random-diffusivity models considered here. Our exact results are in excellent agreement with extensive numerical simulations.

1. Introduction

Diffusive processes came to the attention of the broader scientific community with the experiments on ‘active molecules’ by Brown, who reported the jittery motion of granules of ‘1/4000th to 1/5000th of an inch in length’ contained in pollen grains as well as control experiments on powdered inorganic rocks [1]. In the mid-19th century physician-physiologist Fick published his studies on salt fluxes between reservoirs of different concentrations connected by tubes [2]. To quantify the observed dynamics Fick introduced the diffusion equation (‘Fick’s second law’) for the spatio-temporal concentration profile. A major breakthrough was the theoretical description of ‘Brownian motion’ and the diffusion equation in terms of probabilistic arguments by Einstein [3], Smoluchowski [4], and Sutherland [5]. Concurrently Pearson introduced the notion of the ‘random walk’ [6], and Langevin proposed the intuitive picture of the random force and the stochastic Langevin equation [7].

More recently, major advances in experimental techniques such as superresolution microscopy continue to provide unprecedented insight into the motion of submicron and even fluorescently tagged molecular tracers in complex environments such as living biological cells [8–11]. Concurrently, simulations are becoming ever more powerful and reveal the molecular dynamics in systems such as lipid membranes [12] or internal protein motion [13]. The data resulting from such complex systems unveil a number of new phenomena in the stochastic particle motion and thus call for new theoretical concepts [14–16] on top of already known approaches [17–19].

Among these new insights is that endogenous and introduced tracers in living biological cells perform anomalous diffusion of the form $\langle r^2(t) \rangle \simeq K_\alpha t^\alpha$ in a wide range of systems [8,9,20]. For instance, subdiffusion with $0 < \alpha < 1$ was measured for messenger RNA probes in bacteria cells [21,22], for DNA loci and telomeres in bacteria and eukaryotic cells [22–24], for granules in yeast and human cells [25,26], as well as for the stochastic motion of biological membrane constituents [27,28]. In these cases the slower than Brownian, passive tracer motion is effected by the highly crowded nature of the environment, as can be studied in *in vitro* systems [29,30]. In fact, even small green fluorescent proteins of some 2 nm in size were shown to subdiffuse [31]. Conversely, superdiffusion with $1 < \alpha < 2$ in biological cells is caused by active motion of molecular motors due to consumption of biochemical energy units. Examples include the motor motion itself [32,33], the transport of introduced plastic beads in fibroblast cells [34], RNA cargo in neuron cells [35], and of granules in amoeba [36].

However, even when the mean squared displacement seemingly suggests Brownian motion based on the observation that $\alpha = 1$, remarkable effects have been reported recently. Thus, the motion of micron-sized tracer beads moving along nanotubes as well as in entangled polymer networks was shown to be ‘Fickian’ ($\alpha = 1$) yet the measured displacement distribution exhibited significant deviations from the expected Gaussian law: namely, an exponential distribution of the form $P(\mathbf{r}, t) \propto \exp(-|\mathbf{r}|/\lambda(t))$ with $\lambda(t) \propto t^{1/2}$ was observed [37,38]. Similar ‘Fickian yet non-Gaussian’ diffusion was found for the tracer dynamics in hard sphere colloidal suspensions [39], for the stochastic motion of nanoparticles in nanopost arrays [40], of colloidal nanoparticles adsorbed at fluid interfaces [41–43] and moving along membranes and inside colloidal suspension [44], and for the motion of nematodes [45]. Even more complicated non-Gaussian distributions of displacements were recently observed in *Dictyostelium discoideum* cells [46,47] and protein-crowded lipid bilayer membranes [48]. While in some experiments the non-Gaussian shape of $P(\mathbf{r}, t)$ is observed over the entire experimental window, others report clear crossover behaviours from a non-Gaussian shape at shorter time scales to an effective Gaussian behaviour at longer time scales, for instance, see [37,38].

A non-Gaussian probability density along with the scaling exponent $\alpha = 1$ of the mean squared displacement can be achieved in the superstatistical approach, in which it is assumed that individual Gaussian densities are averaged over a distribution of diffusivities [49–53]. A microscopic realisation of such a behaviour was proposed for a model of diffusion during a polymerisation process [54]. However, in superstatistics (and in the related process called generalised grey Brownian motion [55–57]) the distribution is a constant of the motion and thus no crossover behaviour as mentioned above can be described. In order to include such a non-Gaussian to Gaussian crossover models were introduced in which the diffusion coefficient is considered as a stochastic process itself. In this diffusing-diffusivity picture, originally proposed by Chubynsky and Slater [58], the stochastic dynamics of the diffusivity is characterised by a well-defined correlation time above which the diffusivity becomes equilibrated. Concurrently to this equilibration the ensuing form of $P(\mathbf{r}, t)$ becomes effectively Gaussian. Random-diffusivity models have since then been developed and analysed further, and their application is mainly the diffusive dynamics in heterogeneous systems [59–70].

In fact, stochastic models based on random diffusivities are ubiquitous in financial mathematics for the modelling of stock price dynamics. They are commonly known as stochastic volatility models and many different examples have been analysed in order to identify a proper description for the volatility [71]. Among them, one can find diffusion-based models, where the volatility is described with continuous sample paths, as well as more complicated dynamics where, for instance, jumps are also allowed or where the volatility is defined as a function of separate stochastic processes [72]. Financial mathematics hosts a rich variety of random-diffusivity models, motivated by various aspects of the observed financial market data. Here we present a range of additional, new random-diffusivity models in the context of time series analysis, extending the range of available models beyond the diffusing-diffusivity model developed for Fickian yet non-Gaussian diffusion processes. These may in turn be useful for financial mathematics. As both fields are quickly expanding and new facets are being continuously unveiled, we are confident that the different models introduced here and their detailed features offer the necessary flexibility to account for the new observations.

The central purpose of our study here is twofold. First we analyse several new classes of random-diffusivity models, divided into two groups, jump models and functionals of Brownian motion. For both groups we consider several concrete examples and derive analytic solutions for the probability density function (PDF) $\Pi(x, t)$. The PDF turns out to delicately depend on the precise formulation of the model: the central part may be Gaussian or non-Gaussian, and the tails may be of Gaussian, exponential, log-normal, or even power-law shape. The second goal we pursue here are the *spectral* properties of random-diffusivity processes. Namely, while earlier studies of the random-diffusivity dynamics were mainly concerned with the PDF and the mean squared displacement encoded in the process we assume a different stance and derive the spectral properties of single particle trajectories with finite observation time, geared for the description of contemporary single particle tracking experiments. Such an analysis was worked out in detail for specific systems of normal and anomalous diffusion [73–78], and we here study the commonalities and differences emerging for random-diffusivity scenarios.

Traditionally, power spectral analyses are based on the textbook definition of the spectral density

$$\mu(f) = \lim_{T \rightarrow \infty} \frac{1}{T} \left\langle \left| \int_0^T e^{ift} x(t) dt \right|^2 \right\rangle. \quad (1)$$

This definition involves taking the limit of infinite (practically, very long) measurement times as well as averaging over an ensemble (practically, a large number of) of particles, here and in the following denoted by angular brackets, $\langle \cdot \rangle$. Typical single particle tracking experiments, however, are limited in the measurement time, for instance, due to the lifetime of the employed fluorescent tags or the time a particle stays in the microscope focus. At the same time, such experiments are often limited to a relatively small number of individual trajectories. To cater for this common type of experimental situations we avoid taking the long time and ensemble limits by considering the single-trajectory power spectral density (PSD)

$$S_T(f) = \frac{1}{T} \left| \int_0^T e^{ift} x(t) dt \right|^2 \quad (2)$$

as functions of frequency f and measurement time T . We previously analysed the behaviour of $S_T(f)$ for different diffusion scenarios [76–78] and demonstrated that it is practically useful in the analysis of experimental data [76,77]. In what follows we derive the moment-generating function (MGF) of the PSD (2) for different classes of random-diffusivity processes, including several cases not yet studied in literature. In particular, we obtain the probability density $P(A)$ of the single PSD amplitude, an intrinsically random quantity for a finite-time measurement of a stochastic motion that was demonstrated to be a very useful quantity for the analysis of measured particle trajectories. In addition to analytical derivations we present detailed numerical analyses. This study provides a quite general approach to obtain the PDF for any diffusing-diffusivity model, providing new insights on this class of processes.

This work is structured as follows. We start from section 2 with a description of the model and in section 3 we report general results on the spectral properties of this class of processes. Specific examples of diffusing-diffusivity models are described in sections 4–6. The first example is the well known case in which the diffusivity is modelled as the squared Ornstein–Uhlenbeck process. In the second group of examples we analyse two cases in which the diffusivity is defined as a jump process. The third and last group shows three examples in which the diffusivity is described as a functional of Brownian motion. Finally, in section 7 we draw our conclusions. In the appendix we report details on the explicit derivations of our results.

2. Random-diffusivity processes

We consider a class of one-dimensional stochastic processes x_t that obey the Langevin equation in the Itô convention,

$$\dot{x}_t = \sqrt{2D_0\Psi_t}\xi_t. \quad (3)$$

Here D_0 is a constant, dimensional coefficient in units length²/time, and in our analysis we will assume the initial condition $x_0 = 0$. In equation (3) ξ_t denotes a standard Gaussian white noise with zero mean and covariance function $\overline{\xi_t\xi_{t'}} = \delta(t - t')$. The bar here and henceforth denotes averaging with respect to the noise ξ_t . Lastly Ψ_t is a positive-definite random function, which multiplies D_0 and thus introduces a time-dependent randomness into the effective noise amplitude. In the following we stipulate that Ψ_t is Riemann-integrable on a finite interval $(0, T)$ such that $\int_0^T dt\Psi_t$ exists with probability 1. Note that the case $\Psi_t \equiv 1$ corresponds to standard Brownian motion, while a deterministic choice of the form $\Psi_t = t^{\alpha-1}$ produces so-called scaled Brownian motion [79,80]. We will here discuss several particular

choices for the random function Ψ_t . In addition to the previously made choice of a squared Ornstein–Uhlenbeck process we will consider the case when Ψ_t is a jump-process, that attains independent, identically distributed random values. We also present several examples when Ψ_t is subordinated to standard unbiased Brownian motion B_t : namely, $\Psi_t = B_t^2/a^2$, where a is a model parameter, $\Psi_t = \Theta(B_t)$, where $\Theta(x)$ is the Heaviside theta function, and geometric Brownian motion $\Psi_t = \exp(-B_t/a)$.

Regardless of the choice of the random function Ψ_t , we can solve the Langevin equation (3) for the trajectory x_t for a fixed realisation of the noise and a given realisation of Ψ_t , to obtain

$$x_t = (2D_0)^{1/2} \int_0^t d\tau \Psi_\tau^{1/2} \xi_\tau. \quad (4)$$

The characteristic function of x_t can be written down in the form

$$\Phi_w = \left\langle \exp \left(iw(2D_0)^{1/2} \int_0^t d\tau \Psi_\tau^{1/2} \xi_\tau \right) \right\rangle_\Psi, \quad (5)$$

where the bar stands for averaging over thermal histories, while the angular brackets denote averaging over the realisations of the random function Ψ_t . The thermal average can be performed straightforwardly to give

$$\Phi_w = \left\langle \exp \left(-D_0 w^2 \int_0^t d\tau \Psi_\tau \right) \right\rangle_\Psi. \quad (6)$$

The desired PDF $\Pi(x, t)$ can then be written as

$$\Pi(x, t) = \frac{1}{2\pi} \int_{-\infty}^{\infty} dw e^{-iwx} \Phi_w. \quad (7)$$

In the following section 4 we provide several examples with explicit expressions for the probability density, and we will see how different choices of Ψ_t may lead to PDFs of considerably different shapes.

3. General theory

We first obtain exact expressions for the PSD (2) and then study the limiting behaviour for high frequencies.

3.1. Exact expressions for arbitrary frequency and observation time

We investigate the PSD of an individual trajectory x_t encoded in the stochastic dynamics (3) with $t \in (0, T)$,

$$S_T(f) = \frac{1}{T} \int_0^T dt_1 \int_0^T dt_2 \cos(f(t_1 - t_2)) x_{t_1} x_{t_2}, \quad (8)$$

as function of the frequency f and the observation time T . We determine the MGF and the PDF of the random variable $S_T(f)$.

The MGF of the single-trajectory PSD in (8) is defined as

$$\phi_\lambda = \left\langle \exp \left(-\frac{\lambda}{T} \int_0^T dt \int_0^T dt' \cos(f(t - t')) x_t x_{t'} \right) \right\rangle_\Psi \quad (9)$$

with $\lambda \geq 0$. Relegating some intermediate calculations to appendix A we find the following expression for ϕ_λ in (9) averaged over thermal noises,

$$\phi_\lambda = \frac{1}{4\pi\lambda} \int_{-\infty}^{\infty} dz_1 \int_{-\infty}^{\infty} dz_2 \exp \left(-\frac{z_1^2 + z_2^2}{4\lambda} \right) \left\langle \exp \left(-D_0 \int_0^T dt \Psi_t \left(\int_t^T d\tau Q_\tau \right)^2 \right) \right\rangle_\Psi, \quad (10)$$

where

$$Q_t = z_1 \frac{\cos(ft)}{\sqrt{T}} + z_2 \frac{\sin(ft)}{\sqrt{T}}. \quad (11)$$

Performing the inverse Laplace transform of expression (10) we find the general result for the PDF

$$p(S_T(f) = S) = \frac{1}{4\pi} \int_{-\infty}^{\infty} dz_1 \int_{-\infty}^{\infty} dz_2 J_0 \left(\sqrt{z_1^2 + z_2^2} S \right) \left\langle \exp \left(-D_0 \int_0^T dt \Psi_t \left(\int_t^T d\tau Q_\tau \right)^2 \right) \right\rangle_\Psi, \quad (12)$$

where $J_0(z)$ denotes the Bessel function of the first kind. A more explicit dependence on the frequency f can

be obtained in the form (see appendix A for more details)

$$\phi_\lambda = \left\langle \left[1 + \frac{8\lambda D_0}{f^2 T} \int_0^T dt \Psi_t (1 - \cos(f(T-t))) + \frac{16\lambda^2 D_0^2}{f^4 T^2} \int_0^T dt_1 \Psi_{t_1} \int_0^T dt_2 \Psi_{t_2} \left(\frac{3}{4} + L_f(t_1, t_2) \right) \right]^{-1/2} \right\rangle_\Psi, \tag{13}$$

where $L_f(t_1, t_2)$ is defined by the somewhat lengthy expression (A.6).

The expression within the angular brackets in relation (13) is the exact MGF of the PSD of the process x_t in (3) for any fixed realisation of Ψ_t and holds for arbitrary T and arbitrary f . It also represents the exact form of the MGF in the case when Ψ_t is non-fluctuating: as mentioned, in particular, for $\Psi_t = 1$ it describes the MGF in case of standard Brownian motion [76], while the choice $\Psi_t = t^{\alpha-1}$ corresponds to the case of scaled Brownian motion recently studied in [78].

3.2. Exact high frequency limiting behaviour

As already remarked we here concentrate on random processes Ψ_t which, for any finite T , are Riemann-integrable with probability 1, which implies that in the limit $f \rightarrow \infty$ certain integrals vanish, as shown in appendix B. As a consequence, expression (13) attains the following exact analytic high-frequency form

$$\phi_\lambda \sim \left\langle \left[1 + \frac{8\lambda D_0}{f^2 T} \int_0^T dt \Psi_t + \frac{12\lambda^2 D_0^2}{f^4 T^2} \left(\int_0^T dt \Psi_t \right)^2 \right]^{-1/2} \right\rangle_\Psi, \tag{14}$$

in which we dropped the vanishing terms and kept only the leading terms in $1/f$.

We note that the Laplace parameter λ appears in the combination $D_0\lambda/f^2$ so that the high- f spectrum of a single-trajectory PSD has the universal form

$$S_T(f) \sim \frac{4D_0A}{f^2}, \tag{15}$$

regardless of the specific choice of Ψ_t . Here A is a dimensionless, random amplitude, which differs from realisation to realisation. This means that the characteristic high-frequency dependence of the PSD can be learned, in principle, from just a single trajectory, in agreement with the conclusions in [76–78].

The MGF Φ_λ of the random amplitude A follows from (14) and can be written as

$$\begin{aligned} \Phi_\lambda &= \int_0^\infty dA e^{-\lambda A} P(A) \\ &= \frac{2}{\sqrt{3}} \int_0^\infty dp \exp\left(-\frac{4p}{3}\right) I_0\left(\frac{2p}{3}\right) \Upsilon(T; \lambda p/T), \end{aligned} \tag{16}$$

where $I_0(z)$ is the modified Bessel function of the first kind, and

$$\Upsilon(T; \lambda) = \left\langle \exp\left(-\lambda \int_0^T dt \Psi_t\right) \right\rangle_\Psi \tag{17}$$

is the MGF of the integrated diffusivity (see [64,66])

$$\tau_T = \int_0^T dt \Psi_t. \tag{18}$$

Relation (16) links the MGFs of A and τ_T . Moreover, note that the characteristic function of the diffusing-diffusivity model in (6) is tightly related to the MGF of τ_T in (17), specifically

$$\Upsilon(T; D_0 w^2) = \Phi_w. \tag{19}$$

As shown in [64] the function $\Upsilon(T; \lambda)$ determines the first-passage time properties of the stochastic process x_t . Here we show how this function controls the high-frequency behaviour of the PSD.

Taking the inverse Laplace transform with respect to the parameter λ we evaluate the PDF of A ,

$$P(A) = \frac{2}{\sqrt{3}} \int_0^\infty dz J_0\left(\left(1 + \frac{1}{\sqrt{3}}\right) \sqrt{2zA}\right) J_0\left(\left(1 - \frac{1}{\sqrt{3}}\right) \sqrt{2zA}\right) \Upsilon(T; z/T). \tag{20}$$

This exact expression determines the high- f behaviour of the PDF $p(S_T(f) = S)$,

$$p(S_T(f) = S) \sim \frac{f^2}{4D_0} P\left(A = \frac{Sf^2}{4D_0}\right) \tag{21}$$

as $f \rightarrow \infty$. The exact high- f forms in (16) and (20) will serve as the basis of our analysis for several particular choices of the process Ψ_t in section 4.

Before proceeding, we stop to make several general statements.

- (a) Expanding the exponential function on the right-hand side of (16) into the Taylor series in powers of λ we obtain straightforwardly the relation between the moments of A and the moments of the integrated diffusivity τ_T , which is valid for any n ,

$$\mathbb{E}\{A^n\} = \left(\frac{3}{4}\right)^{n+1/2} n! {}_2F_1\left(\frac{n+1}{2}, \frac{n+2}{2}; 1; \frac{1}{4}\right) \left\langle \frac{\tau_T^n}{T^n} \right\rangle_\Psi, \tag{22}$$

where ${}_2F_1(a, b; c; z)$ is the Gauss hypergeometric function. Since the moments of τ_T are related to the moments of the process x_T [66] we also find

$$\mathbb{E}\{A^n\} = \left(\frac{3}{4}\right)^{n+1/2} \frac{(n!)^2}{(2n)!} {}_2F_1\left(\frac{n+1}{2}, \frac{n+2}{2}; 1; \frac{1}{4}\right) \left\langle \frac{x_T^{2n}}{(D_0 T)^n} \right\rangle_\Psi. \tag{23}$$

- (b) Starting from the results in (22) and (23) we can readily obtain the moments of $S_T(f)$ as well. In particular, if we focus on its average value, we have

$$\langle S_T(f) \rangle = \frac{4D_0 C_1}{f^2 T} \langle \tau_T \rangle_\Psi = \frac{2C_1}{f^2 T} \langle x_T^2 \rangle_\Psi, \tag{24}$$

where $C_1 = (3/4)^{3/2} {}_2F_1(1, 3/2; 1; 1/4)$. This suggests that those random-diffusivity models that display anomalous scaling of the MSD, i.e., $\langle x_T^2 \rangle_\Psi \propto T$, exhibit ageing behaviour, namely, a dependence of the PSD properties on the trajectory length T .

- (c) Equations (15) and (22) permit us to directly access the coefficient of variation γ of the PDF $p(S_T(f) = S)$ in the high- f limit. We get straightforwardly

$$\begin{aligned} \gamma &= \left(\frac{\langle S_T^2(f) \rangle_\Psi - \langle S_T(f) \rangle_\Psi^2}{\langle S_T(f) \rangle_\Psi^2} \right)^{1/2} \approx \left(\frac{\langle A^2 \rangle_\Psi - \langle A \rangle_\Psi^2}{\langle A \rangle_\Psi^2} \right)^{1/2} \\ &= \left(\frac{3}{4} \frac{\langle x_T^4 \rangle_\Psi}{\langle x_T^2 \rangle_\Psi^2} - 1 \right)^{1/2} = \left(\frac{9}{4} \frac{\langle \tau_T^2 \rangle_\Psi}{\langle \tau_T \rangle_\Psi^2} - 1 \right)^{1/2} \\ &= \left(\frac{9}{4} \frac{\partial_\lambda^2 \Upsilon(T; \lambda)|_{\lambda=0}}{(\partial_\lambda \Upsilon(T; \lambda)|_{\lambda=0})^2} - 1 \right)^{1/2}, \end{aligned} \tag{25}$$

which implies that the effective broadness of $p(S_T(f) = S)$ is entirely defined by the first two moments of the random variable τ_T in (18). Specifically, it is independent of D_0 and f when f is only large enough.

- (d) The behaviour of the left tail of $p(S_T(f) = S)$ can be assessed in the following way. Note that the product of the two Bessel functions in (20) can be represented as a power series with an infinite radius of convergence (see (C.1) in appendix C). Inserting the expansion in (C.1) in (20) and integrating over z we find

$$P(A) = \frac{2}{\sqrt{3}} \sum_{n=0}^{\infty} \frac{(-1)^n}{n!} \left(\frac{\sqrt{3}+1}{\sqrt{6}} \right)^{2n} {}_2F_1\left(-n, -n; 1; \frac{1-\sqrt{3}/2}{1+\sqrt{3}/2}\right) \left\langle \frac{T^{n+1}}{\tau_T^{n+1}} \right\rangle_\Psi A^n, \tag{26}$$

if the inverse moments of the variable τ_T exist (and do not grow too fast with n). Therefore, the PDF $P(A)$ is an analytic function of A in the vicinity of $A = 0$, with

$$P(0) = \frac{2}{\sqrt{3}} \left\langle \frac{T}{\tau_T} \right\rangle_\Psi. \tag{27}$$

We note that below we will encounter both situations when $P(A)$ is analytic and when it is not. In the latter situation we will show that $p(S_T(f) = S)$ diverges as $S \rightarrow 0$, which can be already inferred from (27).

4. Diffusivity modelled as squared Ornstein–Uhlenbeck process

In this and the following sections we apply the above general theory to several random-diffusivity models. According to our main results (16) and (20) one first needs to evaluate the MGF $\Upsilon(T; \lambda)$ of the integrated diffusivity τ_T for a chosen diffusivity process Ψ_t . To illustrate the quality of the theoretical predictions in the high-frequency limit we also performed numerical simulations using a Python code. The Euler integration scheme is used to compute (3), where Ψ_t is obtained by a numerical integration of the proper stochastic equation for each case. The PSD is obtained by fast Fourier transform for each trajectory. Starting from the single-trajectory power spectra the random amplitude A is calculated according to (15).

Concretely when Ψ_t in the diffusing-diffusivity model is defined as a stochastic process satisfying some Langevin equation, the distribution of A is determined by (16) and (20) through the MGF $\Upsilon(T; \lambda)$ of the integrated diffusivity τ_T that can be obtained by solving the associated backward Fokker–Planck equation (see [66] for details). Here we consider the common example of squared Ornstein–Uhlenbeck process and related models.

The Ornstein–Uhlenbeck process Y_t defined by the stochastic equation

$$\dot{Y}_t = -\tau_*^{-1} Y_t + \sigma_* \xi'_t \quad (28)$$

is a stationary Gaussian process mean-reverting to zero at a time scale τ_* and driven by standard Gaussian white noise ξ'_t with volatility σ_* . The process $\Psi_t = Y_t^2$ is one of the most common models of diffusing-diffusivity, which satisfies, due to Itô's formula,

$$\dot{\Psi}_t = \tau^{-1}(\bar{\Psi} - \Psi_t) + \sigma\sqrt{2\Psi_t}\xi'_t, \quad (29)$$

where $\tau = \tau_*/2$, $\sigma = \sqrt{2}\sigma_*$, and $\bar{\Psi} = \sigma_*^2\tau_*/2 = \sigma^2\tau/2$. This model was extended in [59–61] by considering Ψ_t as the sum of n independent squared Ornstein–Uhlenbeck processes, when (29) still holds with $\bar{\Psi} = n\sigma^2\tau/2$. More generally, setting $\bar{\Psi}$ to be any positive constant, the Langevin equation (29) defines the so-called Feller process [81], also known as square root process or the Cox–Ingersoll–Ross process [82], and related in the Heston model [83]. This process was used to model the diffusing-diffusivity in [63,64], see also the discussion in [61].

The MGF $\Upsilon(T; \lambda)$ for the integrated squared Ornstein–Uhlenbeck process was first computed by Dankel [84] and employed in [59–61]. Its computation for the Feller process in (29) was presented in [63],

$$\Upsilon(T; \lambda) = \left(\frac{4\omega e^{-(\omega-1)T/(2\tau)}}{(\omega+1)^2 - (\omega-1)^2 e^{-\omega T/\tau}} \right)^\nu, \quad (30)$$

where $\omega = \sqrt{1 + 4\sigma^2\tau^2\lambda}$ and $\nu = \bar{\Psi}/(\tau\sigma^2)$. In particular, setting $\bar{\Psi} = \sigma^2\tau/2$ (and thus $\nu = 1/2$) one retrieves the MGF for the squared Ornstein–Uhlenbeck process. A detailed discussion on the PDF of this model is presented in [59–61,63,64]. Using the explicit formulas for $\langle x_T^2 \rangle_\Psi$ and $\langle x_T^4 \rangle_\Psi$ from [61,63] we get from (25) that

$$\gamma = \left[\frac{3}{4} \left(3 + \frac{6\tau}{\nu T} \left(1 - \frac{\tau}{T} (1 - e^{-T/\tau}) \right) \right) - 1 \right]^{1/2}. \quad (31)$$

Moreover, as the second moment $\langle x_T^2 \rangle$ shows a linear trend in time [61,63], no ageing of the PSD occurs, as suggested in (24).

The PDF of A is determined via (20). Since an explicit calculation of this integral is not straightforward we perform a numerical integration. The results are shown in figure 1, in which we observe excellent agreement between the simulations and the theoretical results. The $1/f^2$ scaling is recovered for any value of τ_* . The coefficient of variation γ converges to different values when we change τ_* , according to (31). Note that this result reflects the different degrees of broadness of the PDF of the random amplitude A . In particular for $\tau_* \ll T$ we obtain a result that is very similar to the one of Brownian motion, while for increasing τ_* the PDF of the random amplitude A becomes increasingly broader.

5. Diffusivity modelled as a jump process

We divide the interval $(0, T)$ into N equal subintervals of duration $\delta = T/N$ and suppose that Ψ_t is a jump process on these intervals, of the form

$$\Psi_t = \psi_k \text{ on } t \in ([k-1]\delta, k\delta), \quad k = 1, \dots, N. \quad (32)$$

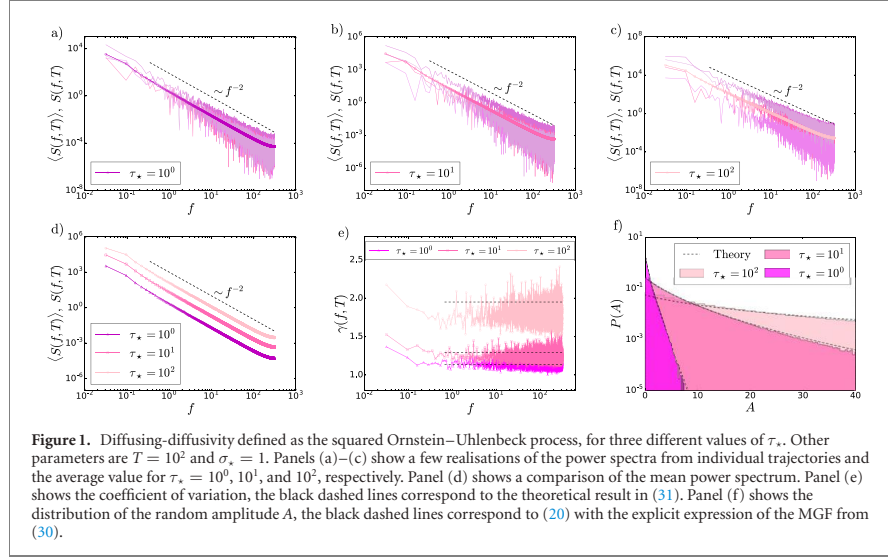


Figure 1. Diffusing-diffusivity defined as the squared Ornstein–Uhlenbeck process, for three different values of τ_* . Other parameters are $T = 10^2$ and $\sigma_* = 1$. Panels (a)–(c) show a few realisations of the power spectra from individual trajectories and the average value for $\tau_* = 10^0, 10^1$, and 10^2 , respectively. Panel (d) shows a comparison of the mean power spectrum. Panel (e) shows the coefficient of variation, the black dashed lines correspond to the theoretical result in (31). Panel (f) shows the distribution of the random amplitude A , the black dashed lines correspond to (20) with the explicit expression of the MGF from (30).

Furthermore we stipulate that the ψ_k are independent, identically distributed, positive-definite random variables with PDF $\rho(\psi)$. In other words, we take that Ψ_t at each discrete time instant $(k-1)\delta$ attains a new random value, taken from the common distribution, and stays constant and equal to this value up to the next discrete instant $k\delta$. For a given realisation of the process Ψ_t we thus have

$$\tau_T = \int_0^T dt \Psi_t = \delta \sum_{k=1}^N \psi_k, \quad (33)$$

and hence

$$\Upsilon(T; \lambda) = \left(\int_0^\infty d\psi \rho(\psi) e^{-\lambda \delta \psi} \right)^{T/\delta}. \quad (34)$$

Evaluating explicitly the derivatives $\partial_\lambda \Upsilon(T; \lambda)$ and $\partial_\lambda^2 \Upsilon(T; \lambda)$ at $\lambda = 0$, we get

$$\langle \tau_T \rangle = T \mathbb{E}\{\psi_k\}, \quad (35)$$

when the first moment $\mathbb{E}\{\psi_k\}$ exists. From this we infer $\langle x_T^2 \rangle_\Psi$ and thus the respective ageing behaviour. Moreover, the coefficient of variation becomes

$$\gamma = \left[\frac{9}{4} \left(1 - \frac{\delta}{T} + \frac{\delta}{T} \frac{\mathbb{E}\{\psi_k^2\}}{\mathbb{E}\{\psi_k\}^2} \right) - 1 \right]^{1/2}, \quad (36)$$

when the first two moments $\mathbb{E}\{\psi_k\}$ and $\mathbb{E}\{\psi_k^2\}$ exist.

Modelling the diffusivity as a jump process can be seen as a way to describe the model in section 4 through a different parametrisation. Indeed, we define a time scale, which is given by the duration δ of each step interval, and we then introduce a random variability of the diffusivity from one interval to the next. These diffusivity fluctuations are chosen according to the PDF $\rho(\psi)$. Of course, the main difference comes from the fact that in this model we do not have any correlation between successive diffusivities. In what follows we analyse two examples in detail. In the first one we select a Gamma distribution for $\rho(\psi)$, in analogy with the diffusing-diffusivity model in section 4, where the diffusion coefficient shows a Gamma distribution as well. In the second example we select a Lévy–Smirnov distribution for $\rho(\psi)$. This allows us to model a system in which a high probability of having small values of the diffusivity is combined with the presence of few outliers, which can be related, for instance, to values of the diffusivity at boundaries of the system.

5.1. Example I: Gamma distribution

First, we consider the Gamma distribution,

$$\rho(\psi) = \frac{\psi^{\nu-1}}{\Gamma(\nu)\psi_0^\nu} \exp(-\psi/\psi_0) \tag{37}$$

with the shape parameter $\nu > 0$ and the scale parameter $\psi_0 > 0$. From (34), we deduce

$$\Upsilon(T; \lambda) = (1 + \lambda\delta\psi_0)^{-\nu T/\delta}. \tag{38}$$

Position-PDF $\Pi(x, t)$

A direct calculation of the PDF for this model can be performed. Starting from (7) and recalling that $\Phi_w = \Upsilon(T; D_0 w^2)$, we get

$$\Pi(x, t) = \mathcal{N}_t \left(\frac{|x|}{2\sqrt{D_0\delta\psi_0}} \right)^{\frac{\nu t}{\delta} - \frac{1}{2}} K_{\frac{1}{2} - \frac{\nu t}{\delta}} \left(\frac{|x|}{\sqrt{D_0\delta\psi_0}} \right), \tag{39}$$

where the normalisation coefficient is

$$\mathcal{N}_t = \sqrt{\frac{2}{\pi}} / \left((D_0\delta\psi_0)^{3/4} \Gamma\left(\frac{\nu t}{\delta}\right) \right). \tag{40}$$

With the properties

$$z^\nu K_{-\nu}(z) \sim 2^{\nu-1} \Gamma(\nu) - \frac{2^{\nu-3} \Gamma(\nu)}{\nu-1} z^2 \tag{41}$$

for $|z| \rightarrow 0$ and $\nu > 1$, as well as

$$K_{-\nu} \sim \sqrt{\frac{\pi}{2z}} e^{-z} \tag{42}$$

for $|z| \rightarrow \infty$, the asymptotic behaviours of the PDF are given by

$$\Pi(x, t) \sim \mathcal{N}_t 2^{\frac{\nu t}{\delta} - \frac{3}{2}} \Gamma\left(\frac{\nu t}{\delta} - \frac{1}{2}\right) \left[1 - \frac{x^2}{4 \left(\frac{\nu t}{\delta} - \frac{3}{2}\right) D_0\delta\psi_0} \right] \tag{43}$$

for $|x| \rightarrow 0$ and $\nu t > 3\delta/2$, as well as

$$\Pi(x, t) \sim \frac{2}{\sqrt{D_0\delta\psi_0} \Gamma\left(\frac{\nu t}{\delta}\right)} \left(\frac{|x|}{2\sqrt{D_0\delta\psi_0}} \right)^{\frac{\nu t}{\delta} - 1} \exp\left(-\frac{|x|}{\sqrt{D_0\delta\psi_0}}\right) \tag{44}$$

for $|x| \rightarrow \infty$.

The functional behaviour of the PDF $\Pi(x, t)$ is shown in figure 2. We see that by changing δ we can observe different shapes of $\Pi(x, t)$. When $\delta = 1$ [panels (a) and (c)] the Gaussian approximation (51) already provides a good estimate of the PDF over a wide range. We start observing discrepancies only far out in the tails, for values which can hardly be reached with real data. When $\delta = 100$ [panels (b) and (d)], in contrast, the exponential tails are distinct. The behaviours at small and large x are well described by the asymptotic expansions in (43) and (44). Note that the value of δ in here plays a role similar to the correlation time τ_* in the diffusing-diffusivity model defined in section 4. The only difference is that by changing τ_* in the model above we also change the average diffusivity while, in this case, changes in the value of δ do not affect the average diffusivity, which is fixed once we choose the jumps PDF in (37).

Amplitude-PDF $P(A)$

The MGF of the amplitude A of the jump process-diffusivity model is given by

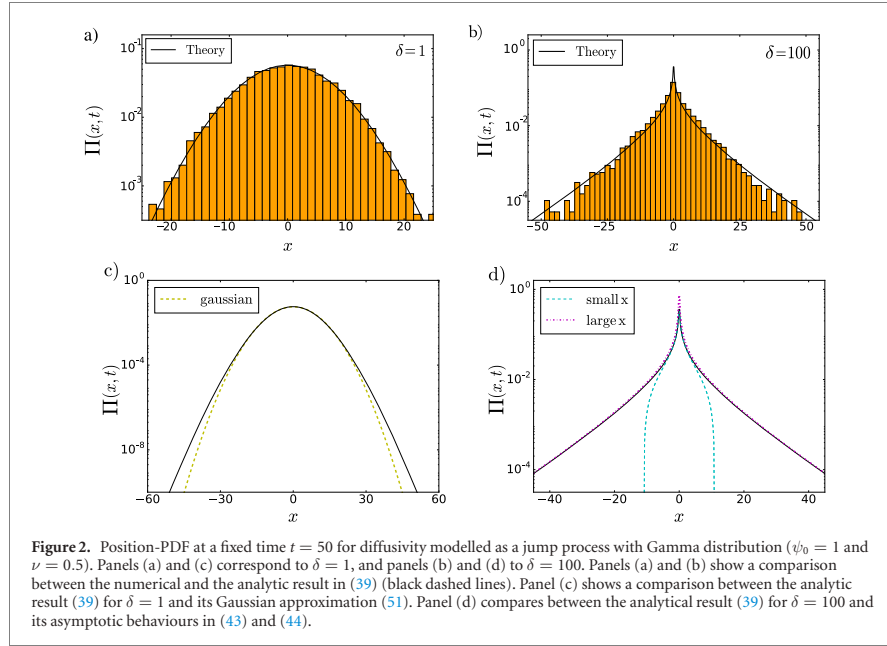
$$\Phi_\lambda = \frac{2}{\sqrt{3}} \int_0^\infty dp \frac{\exp(-4p/3) I_0(2p/3)}{(1 + p\psi_0\lambda\delta/T)^{\nu T/\delta}}, \tag{45}$$

so that

$$P(A) = \frac{2}{\sqrt{3}} \int_0^\infty dz \frac{J_0\left(\frac{(1 + 1/\sqrt{3})\sqrt{2zA}}{(1 + z\psi_0\delta/T)^{\nu T/\delta}}\right) J_0\left(\frac{(1 - 1/\sqrt{3})\sqrt{2zA}}{(1 + z\psi_0\delta/T)^{\nu T/\delta}}\right)}{(1 + z\psi_0\delta/T)^{\nu T/\delta}}. \tag{46}$$

In particular one has $\mathbb{E}\{\psi_k\} = \nu\psi_0$ and $\mathbb{E}\{\psi_k^2\} = \psi_0^2\nu(\nu + 1)$, thus from (35) we readily obtain $\langle \overline{x_T^2} \rangle_\Psi \simeq T$, demonstrating that in this process no ageing behaviour is displayed. Moreover, from (36) we get

$$\gamma = \left[\frac{9}{4} \left(1 + \frac{\delta}{\nu T} \right) - 1 \right]^{1/2}. \tag{47}$$



In the limit $\delta \rightarrow 0$ and $N \rightarrow \infty$, with $\delta N = T$ fixed, we have

$$\Upsilon(T; \lambda) \sim \exp(-\nu\psi_0 T\lambda). \quad (48)$$

Hence,

$$\begin{aligned} \Phi_\lambda &= \frac{2}{\sqrt{3}} \int_0^\infty dp \exp\left(-\left(\frac{4}{3} + \nu\psi_0\lambda\right)p\right) I_0\left(\frac{2p}{3}\right) \\ &= \left(1 + 2\nu\psi_0\lambda + \frac{4}{3}(\nu\psi_0\lambda)^2\right)^{-1/2} \end{aligned} \quad (49)$$

and

$$\begin{aligned} P(A) &= \frac{2}{\sqrt{3}} \int_0^\infty dz J_0\left(\left(1 + 1/\sqrt{3}\right)\sqrt{2zA}\right) J_0\left(\left(1 - 1/\sqrt{3}\right)\sqrt{2zA}\right) e^{-\nu\psi_0 z} \\ &= \frac{2}{\sqrt{3}\nu\psi_0} \exp\left(-\frac{4A}{3\nu\psi_0}\right) I_0\left(\frac{2A}{3\nu\psi_0}\right). \end{aligned} \quad (50)$$

This means that we have essentially the same behaviour as for standard one-dimensional Brownian motion, however, with renormalised coefficients (compare with the result in [76]), in agreement also with what we obtained for the diffusing-diffusivity model in section 4, when selecting $\tau_* \ll T$. Indeed, if we use (48) and recall that $\Phi_w = \Upsilon(T; D_0 w^2)$, we readily obtain

$$\Pi(x, t) \sim \frac{1}{2\sqrt{\pi\nu\psi_0 D_0 t}} \exp\left(-\frac{x^2}{4\nu\psi_0 D_0 t}\right). \quad (51)$$

In figure 3 we show a direct comparison between the numerical and theoretical results for the Gamma distribution with $\psi_0 = 1$ and $\nu = 0.5$. We observe that the average value of the power spectrum is not affected by the value of δ . Nevertheless, when we plot some sample single-trajectory power spectra we notice a larger amplitude scatter for larger values of δ . This may be clearly seen in the distribution of the random variable A , which is broader for larger values of δ , and consequently in the different limiting values of the coefficient of variation. Thus, the fluctuations are sensitive to different parameters of the distribution (37), while the mean behaviour is not.

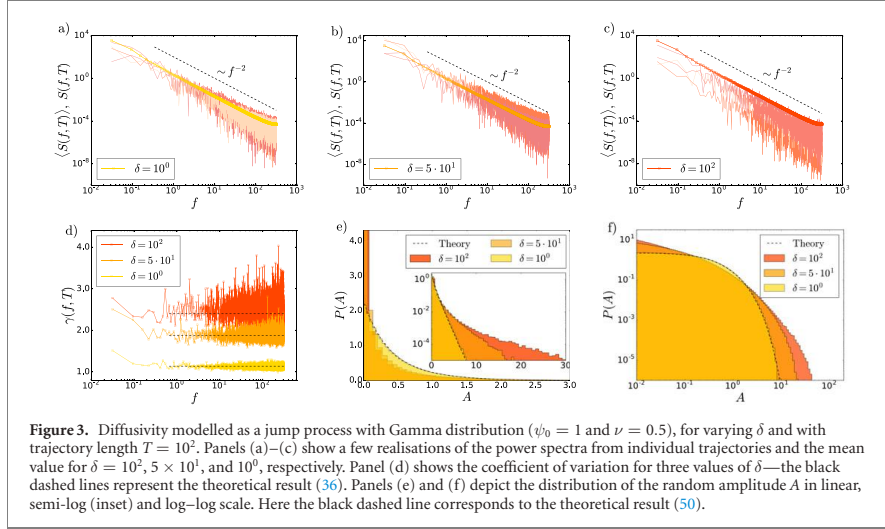


Figure 3. Diffusivity modelled as a jump process with Gamma distribution ($\psi_0 = 1$ and $\nu = 0.5$), for varying δ and with trajectory length $T = 10^2$. Panels (a)–(c) show a few realisations of the power spectra from individual trajectories and the mean value for $\delta = 10^2, 5 \times 10^1$, and 10^0 , respectively. Panel (d) shows the coefficient of variation for three values of δ —the black dashed lines represent the theoretical result (36). Panels (e) and (f) depict the distribution of the random amplitude A in linear, semi-log (inset) and log–log scale. Here the black dashed line corresponds to the theoretical result (50).

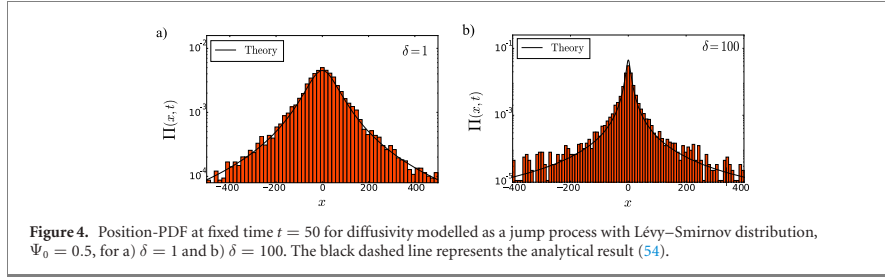


Figure 4. Position-PDF at fixed time $t = 50$ for diffusivity modelled as a jump process with Lévy–Smirnov distribution, $\Psi_0 = 0.5$, for a) $\delta = 1$ and b) $\delta = 100$. The black dashed line represents the analytical result (54).

5.2. Example II: Lévy–Smirnov distribution

In our second example we consider the Lévy–Smirnov distribution

$$\rho(\psi) = \sqrt{\frac{\psi_0}{\pi}} \frac{\exp(-\psi_0/\psi)}{\psi^{3/2}}, \tag{52}$$

for which equation (34) yields

$$\Upsilon(T; \lambda) = \exp\left(-2T\sqrt{\psi_0\lambda/\delta}\right). \tag{53}$$

Note that in this case $\mathbb{E}\{\psi_k\}$ and $\mathbb{E}\{\psi_k^2\}$ are not defined, such that $\langle x_T^2 \rangle_\Psi$ does not exist either. This suggests that a clear ageing behaviour cannot be defined and that fluctuations are what dominates the system.

Position-PDF $\Pi(x, t)$

As a consequence, we obtain the following analytical expression for the PDF,

$$\Pi(x, t) = \frac{2t\sqrt{D_0\psi_0/\delta}}{\pi} \frac{1}{4t^2D_0\psi_0/\delta + x^2}, \tag{54}$$

where we recognise the power-law behaviour, that is already built into relation (52). Note that expression (54) represents the Cauchy distribution, whose median grows with time t .

The PDF is shown for two different values of δ in figure 4. We observe that, differently from the case with the Gamma distribution above, we do not see significant changes in the shape of the distribution when varying δ . For both cases, $\delta = 1$ and $\delta = 100$, the power-law behaviour (54) is readily discernible.

Amplitude-PDF $P(A)$

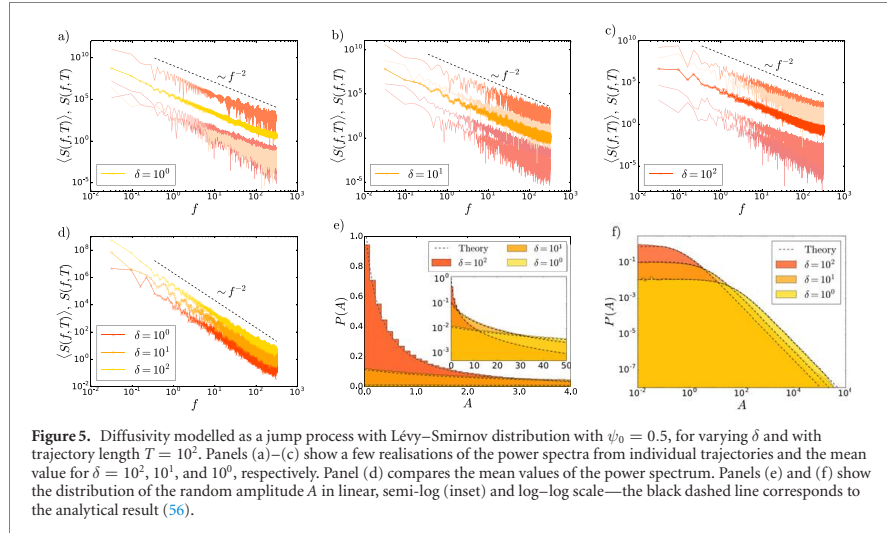


Figure 5. Diffusivity modelled as a jump process with Lévy–Smirnov distribution with $\psi_0 = 0.5$, for varying δ and with trajectory length $T = 10^2$. Panels (a)–(c) show a few realisations of the power spectra from individual trajectories and the mean value for $\delta = 10^2, 10^1$, and 10^0 , respectively. Panel (d) compares the mean values of the power spectrum. Panels (e) and (f) show the distribution of the random amplitude A in linear, semi-log (inset) and log–log scale—the black dashed line corresponds to the analytical result (56).

The MGF for the random amplitude A reads

$$\Phi_\lambda = \frac{2}{\sqrt{3}} \int_0^\infty dp \exp\left(-\frac{4}{3}p - 2\sqrt{p\psi_0\lambda T/\delta}\right) I_0\left(\frac{2p}{3}\right) \tag{55}$$

and

$$P(A) = \frac{2}{\sqrt{3}} \int_0^\infty dz J_0\left(\left(1 + 1/\sqrt{3}\right)\sqrt{2zA}\right) J_0\left(\left(1 - 1/\sqrt{3}\right)\sqrt{2zA}\right) \exp\left(-2\sqrt{z\psi_0 T/\delta}\right) \\ = \frac{\delta}{\sqrt{3}\psi_0 T} \frac{1}{(1 + \xi)^{3/2}} {}_2F_1\left(\frac{3}{4}, \frac{5}{4}; 1; \frac{\xi^2}{4(1 + \xi)^2}\right), \tag{56}$$

with $\xi = (4A\delta)/(3\psi_0 T)$. Note that in the limit $A \rightarrow \infty$, the leading behaviour of $P(A)$ follows

$$P(A) \sim \frac{1}{A^{3/2}}. \tag{57}$$

Thus, the PDF $P(A)$ inherits the property of diverging moments from the parental Lévy–Smirnov distribution.

Figure 5 summarises the properties of the PSD for the jump process with Lévy–Smirnov distribution ($\psi_0 = 0.5$). We observe that, despite the fat-tailed PDF in (54) we still observe the universal $1/f^2$ scaling of the PDF. Concurrently, the PDF of the random amplitude A features the power-law behaviour according to (56). Note that the non-existence of the moments of $P(A)$ generates a pronounced scatter in the amplitude of the average power spectrum.

6. Diffusivity modelled as a functional of Brownian motion

We now focus on the case when Ψ_t is a genuine ‘diffusing-diffusivity’ in the sense that it is subordinated to Brownian motion B_t starting at the origin at $t = 0$, with zero mean and covariance function

$$\langle B_t B_{t'} \rangle = 2D_B \min\{t, t'\}. \tag{58}$$

We here choose $\Psi_t = V[B_t]$, where V is some prescribed, positive-definite function. Note that random variables of the form $\int_0^T dt V[B_t]$ appear across many disciplines, including probability theory, statistical analysis, computer science, mathematical finance and physics. Starting from earlier works [87–92], much effort has been invested in the analysis of the PDF and the corresponding Laplace transforms of these processes. A large body of exact results has been obtained within the last seven decades (see, e.g., [93–98] and further references therein). In the following, we consider three particular examples of $V[B_t]$, for which we can carry out exact calculations and obtain insightful results.

6.1. Example I: $\Psi_t = \Theta(B_t)$

First, we choose the cut-off Brownian motion

$$\Psi_t = \Theta(B_t), \quad (59)$$

where $\Theta(x)$ is the Heaviside theta function. The process x_t exhibits standard diffusive motion, once $B_t > 0$, and pauses, remaining at the position it has reached when B_t goes to negative values. The random variable $\int_0^T dt \Psi_t$ defines the time spent by a Brownian trajectory, starting at the origin, on the positive real line within the time interval $(0, T)$. The time intervals between any two 'diffusion tours', as well as their duration, are random variables with a broad distribution.

This example is of particular interest as it represents an alternative to other standard models describing waiting times and trapping events. One could think, for instance, of the comb model, where a particle, while performing standard Brownian motion along one direction, gets stuck for a random time in branches perpendicular to the direction of the diffusive motion [99,100].

The MSD of the process x_t , as one can straightforwardly check, is just

$$\langle x_t^2 \rangle_\Psi = D_0 t, \quad (60)$$

that is, a standard diffusion law in which the diffusion coefficient is reduced by the factor $1/2$. This means that no ageing behaviour is observed. For higher order moments one expects, of course, significant departures from the standard diffusive behaviour.

Position-PDF $\Pi(x, t)$

The MGF of the random variable $\tau_T = \int_0^T dt \Theta(B_t)$, which has a bounded support on $(0, T)$, was first derived by Kac [90], and Erdős and Kac [91]. Rewriting their result in our notation we have

$$\begin{aligned} \Upsilon(T; \lambda) &= \left\langle \exp \left(-\lambda \int_0^T dt \Theta(B_t) \right) \right\rangle_\Psi \\ &= e^{-\lambda T/2} I_0 \left(\frac{\lambda T}{2} \right). \end{aligned} \quad (61)$$

Note that the inverse Laplace transform of this expression produces the celebrated Lévy arcsine law [101]. With result (61), the desired PDF is given by

$$\begin{aligned} \Pi(x, t) &= \frac{1}{\pi} \int_0^\infty dw \cos(wx) \exp \left(-\frac{D_0 t}{2} w^2 \right) I_0 \left(\frac{D_0 t}{2} w^2 \right) \\ &= \frac{\exp \left(-x^2 / (8D_0 t) \right)}{2\sqrt{\pi^3 D_0 t}} K_0 \left(\frac{x^2}{8D_0 t} \right). \end{aligned} \quad (62)$$

Recalling that $K_0(z) \sim -\ln(z/2) - \gamma_{EM}$ for $|z| \rightarrow 0$, where γ_{EM} is the Euler–Mascheroni constant, for small x we have

$$\Pi(x, t) \sim \frac{-\ln \left(\frac{x^2}{8D_0 t} \right) - \gamma_{EM}}{2\sqrt{\pi^3 D_0 t}}, \quad |x| \rightarrow 0. \quad (63)$$

For large x we use (42) and obtain the asymptotic behaviour for the PDF,

$$\Pi(x, t) \sim \frac{1}{\pi|x|} \exp \left(-\frac{x^2}{4D_0 t} \right), \quad |x| \rightarrow \infty. \quad (64)$$

The PDF for this process is shown in figure 6. We see that the central part of the PDF is strongly non-Gaussian, while the tails are Gaussian, in agreement with the asymptotic behaviours (63) and (64).

Amplitude-PDF $P(A)$

Inserting expression (61) into (16) and performing the integration over z , we arrive at the following, remarkably compact expression for the MGF,

$$\Phi_\lambda = \frac{2\sqrt{2}}{\pi\sqrt{2+3\lambda}} \mathbf{K} \left(\frac{2\lambda}{2+3\lambda} \right) \quad (65)$$

where $\mathbf{K}(x)$ is the complete elliptic integral of the first kind,

$$\mathbf{K}(x) = \int_0^{\pi/2} \frac{d\phi}{\sqrt{1-x^2 \sin^2(\phi)}}. \quad (66)$$

Note that the high- f asymptotic form in (65) is independent of the observation time T .

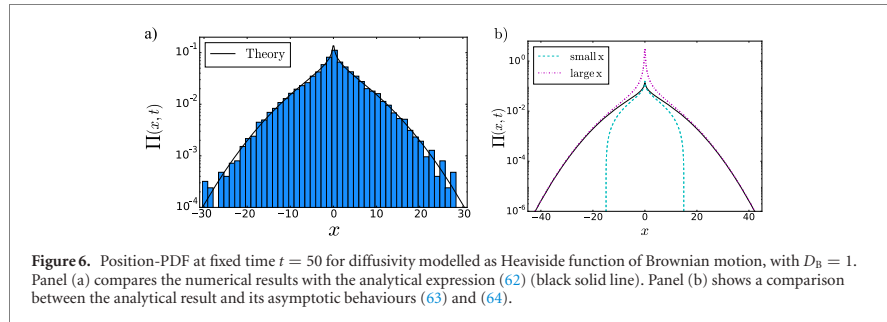


Figure 6. Position-PDF at fixed time $t = 50$ for diffusivity modelled as Heaviside function of Brownian motion, with $D_B = 1$. Panel (a) compares the numerical results with the analytical expression (62) (black solid line). Panel (b) shows a comparison between the analytical result and its asymptotic behaviours (63) and (64).

To proceed we take advantage of the definition of the complete elliptic integral and perform the inverse Laplace transform of (65). After some formal manipulations this yields the following expression for the PDF,

$$P(A) = 2\sqrt{\frac{2}{3\pi^3 A}} \int_0^{\pi/2} \frac{d\phi}{\sqrt{1 - \frac{2}{3} \sin^2(\phi)}} \exp\left(-\frac{2A}{3(1 - \frac{2}{3} \sin^2(\phi))}\right). \quad (67)$$

Multiplying both sides of the latter equation by A^n and integrating over A from 0 to ∞ , we get the following simple expression for the moments of the random amplitude A of arbitrary order,

$$\mathbb{E}\{A^n\} = \frac{\Gamma(n + \frac{1}{2})}{\sqrt{\pi}} \left(\frac{3}{2}\right)^n {}_2F_1\left(-n, \frac{1}{2}; 1; \frac{2}{3}\right). \quad (68)$$

Then, from (25), we readily get the coefficient of variation, $\gamma = \sqrt{19/8}$.

Note that the integrals $\int_0^\infty d\lambda \lambda^n \Upsilon(T; \lambda)$ diverge for any $n > 0$, which means that τ_T does not have negative moments. One therefore expects that $P(A)$ is a non-analytic, diverging function in the limit $A \rightarrow 0$. The small- A asymptotic behaviour of $P(A)$ can be deduced directly from (67). Expanding the exponential function in the integral into the Taylor series in powers of A and expressing the emerging generalised elliptic integrals via their representations in terms of the toroidal functions $P_{n-1/2}(\cosh(\eta))$ (see (C.3) in appendix C), we get

$$P(A) = \sqrt{\frac{2}{3\pi^3 A}} \sum_{n=0}^\infty \frac{(-1)^n}{n!} \left(\frac{2}{\sqrt{3}}\right)^n P_{n-1/2}\left(\frac{2}{\sqrt{3}}\right) A^n. \quad (69)$$

For the opposite limit $A \rightarrow \infty$, we conveniently rewrite equation (56) in the form

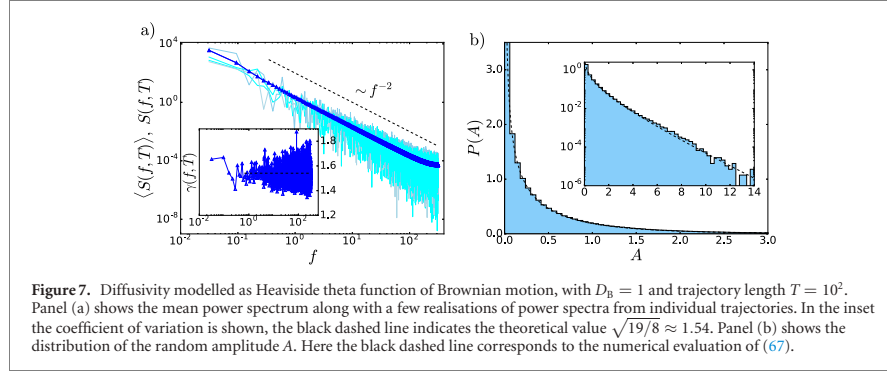
$$\begin{aligned} P(A) &= 2\sqrt{\frac{2}{3\pi^3 A}} \exp\left(-\frac{2A}{3}\right) \int_0^{\pi/2} \frac{d\phi}{\sqrt{(1 - \frac{2}{3} \sin^2(\phi))}} \exp\left(-\frac{2A}{3} \frac{\frac{2}{3} \sin^2(\phi)}{1 - \frac{2}{3} \sin^2(\phi)}\right) \\ &= 2\sqrt{\frac{2}{3\pi^3 A}} \exp\left(-\frac{2A}{3}\right) \sum_{n=0}^\infty \left(\int_0^{\pi/2} \sin^{2n}(\phi) d\phi\right) \left(\frac{2}{3}\right)^n L_n^{(-1/2)}\left(\frac{2A}{3}\right) \\ &= \frac{2}{3\pi} \sqrt{\frac{3}{2A}} \exp\left(-\frac{2A}{3}\right) \sum_{n=0}^\infty \frac{\Gamma(n + 1/2)}{n!} \left(\frac{2}{3}\right)^n L_n^{(-1/2)}\left(\frac{2A}{3}\right), \end{aligned} \quad (70)$$

where $L_n^{(-1/2)}(x)$ are associated Laguerre polynomials. We focus next on the asymptotic behaviour of the function

$$g(u) = u^{-1/2} \sum_{n=0}^\infty \frac{\Gamma(n + 1/2)}{n!} \left(\frac{2}{3}\right)^n L_n^{(-1/2)}(u) \quad (71)$$

in the limit $u \rightarrow \infty$. Performing a Laplace transform of $g(u)$ we readily get

$$\begin{aligned} \mathcal{L}_s\{g(u)\} &= \int_0^\infty du \exp(-su) g(u) \\ &= \frac{1}{s^{1/2}} \sum_{n=0}^\infty \frac{\Gamma^2(n + 1/2)}{(n!)^2} \left(\frac{2(s-1)}{3s}\right)^n \\ &= \frac{2}{s^{1/2}} \mathbf{K}\left(\frac{2(s-1)}{3s}\right), \end{aligned} \quad (72)$$



where \mathbf{K} is the complete elliptic integral defined in equation (66). In the limit $s \rightarrow 0$ (corresponding to $A \rightarrow \infty$),

$$\mathcal{L}_s \{g(u)\} \sim \frac{2}{s^{1/2}} \mathbf{K} \left(-\frac{2}{3s} \right) = 2 \int_0^{\pi/2} \frac{d\phi}{\sqrt{s + \frac{2}{3} \sin^2(\phi)}}. \quad (73)$$

Inverting the Laplace transform and integrating over ϕ , we find

$$g(u) \sim \frac{\pi}{\sqrt{u}} \exp\left(-\frac{u}{3}\right) I_0\left(\frac{u}{3}\right) \rightarrow \sqrt{\frac{3}{2}} \frac{1}{u}. \quad (74)$$

Thus, in the limit $A \rightarrow \infty$, the leading behaviour of the PDF $P(A)$ yields in the form

$$P(A) \sim \frac{1}{\pi A} \sqrt{\frac{3}{2}} \exp\left(-\frac{2A}{3}\right). \quad (75)$$

Figure 7 summarises the numerical results for this case. Again we observe excellent agreement with the theoretical results.

6.2. Example II: $\Psi_t = \exp(-B_t/a)$

As the second example, we link the process Ψ_t to so-called geometric Brownian motion. Random variables of this form have been widely studied in the mathematical finance literature (see, e.g., [93]). Within the latter domain, they emerge very naturally as representation of the solution of the celebrated Black–Scholes equation. Their time-averaged counterpart is related to the so-called asian options [102–104] (see also [105,106]) and also appears in different contexts in the analysis of transport phenomena in disordered media (see, e.g., [107–113]) as well as characterises some features of the melting transition of heteropolymers [114].

In our notation, we set

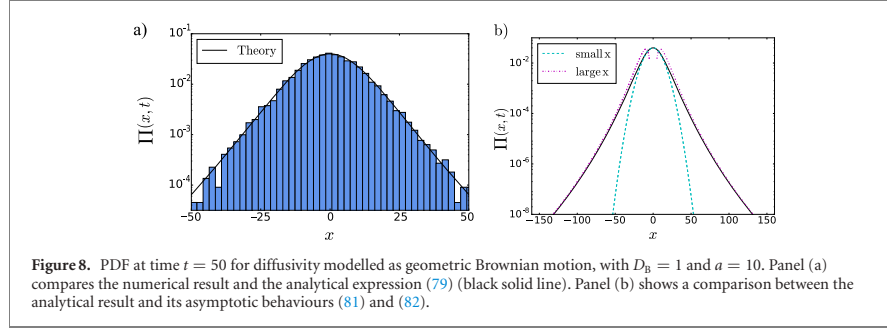
$$\Psi_t = \exp\left(-\frac{B_t}{a}\right), \quad (76)$$

where a is a parameter of unit length. In this case, x_t exhibits an anomalously strong superdiffusion such that

$$\begin{aligned} \langle x_t^2 \rangle &= 2D_0 \int_0^t d\tau \langle \Psi_\tau \rangle_\Psi = 2D_0 \int_0^t d\tau \exp(D_B \tau / a^2) \\ &= \frac{2D_0 a^2}{D_B} (\exp(D_B t / a^2) - 1). \end{aligned} \quad (77)$$

Note that when $D_B t / a^2 \ll 1$ we have $\langle x_t^2 \rangle \sim 2D_0 t$. These results for the MSD demonstrate that for this model, in general, we observe ageing behaviour, though the latter may be hidden while analysing very short trajectories.

Position-PDF $\Pi(x, t)$



The Laplace transform of the time-averaged geometric Brownian motion in our notation reads [108–110]

$$\begin{aligned} \Upsilon(T; \lambda) &= \left\langle \exp \left(-\lambda \int_0^T dt \exp \left(-\frac{B_t}{a} \right) \right) \right\rangle_{\Psi} \\ &= \frac{2a}{\sqrt{\pi D_B T}} \int_0^{\infty} dx \exp \left(-\frac{a^2 x^2}{D_B T} \right) \cos \left(2a \sqrt{\frac{\lambda}{D_B}} \sinh(x) \right) \\ &= \frac{2}{\pi} \int_0^{\infty} dx \exp \left(-\frac{D_B T}{4a^2} x^2 \right) \cosh \left(\frac{\pi x}{2} \right) K_{ix} \left(2a \sqrt{\frac{\lambda}{D_B}} \right), \end{aligned} \quad (78)$$

where K_{ix} is the modified Bessel function of the second kind with purely imaginary index. As a consequence, the PDF is given by

$$\begin{aligned} \Pi(x, t) &= \left(\frac{2}{\pi} \right)^{3/2} \int_0^{\infty} dz \exp \left(-\frac{D_B t}{4a^2} z^2 \right) \cosh \left(\frac{\pi z}{2} \right) \int_0^{\infty} dw \cos(wx) K_{iz} \left(2a|w| \sqrt{\frac{D_0}{D_B}} \right) \\ &= \frac{1}{2\sqrt{\pi b_2 t (b_1^2 + x^2)}} \exp \left(-\frac{\operatorname{arcsinh}^2(x/b_1)}{4b_2 t} \right), \end{aligned} \quad (79)$$

where

$$b_1 = 2a \sqrt{\frac{D_0}{D_B}}, \quad b_2 = \frac{D_B}{4a^2}. \quad (80)$$

Recalling that $\operatorname{arcsinh}(z) \sim z$ for $z \rightarrow 0$ and $\operatorname{arcsinh}(z) \sim \ln(2z)$ for $z \rightarrow \infty$, we express the asymptotic behaviour of the PDF as

$$\Pi(x, t) \sim \frac{1}{2\sqrt{\pi b_2 t (b_1^2 + x^2)}} \exp \left(-\frac{x^2}{4b_2 t b_1^2} \right) \quad (81)$$

for $|x| \rightarrow 0$ and

$$\Pi(x, t) \sim \frac{1}{2\sqrt{\pi b_2 t (b_1^2 + x^2)}} \exp \left(-\frac{\ln^2(2x/b_1)}{4b_2 t} \right) \quad (82)$$

for $|x| \rightarrow \infty$.

The PDF is shown in figure 8. In this case, according to the asymptotic expansions (81) and (82) we observe that the central part of the PDF is approximately Gaussian, while the tails follow a log-normal shape.

Amplitude-PDF $P(A)$

Evaluating explicitly $\partial_{\lambda} \Upsilon(T; \lambda)$ and $\partial_{\lambda}^2 \Upsilon(T; \lambda)$ at $\lambda = 0$, we get

$$\gamma = \left[\frac{3}{8} \left(3 + e^{D_B T/a^2} \left(2 + e^{D_B T/a^2} \right) \right) - 1 \right]^{1/2}. \quad (83)$$

Figure 9 summarises our numerical results, which show excellent agreement with the theoretical prediction.

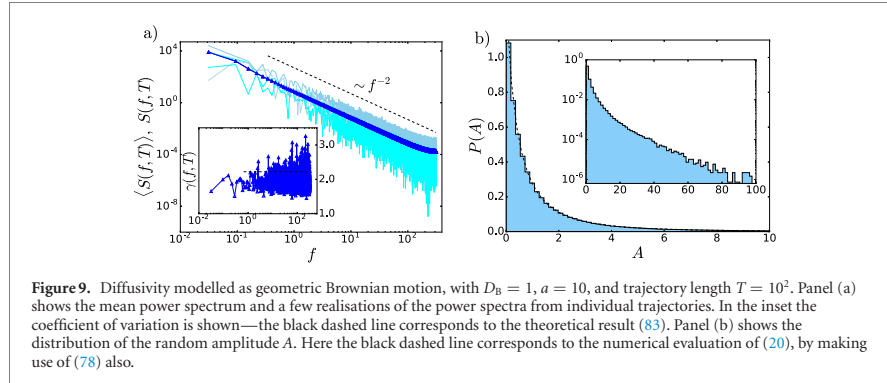


Figure 9. Diffusivity modelled as geometric Brownian motion, with $D_B = 1$, $a = 10$, and trajectory length $T = 10^2$. Panel (a) shows the mean power spectrum and a few realisations of the power spectra from individual trajectories. In the inset the coefficient of variation is shown—the black dashed line corresponds to the theoretical result (83). Panel (b) shows the distribution of the random amplitude A . Here the black dashed line corresponds to the numerical evaluation of (20), by making use of (78) also.

6.3. Example III: $\Psi_t = B_t^2/a^2$

Finally, we consider squared Brownian motion

$$\Psi_t = \frac{B_t^2}{a^2}, \tag{84}$$

where a is a parameter of unit length. Note that here the process x_t in (3) is superdiffusive, such that its mean-squared displacement obeys

$$\langle \overline{x_t^2} \rangle_\Psi = \frac{2D_0 D_B}{a^2} t^2, \tag{85}$$

and thus a pronounced ageing behaviour occurs.

This example, similarly to the diffusing-diffusivity model in section 4, defines the diffusivity as the squared of an auxiliary variable, though in this case the variable follows a Brownian motion instead of the OU process. This choice implies that there is no crossover time, in contrast to the standard diffusing-diffusivity model, and thus we obtain a model which is always non-stationary. In particular, we introduce a larger separation between small and large values of the diffusivity, which may be interpreted as non-linear effects of the heterogeneity. Note that, if we were to define a random duration δ of the intervals, this model could be linked to a correlated CTRW [85,86].

Position-PDF $\Pi(x, t)$

The Laplace transform of the PDF of integrated squared Brownian motion was first calculated in the classical paper by Cameron and Martin [88,89] (see also [90]). In our notation,

$$\begin{aligned} \Upsilon(T; \lambda) &= \left\langle \exp \left(-\frac{\lambda}{a^2} \int_0^T dt B_t^2 \right) \right\rangle_\Psi \\ &= \frac{1}{\sqrt{\cosh \left(\sqrt{4D_B T^2 \lambda} / a^2 \right)}}, \end{aligned} \tag{86}$$

and the PDF $\Pi(x, t)$ for this process is given by

$$\begin{aligned} \Pi(x, t) &= \frac{1}{\pi} \int_0^\infty \frac{dw \cos(wx)}{\sqrt{\cosh \left(w \sqrt{4D_B D_0 t^2} / a^2 \right)}} \\ &= \frac{1}{\sqrt{2ct}} \operatorname{sech} \left(\frac{\pi x}{ct} \right) P_{\frac{ix}{ct} - \frac{1}{2}}(0), \end{aligned} \tag{87}$$

where $c = 2\sqrt{D_0 D_B}/a$ and $P_\nu(z)$ is the Legendre function of the first kind. The latter admits the representation

$$P_{ix/ct-1/2}(0) = \sqrt{\pi} \left/ \left[\Gamma \left(\frac{ix}{2ct} + \frac{3}{4} \right) \Gamma \left(-\frac{ix}{2ct} + \frac{3}{4} \right) \right] \right., \tag{88}$$

such that

$$\Pi(x, t) = \frac{\sqrt{\pi}}{ct\sqrt{2}} \frac{\operatorname{sech} \left(\frac{\pi x}{ct} \right)}{\Gamma \left(\frac{ix}{2ct} + \frac{3}{4} \right) \Gamma \left(-\frac{ix}{2ct} + \frac{3}{4} \right)}. \tag{89}$$

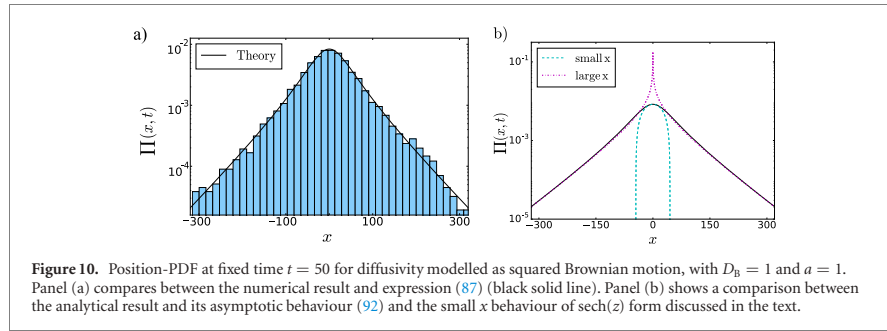


Figure 10. Position-PDF at fixed time $t = 50$ for diffusivity modelled as squared Brownian motion, with $D_B = 1$ and $a = 1$. Panel (a) compares between the numerical result and expression (87) (black solid line). Panel (b) shows a comparison between the analytical result and its asymptotic behaviour (92) and the small x behaviour of $\text{sech}(z)$ form discussed in the text.

In the limits,

$$\Gamma\left(\frac{ix}{2ct} + \frac{3}{4}\right) \Gamma\left(-\frac{ix}{2ct} + \frac{3}{4}\right) \sim \Gamma\left(\frac{3}{4}\right)^2 \tag{90}$$

for $|x| \rightarrow 0$, and

$$\Gamma\left(\frac{ix}{2ct} + \frac{3}{4}\right) \Gamma\left(-\frac{ix}{2ct} + \frac{3}{4}\right) \sim \pi \sqrt{\frac{2|x|}{ct}} \exp\left(-\frac{\pi|x|}{2ct}\right) \tag{91}$$

for $|x| \rightarrow \infty$. As a consequence, the behaviour of the PDF for small x is approximately Gaussian, $\simeq \exp(-\text{const.}x^2)$, where const. is a constant that can be expressed via the polylogarithm function. Conversely,

$$\Pi(x, t) \sim \frac{1}{\pi ct|x|} \exp\left(-\frac{\pi|x|}{2ct}\right) \tag{92}$$

for $|x| \rightarrow \infty$. The shape of the PDF is shown in figure 10. We clearly observe that the central part is approximately Gaussian while the tails have an exponential trend, as expressed explicitly by the asymptote (92).

Amplitude-PDF $P(A)$

Using (86) we then find that the MGF of the random amplitude A and the corresponding PDF are given by the integrals

$$\Phi_\lambda(A) = \frac{2}{\sqrt{3}} \int_0^\infty dp \frac{\exp(-4p/3) I_0(2p/3)}{\sqrt{\cosh(\sqrt{4D_B T} \lambda p/a^2)}} \tag{93}$$

and

$$P(A) = \frac{2}{\sqrt{3}} \int_0^\infty dz \frac{J_0\left(\frac{(1+1/\sqrt{3})\sqrt{2Az}}{\sqrt{4D_B Tz/a^2}}\right) J_0\left(\frac{(1-1/\sqrt{3})\sqrt{2Az}}{\sqrt{4D_B Tz/a^2}}\right)}{\cosh(\sqrt{4D_B Tz/a^2})} \tag{94}$$

The series representation of $P(A)$ in (94) can be found directly by taking advantage of expansion (C.2) in appendix C and our result (56), to yield

$$P(A) = \frac{1}{2\sqrt{6\pi} D_B T} \sum_{n=0}^\infty \frac{(-1)^n \Gamma(n+1/2)}{(n+1/4)^2 n! (1+\xi_n)^{3/2}} {}_2F_1\left(\frac{3}{4}, \frac{5}{4}; 1; \frac{\xi_n^2}{4(1+\xi_n)^2}\right) \tag{95}$$

with

$$\xi_n = \frac{a^2 A}{3(n+1/4)^2 D_B T} \tag{96}$$

Note that the integrals

$$\int_0^\infty d\lambda \lambda^n \Upsilon(T; \lambda) \tag{97}$$

exist for any $n > 0$ and, hence, all negative moments of $\int_0^T dt B_t^2$ exist, as well. As a consequence, $P(A)$ is an analytic function of A . We immediately obtain the coefficient of variation from (25) as $\gamma = \sqrt{17}/2$. Figure 11 displays numerical results for which we observe excellent agreement with the theoretical expressions.

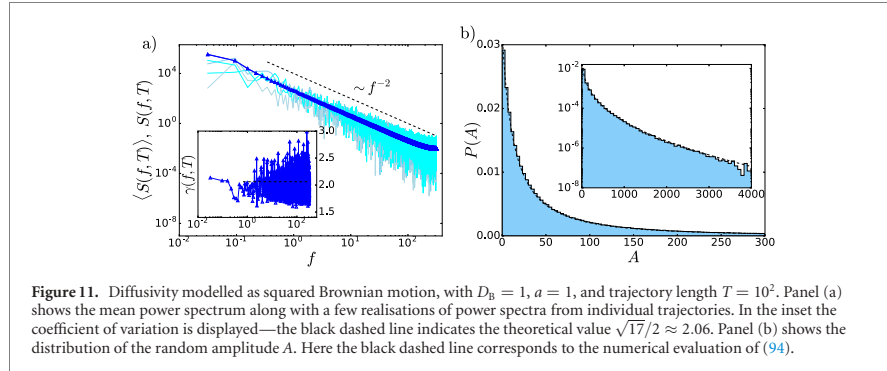


Figure 11. Diffusivity modelled as squared Brownian motion, with $D_B = 1$, $a = 1$, and trajectory length $T = 10^2$. Panel (a) shows the mean power spectrum along with a few realisations of power spectra from individual trajectories. In the inset the coefficient of variation is displayed—the black dashed line indicates the theoretical value $\sqrt{17}/2 \approx 2.06$. Panel (b) shows the distribution of the random amplitude A . Here the black dashed line corresponds to the numerical evaluation of (94).

Table 1. Collection of the main results for the different random-diffusivity models with respective equation numbers. Next to the definitions of the models we refer to the MGF of the integrated diffusivity τ_T , the coefficient of variation γ , which can play the role of an indicator for each model, and the ageing behaviour.

Random-diffusivity model	MGF of τ_T	γ	Ageing
$\Psi_t = Y_t^2, Y_t = \text{OU process}$	equation (30)	equation (31)	×
$\Psi_t = \psi_k$	$\rho(\psi)$ gamma distr.	equation (38)	×
	$\rho(\psi)$ Lévy–Smirnov distr.	equation (53)	not defined
$\Psi_t = V[B_t]$	$V[Z] = \theta(Z)$	equation (61)	$\sqrt{19/8}$
	$V[Z] = \exp(-Z)$	equation (78)	equation (83)
	$V[Z] = Z^2$	equation (86)	$\sqrt{17}/2$

7. Conclusions

Quite typically stochastic time series are evaluated in terms of the ensemble averaged MSD $\langle \overline{x_t^2} \rangle_\Psi$. It has the advantage that fluctuations are reduced due to the averaging over many individual trajectories. However, this is not always possible. Namely, for the by-now routine results from single particle tracking experiments typically rather few, finite time series are obtained. These are then evaluated in terms of the time-averaged MSD. While this quantity may also be averaged over the available individual trajectories, it is increasingly realised that the amplitude fluctuations between individual trajectories in fact harbours important quantitative information characteristic for a given stochastic process [14,15,115–117].

Similar to the consideration of time averaged MSDs for trajectories of finite measurement time T , we here analysed the single-trajectory PSD of stochastic trajectories characterised by random diffusivities. Following our previous work on standard Brownian motion [76], as well as fractional [77] and scaled Brownian motion [78], we here investigated the detailed behaviour of single-trajectory PSDs of a broad class of diffusing-diffusivity models. These have recently gained considerable attention as simple models for diffusion processes in heterogeneous media. We described a general procedure to obtain the position PDF $\Pi(x, t)$ for all such models. The main ingredient in the calculation is the MGF of the integrated diffusivity, showing explicitly that different choices of the underlying diffusivity Ψ_t lead to distinctly different emerging behaviours, as summarised in table 1.

We started our discussion from the by-now well-established and widely studied model of ‘diffusing-diffusivity’, namely the case when Ψ_t is chosen as the squared of the Ornstein–Uhlenbeck process. We then discussed the second case, in which Ψ_t is defined as a jump process. The properties of this model depend strongly on the exact distribution chosen for the increment variables. We considered two examples, a Gamma distribution and a Lévy–Smirnov distribution. Finally, three cases in which the diffusivity is modelled as a functional of Brownian motion were discussed.

The main result of this work is that, regardless of the different properties of all these diffusing-diffusivity models we obtained a universal high- f asymptote of the PSD. This behaviour is characterised by a $1/f^2$ scaling, in analogy to Brownian motion [76] and scaled Brownian motion [78]. A first way to discriminate among models lies in the study of the ageing behaviour of the PSD, as already discussed in [78]. Indeed, we showed that the dependence of the PSD on the trajectory length T appears only for those random-diffusivity models that are characterised by an anomalous scaling of the MSD. We also showed that

differences from one model to another appear in higher order moments. In particular, we obtained exact expressions for the coefficient of variation in all cases, proving that the latter can be a good indicator of the specific model (see table 1).

Finally, we established that the PDF of the random amplitude A carries most of the meaningful information. Namely, the coefficient of variation may be directly calculated from its moments. Moreover, its MGF is tightly related to that of the integrated diffusivity, thus reflecting the particular properties of the process Ψ_t . As we showed before [76,77], the distribution $P(A)$ can even be evaluated meaningfully from experimental data of fairly short trajectories. In its useful role in data analysis the single-trajectory PSD approach thus complements other methods such as the time-averaged MSD and its amplitude variation [14,115,118–124], ageing analyses [77,115], or, in the context of non-Gaussian diffusion, the codifference methods [125].

The role of distinguishing different physical processes from measured single trajectory data therefore heavily lies on the amplitude fluctuations and the coefficient of variation encoded in them. This improved understanding of the single-trajectory PSD should therefore replace a common claim in many textbooks according to which the $1/f^2$ -dependence of the spectrum was a fingerprint of Brownian motion. In line to previous works [76–78], in which we already alerted that this may be a deceptive concept, we have shown here that a wide range of random-diffusivity models with distinctly different behaviour and showing anomalous diffusion, exhibit precisely the $1/f^2$ -dependence. Therefore, any experimental observation of the spectral density varying as $1/f^2$ alone cannot be taken as proof of standard Brownian motion. One necessarily needs to consider the ageing behaviour of the spectral density, as in the case of superdiffusive fractional Brownian motion or scaled Brownian motion, evaluate the coefficient of variation of the spectral density, or determine the functional form of the PDF $P(A)$ of the amplitude fluctuations.

In light of this the relevance of the presented results is twofold. First, they provide new and useful insights into the increasingly popular class of stochastic processes with random diffusivity used in the description of Fickian yet non-Gaussian diffusion in heterogeneous systems. Second, the results continue our ongoing analysis based on the single-trajectory PSD for different classes of stochastic processes, showing in particular the persistence of the $1/f^2$ -scaling of the PSD, which appears to be robust—as long as we do not introduce correlations in the driving noise of the system, as studied in [77].

We note that if we redefine \dot{x}_t in the Langevin equation (3) as S_t/S_t , we recover the seminal Black–Scholes (or Black–Scholes–Merton) equation for an asset price S_t with zero-constant trend and stochastic volatility $\sqrt{D_0\Psi_t}$ used in financial market models [126–128]. The relevance of diffusing-diffusivity approaches to economic and financial modelling was also discussed for the case of the squared Ornstein–Uhlenbeck process [61]. Namely, the resulting stochastic equation for $D_0\Psi_t$ in this case is nothing else than the Heston model [83], a special class of the Cox–Ingersson–Ross model [82,129], and as such specifies the time evolution of the stochastic volatility of a given asset [63,83,130]. We note in this context that diffusing-diffusivity models are intimately related to random-coefficient autoregressive processes used in financial market analysis [131].

We finally note that realisation-to-realisation fluctuations of a stochastic process also turn out to be relevant in many scenarios of first-passage time statistics [132,133]. These fluctuations are connected to the typically broad (‘defocused’) PDFs of first-passage times even in simple geometries and the related feature of geometry-control [134–136]. It will be interesting to extend the existing first-passage time analyses of diffusing-diffusivity models [64,68] to the different processes studied herein, and to more complex geometries. In particular, given that for fractional Brownian motion the first-passage time distributions and the return-intervals distribution (the times between consecutive crossings of the diffusion process through a given level) have power-law exponents that are directly related to the scaling exponent of the power spectrum [137,138], one might speculate whether the corresponding distributions here are universal. However, the universal spectral behaviour predicted in this paper for a variety of random-diffusing models does not necessarily imply that the first-passage time properties will be the same for all the models. In fact, we expect that the first-passage time densities will exhibit different behaviours for the various models, to the same extent as the position PDFs unveiled here are significantly different from each other. The detailed analysis of the first-passage time properties of the new random-diffusivity models studied here constitutes one of the main directions of our future research.

Acknowledgments

VS is supported by the Basque Government through the BERC 2018-2021 program and by the Spanish Ministry of Economy and Competitiveness MINECO through BCAM Severo Ochoa accreditation SEV-2017-0718. FS acknowledges Padova University for support within grant PRD-BIRD191017. RM

acknowledges Deutsche Forschungsgemeinschaft (DFG) for support within grant ME 1535/7-1, as well as the Foundation for Polish Science (Fundacja na rzecz Nauki Polskiej, FNP) for an Alexander von Humboldt Polish Honorary Research Scholarship. We acknowledge the support of the Deutsche Forschungsgemeinschaft (German Research Foundation) and the Open Access Publication Fund of Potsdam University.

Appendix A. Derivation of the moment-generating function of the power spectral density

It is convenient to rewrite formally the definition of the PSD in (8) in the form

$$S_T(f) = \frac{1}{T} \left(\int_0^T dt \cos(ft) x_t \right)^2 + \frac{1}{T} \left(\int_0^T dt \sin(ft) x_t \right)^2. \quad (\text{A.1})$$

Our first step then consists in a standard linearisation of the expression in the exponential in (9). Taking advantage of the integral identity

$$\exp(-b^2/(4c)) = \sqrt{\frac{c}{\pi}} \int_{-\infty}^{\infty} dz \exp(-cz^2 + ibz) \quad (\text{A.2})$$

for $c > 0$, we formally recast (9) into the form

$$\phi_\lambda = \frac{1}{4\pi\lambda} \int_{-\infty}^{\infty} dz_1 \int_{-\infty}^{\infty} dz_2 \exp\left(-\frac{z_1^2 + z_2^2}{4\lambda}\right) \left\langle \overline{\exp\left(i \int_0^T dt Q_t x_t\right)} \right\rangle_\Psi, \quad (\text{A.3})$$

where Q_t is defined in (11). Now, the averaging over thermal noise realisations can be performed straightforwardly, yielding

$$\begin{aligned} \overline{\exp\left(i \int_0^T dt Q_t x_t\right)} &= \overline{\exp\left(i \sqrt{2D_0} \int_0^T dt \sqrt{\Psi_t} \xi_t \int_t^T d\tau Q_\tau\right)} \\ &= \exp\left(-D_0 \int_0^T dt \Psi_t \left(\int_t^T d\tau Q_\tau\right)^2\right), \end{aligned} \quad (\text{A.4})$$

where we integrated by parts and used (3). Combining (A.3) and (A.4) we arrive at our general result (10).

The derivation of our main result (13) takes advantage of the explicit form of Q in (11) and the following calculation,

$$\begin{aligned} \int_0^T dt \Psi_t \left(\int_t^T d\tau Q_\tau\right)^2 &= \frac{z_1^2}{f^2 T} \int_0^T dt \Psi_t (\sin(fT) - \sin(ft))^2 + \frac{z_2^2}{f^2 T} \int_0^T dt \Psi_t (\cos(ft) - \cos(fT))^2 \\ &\quad + \frac{2z_1 z_2}{f^2 T} \int_0^T dt \Psi_t (\sin(fT) - \sin(ft)) (\cos(ft) - \cos(fT)). \end{aligned} \quad (\text{A.5})$$

Inserting the latter expression into (10) and performing the integrations over z_1 and z_2 we find the expression in (13) with $L_f(t_1, t_2)$ explicitly defined by

$$\begin{aligned} L_f(t_1, t_2) &= \frac{1}{2} \cos(2ft_2) - \frac{1}{2} \cos(2ft_1) - \frac{1}{2} \cos(f(T-t_1)) - \frac{1}{2} \cos(f(T-t_2)) - \frac{1}{4} \cos(2f(T-t_1)) \\ &\quad - \frac{1}{2} \cos(2f(T-t_2)) + \frac{1}{4} \cos(f(3T-t_2)) - \frac{1}{4} \cos(f(3T-t_1)) + \frac{3}{4} \cos(f(T+t_1)) - \frac{3}{4} \cos(f(T+t_2)) \\ &\quad - \frac{1}{2} \cos(f(t_1-t_2)) - \frac{1}{4} \cos(2f(t_1-t_2)) + \frac{1}{4} \cos(f(T-2t_1-t_2)) - \frac{1}{4} \cos(f(T-t_1-2t_2)) \\ &\quad + \frac{1}{2} \cos(f(T+t_1-2t_2)) + \frac{1}{2} \cos(f(T-2t_1+t_2)) + \frac{1}{4} \cos(f(T+2t_1-t_2)) \\ &\quad - \frac{1}{4} \cos(f(T-t_1+2t_2)) + \frac{1}{2} \cos(f(2T-t_1-t_2)) - \frac{1}{2} \cos(f(2T+t_1-t_2)) \\ &\quad + \frac{1}{2} \cos(f(2T-t_1+t_2)). \end{aligned} \quad (\text{A.6})$$

Appendix B. High- f behaviour of the Riemann-integrable diffusivities

For Riemann-integrable functions, according to the Riemann–Lebesgue lemma we have

$$\lim_{f \rightarrow \infty} \int_0^T dt \Psi_t \cos(f(T-t)) = 0 \quad (\text{B.1})$$

with probability 1 (however, nothing can be said about how fast zero is approached in the general case).

Once (B.1) holds, one finds that for $L_f(t_1, t_2)$ defined in (A.6),

$$\lim_{f \rightarrow \infty} \int_0^T dt_1 \Psi_{t_1} \int_0^T dt_2 \Psi_{t_2} L_f(t_1, t_2) = 0. \quad (\text{B.2})$$

Appendix C. Useful formulae

Our expression for the PDF $P(A)$ in (26) and (27) rely on the following series expansion of the product of two Bessel functions,

$$J_0\left(\left(1 + \frac{1}{\sqrt{3}}\right)\sqrt{2zA}\right) J_0\left(\left(1 - \frac{1}{\sqrt{3}}\right)\sqrt{2zA}\right) = \sum_{n=0}^{\infty} \frac{(-1)^n}{(n!)^2} \left(\frac{\sqrt{3}+1}{\sqrt{6}}\right)^{2n} {}_2F_1\left(-n, -n; 1; \frac{1-\sqrt{3}/2}{1+\sqrt{3}/2}\right) (zA)^n. \quad (\text{C.1})$$

The form of the PDF in (95) stems from the expansion

$$\frac{1}{\sqrt{\cosh\left(\sqrt{4D_B Tz/a^2}\right)}} = \sqrt{2} \sum_{n=0}^{\infty} \binom{-1/2}{n} \exp\left(-2\sqrt{\frac{D_B Tz}{a^2}} \left(2n + \frac{1}{2}\right)\right). \quad (\text{C.2})$$

The result in (69) involves toroidal functions defined by

$$P_{n-1/2}(\cosh(\eta)) = \frac{2}{\pi} e^{-(n+1/2)\eta} \int_0^{\pi/2} \frac{d\phi}{(1 - 2e^{-\eta} \sinh(\eta) \sin^2(\phi))^{n+1/2}}. \quad (\text{C.3})$$

Setting $\exp(-\eta)\sinh(\eta) = 1/3$, i.e., $\eta = \ln(\sqrt{3})$, we obtain expression (69).

ORCID iDs

Vittoria Sposini  <https://orcid.org/0000-0003-0915-4746>

Denis S Grebenkov  <https://orcid.org/0000-0002-6273-9164>

Ralf Metzler  <https://orcid.org/0000-0002-6013-7020>

Gleb Oshanin  <https://orcid.org/0000-0001-8467-3226>

References

- [1] Brown R 1828 A brief account of microscopical observations made in the months of June, July and August 1827, on the particles contained in the pollen of plants; and on the general existence of active molecules in organic and inorganic bodies *Philos. Mag.* **4** 161
- [2] Fick A 1855 Über Diffusion (On diffusion) *Ann. Phys.* **170** 59
- [3] Einstein A 1905 Über die von der molekularkinetischen Theorie der Wärme geforderte Bewegung von in ruhenden Flüssigkeiten suspendierten Teilchen (On the motion of small particles suspended in liquids at rest required by the molecular-kinetic theory of heat) *Ann. Phys.* **322** 549
- [4] von Smoluchowski M 1906 Zur kinetischen Theorie der Brownschen molekularenbewegung und der Suspensionen (On the kinetic theory of Brownian molecular motion and suspensions) *Ann. Phys.* **21** 756
- [5] Sutherland W 1905 A dynamical theory of diffusion for non-electrolytes and the molecular mass of albumin *Philos. Mag.* **9** 781
- [6] Pearson K 1905 The problem of the random walk *Nature* **72** 294
- [7] Langevin P 1908 On the theory of Brownian motion *C. R. Acad. Sci. Paris* **146** 530
- [8] Höfling F and Franosch T 2013 Anomalous transport in the crowded world of biological cells *Rep. Prog. Phys.* **76** 046602
- [9] Nørregaard K, Metzler R, Ritter C M, Berg-Sørensen K and Oddershede L B 2017 Manipulation and motion of organelles and single molecules in living cells *Chem. Rev.* **117** 4342
- [10] Xie X S, Choi P J, Li G-W, Lee N K and Lia G 2008 Single-molecule approach to molecular biology in living bacterial cells *Annu. Rev. Biophys.* **37** 417
- [11] Bräuchle C, Lamb D C and Michaelis J 2012 *Single Particle Tracking and Single Molecule Energy Transfer* (New York: Wiley)
- [12] Javanainen M, Martinez-Seara H, Metzler R and Vattulainen I 2017 Diffusion of integral membrane proteins in protein-rich membranes *J. Phys. Chem. Lett.* **8** 4308

- [13] Hu X, Hong L, Smith M D, Neusius T, Cheng X and Smith J C 2016 The dynamics of single protein molecules is non-equilibrium and self-similar over thirteen decades in time *Nat. Phys.* **12** 171
- [14] Barkai E, Garini Y and Metzler R 2012 Strange kinetics of single molecules in living cells *Phys. Today* **65** 29
- [15] Krapf D and Metzler R 2019 Strange interfacial molecular dynamics *Phys. Today* **72** 48
- [16] Metzler R 2019 Brownian motion and beyond: first-passage, power spectrum, non-Gaussianity, and anomalous diffusion *J. Stat. Mech.: Theor. Exp.* **2019** 114003
- [17] Klafter J, Shlesinger M F and Zumofen G 1996 Beyond Brownian Motion *Phys. Today* **49** 33
- [18] Shlesinger M, Zaslavsky G and Klafter J 1993 Strange kinetics *Nature* **363** 31
- [19] Scher H, Shlesinger M F and Bendler J T 1991 Time-scale invariance in transport and relaxation *Phys. Today* **44** 26
- [20] Saxton M J and Jacobsen K 1997 Single-particle tracking: applications to membrane dynamics *Annu. Rev. Biophys. Biomol. Struct.* **26** 373
- [21] Golding I and Cox E C 2006 Physical nature of bacterial cytoplasm *Phys. Rev. Lett.* **96** 098102
- [22] Weber S C, Spakowitz A J and Theriot J A 2010 Bacterial chromosomal loci move subdiffusively through a viscoelastic cytoplasm *Phys. Rev. Lett.* **104** 238102
- [23] Burnecki K, Kepten E, Janczura J, Bronshtein I, Garini Y and Weron A 2012 Universal algorithm for identification of fractional Brownian motion. A case of telomere subdiffusion *Biophys. J.* **103** 1839
- [24] Bronstein I, Israel Y and Garini Y 2009 Transient anomalous diffusion of telomeres in the nucleus of mammalian cells *Phys. Rev. Lett.* **103** 018102
- [25] Jeon J-H, Tejedor V, Burov S, Barkai E, Selhuber-Unkel C, Berg-Sorensen K, Oddershede L and Metzler R 2011 *In vivo* anomalous diffusion and weak ergodicity breaking of lipid granules *Phys. Rev. Lett.* **106** 048103
- [26] Bertseva E, Grebenkov D S, Schmidhauser P, Gribkova S, Jeney S and Forro L 2012 Optical trapping microrheology in cultured human cells *Eur. Phys. J. E* **35** 63
- [27] Weigel A V, Simon B, Tamkun M M and Krapf D 2011 Ergodic and nonergodic processes coexist in the plasma membrane as observed by single-molecule tracking *Proc. Natl. Acad. Sci.* **108** 6438
- [28] Manzo C, Torreno-Pina J A, Massignon P, Lapeyre G J Jr, Lewenstein M and Garcia Parajo M F 2015 Weak ergodicity breaking of receptor motion in living cells stemming from random diffusivity *Phys. Rev. X* **5** 011021
- [29] Szymanski J and Weiss M 2009 Elucidating the origin of anomalous diffusion in crowded fluids *Phys. Rev. Lett.* **103** 038102
- [30] Jeon J-H, Leijne N, Oddershede L B and Metzler R 2013 Anomalous diffusion and power-law relaxation in wormlike micellar solution *New J. Phys.* **15** 045011
- [31] Di Rienzo C, Piazza V, Gratton E, Beltram F and Cardarelli F 2014 Probing short-range protein Brownian motion in the cytoplasm of living cells *Nat. Commun.* **5** 5891
- [32] Chen K, Wang B and Granick S 2015 Memoryless self-reinforcing directionality in endosomal active transport within living cells *Nat. Mater.* **14** 589
- [33] Robert D, Nguyen T H, Gallet F and Wilhelm C 2010 *In vivo* determination of fluctuating forces during endosome trafficking using a combination of active and passive microrheology *PLoS One* **4** e10046
- [34] Caspi A, Granek R and Elbaum M 2000 Enhanced diffusion in active intracellular transport *Phys. Rev. Lett.* **85** 5655
- [35] Song M S, Moon H C, Jeon J-H and Park H Y 2018 Neuronal messenger ribonucleoprotein transport follows an aging Lévy walk *Nat. Commun.* **9** 344
- [36] Revery J F, Jeon J-H, Bao H, Leippe M, Metzler R and Selhuber-Unkel C 2015 Superdiffusion dominates intracellular particle motion in the supercrowded space of pathogenic *Acanthamoeba castellanii* *Sci. Rep.* **5** 11690
- [37] Wang B, Kuo J, Bae S C and Granick S 2012 When Brownian diffusion is not Gaussian *Nat. Mater.* **11** 481
- [38] Wang B, Anthony S M, Bae S C and Granick S 2009 Anomalous yet Brownian *Proc. Natl. Acad. Sci.* **106** 15160
- [39] Guan J, Wang B and Granick S 2014 Single-molecule observation of long jumps in polymer adsorption *ACS Nano* **8** 3331
- [40] He K, Khorasani F B, Retterer S T, Tjomasn D K, Conrad J C and Krishnamoorti R 2013 Diffusive dynamics of nanoparticles in arrays of nanoposts *ACS Nano* **7** 5122
- [41] Xue C, Zheng X, Chen K, Tian Y and Hu G 2016 Probing non-Gaussianity in confined diffusion of nanoparticles *J. Phys. Chem. Lett.* **7** 514
- [42] Wang D, Hu R, Skaug M J and Schwartz D 2015 Temporally anticorrelated motion of nanoparticles at a liquid interface *J. Phys. Chem. Lett.* **6** 54
- [43] Dutta S and Chakrabarti J 2016 Anomalous dynamical responses in a driven system *Europhys. Lett.* **116** 38001
- [44] Leptos K C, Guasto J S, Gollub J P, Pesci A I and Goldstein R E 2009 Dynamics of enhanced tracer diffusion in suspensions of swimming eukaryotic microorganisms *Phys. Rev. Lett.* **103** 198103
- [45] Hapca S, Crawford J W and Young I M 2009 Anomalous diffusion of heterogeneous populations characterized by normal diffusion at the individual level *J. R. Soc. Interface* **6** 111
- [46] Witzel P, Götz M, Lanoiselée Y, Franosch T, Grebenkov D S and Heinrich D 2019 Heterogeneities shape passive intracellular transport *Biophys. J.* **117** 203
- [47] Cherstvy A G, Nagel O, Beta C and Metzler R 2018 Non-Gaussianity, population heterogeneity, and transient superdiffusion in the spreading dynamics of amoeboid cells *Phys. Chem. Chem. Phys.* **20** 23034
- [48] Jeon J-H, Javanainen M, Martinez-Seara H, Metzler R and Vattulainen I 2016 Protein crowding in lipid bilayers gives rise to non-Gaussian anomalous lateral diffusion of phospholipids and proteins *Phys. Rev. X* **6** 021006
- [49] Beck C and Cohen E G D 2003 Superstatistics *Phys. A* **332** 267
- [50] Beck C 2007 Statistics of three-dimensional Lagrangian turbulence *Phys. Rev. Lett.* **98** 064502
- [51] Beck C 2006 Stretched exponentials from superstatistics *Phys. A* **365** 96
- [52] van der Straeten E and Beck C 2009 Superstatistical fluctuations in time series: applications to share-price dynamics and turbulence *Phys. Rev. E* **80** 036108
- [53] Metzler R 2020 Superstatistics and non-Gaussian diffusion *Eur. Phys. J. Spec. Top.* **229** 711–28
- [54] Baldovin F, Orlandini E and Seno F 2019 Polymerization induces non-Gaussian diffusion *Front. Phys.* **7** 124
- [55] Mura A, Taqqu M S and Mainardi F 2008 Non-Markovian diffusion equations and processes: analysis and simulations *Phys. A* **387** 5033
- [56] Mura A and Pagnini G 2008 Characterizations and simulations of a class of stochastic processes to model anomalous diffusion *J. Phys. A* **41** 285003
- [57] Molina-García D, Minh Pham T, Paradisi P, Manzo C and Pagnini G 2016 Fractional kinetics emerging from ergodicity breaking in random media *Phys. Rev. E* **94** 052147

- [58] Chubynsky M V and Slater G W 2014 Diffusing diffusivity: a model for anomalous, yet Brownian, diffusion *Phys. Rev. Lett.* **113** 098302
- [59] Jain R and Sebastian K L 2016 Diffusion in a crowded, rearranging environment *J. Phys. Chem. B* **120** 3988
- [60] Jain R and Sebastian K L 2016 Diffusing diffusivity: survival in a crowded rearranging and bounded domain *J. Phys. Chem. B* **120** 9215
- [61] Chechkin A V, Seno F, Metzler R and Sokolov I M 2017 Brownian yet non-Gaussian diffusion: from superstatistics to subordination of diffusing diffusivities *Phys. Rev. X* **7** 021002
- [62] Tyagi N and Cherayil B J 2017 Non-Gaussian Brownian diffusion in dynamically disordered thermal environments *J. Phys. Chem. B* **121** 7204
- [63] Lanoiselée Y and Grebenkov D S 2018 A model of non-Gaussian diffusion in heterogeneous media *J. Phys. A* **51** 145602
- [64] Lanoiselée Y, Moutal N and Grebenkov D S 2018 Diffusion-limited reactions in dynamic heterogeneous media *Nat. Commun.* **9** 4398
- [65] Sposini V, Chechkin A V, Seno F, Pagnini G and Metzler R 2018 Random diffusivity from stochastic equations: comparison of two models for Brownian yet non-Gaussian diffusion *New J. Phys.* **20** 043044
- [66] Grebenkov D S 2019 A unifying approach to first-passage time distributions in diffusing diffusivity and switching diffusion models *J. Phys. A* **52** 174001
- [67] Lanoiselée Y and Grebenkov D S 2019 Non-Gaussian diffusion of mixed origins *J. Phys. A* **52** 304001
- [68] Sposini V, Chechkin A V and Metzler R 2019 First passage statistics for diffusing diffusivity *J. Phys. A* **52** 04LT01
- [69] Hidalgo-Soria M and Barkai E 2019 The Hitchhiker model for Laplace diffusion processes in the cell environment arXiv:1909.07189
- [70] Chakraborty I and Roichman Y 2019 Two coupled mechanisms produce Fickian, yet non-Gaussian diffusion in heterogeneous media arXiv:1909.11364
- [71] Shephard N 2010 Stochastic volatility models *Macroeconomics and Time Series Analysis. The New Palgrave Economics Collection* ed S N Durlauf and L E Blume (London: Palgrave Macmillan)
- [72] Barndorff-Nielsen O and Shephard N 2001 Non-Gaussian OU based models and some of their uses in financial economics *J. R. Stat. Soc. B* **63** 167–241
- [73] Sadegh S, Barkai E and Krapf D 2014 $1/f$ noise for intermittent quantum dots exhibits non-stationarity and critical exponents *New J. Phys.* **16** 113054
- [74] Leibovich N, Dechant A, Lutz E and Barkai E 2016 Aging Wiener–Khinchin theorem and critical exponents of $1/f$ noise *Phys. Rev. E* **94** 052130
- [75] Leibovich N and Barkai E 2017 Conditional $1/f^\alpha$ noise: from single molecules to macroscopic measurement *Phys. Rev. E* **96** 032132
- [76] Krapf D, Marinari E, Metzler R, Oshanin G, Xu X and Squarcini A 2018 Power spectral density of a single Brownian trajectory: what one can and cannot learn from it *New J. Phys.* **20** 023029
- [77] Krapf D et al 2019 Spectral content of a single non-brownian trajectory *Phys. Rev. X* **9** 011019
- [78] Sposini V, Metzler R and Oshanin G 2019 Single-trajectory spectral analysis of scaled Brownian motion *New J. Phys.* **21** 073043
- [79] Lim S C and Muniandy S V 2002 Self-similar Gaussian processes for modeling anomalous diffusion *Phys. Rev. E* **66** 021114
- [80] Jeon J-H, Chechkin A V and Metzler R 2014 Scaled Brownian motion: a paradoxical process with a time dependent diffusivity for the description of anomalous diffusion *Phys. Chem. Chem. Phys.* **16** 15811
- [81] Feller W 1951 Two singular diffusion problems *Ann. Math.* **54** 173
- [82] Cox J C, Ingersoll J E and Ross S A 1985 A theory of the term structure of interest rates *Econometrica* **53** 385
- [83] Heston S L 1993 A closed-form solution for options with stochastic volatility with applications to bond and currency options *Rev. Financ. Stud.* **6** 327
- [84] Dankel T 1991 On the distribution of the integrated square of the Ornstein–Uhlenbeck process *SIAM J. Appl. Math.* **5** 568
- [85] Tejedor V and Metzler R 2010 Anomalous diffusion in correlated continuous time random walks *J. Phys. A* **43** 082002
- [86] Magdziarz M, Metzler R, Szczotka W and Zebrowski P 2012 Correlated continuous-time random walks—scaling limits and Langevin picture *J. Stat. Mech.* **2012** P04010
- [87] Lévy P 1940 Sur certains processus stochastiques homogènes (On certain homogeneous stochastic processes) *Compos. Math.* **7** 283
- [88] Cameron R H and Martin W T 1945 Transformations of Wiener integrals under a general class of linear transformation *Trans. Am. Math. Soc.* **58** 184
- [89] Cameron R H and Martin W T 1945 Evaluation of various Wiener integrals by use of certain Sturm–Liouville differential equations *Bull. Am. Math. Soc.* **51** 73
- [90] Kac M 1949 On distributions of certain Wiener functionals *Trans. Am. Math. Soc.* **65** 1
- [91] Erdős P and Kac M 1947 On the number of positive sums of independent random variables *Bull. Am. Math. Soc.* **53** 1011
- [92] Lamperti J 1958 An occupation time theorem for a class of stochastic processes *Trans. Am. Math. Soc.* **88** 380
- [93] Yor M 2000 *Exponential Functionals of Brownian Motion and Related Processes* (Berlin: Springer)
- [94] Majumdar S N 2005 Brownian functionals in physics and computer science *Curr. Sci.* **89** 2076
- [95] Perret A, Comtet A, Majumdar S N and Schehr G 2015 On certain functionals of the maximum of brownian motion and their applications *J. Stat. Phys.* **161** 1112
- [96] Boyer D, Dean D S, Mejia-Monasterio C and Oshanin G 2013 Distribution of the least-squares estimators of a single Brownian trajectory diffusion coefficient *J. Stat. Mech.* **2013** P04017
- [97] Boyer D, Dean D S, Mejia-Monasterio C and Oshanin G 2012 Optimal estimates of the diffusion coefficient of a single Brownian trajectory *Phys. Rev. E* **85** 031136
- [98] Borodin A N and Salminen P 1996 *Handbook of Brownian Motion: Facts and Formulae* (Basel: Birkhäuser)
- [99] Arkhincheev V E and Baskin E M 1991 Anomalous diffusion and drift in a comb model of percolation clusters *Sov. Phys. JETP* **73** 161
- [100] Sandev T, Iomin A, Kantz H, Metzler R and Chechkin A 2016 Comb model with slow and Ultraslow diffusion *Math. Model. Nat. Phenom.* **11** 18
- [101] Lévy P 1939 Sur certains processus stochastiques homogènes *Compos. Math.* **7** 283
- [102] Geman H and Yor M 1993 Bessel processes, asian options, and perpetuities *Math. Finance* **3** 349
- [103] Wilmott P, Dewynne J and Howison S 2000 *Option Pricing: Mathematical Models and Computation* (Oxford: Oxford Financial Press)

- [104] Oshanin G and Schehr G 2012 Two stock options at the races: Black–Scholes forecasts *Quant. Finance* **12** 1325
- [105] Peters O and Klein W 2013 Ergodicity breaking in geometric Brownian motion *Phys. Rev. Lett.* **110** 100603
- [106] Cherstvy A G, Vinod D, Aghion E, Chechkin A V and Metzler R 2017 Time averaging, ageing and delay analysis of financial time series *New J. Phys.* **19** 063045
- [107] Burlatsky S F, Oshanin G, Mogutov A and Moreau M 1992 Non-Fickian steady flux in a one-dimensional Sinai-type disordered system *Phys. Rev. A* **45** R6955
- [108] Oshanin G, Mogutov A and Moreau M 1993 Steady flux in a continuous-space Sinai chain *J. Stat. Phys.* **73** 379
- [109] Monthus C and Comtet A 1994 On the flux distribution in a one dimensional disordered system *J. Phys. I.* **4** 635
- [110] Comtet A, Monthus C and Yor M 1998 Exponential functionals of Brownian motion and disordered systems *J. Appl. Probab.* **35** 255
- [111] Oshanin G, Rosso A and Schehr G 2013 Anomalous fluctuations of currents in Sinai-type random chains with strongly correlated disorder *Phys. Rev. Lett.* **110** 100602
- [112] Cherstvy A G, Chechkin A V and Metzler R 2013 Anomalous diffusion and ergodicity breaking in heterogeneous diffusion processes *New J. Phys.* **15** 083039
- [113] Cherstvy A G and Metzler R 2014 Non-ergodicity, fluctuations, and criticality in heterogeneous diffusion processes *Phys. Rev. E* **90** 012134
- [114] Oshanin G and Redner S 2009 Helix or coil? Fate of a melting heteropolymer *Europhys. Lett.* **85** 10008
- [115] Metzler R, Jeon J-H, Cherstvy A G and Barkai E 2014 Anomalous diffusion models and their properties: non-stationarity, non-ergodicity, and ageing at the centenary of single particle tracking *Phys. Chem. Chem. Phys.* **16** 24128
- [116] Stefani F D, Hoogenboom J P and Barkai E 2009 Beyond quantum jumps: blinking nanoscale light emitters *Phys. Today* **62** 34
- [117] Lanoiselée Y and Grebenkov D S 2016 Revealing nonergodic dynamics in living cells from a single particle trajectory *Phys. Rev. E* **93** 052146
- [118] Weron A, Janczura J, Boryczka E, Sungkaworn T and Calebiro D 2019 Statistical testing approach for fractional anomalous diffusion classification *Phys. Rev. E* **99** 042149
- [119] Bo S, Schmidt F, Eichhorn R and Volpe G 2019 Measurement of anomalous diffusion using recurrent neural networks *Phys. Rev. E* **100** 010102
- [120] Thapa S, Lomholt M A, Krog J, Cherstvy A G and Metzler R 2018 Bayesian nested sampling analysis of single particle tracking data: maximum likelihood model selection applied to stochastic diffusivity data *Phys. Chem. Chem. Phys.* **20** 29018
- [121] Cherstvy A G, Thapa S, Wagner C E and Metzler R 2019 Non-Gaussian, non-ergodic, and non-Fickian diffusion of tracers in mucin hydrogels *Soft Matter* **15** 2526
- [122] Jeon J-H and Metzler R 2010 Analysis of short subdiffusive time series: scatter of the time averaged mean squared displacement *J. Phys. A* **43** 252001
- [123] Grebenkov D S 2011 Probability distribution of the time-averaged mean-square displacement of a Gaussian process *Phys. Rev. E* **84** 031124
- [124] Andrianov A and Grebenkov D S 2012 Time-averaged MSD of Brownian motion *J. Stat. Mech.* **2012** P07001
- [125] Ślęzak J, Metzler R and Magdziarz M 2019 Codifference can detect ergodicity breaking and non-Gaussianity *New J. Phys.* **21** 053008
- [126] Black F and Scholes M 1973 The pricing of options and corporate liabilities *J. Polit. Econ.* **81** 637
- [127] Merton R C 1971 Optimum consumption and portfolio rules in a continuous-time model *J. Econ. Theor.* **3** 373
- [128] Merton R C 1976 Option pricing when underlying stock returns are discontinuous *J. Financ. Econ.* **3** 125
- [129] Cox J C and Ross S A 1976 The valuation of options for alternative stochastic processes *J. Financ. Econom.* **3** 145
- [130] Dragulescu A A and Yakovenko V M 2002 Probability distribution of returns in the Heston model with stochastic volatility *Quant. Finance* **2** 443
- [131] Ślęzak J, Burnecki K and Metzler R 2019 Random coefficient autoregressive processes describe Brownian yet non-Gaussian diffusion in heterogeneous systems *New J. Phys.* **21** 073056
- [132] Mejía-Monasterio C, Oshanin G and Schehr G 2011 First passages for a search by a swarm of independent random searchers *J. Stat. Mech.* **2011** P06022
- [133] Mattos T, Mejía-Monasterio C, Metzler R and Oshanin G 2012 First passages in bounded domains: When is the mean first passage time meaningful? *Phys. Rev. E* **86** 031143
- [134] Pulkkinen O and Metzler R 2013 Distance matters: the impact of gene proximity in bacterial gene regulation *Phys. Rev. Lett.* **110** 198101
- [135] Godec A and Metzler R 2016 Universal proximity effect in target search kinetics in the few encounter limit *Phys. Rev. X* **6** 041037
- [136] Grebenkov D, Metzler R and Oshanin G 2018 Strong defocusing of molecular reaction times: geometry and reaction control *Commun. Chem.* **1** 96
- [137] Carretero-Campos C, Bernaola-Galván P, Ivanov P C and Carpena P 2012 Phase transitions in the first-passage time of scale-invariant correlated processes *Phys. Rev. E* **85** 011139
- [138] Carpena P, Coronado A V, Carretero-Campos C, Bernaola-Galvan P and Ivanov P C 2015 First-passage time properties of correlated time series with scale-invariant behavior and with crossovers in the scaling *Time Series Analysis and Forecasting* ed I Rojas and H S Pomares (Berlin: Springer)

Bibliography

- [1] Brown R 1828 A brief account of microscopical observations made on the particles contained in the pollen of plants *Phil. Mag.* **4**, 161.
- [2] Fick A 1855 On liquid diffusion *Ann. Phys. (Leipzig)* **94**, 59. Reprinted in: Fick A 1995 On liquid diffusion *J. Membr. Sci.* **100**, 33.
- [3] Perrin J 1908 L'agitation moléculaire et le mouvement brownien *Compt. Rend.* **146** 967.
Perrin J 1909 Mouvement brownien et réalité moléculaire *Ann. Chim. Phys.* **18**, 5.
- [4] Nordlund I 1914 A new determination of Avogadro's number from Brownian motion of small mercury spherules *Z. Phys. Chem.* **87**, 40.
- [5] Kappler E 1931 Versuche zur Messung der Avogadro-Loschmidtschen Zahl aus der Brownschen Bewegung einer Drehwaage *Ann. Phys. (Leipzig)* **11**, 233.
- [6] Einstein A 1905 Über die von der molekularkinetischen Theorie der Wärme geforderte Bewegung von in ruhenden Flüssigkeiten suspendierten Teilchen *Ann. Phys.* **322**, 549.
- [7] Sutherland W 1905 A dynamical theory of diffusion for non-electrolytes and the molecular mass of albumin *Phil. Mag.* **9**, 781.
- [8] von Smoluchowski M 1906 Zur kinetischen Theorie der Brownschen Molekularbewegung und der Suspensionen *Ann. Phys.* **21**, 756.
- [9] Langevin P 1908 Sur la théorie de mouvement brownien *C.R. Hebd. Seances Acad. Sci.* **146**, 530.
- [10] van Kampen N G 1981 Stochastic processes in physics and chemistry (North Holland Publishing Company, Amsterdam).
- [11] Kärger J 1985 NMR self-diffusion studies in heterogenous systems *Adv. Colloid Interface Sci.* **23**, 129.

- [12] Mandelbrot B B & van Ness J W 1968, Fractional Brownian motions, fractional noises and applications *SIAM Review* **10**, 422.
- [13] Qian H 2003 *in Processes with long-range correlations: theory and applications*, edited by Rangarajan G & Ding M (Springer, Berlin, Heidelberg), 22.
- [14] Zwanzig R 2001 Nonequilibrium statistical mechanics (Oxford University Press, Oxford).
- [15] Hänggi P 1978 Correlation functions and master equations of generalized (non-Markovian) Langevin equations *Z. Phys. B* **31**, 407.
- [16] Goychuk I 2012 Viscoelastic subdiffusion: generalized Langevin equation approach *in Advances in Chemical Physics (John Wiley & Sons, Ltd)*, 187.
- [17] Metzler R & Klafter J 2004 The restaurant at the end of the random walk: recent developments in the description of anomalous transport by fractional dynamics *J. Phys. A* **37**, R161.
- [18] Wang B, Antony S M, Bae S C & Granick S 2009 Anomalous yet Brownian *Proc. Nat. Acad. Sci. U.S.A.* **106**, 15160.
- [19] Wang B, Kuo J, Bae S C & Granick S 2012 When Brownian diffusion is not Gaussian *Nat. Mater.* **11**, 481.
- [20] Leptos K C, Guasto J S, Gollub J P, Pesci A I & Goldstein R E 2009 Dynamics of enhanced tracer diffusion in suspensions of swimming eukaryotic microorganisms *Phys. Rev. Lett.* **103**, 198103.
- [21] Xue C, Zheng X, Chen K, Tian Y & Hu G 2016 Probing Non-Gaussianity in confined diffusion of nanoparticles *J. Phys. Chem. Lett.* **7**, 514.
- [22] Wang D, Hu R, Skaug M J & Schwartz D K 2015 Temporally anticorrelated motion of nanoparticles at a liquid Interface *J. Phys. Chem. Lett.* **6**, 54.
- [23] Dutta S & Chakrabarti J 2016 Anomalous dynamical responses in a driven system *EPL* **116**, 38001.
- [24] Hapca S, Crawford J W & Young I M 2009 Anomalous diffusion of heterogeneous populations characterized by normal diffusion at the individual level *J. R. Soc. Interface* **6**, 111.
- [25] Kob W & Andersen H C 1995 Testing mode-coupling theory for a supercooled binary Leonard-Jones mixture: the van Hove correlation function *Phys. Rev. E* **51**, 4626.

- [26] Chaudhuri P, Berthier L & Kob W 2007 Universal nature of particle displacements close to glass and jamming transitions *Phys. Rev. Lett.* **99**, 060604.
- [27] R-Vargas S, Rovigatti L & Sciortino F 2017 Connectivity, dynamics, and structure in a tetrahedral network liquid *Soft Matt.* **13**, 514.
- [28] Samanta N & Chakrabarti R 2016 Tracer diffusion in a sea of polymers with binding zones: mobile vs. frozen traps *Soft Matter* **12**, 8554.
- [29] Skaug M J, Wang L, Ding Y & Schwartz D K 2015 Hindered nanoparticle diffusion and void accessibility in a three-dimensional porous medium *ACS Nano* **9**, 2148.
- [30] Stuhrmann B, Soares e Silva M, Depken M, Mackintosh F C & Koenderink G H 2012 Nonequilibrium fluctuations of a remodeling in vitro cytoskeleton *Phys. Rev. E* **86**, 020901.
- [31] Lampo T, Stylianido S, Backlund M P, Wiggins P A & Spakowitz A J 2017 Cytoplasmic RNA-protein particles exhibit non-Gaussian subdiffusive behaviour *Biophys. J.* **112**, 532.
- [32] Soares de Silva M, Stuhrmann B, Betz T & Koenderink G H 2014 Time-resolved microrheology of actively remodeling actomyosin networks *New J. Phys.* **16**, 075010.
- [33] Jeon J-H, Javanainen M, Martinez-Seara H, Metzler R & Vattulainen I 2016 Protein crowding in lipid bilayers gives rise to non-Gaussian anomalous lateral diffusion of phospholipids and proteins *Phys. Rev. X* **6**, 021006.
- [34] Cox J C, Ingersoll J E & Ross S A 1985 A theory of the term structure of interest rates, *Econometrica* **53**, 385.
- [35] Heston S L 1993 A Closed-form solution for options with stochastic volatility with applications to bond and currency options *Rev. Financ. Stud.* **6**, 327.
- [36] Barndorff-Nielsen O & Shephard N Non-Gaussian OU based models and some of their uses in financial economics *J. R. Stat. Soc. B* **63**, 167.
- [37] Shephard N 2010 Stochastic volatility models. *In: S. N. Durlauf, L.E. Blume (eds) Macroeconometrics and Time Series Analysis.* The New Palgrave Economics Collection. Palgrave Macmillan, London.
- [38] El Euch O & Rosenbaum M 2019 The characteristic function of rough Heston models *Math. Financ.* **29**, 3.

- [39] Pagnini G & Paradisi P 2016 A stochastic solution with gaussian stationary increments of the symmetric space-time fractional diffusion equation *Fract. Calc. Appl. Anal.* **19**, 408.
- [40] Mura A & Pagnini G 2008 Characterizations and simulations of a class of stochastic processes to model anomalous diffusion *J. Phys. A: Math. Theor.* **41**, 285003.
- [41] Schneider W R 1990 Grey noise in *Stochastic Processes, Physics and Geometry*, Albeverio S, Casati G, Cattaneo U, Merlini D & Moresi R (World Scientific, Singapore), 76; Schneider W R 1990 Grey noise in *Ideas and Methods in Mathematical Analysis, Stochastics and Applications*, Vol. I, Albeverio S, Fenstad J E, Holden H, Lindstrøm T (Cambridge University Press, Cambridge), 261.
- [42] Pagnini, G 2014 Short note on the emergence of fractional kinetics. *Physica A* **409**, (2014), 29.
- [43] Sposini V, Chechkin A V, Seno F, Pagnini G & Metzler R 2018 Random diffusivity from stochastic equations: comparison of two models for Brownian yet non-Gaussian diffusion *New J. Phys.*, **20**, 043044.
- [44] Vitali S, Sposini V, Sliusarenko O, Paradisi P, Castellani G & Pagnini G 2018 Langevin equation in complex media and anomalous diffusion *J. R. Soc. Interface* **15**, 20180282.
- [45] D'Ovidio M, Vitali S, Sposini V, Sliusarenko O, Paradisi P, Castellani G & Pagnini G 2018 Center-of-mass like superposition of Ornstein-Uhlenbeck processes: a pathway to non-autonomous stochastic differential equations and fractional diffusion *Fract. Calc. Appl. Anal.* **21**, 1420.
- [46] Sliusarenko O, Vitali S, Sposini V, Paradisi P, Chechkin A V, Castellani G & Pagnini P 2019 Finite-energy Lévy-type motion through heterogeneous ensemble of Brownian particles *J. Phys. A: Math. Theor.* **52**, 095601.
- [47] Maćkała A & Magdziarz M 2019 Statistical analysis of superstatistical fractional Brownian motion and applications *Phys. Rev. E* **99**, 012143.
- [48] Golding I & Cox E C Physical nature of bacterial cytoplasm *Phys. Rev. Lett.* **96**, 098102.
- [49] J. Ślęzak, R. Metzler & Magdziarz M 2018 Superstatistical generalised Langevin equation: non-Gaussian viscoelastic anomalous diffusion *New J. Phys.* **20**, 023026.
- [50] Beck C & Cohen E D B 2003 Superstatistics *Physica A* **322**, 267.

- [51] Beck C 2006 Superstatistical Brownian motion *Prog. Theor. Phys. Suppl.* **162**, 29.
- [52] Abe S, Beck C & Cohen E D B 2007 Superstatistics, thermodynamics, and fluctuations *Phys. Rev. E* **76**, 031102.
- [53] Chubynsky M V & Slater G W 2014 Diffusing diffusivities: a model for anomalous, yet Brownian diffusion *Phys. Rev. Lett.* **113**, 098302.
- [54] Checkkin A V, Seno F, Metzler R & Sokolov I 2017 Brownian yet non-Gaussian diffusion: from superstatistics to subordination of diffusing diffusivities *Phys. Rev. X* **7**, 021002.
- [55] Jain R & Sebastian K L 2016 Diffusion in a crowded, rearranging environment *J. Phys. Chem. B* **120**, 3988.
- [56] Jain R & Sebastian K L 2017 Diffusing diffusivity: a new derivation and comparison with simulations *J. Chem. Sci.* **129**, 929.
- [57] Matse M, Chubynsky M V & Bechhoefer J 2017 Test of the diffusing-diffusivity mechanism using nearwall colloidal dynamics *arXiv:1706.02039v1*.
- [58] Feller W 1968 An Introduction to Probability Theory and Its Applications, Vol. 2 *John Wiley & Sons, New York*.
- [59] Lanoiselée Y & Grebenkov D 2018 A model of non-Gaussian diffusion in heterogeneous media *J. Phys. A: Math. Theor.*, **51**, 145602.
- [60] Tyagi N & Cherayil B J 2017 Non-Gaussian Brownian diffusion in dynamically disordered thermal environments *J. Phys. Chem. B*, **121**, 7204.
- [61] Ambaye H & Kehr K W 1999 A toy model for molecular motors *Physica A* **267**, 111.
- [62] Bressloff P C 2017 Stochastic switching in biology: from genotype to phenotype *J. Phys. A: Math. Theor.* **50**, 133001.
- [63] Yin G & Zhu C 2010 Hybrid switching diffusions: properties and applications (Springer, New York).
- [64] Miyaguchi T, Akimoto T & Yamamoto E 2016 Langevin equation with fluctuating diffusivity: a two-state model *J. Phys. Rev. E*, **94**, 012109.
- [65] Metzler R 2017 Gaussianity fair: the riddle of anomalous yet non-Gaussian diffusion *Biophys. J.* **112**, 413.

- [66] Sabri A, Xu X, Krapf D & Weiss M 2019 Elucidating the origin of heterogeneous anomalous diffusion in the cytoplasm of mammalian cells *pre-print*: arXiv:1910.00102v1.
- [67] Wang W, Seno F, Sokolov I S, Chechkin A V & Metzler R 2020 Unexpected crossovers in correlated random-diffusivity processes *New J. Phys.* (in press) DOI:10.1088/1367-2630/aba390.
- [68] Ahamad N & Debnath P 2020 Rouse model in crowded environment modeled by "diffusing diffusivity" *Physica A* **549** (C).
- [69] Hidalgo-Soria M & Barkai E S 2020 The Hitchhiker model for Laplace diffusion processes in the cell environment *pre-print*: arXiv:1909.07189v2.
- [70] Barkai E & Burov S 2020 Packets of diffusing particles exhibit universal exponential tails *Phys. Rev. Lett.* **124**, 060603.
- [71] Wang, W, Barkai E & Burov S 2020 Large deviations for continuous time random walks *Entropy* **22**, 697.
- [72] Thapa S, Lomholt M A, Krog J, Cherstvy A G & Metzler R 2018 Bayesian analysis of single-particle tracking data using the nested-sampling algorithm: maximum-likelihood model selection applied to stochastic-diffusivity data *Phys. Chem. Chem. Phys.* **20** (46), 29018.
- [73] Sposini V, Metzler R and Oshanin G 2019 Single-trajectory spectral analysis of scaled Brownian motion *New J. Phys.* **21**, 073043.
- [74] Sposini V, Grebenkov D S, Metzler R , Oshanin G & Seno F 2020 Universal spectral features of different classes of random diffusivity processes *New J. Phys.* **22**, 063056.
- [75] Sposini V, Chechkin A V & Metzler R 2019 First passage statistics for diffusing diffusivity *J. Phys. A: Math. Theor.* **52**, 04LT01.
- [76] Lim S C & Muniandy S V 2002 Self-similar Gaussian processes for modeling anomalous diffusion *Phys. Rev. E* **66**, 021114.
- [77] Jeon, J-H, Chechkin A V & Metzler R 2014 Scaled Brownian motion: a paradoxical process with a time dependent diffusivity for the description of anomalous diffusion *Phys. Chem. Chem. Phys.* **16**, 15811.
- [78] Norton M P & Karczub D G 2003 Fundamentals of Noise and Vibration Analysis for Engineers (Cambridge: Cambridge University Press).

- [79] Krapf D, Marinari E, Metzler R, Oshanin G, Xu X & Squarcini A 2018 Power spectral density of a single Brownian trajectory: what one can and cannot learn from it *New J. Phys.* **20**, 023029.
- [80] Krapf D, Lukat N, Marinari E, Metzler R, Oshanin G, Selhuber-Unkel C, Squarcini A, Stadler L, Weiss M & Xu X 2019 Spectral content of a single non-Brownian trajectory *Phys. Rev. X* **9**, 011019.
- [81] Metzler R 2019 Brownian motion and beyond: first-passage, power spectrum, non-Gaussianity, and anomalous diffusion *J. Stat. Mech.* **2019**, 114003.
- [82] Redner S 2001 A Guide to First Passage Processes (Cambridge: Cambridge University Press).
- [83] Metzler R, Oshanin G and Redner S 2014 First-passage phenomena and their applications (Singapore: World Scientific).
- [84] Mattos T G, Mejía-Monasteria C, Metzler R & Oshanin G 2012 First passages in bounded domains: when is the mean first passage time meaningful? *Phys. Rev. E* **86**, 031143.
- [85] Godec A & Metzler R 2016 First passage time distribution in heterogeneity controlled kinetics: going beyond the mean first passage time *Sci. Rep.* **6**, 20349.
- [86] Godec A & Metzler R 2016 Universal proximity effect in target search kinetics in the few-encounter limit *Phys. Rev. X* **6**, 041037.
- [87] Budini A A & Cáceres M O 2018 First-passage time for superstatistical Fokker-Planck models *Phys. Rev. E* **97**, 012137.
- [88] Jain R & Sebastian K L 2016 Diffusing diffusivity: survival in a crowded rearranging and bounded domain *J. Phys. Chem. B* **120**, 9215.
- [89] Bressloff P C & Lawley S D 2017 Residence times of a Brownian particle with temporal heterogeneity *J. Phys. A: Math. Theor.* **50**, 195001.
- [90] Tyagi N & Cherayil B J 2018 Enhancement of target location rates by stochastic modulation of Brownian motion *J. Stat. Mech.* **2018**, 063208.
- [91] Lanoiselée Y, Moutal N, Grebenkov D 2019 Diffusion-limited reactions in dynamic heterogeneous media *Nat. Comm.* **9**, 4398.
- [92] Grebenkov D 2019 A unifying approach to first-passage time distributions in diffusing diffusivity and switching diffusion models *J. Phys. A: Math. Theor.* **52**, 174001.

- [93] Grebenkov S D, Sposini V, Metzler R, Oshanin G and Seno F 2020 Universal spectral features of different classes of random diffusivity processes *pre-print*: arXiv:2007.05765.
- [94] Hartich D & Godec A 2018 Duality between relaxation and first passage in reversible Markov dynamics: rugged energy landscapes disentangled *New J. Phys.* **20**, 112002.
- [95] Hartich D & Godec A 2019 Interlacing relaxation and first-passage phenomena in reversible discrete and continuous space Markovian dynamics *J. Stat. Mech.* **2019**, 024002.
- [96] Baldovin F, Orlandini E & Seno F 2019 Polymerization induces non-Gaussian diffusion *Front. Phys.* **7**, 124.
- [97] Postnikov E B, Chechkin A V & Sokolov I M 2020 Brownian yet non-Gaussian diffusion in heterogeneous media: from superstatistics to homogenization *New J. Phys.* **22**, 063046.
- [98] Spakowitz A J (2019) Transient anomalous diffusion in a heterogeneous environment. *Front. Phys.* **7**, 119.
- [99] Chakraborty I & Roichman Y 2020 Disorder-induced Fickian, yet non-Gaussian diffusion in heterogeneous media *Phys. Rev. Res.* **2**, 022020(R).